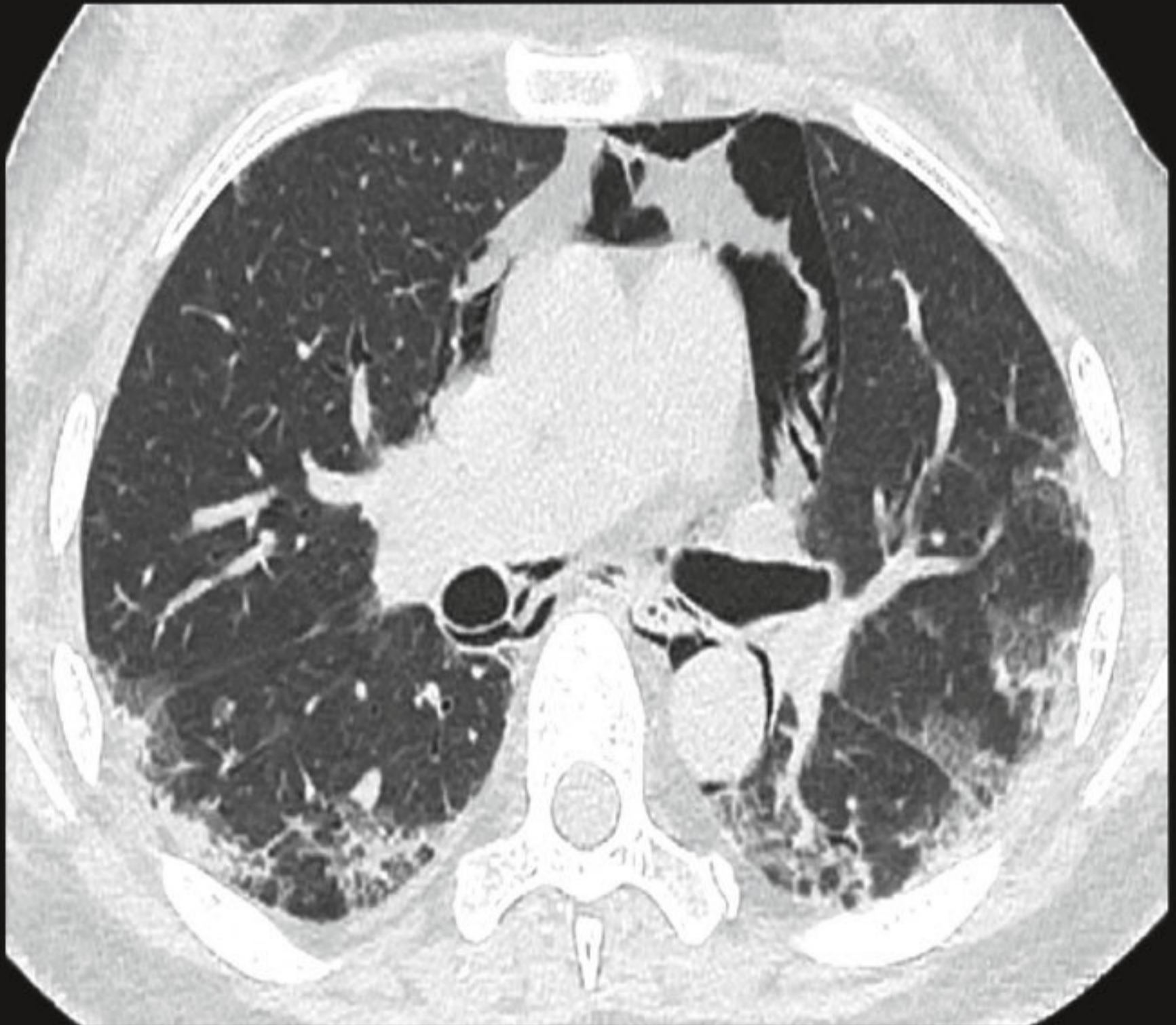


Arthritis & Rheumatology

AN OFFICIAL JOURNAL OF THE AMERICAN COLLEGE OF RHEUMATOLOGY



Arthritis & Rheumatology

An Official Journal of the American College of Rheumatology
www.arthritisrheum.org and wileyonlinelibrary.com

Editor

Richard J. Bucala, MD, PhD
Yale University School of Medicine, New Haven

Deputy Editor

Daniel H. Solomon, MD, MPH, *Boston*

Co-Editors

Joseph E. Craft, MD, *New Haven*
David T. Felson, MD, MPH, *Boston*
Richard F. Loeser Jr., MD, *Chapel Hill*
Peter A. Nigrovic, MD, *Boston*
Janet E. Pope, MD, MPH, FRCPC, *London, Ontario*
Christopher T. Ritchlin, MD, MPH, *Rochester*
Betty P. Tsao, PhD, *Charleston*
John Varga, MD, *Chicago*

Co-Editor and Review Article Editor

Robert Terkeltaub, MD, *San Diego*

Clinical Trials Advisor

Michael E. Weinblatt, MD, *Boston*

Social Media Editor

Paul H. Sufka, MD, *St. Paul*

Journal Publications Committee

Shervin Assassi, MD, MS, *Chair, Houston*
Vivian Bykerk, MD, FRCPC, *New York*
Kristin D'Silva, MD, *Boston*
Deborah Feldman, PhD, *Montreal*
Meenakshi Jolly, MD, MS, *Chicago*
Linda C. Li, PT, MSc, PhD, *Vancouver*
Uyen-Sa Nguyen, MPH, DSc, *Fort Worth*
R. Hal Scofield, MD, *Oklahoma City*

Editorial Staff

Jane S. Diamond, MPH, *Managing Editor, Atlanta*
Ilani S. Lorber, MA, *Assistant Managing Editor, Atlanta*
Lesley W. Allen, *Senior Manuscript Editor, Atlanta*
Kelly Barraza, *Manuscript Editor, Atlanta*
Jessica Hamilton, *Manuscript Editor, Atlanta*
Sara Omer, *Manuscript Editor, Atlanta*
Emily W. Wehby, MA, *Manuscript Editor, Atlanta*
Stefanie L. McKain, *Editorial Coordinator, Atlanta*
Brittany Swett, *Assistant Editor, New Haven*
Will Galanis, *Production Editor, Boston*

Associate Editors

Daniel Aletaha, MD, MS, <i>Vienna</i>	Insoo Kang, MD, <i>New Haven</i>	Andras Perl, MD, PhD, <i>Syracuse</i>
Heather G. Allore, PhD, <i>New Haven</i>	Wan-Uk Kim, MD, PhD, <i>Seoul</i>	Jack Porrino, MD, <i>New Haven</i>
Daniel J. Clauw, MD, <i>Ann Arbor</i>	Carol Langford, MD, MHS, <i>Cleveland</i>	Timothy R. D. J. Radstake, MD, PhD, <i>Utrecht</i>
Robert A. Colbert, MD, PhD, <i>Bethesda</i>	Katherine Liao, MD, MPH, <i>Boston</i>	William Robinson, MD, PhD, <i>Palo Alto</i>
Karen H. Costenbader, MD, MPH, <i>Boston</i>	S. Sam Lim, MD, MPH, <i>Atlanta</i>	Georg Schett, MD, <i>Erlangen</i>
Nicola Dalbeth, MD, FRACP, <i>Auckland</i>	Anne-Marie Malfait, MD, PhD, <i>Chicago</i>	Nan Shen, MD, <i>Shanghai</i>
Kevin D. Deane, MD, <i>Denver</i>	Paul A. Monach, MD, PhD, <i>Boston</i>	Ronald van Vollenhoven, MD, PhD, <i>Amsterdam</i>
Mark C. Genovese, MD, <i>Palo Alto</i>	Chester V. Oddis, MD, <i>Pittsburgh</i>	Fredrick M. Wigley, MD, <i>Baltimore</i>

Advisory Editors

Abhishek Abhishek, MD, PhD, <i>Nottingham</i>	Erica Herzog, MD, PhD, <i>New Haven</i>	Rik Lories, MD, PhD, <i>Leuven</i>
Tom Appleton, MD, PhD, <i>London, Ontario</i>	Hui-Chen Hsu, PhD, <i>Birmingham</i>	Bing Lu, PhD, <i>Boston</i>
Bonnie Bermas, MD, <i>Dallas</i>	J. Michelle Kahlenberg, MD, PhD, <i>Ann Arbor</i>	Suresh Mahalingam, PhD, <i>Southport, Queensland</i>
Liana Fraenkel, MD, MPH, <i>New Haven</i>	Mariana J. Kaplan, MD, <i>Bethesda</i>	Aridaman Pandit, PhD, <i>Utrecht</i>
Monica Guma, MD, PhD, <i>La Jolla</i>	Jonathan Kay, MD, <i>Worcester</i>	Kevin Winthrop, MD, MPH, <i>Portland</i>
Nigil Haroon, MD, PhD, <i>Toronto</i>	Francis Lee, MD, PhD, <i>New Haven</i>	Kazuki Yoshida, MD, MPH, MS, <i>Boston</i>
	Sang-Il Lee, MD, PhD, <i>Jinju</i>	

AMERICAN COLLEGE OF RHEUMATOLOGY

Ellen M. Gravallese, MD, *Boston*, **President**
David R. Karp, MD, PhD, *Dallas*, **President-Elect**
Douglas White, MD, PhD, *La Crosse*, **Treasurer**

Kenneth G. Saag, MD, MSc, *Birmingham*, **Secretary**
Steven Echard, IOM, CAE, *Atlanta*, **Executive Vice-President**

© 2020 American College of Rheumatology. All rights reserved. No part of this publication may be reproduced, stored or transmitted in any form or by any means without the prior permission in writing from the copyright holder. Authorization to copy items for internal and personal use is granted by the copyright holder for libraries and other users registered with their local Reproduction Rights Organization (RRO), e.g. Copyright Clearance Center (CCC), 222 Rosewood Drive, Danvers, MA 01923, USA (www.copyright.com), provided the appropriate fee is paid directly to the RRO. This consent does not extend to other kinds of copying such as copying for general distribution, for advertising or promotional purposes, for creating new collective works or for resale. Special requests should be addressed to: permissions@wiley.com

Access Policy: Subject to restrictions on certain backfiles, access to the online version of this issue is available to all registered Wiley Online Library users 12 months after publication. Subscribers and eligible users at subscribing institutions have immediate access in accordance with the relevant subscription type. Please go to onlinelibrary.wiley.com for details.

The views and recommendations expressed in articles, letters, and other communications published in *Arthritis & Rheumatology* are those of the authors and do not necessarily reflect the opinions of the editors, publisher, or American College of Rheumatology. The publisher and the American College of Rheumatology do not investigate the information contained in the classified advertisements in this journal and assume no responsibility concerning them. Further, the publisher and the American College of Rheumatology do not guarantee, warrant, or endorse any product or service advertised in this journal.

Cover design: Todd Machen

Ⓜ This journal is printed on acid-free paper.

Arthritis & Rheumatology

An Official Journal of the American College of Rheumatology
www.arthritisrheum.org and wileyonlinelibrary.com

VOLUME 72 • March 2020 • NO. 3

In This Issue	A15
Clinical Connections	A17
Special Articles	
Editorial: Tissue-Resident Memory T Cells: Sequestered Immune Sensors and Effectors of Inflammation in Spondyloarthritis <i>Christopher Ritchlin</i>	379
Editorial: More Than Skin Deep: Bringing Precision Medicine to Systemic Sclerosis <i>Christopher A. Mecoli and Ami A. Shah</i>	383
Advances in Disease Mechanisms and Translational Technologies: Clinicopathologic Significance of Inflammasome Activation in Autoimmune Diseases <i>J. Michelle Kahlenberg and Insoo Kang</i>	386
ACR Presidential Address: A Story to Tell, a Promise to Keep <i>Paula Marchetta</i>	396
Rheumatoid Arthritis	
Impact of Cumulative Inflammation, Cardiac Risk Factors, and Medication Exposure on Coronary Atherosclerosis Progression in Rheumatoid Arthritis <i>George A. Karpouzas, Sarah R. Ormseth, Elizabeth Hernandez, and Matthew J. Budoff</i>	400
Comparative Profiling of Serum Protein Biomarkers in Rheumatoid Arthritis-Associated Interstitial Lung Disease and Idiopathic Pulmonary Fibrosis <i>Daniel J. Kass, Mehdi Nouraie, Marilyn K. Glassberg, Nitya Ramreddy, Karen Fernandez, Lisa Harlow, Yingze Zhang, Jean Chen, Gail S. Kerr, Andreas M. Reimold, Bryant R. England, Ted R. Mikuls, Kevin F. Gibson, Paul F. Dellaripa, Ivan O. Rosas, Chester V. Oddis, and Dana P. Ascherman</i>	409
Osteoarthritis	
Mediating Role of Bone Marrow Lesions, Synovitis, Pain Sensitization, and Depressive Symptoms on Knee Pain Improvement Following Substantial Weight Loss <i>S. Reza Jafarzadeh, Tuhina Neogi, Joshua J. Stefanik, Jing-Sheng Li, Ali Guermazi, Caroline M. Apovian, and David T. Felson</i>	420
Spondyloarthritis	
Brief Report: Altered Cytotoxicity Profile of CD8+ T Cells in Ankylosing Spondylitis <i>Eric Gracey, Yuchen Yao, Zoya Qaiyum, Melissa Lim, Michael Tang, and Robert D. Inman</i>	428
Psoriatic Arthritis	
Polyfunctional, Proinflammatory, Tissue-Resident Memory Phenotype and Function of Synovial Interleukin-17A+CD8+ T Cells in Psoriatic Arthritis <i>Kathryn J. A. Steel, Ushani Srenathan, Michael Ridley, Lucy E. Durham, Shih-Ying Wu, Sarah E. Ryan, Catherine D. Hughes, Estee Chan, Bruce W. Kirkham, and Leonie S. Taams</i>	435
Systemic Lupus Erythematosus	
Hydroxychloroquine Blood Levels Predict Hydroxychloroquine Retinopathy <i>Michelle Petri, Marwa Elkhailifa, Jessica Li, Laurence S. Magder, and Daniel W. Goldman</i>	448
Improved Mitochondrial Metabolism and Reduced Inflammation Following Attenuation of Murine Lupus With Coenzyme Q10 Analog Idebenone <i>Luz P. Blanco, Hege L. Pedersen, Xinghao Wang, Yaíma L. Lightfoot, Nickie Seto, Carmelo Carmona-Rivera, Zu-Xi Yu, Victoria Hoffmann, Peter S. T. Yuen, and Mariana J. Kaplan</i>	454
Systemic Sclerosis	
Using Autoantibodies and Cutaneous Subset to Develop Outcome-Based Disease Classification in Systemic Sclerosis <i>Svetlana I. Nihtyanova, Alper Sari, Jennifer C. Harvey, Anna Leslie, Emma C. Derrett-Smith, Carmen Fonseca, Voon H. Ong, and Christopher P. Denton</i>	465

Spontaneous Pulmonary Hypertension Associated With Systemic Sclerosis in P-Selectin Glycoprotein Ligand 1-Deficient Mice <i>Rafael González-Tajuelo, María de la Fuente-Fernández, Daniel Morales-Cano, Antonio Muñoz-Callejas, Elena González-Sánchez, Javier Silván, Juan Manuel Serrador, Susana Cadenas, Bianca Barreira, Marina Espartero-Santos, Carlos Gamallo, Esther F. Vicente-Rabaneda, Santos Castañeda, Francisco Pérez-Vizcaíno, Ángel Cogolludo, Luis Jesús Jiménez-Borreguero, and Ana Urzainqui</i>	477
Multicenter Prospective Study of the Efficacy and Safety of Combined Immunosuppressive Therapy With High-Dose Glucocorticoid, Tacrolimus, and Cyclophosphamide in Interstitial Lung Diseases Accompanied by Anti-Melanoma Differentiation-Associated Gene 5-Positive Dermatomyositis <i>Hideaki Tsuji, Ran Nakashima, Yuji Hosono, Yoshitaka Imura, Masato Yagita, Hajime Yoshifuji, Shintaro Hirata, Takaki Nojima, Eiji Sugiyama, Kazuhiro Hatta, Yoshio Taguchi, Masaki Katayama, Kiminobu Tanizawa, Tomohiro Handa, Ryuji Uozumi, Shuji Akizuki, Kosaku Murakami, Motomu Hashimoto, Masao Tanaka, Koichiro Ohmura, and Tsuneyo Mimori</i>	488
Applications Invited for <i>Arthritis Care & Research</i> Editor-in-Chief (2021–2026 Term)	498
Pediatric Rheumatology	
Brief Report: Impact of <i>IL1RN</i> Variants on Response to Interleukin-1 Blocking Therapy in Systemic Juvenile Idiopathic Arthritis <i>Claas Hinze, Sabrina Fuehner, Christoph Kessel, Helmut Wittkowski, Elke Lainka, Melanie Baehr, Boris Hügler, Johannes-Peter Haas, Gerd Ganser, Elisabeth Weißbarth-Riedel, Annette Jansson, and Dirk Foell</i>	499
Letters	
Immune Checkpoint Inhibitors in Preexisting Autoimmune Disease: Comment on the Article by Tison et al <i>Wen-hui Xie and Zhuo-li Zhang</i>	506
Reply <i>Alice Tison, Marie Kostine, and Divi Cornec</i>	506
The First Epidemiologic Perspective on Takotsubo Syndrome in Patients With Takayasu Arteritis and Its Impact on Inpatient Outcomes: Comment on the Report by Lim et al <i>Rupak Desai, Sandeep Singh, Rajesh Sachdeva, and Gautam Kumar</i>	508
Reply <i>Sen Hee Tay, D. P. S. Dissanayake, Shir Lynn Lim, and Weiqin Lin</i>	509
ACR Announcements	A26

Cover image: The figure on the cover shows lung high-resolution computed tomography of an anti-MDA-5-positive dermatomyositis patient with interstitial lung disease. The patient had had dyspnea, and high-resolution computed tomography showed ground-glass opacity and consolidation with subpleural distribution mainly in the lower lobe but also in the upper lobe, accompanied by pneumomediastinum. This issue of *Arthritis & Rheumatology* features a report on the results of a prospective study examining the efficacy and safety of combined immunosuppressive therapy in anti-MDA-5-positive dermatomyositis patients with interstitial lung disease (Tsuji et al, pages 488–498). Image courtesy of Ran Nakashima, MD, PhD.

In this Issue

Highlights from this issue of *A&R* | By Lara C. Pullen, PhD

Coronary Atherosclerosis Progression in Rheumatoid Arthritis

In this issue, Karpouzas et al (p. 400) report the results of the first long-term study to explore predictors of coronary plaque progression in a well-characterized, prospective cohort of patients with rheumatoid arthritis (RA) without known cardiovascular (CV) disease.

p. 400

They found that, in patients with RA, inflammation is a consistent and independent predictor of coronary atherosclerosis progression, suggesting that CV risk can be mitigated by specifically targeting inflammation. When the investigators

examined individuals in their cohort, they found that total plaque increased in 48% of patients with RA. Progression was predicted by older age, higher cumulative inflammation, and total prednisone dose. Additionally, coronary artery calcium (CAC) progressors were older, more obese, hypertensive, and had higher cumulative inflammation compared to nonprogressors. In contrast, patients without baseline calcification who had longer exposure to biologics were less likely to have noncalcified plaque progression, lesion remodeling, and constrained CAC change.

This association was independent of inflammation, prednisone dose, or statin exposure.

The researchers also found that longer statin treatment further restricted noncalcified plaque progression and attenuated the effect of inflammation on increased plaque and CAC. Stringent systolic blood pressure (BP) control further weakened the effect of inflammation on total plaque progression. Thus, biologic disease-modifying antirheumatic drugs, statins, and BP control may further constrain plaque progression directly or indirectly.

Comparative Profiling of RA-Associated Interstitial Lung Disease and Idiopathic Pulmonary Fibrosis

As many as 40% of patients with rheumatoid arthritis (RA) will develop the complication of interstitial lung disease (ILD). Advanced RA-associated ILD (RA-ILD) resembles idiopathic pulmonary fibrosis (IPF), however, making it difficult for rheumatologists to tease out the distinct pathophysiology that appears to underlie the 2 diseases.

p. 409

In this issue, Kass et al (p. 409) describe their efforts to use comparative profiling of serum proteins in RA-ILD and IPF to define the molecular basis of the overlap between the 2 diseases. They used multiplex enzyme-linked immunosorbent assays and a series of complementary statistical models to show that several serum protein biomarkers are associated with the presence of ILD in independent cohorts of RA patients. They conclude that comparative serum protein biomarker profiling represents a viable method for distinguishing RA-ILD from RA–no ILD and identifying population-specific mediators shared with IPF.

The researchers analyzed sera from 2 independent cohorts (Veterans Affairs [VA] and Non-VA) to identify many non-overlapping biomarkers that distinguished RA-ILD from RA–no ILD in adjusted regression models. The presence of concomitant emphysema is higher in the VA cohort compared to the Non-VA cohort. Their comparative analysis of fully adjusted models revealed that the range of biomarkers associated with RA-ILD differed in the 2 cohorts. When the researchers performed parallel analysis of sera from IPF patients, they were able to identify a discriminatory panel

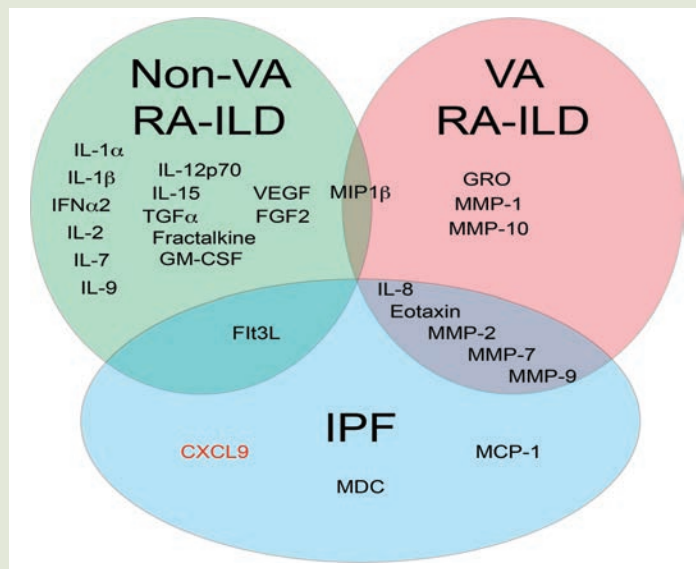


Figure 1. Differential overlap between IPF and RA-ILD in a VA cohort and a Non-VA cohort of RA patients.

of protein markers in models adjusted for age/sex/smoking, which showed differential overlap with profiles linked to RA-ILD in the VA cohort versus the Non-VA cohort. Principal components analysis further revealed several distinct functional groups of RA-ILD–associated markers that, in the VA cohort, encompassed proinflammatory cytokines/chemokines as well as 2 different subsets of metalloproteinases. When the researchers performed least absolute shrinkage and selection operator regression modeling in both cohorts, they identified distinct biomarker combinations that were capable of discriminating RA-ILD from RA–no ILD.

A New Outcome-Based Disease Classification for Systemic Sclerosis

In this issue, Nihtyanova et al (p. 465) describe how autoantibodies, cutaneous subset, and disease duration are all important for assessing morbidity and mortality in patients with systemic sclerosis (SSc). Their observations are based upon a large (n = 1,325) single-center cohort of patients with SSc, and they use their observations to propose a novel classification scheme that may improve disease monitoring and benefit future clinical trial designs in SSc.

The cohort included multiple antibody/skin disease subsets. The investigators found that anticentromere antibody-positive patients with limited cutaneous SSc (lcSSc) had the highest 20-year survival, lowest incidence of clinically significant pulmonary fibrosis (PF) and scleroderma renal crisis (SRC), and lowest incidence of cardiac SSc. In contrast, the frequency of pulmonary hypertension (PH) in the anticentromere antibody-positive patients was similar to the mean value in the SSc cohort overall.

The anti-Scl-70+ groups of patients with lcSSc and patients with diffuse cutaneous SSc (dcSSc) had the highest incidence of

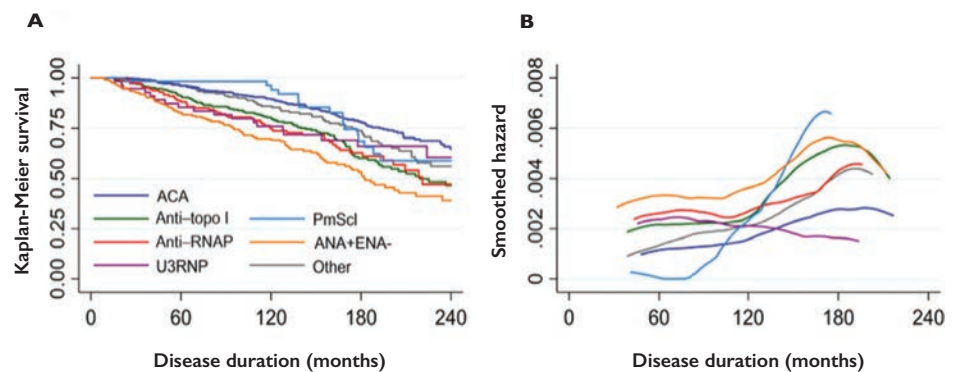


Figure 1. Associations of autoantibodies with survival estimates and incidence of organ complications over time in patients with systemic sclerosis. Kaplan-Meier survival estimates (A) and smoothed hazards of death over time (B) in subgroups by antibody specificity.

clinically significant PF. Anti-Scl-70+ patients with dcSSc also had the lowest survival and the second highest incidence of cardiac SSc at 20 years. Other complications were rare, however, in anti-Scl-70+ patients with lcSSc, and these patients demonstrated the lowest incidence of PH and second highest survival at 20 years.

The researchers found that anti-RNA polymerase antibody-positive SSc patients had the highest incidence of SRC at 20 years, and the anti-U3 RNP+ SSc

group had the highest incidence of PH and cardiac SSc at 20 years. When the investigators evaluated lcSSc patients with other defined autoantibodies, they found that the risk of SRC and cardiac SSc was low at 20 years, while the frequencies of other outcomes were similar to the mean values in the full SSc cohort. In addition, patients with dcSSc who were positive for other defined autoantibodies had a poor prognosis, demonstrating the second lowest survival and frequent organ complications.

Altered CD8+ Cytotoxicity Profile in Ankylosing Spondylitis

Ankylosing spondylitis (AS), an inflammatory arthritis, affects more men than women and results in progressive axial disease. Even though HLA-B27 is associated with a high risk for the development of AS, studies of AS have revealed a limited role for CD8+ T cells in disease. In this issue, Gracey et al (p. 428) report that AS patients have an altered cytotoxic T cell profile and that activated CD8+ T cells with a cytotoxic profile can be found in the joints of patients with AS.

The researchers began the study with the goal of validating their previously published observation of lower cytotoxic gene expression in the whole blood of AS patients. They hypothesized from this observation that an alteration in CD8+ T cells might explain the aberrant cytotoxic profile observed in patients. Their new data expands upon their earlier observation and suggests that researchers may have overlooked a central role for CD8+ T cells in AS.

In the current study, the investigators report that granzyme (GZM) and perforin 1 (PRF1) gene expression were both reduced in AS patients compared to healthy controls. They note that this finding was especially pronounced in men. Moreover, perforin 1, but not granzyme, protein levels were reduced in AS patient serum.

When the researchers analyzed synovial fluid (SF), they found that granzymes were elevated in patients with AS, but not in those with rheumatoid arthritis or osteoarthritis. When they performed flow cytometry, they found a reduction in granzyme-positive and perforin 1-positive lymphocytes, but not an intrinsic defect in CD8+ T cell granzyme or perforin 1 production. Further analysis of AS patients revealed that CD8+ T cell frequency was, however, reduced in the blood and increased in the SF of AS patients.

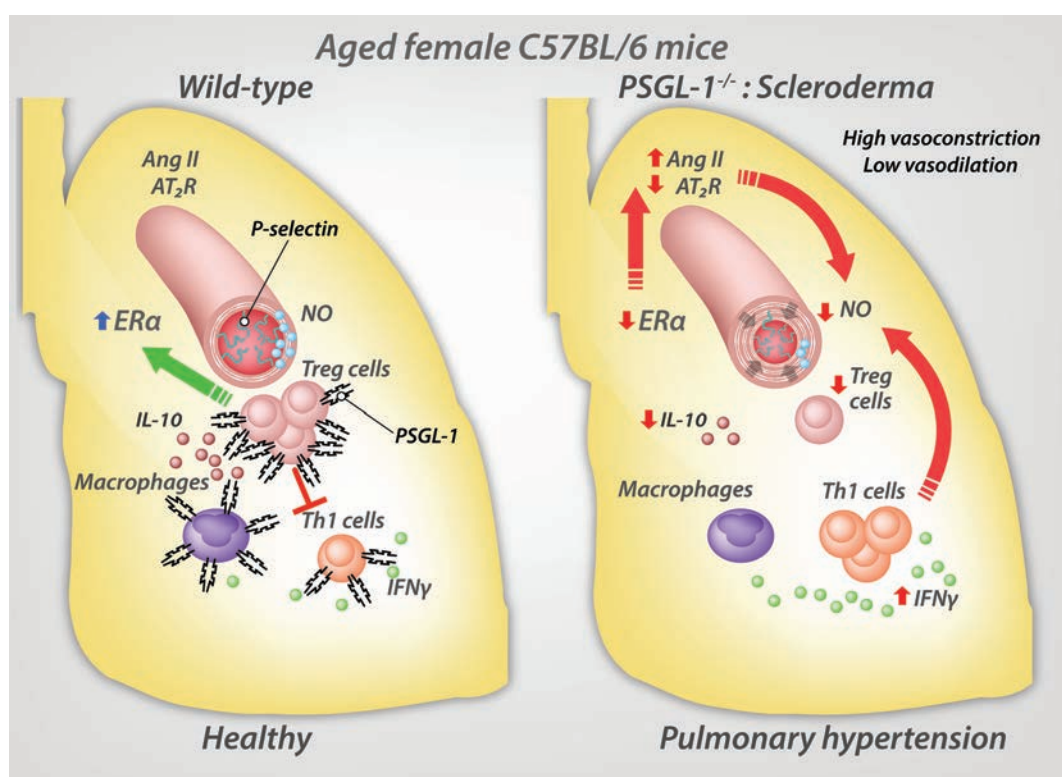
Clinical Connections

Spontaneous Pulmonary Hypertension Associated With Systemic Sclerosis in P-Selectin Glycoprotein Ligand I–Deficient Mice

González-Tajuelo et al, *Arthritis Rheumatol* 2020;74:477–487

CORRESPONDENCE

Ana Urzainqui, PhD: ana.urzainqui@salud.madrid.org



KEY POINTS

The lungs of aged PSGL-1–deficient female mice show:

- Medial thickening of small lung vessels and increased pulmonary artery pressure.
- Increased Ang II levels and reduced AT₂R expression and NO production.
- Reduced presence of Treg cells.
- Impeded age-related ERα up-regulation.

SUMMARY

Aged female mice lacking leukocytic receptor P-selectin glycoprotein ligand I (PSGL-I) develop pulmonary hypertension associated with scleroderma. González-Tajuelo et al found that PSGL-I deficiency in such subjects increases pulmonary levels of Angiotensin II (Ang II), an endocrine mediator involved in vasoconstriction and vascular remodeling, impedes Ang II type 2 receptor (AT₂R) expression in the lungs, and prevents age-related up-regulation of estrogen receptor α (ER α), a pleiotropic transcription factor with vasoprotective functions. In addition, aged PSGL-I–deficient female mice have endothelial dysfunction and reduced vasodilatory nitric oxide (NO) production by endothelial cells. These events result in vascular medial hypertrophy. At the same time, a lack of PSGL-I reduces the presence of Treg cells in the lungs and leads to increased interferon- γ (IFN γ) and reduced interleukin-10 (IL-10) production by macrophages, T cells, and B cells, as well as an imbalance in the ratio of proinflammatory cells:regulatory cells, further contributing to endothelial dysfunction. Together, these events lead to increased vasoconstriction and reduced vasodilation in lung vessels, promoting resistance to blood flow and favoring the development of pulmonary hypertension.

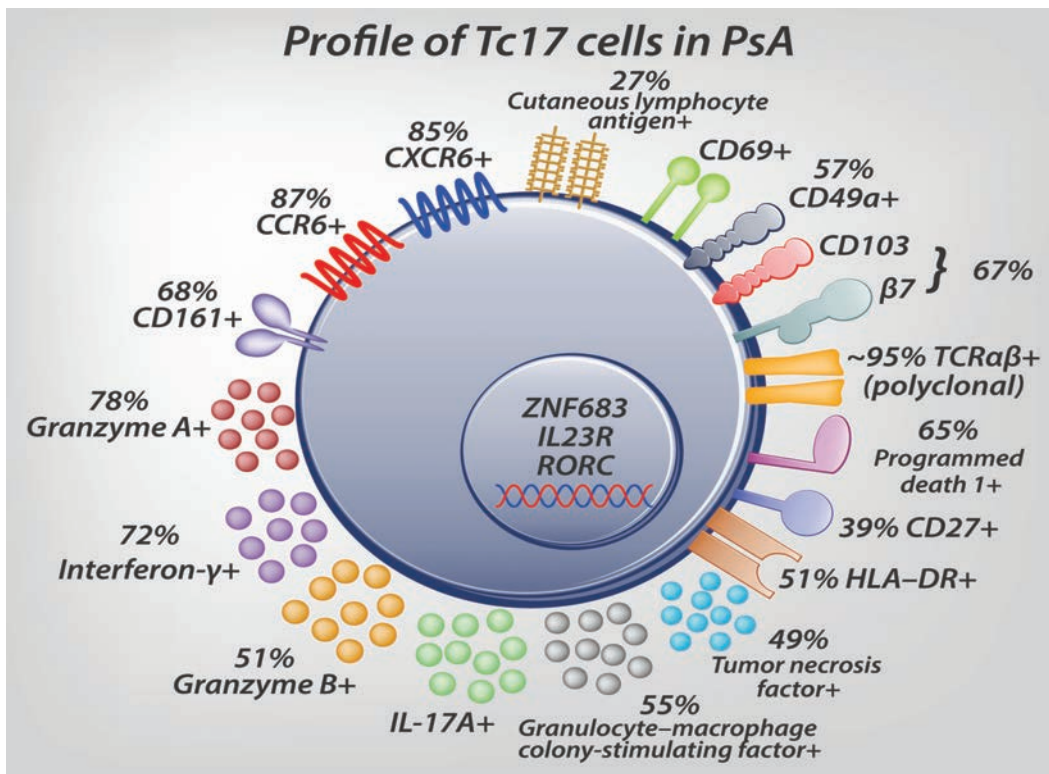
Polyfunctional, Proinflammatory, Tissue-Resident Memory Phenotype and Function of Synovial Interleukin-17A+CD8+ T Cells in Psoriatic Arthritis

Steel et al, *Arthritis Rheumatol* 2020;74:435–447

CORRESPONDENCE

Kathryn J. A. Steel, PhD: kathryn.steel@kcl.ac.uk

Leonie S. Taams, PhD: leonie.taams@kcl.ac.uk



KEY POINTS

- Polyclonal Tc17 cells are enriched in the SF of patients with PsA and SpA but not in rheumatoid arthritis.
- Tc17 cells from PsA SF have hallmarks of synovial Th17 and Tc1 cells and are polyfunctional, secreting a range of proinflammatory mediators.
- Synovial Tc17 cells exhibit a strong Trm cell signature and express enhanced levels of CXCR6, which may aid retention in the PsA synovial joint.

SUMMARY

Genetic associations, taken together with the clinical efficacy of interleukin-17A (IL-17A) blockade, imply a role for CD8+T cells and the IL-23/IL-17 axis in psoriatic arthritis (PsA). Previously, IL-17A+CD8+ (Tc17) T cells were shown to be enriched in the synovial fluid (SF) of patients with PsA, but little was known about their role in PsA pathogenesis. Steel et al addressed this question by determining the immunophenotype, molecular profile, and function of primary human Tc17 cells isolated from the SF of patients with PsA. Synovial Tc17 cells, enriched in both PsA and other types of peripheral spondyloarthritis (SpA), have a polyclonal T cell receptor (TCR) repertoire, with hallmarks of both Th17 (*RORC/IL23R/CCR6/CD161*) and Tc1 cells (*granzyme A/B*). These cells release a polyfunctional range of proinflammatory mediators upon stimulation, which may contribute to the ongoing inflammation. Synovial Tc17 cells display a strong tissue-resident memory (Trm) cell signature composed of known Trm genes and surface markers and express elevated levels of the chemokine receptor CXCR6. These features suggest that Tc17 cells are retained in the inflamed joint, possibly driven by elevated levels of CXCL16 found in PsA SF. The molecular signature and functional profiling of these cells may help explain how Tc17 cells can contribute to synovial inflammation and disease persistence in PsA and possibly other types of SpA.

EDITORIAL

Tissue-Resident Memory T Cells: Sequestered Immune Sensors and Effectors of Inflammation in Spondyloarthritis

Christopher Ritchlin

Despite a ballooning therapeutic toolbox, treatment responses to newer biologic agents and oral small molecules in psoriatic arthritis (PsA) and spondyloarthritis (SpA) are of similar magnitude to those observed with anti-tumor necrosis factor (anti-TNF) agents (1,2). Therapeutic outcomes in PsA and SpA stand in marked contrast to those reported in psoriasis, where blockade of molecules in the interleukin-23 (IL-23)/IL-17 pathway often leads to prolonged, deep responses and in some cases even remission (3). The underlying mechanisms that account for these divergent outcomes in the skin and joint are not well understood and are the subject of much speculation centered primarily on the existence of distinct cell populations or disease pathways unique to the joint.

In rheumatoid arthritis (RA), analysis of synovial tissue with single-cell RNA sequencing and cytometry by time-of-flight mass spectrometry have revealed discrete cell subpopulations with transcriptomic and cell surface expression profiles linked to functional activities (4–7). These analyses, focused on the synovium and not the peripheral blood, provided new insights regarding key pathogenic cell–cell interactions and underscore the necessity of examining cellular and molecular events in the target tissue. Traditionally, the study of T cells centered on sampling T lymphocytes from the peripheral blood to analyze cell subsets, phenotypic features, and functional characteristics. Recent discoveries, however, revealed the presence of a memory T cell population stationed within the tissue that does not recirculate, termed tissue-resident memory T (Trm) cells. These Trm cells are a separate subset from circulating effector memory T cells, which travel in the lymph and blood to patrol peripheral tissues and eliminate pathogens, and central memory T cells, which circulate in the blood and lymph to secondary lymphoid organs but not to peripheral tissues (8).

The first descriptions of Trm cells arose from examination of immune events in the skin. Boyman et al demonstrated the critical importance of skin-resident T cells in the initiation of psoriasis (9). They grafted uninvolved human psoriatic skin onto immunodeficient mice. The T cells in the graft proliferated and were crucial for the development of psoriasiform skin lesions

at 8 weeks. Interestingly, CD8+ T cells were identified in the epidermis and at the epidermal–dermal junction. Some of these cells expressed CD69, which prevents egress of T cells from tissue. Moreover, the proliferation of these T cells was dependent on TNF. In a pivotal study, cutaneous lymphocyte antigen (CLA)–positive cells in normal human skin were shown to be Trm cells that did not recirculate (10). Subsequent work on human psoriasis revealed the presence of a highly enriched population of CCR6+CD103+IL-23+CD8+ cells in resolved psoriatic lesions that produced IL-17 *ex vivo* (11). The T cells in the resolved lesions were oligoclonal, polyfunctional (secreted multiple proinflammatory cytokines), $\alpha\beta$ + T lymphocytes that did not recirculate (12). Cellular profiling showed that these Trm cells expressed the markers CD69 and CD103. The identification of long-lived, site-specific directed memory T cells parked in the skin and other barrier tissues opened new avenues of investigation.

Trm cells are key participants in the immune-sensing network poised to detect pathogens or other perturbations in nonlymphoid tissues (13). They possess several characteristic properties, as listed in Table 1. These cells, first identified in epithelial barrier tissues such as the skin, lung, and gut, are long lived; persist in specific tissues; and provide protection against an array of bacterial, viral, fungal, and parasitic pathogens (14). They carry out these activities through the release of cytokines and by sounding the alarm to attract additional resident and circulating cells. They are the most abundant memory T cell population and mediate inflammation in the absence of circulating T cells. CD8+ Trm cells undergo a distinct differentiation program in response to cues from peripheral tissues.

Trm cells exhibit a high degree of plasticity and receptor expression that can vary from tissue to tissue but several characteristic markers have been identified, as shown in Figure 1 (15). CD69 antagonizes sphingosine 1-phosphate receptor 1 and thus prevents egress of cells from tissues, although other inhibitor migration signals are also likely present. CD69 can be transiently expressed after T cell activation by antigen and is up-regulated by

Christopher Ritchlin, MD, MPH: University of Rochester, Rochester, New York. No potential conflicts of interest relevant to this article were reported. Address correspondence to Christopher Ritchlin, MD, MPH, University of Rochester, Center for Musculoskeletal Research, AIR Division, PO Box

695, Rochester, NY 14642. E-mail: Christopher_ritchlin@URMC.rochester.edu.

Submitted for publication October 31, 2019; accepted in revised form November 14, 2019.

Table 1. Characteristics of tissue-resident memory T cells

1. Heterogeneous long-lived cells
2. Maintain tissue homeostasis by immune sensing and immunosurveillance
3. Cannot be sampled in the blood but traffic to secondary lymphoid organs
4. Capable of triggering a rapid antigen-driven immune response in the absence of circulating T cells
5. Provide tissue-specific protection against a wide range of human pathogens
6. Proliferate locally, produce cytokines, induce dendritic cell maturation, and interact with circulating effector T cells
7. Capable of mediating inflammation in psoriasis, fixed drug eruption, and arthritis

several inflammatory cytokines. CD103 pairs with $\beta 7$ and binds E-cadherin, which is highly expressed on epithelial cells. Granzyme B is a serine protease in cytotoxic granules that, when released, induces cellular apoptosis. This molecule can also degrade matrix and activate cytokines. Programmed death 1 (PD-1) is a surface protein that suppresses T cell activity. Expression of PD-1 marks an exhausted cell phenotype but when expressed by Trm cells in inflamed tissues it signifies an antigen-experienced cell with an effector phenotype (16). Recognition of innocuous or self antigens by CD8+ Trm cells can induce inflammation in tissues that may ultimately lead to chronic and recurring damage. For example, besides psoriasis, CD8+ Trm cells have been implicated in the pathogenesis of other dermatologic diseases, including fixed drug eruption, alopecia areata, and vitiligo (17). The contribution of these cells to neoplastic and inflammatory diseases in the lung, brain, and gut are also areas of active investigation.

Several lines of evidence highlight the role of resident T cells in joints as key effectors of synovial inflammation. First, IL-17-expressing CD8+ T (Tc17) cells were enriched in PsA but not RA synovial fluid, and levels of these cells in the circulation were low. Moreover, the frequency of synovial Tc17 cells correlated with C-reactive protein levels, erythrocyte sedimentation rate, the Disease Activity in Psoriatic Arthritis outcome measure, and joint ultrasound scores (18). Second, Wade et al provided additional evidence of the existence of polyfunctional T cells in the psoriatic joint (19). They analyzed single-cell suspensions of mechanically/enzymatically digested psoriatic synovial tissue. They found that Th17, Th1, and ex-Th17 cells in the synovium, but not the blood, were polyfunctional granulocyte-macrophage colony-stimulating factor (GM-CSF)-positive, TNF-positive, IL-17-positive, or interferon- γ (IFN γ)-positive T cells (19). Third, an enrichment of CD69+PD-1+CD8+ T cells was identified in synovial fluid from patients with juvenile idiopathic arthritis (20). These cells were metabolically active effectors, had a phenotype of activation not exhaustion, expressed IFN γ and granzyme B, and were enriched for a tissue-resident memory cell transcriptional profile. In each of those previous studies, signals from the synovium were presumed to promote the development of an activated phenotype in the memory cell population.

In this issue of *Arthritis & Rheumatology*, Steel et al describe a population of IL-17A+CD8+TCR $\alpha\beta$ + T cells that were enriched in the synovial fluid but not the peripheral blood of PsA and SpA patients (21). These cells were not elevated in RA synovial fluid. They expressed markers of both Th17 cells (*RORC/IL23R/CCR6/CD161*)

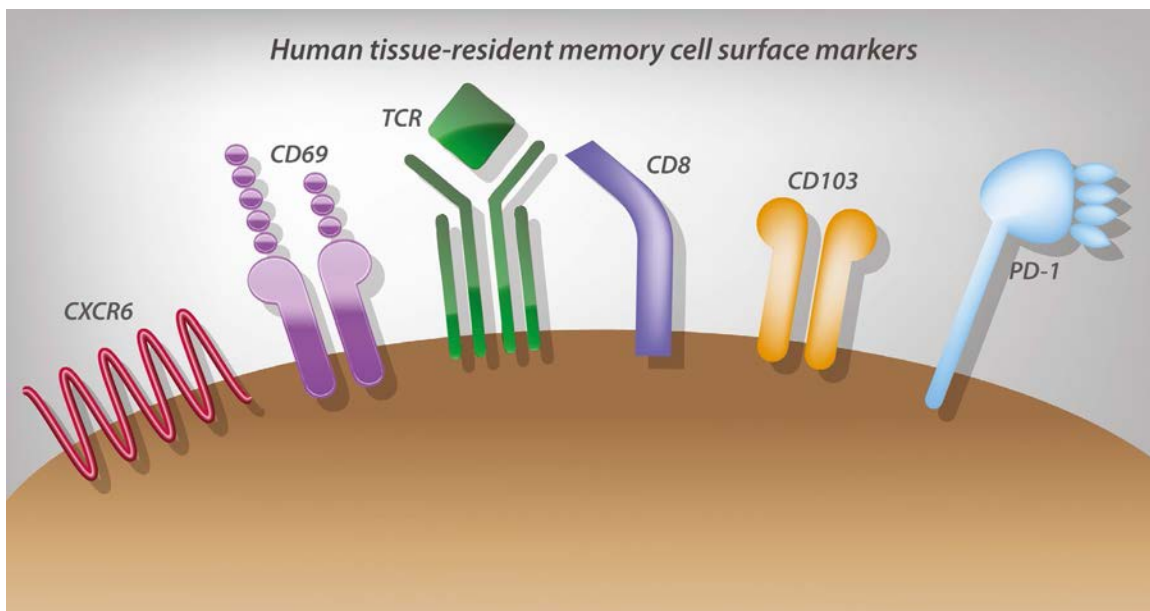


Figure 1. Human CD8+ tissue-resident memory T (Trm) cell surface markers. CXCR6 is a chemokine receptor with CXCL16 as its ligand. CD69 is a C-type lectin that blocks egress of Trm cells from tissues and binds sphingosine 1-phosphate receptor 1. The majority of Trm cells are T cell receptor $\alpha\beta$ (TCR $\alpha\beta$) positive. CD8 is a transmembrane protein and a coreceptor for TCR. CD103 is an integrin that binds $\beta 7$ and has E-cadherin as its ligand. Programmed death 1 (PD-1) down-regulates the immune response in cancer and infection, but during inflammation it is expressed by antigen-experienced Trm cells with effector functions.

and Tc1 cells (granzyme A/B). Synovial Tc17 cells were polyclonal (had a diverse TCR repertoire with a low clonality score), exhibited a Trm cell signature, and secreted several proinflammatory cytokines, including IFN γ , TNF, GM-CSF, and IL-21, and expressed PD-1. CXCR6 was a marker for Tc17 cells and increased levels of its ligand CXCL16 were present in the synovial fluid. A subset of the Trm cells expressed CLA and CD49, homing molecules for trafficking to the skin and gut, respectively.

These results are intriguing, but several caveats deserve mention. First, the Tc17 cells were analyzed in the synovial fluid and not in synovial tissue. It is not known if these cells are representative of those present in the synovial membrane. In addition, given the profiles that signify tissue residence, what are the signals that trigger the transit of these tissue-resident cells into the synovial fluid? Certainly, examination of the synovial tissue is required to investigate the topology, cellular interactions, and regional transcriptomics of these cells. The Tc17 cells were not identified in RA synovial fluid, which is somewhat puzzling given that IL-17A protein levels in psoriatic and rheumatoid synovial tissues do not differ significantly (22). Last, the sample size was small, and correlation with different phenotypes was beyond the scope of this study and will await additional examination. It is important to underscore that the majority of these samples studied by Steel and colleagues were from PsA patients, and the 3 samples that were subjected to T cell receptor sequencing were all from PsA synovial fluid, so the results may not be readily applicable to SpA.

A central question regarding the importance of Trm cells in PsA and SpA is whether these cells are key effectors of inflammation that persist despite therapy. Next steps should focus on examining the phenotype of these cells in the tissue before and after active treatment and correlation with disease response. The inability to gain insights into local joint events by sampling the blood represents a major barrier, but efforts to improve technologies to rapidly and safely sample joint tissues should be a high priority.

These cells, hidden from view, may provide insights into the events that link skin, gut, and joint disease. The finding of skin and gut homing receptors on Trm cells in the joint fluid may provide support for the notion of cellular links that may be pivotal to the etiopathogenesis of these disorders. Presumably, these cells originate in the skin and gut and migrate to the joints where they establish residence. While Trm cells do not recirculate in the blood, they can be mobilized following activation to enter the lymph and traffic to secondary lymph node organs (23) where they may conceivably promote tissue effector cells with cutaneous or gut homing receptors to enter joints. Alternatively, Trm cells may down-regulate CD69, allowing them to enter the circulation and traffic to other peripheral tissues. Last, targeting and eliminating Trm cell populations in joints has the distinct advantage that such a strategy would not impair systemic immune responses. Critical knowledge gaps to be addressed before advancing to therapeutics, however, include a better understanding of Trm

cell heterogeneity and plasticity, Trm cell interactions with other tissue-resident and circulating populations, and how to develop valid and reliable markers to enhance diagnosis and facilitate therapeutic targeting. Confirmation that Trm cells reside in inflamed synovial membranes will propel research focused on eliminating or modulating this subset and further expand the SpA therapeutic toolbox in new directions.

AUTHOR CONTRIBUTIONS

Dr. Ritchlin drafted the article, revised it critically for important intellectual content, and approved the final version to be published.

REFERENCES

- Ritchlin CT, Colbert RA, Gladman DD. Psoriatic arthritis [review]. *N Engl J Med* 2017;376:957–70.
- Sieper J, Poddubnyy D. Axial spondyloarthritis. *Lancet* 2017;390:73–84.
- Erichsen CY, Jensen P, Kofoed K. Biologic therapies targeting the interleukin (IL)-23/IL-17 immune axis for the treatment of moderate-to-severe plaque psoriasis: a systematic review and meta-analysis. *J Eur Acad Dermatol Venereol* 2020;34:30–8.
- Croft AP, Campos J, Jansen K, Turner JD, Marshall J, Attar M, et al. Distinct fibroblast subsets drive inflammation and damage in arthritis. *Nature* 2019;570:246–51.
- Donlin LT, Rao DA, Wei K, Slowikowski K, McGeachy MJ, Turner JD, et al. Methods for high-dimensional analysis of cells dissociated from cryopreserved synovial tissue. *Arthritis Res Ther* 2018;20:139.
- Rao DA, Gurish MF, Marshall JL, Slowikowski K, Fonseka CY, Liu Y, et al. Pathologically expanded peripheral T helper cell subset drives B cells in rheumatoid arthritis. *Nature* 2017;542:110–4.
- Zhang F, Wei K, Slowikowski K, Fonseka CY, Rao DA, Kelly S, et al. Defining inflammatory cell states in rheumatoid arthritis joint synovial tissues by integrating single-cell transcriptomics and mass cytometry. *Nat Immunol* 2019;20:928–42.
- Von Andrian UH, Mackay CR. T-cell function and migration—two sides of the same coin [review]. *N Engl J Med* 2000;343:1020–34.
- Boyman O, Hefti HP, Conrad C, Nickoloff BJ, Suter M, Nestle FO. Spontaneous development of psoriasis in a new animal model shows an essential role for resident T cells and tumor necrosis factor- α . *J Exp Med* 2004;199:731–6.
- Clark RA, Chong B, Mirchandani N, Brinster NK, Yamanaka K, Dowgiert RK, et al. The vast majority of CLA+ T cells are resident in normal skin. *J Immunol* 2006;176:4431–9.
- Cheuk S, Wikén M, Blomqvist L, Nylén S, Talme T, Ståhle M, et al. Epidermal Th22 and Tc17 cells form a localized disease memory in clinically healed psoriasis. *J Immunol* 2014;192:3111–20.
- Matos TR, O'Malley JT, Lowry EL, Hamm D, Kirsch IR, Robins HS, et al. Clinically resolved psoriatic lesions contain psoriasis-specific IL-17-producing $\alpha\beta$ T cell clones. *J Clin Invest* 2017;127:4031–41.
- Masopust D, Soerens AG. Tissue-resident T cells and other resident leukocytes. *Annu Rev Immunol* 2019;37:521–46.
- Schenkel JM, Masopust D. Tissue-resident memory T cells. *Immunity* 2014;41:886–97.
- Watanabe R, Gehad A, Yang C, Scott LL, Teague JE, Schlaupbach C, et al. Human skin is protected by four functionally and phenotypically discrete populations of resident and recirculating memory T cells. *Sci Transl Med* 2015;7:279ra39.
- Petrelli A, van Wijk F. CD8+ T cells in human autoimmune arthritis: the unusual suspects. *Nat Rev Rheumatol* 2016;12:421–8.

17. Ho AW, Kupper TS. T cells and the skin: from protective immunity to inflammatory skin disorders. *Nat Rev Immunol* 2019;19:490–502.
18. Menon B, Gullick NJ, Walter GJ, Rajasekhar M, Garrod T, Evans HG, et al. Interleukin-17+CD8+ T cells are enriched in the joints of patients with psoriatic arthritis and correlate with disease activity and joint damage progression. *Arthritis Rheumatol* 2014;66:1272–81.
19. Wade SM, Canavan M, McGarry T, Low C, Wade SC, Mullan RH, et al. Association of synovial tissue polyfunctional T-cells with DAPSA in psoriatic arthritis. *Ann Rheum Dis* 2019;78:350–4.
20. Petrelli A, Mijnheer G, Hoytema van Konijnenburg DP, van der Wal MM, Giovannone B, Mocholi E, et al. PD-1+CD8+ T cells are clonally expanding effectors in human chronic inflammation. *J Clin Invest* 2018;128:4669–81.
21. Steel KJ, Srenathan U, Ridley M, Durham LE, Wu SY, Ryan SE. Polyfunctional, proinflammatory, tissue-resident memory phenotype and function of synovial interleukin-17A+CD8+ T cells in psoriatic arthritis. *Arthritis Rheumatol* 2020;72:435–47.
22. Van Baarsen LG, Lebre MC, van der Coelen D, Aarrass S, Tang MW, Ramwadhoebe TH, et al. Heterogeneous expression pattern of interleukin 17A (IL-17A), IL-17F and their receptors in synovium of rheumatoid arthritis, psoriatic arthritis and osteoarthritis: possible explanation for nonresponse to anti-IL-17 therapy? *Arthritis Res Ther* 2014;16:426.
23. Beura LK, Wijeyesinghe S, Thompson EA, Macchietto MG, Rosato PC, Pierson MJ, et al. T cells in nonlymphoid tissues give rise to lymph-node-resident memory T cells. *Immunity* 2018;48:327–38.

EDITORIAL

More Than Skin Deep: Bringing Precision Medicine to Systemic Sclerosis

Christopher A. Mecoli  and Ami A. Shah 

Historically, patients with systemic sclerosis (SSc) have been classified by the extent of their skin involvement, given a classification of either diffuse cutaneous SSc (dcSSc), characterized by skin involvement of the torso and proximal limbs, or limited cutaneous SSc (lcSSc), with involved skin predominantly distal to the elbows and knees. Subgrouping based on cutaneous type is grounded in the literature, in which differences in organ involvement and mortality have been demonstrated (1). However, this binary classification system does not capture the marked clinical heterogeneity known to exist within these 2 subgroups. Attempting to risk stratify a given SSc patient's clinical trajectory, organ-specific complications, and response to medications based solely on cutaneous type is an imperfect approach in the modern era.

Over the past few decades, the value of SSc-specific and -associated autoantibodies has been increasingly realized (2,3). As more clinical-serologic associations have been discovered and validated, our ability to phenotype SSc patients has dramatically improved. This increased awareness, in conjunction with improved laboratory capabilities in autoantibody testing, has allowed for the majority of SSc cohorts around the world to have comprehensive and detailed serotyping. However, even within a given autoantibody subtype, there is often heterogeneity in clinical presentation and course; the power of combining both serology and skin subtype identification to predict outcomes has been illustrated by Cottrell et al, who demonstrated that within a given SSc-specific autoantibody group (e.g., anti-Scl-70), different clinical trajectories exist based on cutaneous subtype (4).

In addition to utilizing cutaneous type and autoantibodies to help clinically phenotype SSc patients, a third component—time—is perhaps most critical of all. Epidemiologic issues related to time are integral to characterizing SSc cohorts, given the known fact that organ-specific complications do not occur evenly throughout the life of a patient with SSc (5). These issues include

minimizing immortal person-time (e.g., the time during which the relevant outcome under study could not have been observed), accounting for SSc disease duration, and assessing the timing of events relative to one another. This concept has been eloquently shown by Herrick et al in their development of a model to predict progression of skin disease in SSc (6). Whereas the baseline modified Rodnan skin thickness score (MRSS) alone was a poor predictor, the model improved upon the addition of disease duration, and further improved with the incorporation of RNA polymerase III (anti-RNAP) antibody status (6). Similarly, the power of utilizing cutaneous subtype, autoantibody status, and timing as filters through which to study the cancer-scleroderma relationship has illustrated the value of these tools in risk stratifying SSc patients for the development of malignancy (7).

It is within this landscape that the work by Nihtyanova et al in this issue of *Arthritis & Rheumatology* bolsters the argument for incorporating cutaneous type, serology, and disease duration to subgroup SSc populations (8). Their study included more than 1,300 SSc patients seen at the University College London and stratified them into 1 of 14 subgroups defined a priori based on different combinations of cutaneous disease type (limited or diffuse) and autoantibody status (anticentromere antibody [ACA] positive, anti-topoisomerase I [anti-topo I; anti-Scl-70] positive, anti-RNAP positive, anti-U3 RNP positive, anti-PM/Scl positive, antinuclear antibody [ANA] positive but extractable nuclear antigen [ENA] antibody negative, and “other” [including antibodies to U1 RNP, Th/To, SL, Ku, Jo-1, Ro, La, XR, PL-7, heterogeneous nuclear RNP, and Sm, as well as ANA negative]). For each of the 14 combinations, they performed time-to-event analyses of organ-specific complications and survival at 5, 10, 15, and 20 years of follow-up. Upon collapsing similar strata, they discovered 7 distinct SSc subgroups: ACA+ lcSSc, anti-Scl-70+ lcSSc, anti-Scl-70+ dcSSc, anti-RNAP+, anti-U3 RNP+, lcSSc with other

Supported in part by the Johns Hopkins inHealth Precision Medicine Initiative. Dr. Mecoli's work was supported by the NIH (National Institute of Arthritis and Musculoskeletal and Skin Diseases grant K23-AR-075898), the Jerome L. Greene Foundation, and a Johns Hopkins University School of Medicine Clinician Scientist award. Dr. Shah's work was supported by the NIH (National Institute of Arthritis and Musculoskeletal and Skin Diseases grant R01-AR-073208), the Scleroderma Research Foundation, and the Donald B. and Dorothy L. Stabler Foundation.

Christopher A. Mecoli, MD, MHS, Ami A. Shah, MD, MHS: Johns Hopkins University School of Medicine, Baltimore, Maryland.

No potential conflicts of interest relevant to this article were reported.

Address correspondence to Ami A. Shah, MD, MHS, Johns Hopkins Scleroderma Center, 5501 Hopkins Bayview Circle, Baltimore, MD 21224. E-mail: Ami.Shah@jhmi.edu.

Submitted for publication September 25, 2019; accepted in revised form October 29, 2019.

antibodies, and dcSSc with other antibodies. Based on these clinical subgroupings, the authors report markedly different incidence rates of scleroderma renal crisis (SRC), scleroderma heart disease, pulmonary hypertension (PH), clinically significant pulmonary fibrosis (PF), and overall mortality.

The strengths of the study by Nihtyanova et al (8) are the inclusion of a large number of autoantibodies tested in a systematic manner, prospective follow-up of long duration, standardized clinical outcome measures, and rigorous analytic methods. Their study demonstrates the added value of incorporating antibody status to clinically phenotype SSc patients above and beyond cutaneous subtype. This is particularly apparent when comparing organ-specific outcomes and mortality between anti-Scl-70+ patients with lcSSc and anti-Scl-70+ patients with dcSSc; whereas anti-Scl-70+ dcSSc and lcSSc patients had similar rates of clinically significant PF, the incidence of other organ-specific complications and mortality were increased >2-fold in those with diffuse disease.

With respect to organ-specific complications, the study by Nihtyanova et al highlights the clinical importance of the anti-U3 RNP+ subgroup of SSc patients, particularly their high risk of PH (both group 1 [pulmonary arterial hypertension] and group 3 [PH associated with interstitial lung disease (ILD)]); 1 in 3 anti-U3 RNP+ patients developed PH over 15 years. Interestingly, patients with anti-Scl-70 or anti-PM/Scl antibodies had the lowest hazard of PH development, even when accounting for PH secondary to ILD, and those with ACAs had only average risk of developing PH. In addition, anti-RNAP+ and ANA+ENA- patients had the highest initial MRSS skin thickness scores, but also experienced the most improvement—a factor that may be important to consider in the design of clinical trials focused on active diffuse cutaneous disease.

The proposed classification system has clear benefits when applied in clinical practice, such as improved prognostication as well as informing disease-monitoring strategies (e.g., frequency of hypertension screening for SRC, electrocardiogram for arrhythmia, or pulmonary function testing [PFT] and echocardiogram for clinically significant PF and cardiac scleroderma, respectively). For example, the knowledge that a patient with ACA+ limited disease has a 20-year incidence of clinically significant PF of <10% might inform the treating provider that obtaining frequent PFTs may be unnecessary.

In addition to having a direct impact on the clinical care of SSc patients, this classification framework would allow for better comparisons across different SSc cohorts, as the frequency of different autoantibody subsets tends to vary internationally (9). The failure of validating research findings in different cohorts could be attributable, in part, to this geographic heterogeneity. For example, a cohort with a low prevalence (<10%) of anti-RNAP-positive SSc may not validate findings with regard to the risk of malignancy or SRC found in a different cohort in which the anti-RNAP-positive SSc prevalence is >20%.

Furthermore, the findings from the study by Nihtyanova et al may inform optimal clinical trial study design in SSc. The differential severity and clinical course observed suggests that enrichment of high-risk subgroups—i.e., those who are most likely to progress—should be considered in trials focused on different organ-specific complications.

Moving forward, these results need to be validated in other SSc cohorts, including those with different racial and ethnic compositions. It remains to be seen whether race and ethnicity has an impact on this type of subgrouping, given that certain racial groups, such as African Americans, are known to have more severe disease (10,11). In addition, there remains several unanswered questions with regard to the use of this approach to classify SSc patients. For example, many patients were positive for >1 autoantibody (most notably, anti-Ro antibodies), and the impact that this might have on the clinical trajectory and rate of mortality warrants further study.

We also need to better understand the influence that different treatment strategies have on these subgroups; for example, studies should address whether treatment of diffuse cutaneous disease would impact the incidence rates of clinically significant PF. Moreover, the incorporation of other outcome measures, including SSc-specific patient-reported outcomes, needs to be implemented and standardized, particularly given the current shortcomings of outcome measures pertaining to digital ischemia, calcinosis, and gastrointestinal symptoms.

These data illustrate that multiple measurements in combination, such as cutaneous subtype, autoantibody status, and timing, improve predictive capability compared to a single measurement alone. The approach to incorporate and harmonize multiple clinical and biologic characteristics to subgroup SSc patients is the foundation of precision medicine. In the near future, dynamic genetic, plasma, serum, and/or cellular biomarkers will likely prove even more valuable for classification and provide insight into disease mechanisms; the SSc community should anticipate this accordingly, by storing biospecimens conducive to analysis. In an era of an increasing number of working groups, societies, and cohorts, standardization and validation will be paramount to success. Fortunately, many dedicated researchers and healthcare providers are focused on improving our ability to classify SSc patients, which will in turn advance research programs and, ultimately, clinical care.

AUTHOR CONTRIBUTIONS

Drs. Mecoli and Shah drafted the article, revised it critically for important intellectual content, and approved the final version to be published.

REFERENCES

1. Medsger TA Jr. Natural history of systemic sclerosis and the assessment of disease activity, severity, functional status, and psychologic well-being. *Rheum Dis Clin North Am* 2003;29:255–73.
2. Hamaguchi Y. Autoantibody profiles in systemic sclerosis: predictive value for clinical evaluation and prognosis. *J Dermatol* 2010;37:42–53.

3. Patterson KA, Roberts-Thomson PJ, Lester S, Tan JA, Hakendorf P, Rischmueller M, et al. Interpretation of an extended autoantibody profile in a well-characterized Australian systemic sclerosis (scleroderma) cohort using principal components analysis. *Arthritis Rheumatol* 2015;67:3234–44.
4. Cottrell TR, Wise RA, Wigley FM, Boin F. The degree of skin involvement identifies distinct lung disease outcomes and survival in systemic sclerosis. *Ann Rheum Dis* 2014;73:1060–6.
5. Walker JG, Steele RJ, Schnitzer M, Taillefer S, Baron M, Canadian Scleroderma Research Group, et al. The association between disease activity and duration in systemic sclerosis. *J Rheumatol* 2010;37:2299–306.
6. Herrick AL, Peytrignet S, Lunt M, Pan X, Hesselstrand R, Mouthon L. Patterns and predictors of skin score change in early diffuse systemic sclerosis from the European Scleroderma Observational Study. *Ann Rheum Dis* 2018;77:563–70.
7. Igusa T, Hummers LK, Visvanathan K, Richardson C, Wigley FM, Casciola-Rosen L, et al. Autoantibodies and scleroderma phenotype define subgroups at high-risk and low-risk for cancer. *Ann Rheum Dis* 2018;77:1179–86.
8. Nihtyanova SI, Sari A, Harvey JC, Leslie A, Derrett-Smith EC, Fonseca C, et al. Using autoantibodies and cutaneous subset to develop outcome-based disease classification in systemic sclerosis. *Arthritis Rheumatol* 2020;72:465–76.
9. Sobanski V, Dauchet L, Lefèvre G, Lambert M, Morell-Dubois S, Sy T, et al. Prevalence of anti-RNA polymerase III antibodies in systemic sclerosis: new data from a French cohort and a systematic review and meta-analysis. *Arthritis Rheumatol* 2014;66:407–17.
10. Steen V, Domsic RT, Lucas M, Fertig N, Medsger TA Jr. A clinical and serologic comparison of African American and Caucasian patients with systemic sclerosis. *Arthritis Rheum* 2012;64:2986–94.
11. Gelber AC, Manno RL, Shah AA, Woods A, Le EN, Boin F, et al. Race and association with disease manifestations and mortality in scleroderma: a 20-year experience at the Johns Hopkins Scleroderma Center and review of the literature. *Medicine (Baltimore)* 2013;92:191–205.

ADVANCES IN DISEASE MECHANISMS AND TRANSLATIONAL TECHNOLOGIES

Clinicopathologic Significance of Inflammasome Activation in Autoimmune Diseases

J. Michelle Kahlenberg¹  and Insoo Kang² 

Autoimmune diseases are characterized by dysregulated immune tolerance to self and inflammatory damage to tissues and organs. The development of inflammation involves multiple innate and adaptive immune pathways. Inflammasomes are multimeric cytosolic protein complexes that form to mediate host immune responses upon recognizing pathogen- or damage-associated molecular patterns via pattern-recognition receptors (PRRs). The accelerating pace of inflammasome research has demonstrated important roles for inflammasome activation in many pathologic conditions, including infectious, metabolic, autoinflammatory, and autoimmune diseases. The inflammasome generally comprises a PRR, procaspase 1, and an adaptor molecule connecting the PRR and procaspase 1. Upon inflammasome activation, procaspase 1 becomes active caspase 1 that converts pro–interleukin-1 β (proIL-1 β) and proIL-18 into mature and active IL-1 β and IL-18, respectively. The cytokines IL-1 β and IL-18 have multipotent effects on immune and nonimmune cells and induce and promote systemic and local inflammatory responses. Human studies have shown increased levels of these cytokines, altered activation of inflammasome-related molecules, and/or the presence of inflammasome activators in rheumatic diseases, including systemic lupus erythematosus, rheumatoid arthritis, crystal-induced arthropathies, and Sjögren’s syndrome. Such changes are found in the primary target organs, such as the kidneys, joints, and salivary glands, as well as in the cardiovascular system. In animal models of rheumatic diseases, inflammation and tissue damage improve upon genetic or pharmacologic targeting of the inflammasome, supporting its pathogenic role. Herein, we review the clinicopathologic significance and therapeutic targeting of inflammasome activation in rheumatic diseases and related conditions based on recent findings.

Introduction

Inflammation plays a critical role in the pathogenesis of rheumatic diseases, including systemic lupus erythematosus (SLE), rheumatoid arthritis (RA), and crystal-induced arthropathies. Multiple innate and adaptive immune pathways and molecules are involved in the development of inflammation. Germline-encoded pattern-recognition receptors (PRRs), like Toll-like receptors (TLRs), expressed by innate immune cells recognize pathogen-associated molecular patterns (PAMPs) and damage-associated molecular patterns (DAMPs), which

are derived from invading pathogens and stressed host cells, respectively. Upon recognizing these molecules, the innate immune cells produce an array of inflammatory molecules such as interleukin-1 β (IL-1 β) and IL-18, whose maturation and secretion are regulated by multiprotein complex inflammasomes (1,2). An increasing body of evidence supports the notion that the inflammasome plays a role in rheumatic diseases such as SLE, crystal-induced arthropathies, and RA. In this review, we discuss the biologic processes, clinical significance, and therapeutic targeting of inflammasome activation in rheumatic diseases and related conditions, focusing on recent advances.

Dr. Kahlenberg’s work was supported by the Doris Duke Foundation (Physician Scientist Development Award), the NIH (National Institute of Arthritis and Musculoskeletal and Skin Diseases grant R01-AR-071384), an Innovative Research Award from the Rheumatology Research Foundation, and the Taubman Institute (Parfet Emerging Scholar award). Dr. Kang’s work was supported in part by the NIH (grants 1-R01-AG-056728, R21-AI-126604, and R01-AG-055362).

¹J. Michelle Kahlenberg, MD, PhD: University of Michigan, Ann Arbor;
²Insoo Kang, MD: Yale University, New Haven, Connecticut.

Dr. Kahlenberg has received consulting fees and/or honoraria from Bristol-Myers Squibb, Novartis, AstraZeneca, and Eli Lilly (less than \$10,000

each) and research support from Celgene. No other disclosures relevant to this article were reported.

Address correspondence to J. Michelle Kahlenberg, MD, PhD, 5570A Medical Science Research Building II, 1150 West Medical Center Drive, Ann Arbor, MI 48109 (e-mail: mkahlenb@med.umich.edu); or to Insoo Kang, MD, The Anlyan Center for Medical Research and Education Room S541C, 300 Cedar Street, New Haven, CT 06520 (e-mail: insoo.kang@yale.edu).

Submitted for publication July 9, 2019; accepted in revised form September 24, 2019.

Inflammasome types and activation

Inflammasomes are multimeric cytosolic protein complexes that form to mediate host immune responses upon sensing PAMPs or DAMPs (1,2). Assembly of an inflammasome cleaves

procaspase 1 into active caspase 1 that converts proIL-1 β and proIL-18 into mature and active IL-1 β and IL-18, respectively. Inflammasome activation can lead to pyroptosis, a type of inflammatory cell death, and active caspase 1 enables the unconventional secretion of numerous cytosolic proteins (3). The inflammasome

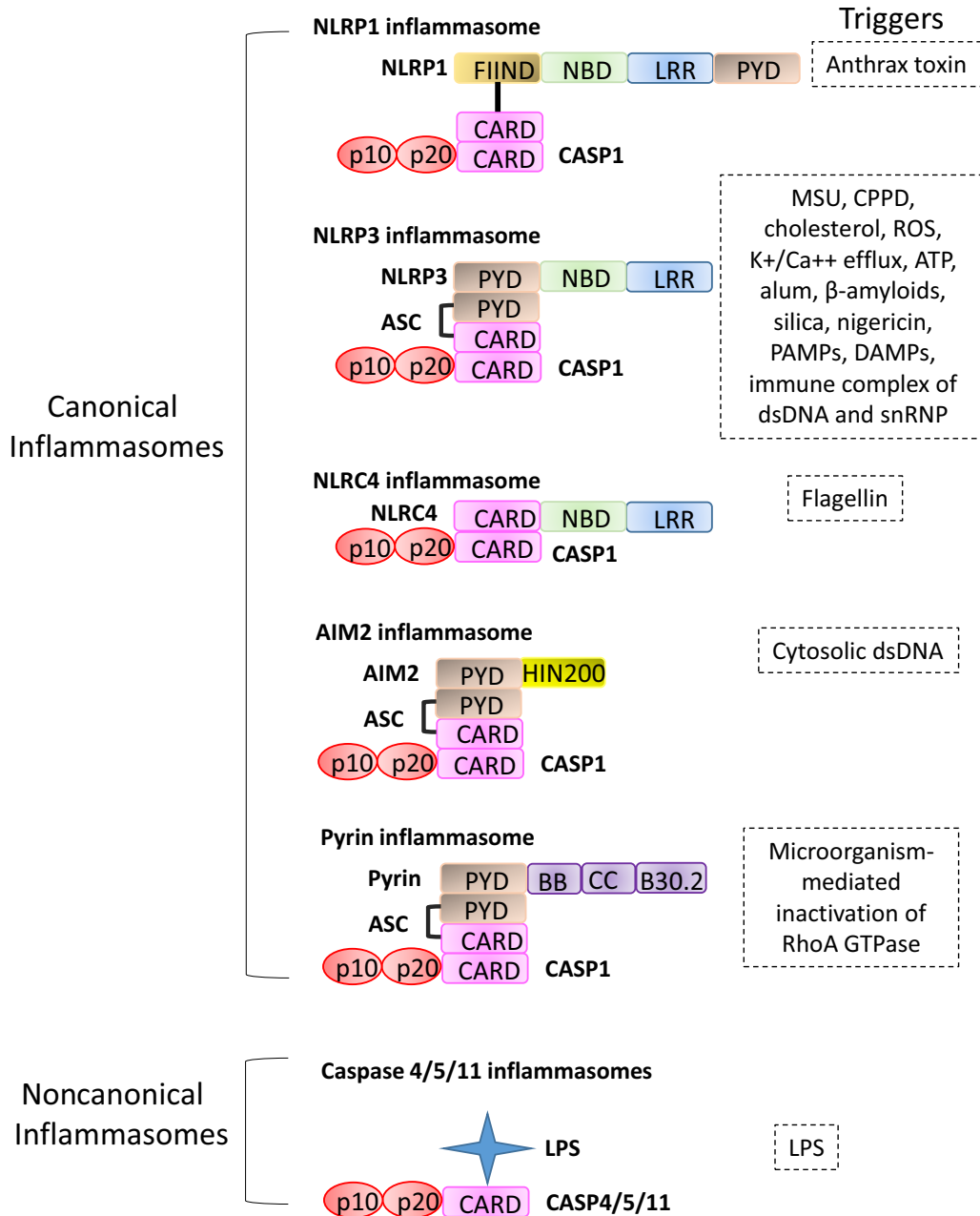


Figure 1. Structures and triggers of canonical and noncanonical inflammasomes. Canonical inflammasomes that contain caspase 1 can be classified into distinct types based on the presence of the sensor proteins NLRP1, NLRP3, NLRC4, AIM2, or pypin, which recognize different triggers. Noncanonical inflammasomes that contain caspase 4 or 5 in humans and caspase 11 in mice can directly interact with the lipid A moiety of lipopolysaccharides (LPS). Triggers of individual inflammasomes are shown. FIIND = function to find domain; NBD = nucleotide-binding domain; LRR = leucine-rich repeat; PYD = pypin domain; CARD = caspase activation and recruitment domain; p10 = caspase 1 p10; CASP1 = caspase 1; MSU = monosodium urate monohydrate; CPPD = calcium pyrophosphate dihydrate; ROS = reactive oxygen species; PAMPs = pathogen-associated molecular patterns; DAMPs = damage-associated molecular patterns; dsDNA = double-stranded DNA; snRNP = small nuclear RNP; HIN200 = hematopoietic interferon-inducible nuclear protein 200; BB = bBox zinc-finger domain; CC = coiled coin domain; B30.2 = B30.2 domain.

typically comprises 3 components: 1) a PRR sensing PAMPs or DAMPs, 2) procaspase 1, and 3) an adaptor molecule like ASC that links the sensor and procaspase 1 (1,2). Based on the types of PRRs present in individual inflammasomes, they can be classified into nucleotide-binding oligomerization domain–like receptor (NLR), absent in melanoma 2 (AIM2)–like receptor (ALR), and pyrin inflammasomes (Figure 1). The NLR inflammasome family members, which include NLRP1, NLRP3, and NLRC4, have a central nucleotide-binding domain, a C-terminal leucine-rich repeat, and a pyrin or caspase activation and recruitment domain (CARD) (1,2). PRRs of individual inflammasomes can sense distinct stimuli (Figure 1). AIM2 recognizes intracytoplasmic DNA, whereas NLRP3 can be triggered by PAMPs, DAMPs, and even environmental chemicals (e.g., silica) (1,2). While caspase 1–containing inflammasomes are classified as canonical inflammasomes, noncanonical inflammasomes containing caspase 4 or 5 and caspase 11 are observed in humans and mice, respectively. The CARD motif of caspases 4, 5, and 11 can directly bind with the lipid A moiety of intracellular lipopolysaccharide, leading to the activation of these caspases and subsequent secretion of IL-1 β and IL-18 (2,3).

The best-characterized inflammasome is the NLRP3 inflammasome (3). While intracellular levels of ASC and procaspase 1 are stable, the quantity of NLRP3 present in resting myeloid cells (e.g., human monocytes) is insufficient to allow activation in response to stimuli, suggesting that NLRP3 is a limiting factor regulating NLRP3 inflammasome activation (3–5). NLRP3 that is up-regulated by PRRs via active NF- κ B can be regulated by post-translational mechanisms including phosphorylation and ubiquitination (3). Reactive oxygen species (ROS), K⁺ efflux, ATP, and lysosomal rupture can mediate the activation of the NLRP3 inflammasome (3). High levels of extracellular ATP also result in K⁺ efflux by activating the P2X purinoceptor 7 (P2X₇ purinoceptor) channel. Many NLRP3 triggers increase mitochondrial ROS production, and NLRP3 inflammasome activation is inhibited by preincubation with some antioxidants (3). Never in mitosis gene–related protein kinase 7 plays an essential role in the formation of the NLRP3 inflammasome in murine macrophages by directly interacting with NLRP3 (6). Bruton's tyrosine kinase (BTK), which is involved in B cell receptor and TLR signaling, physically interacts with ASC and NLRP3, and inhibiting BTK suppresses NLRP3 inflammasome activation (7). These findings highlight the fundamental role of the inflammasome in handling attacks and dangers posed to the host through interacting with multiple cellular and molecular pathways.

The inflammasome and rheumatic diseases

Inflammasomes regulate the maturation and secretion of IL-1 β . IL-1 β has pleiotropic effects on multiple immune and nonimmune cells and is responsible for many clinical manifestations in autoimmune and inflammatory diseases (8). As an endogenous pyrogen, IL-1 β induces fever, which is frequently seen in rheumatic diseases. IL-1 β serves as an upstream regulator of innate and adaptive

immune responses by promoting the production of other inflammatory cytokines, such as IL-6, tumor necrosis factor (TNF), and IL-17 (8,9). Similarly, IL-18 is known to enhance interferon- γ (IFN γ) production by Th1 cytokines. Thus, it is natural to consider the potential role of the inflammasome in inflammation and tissue damage in rheumatic diseases. A body of evidence supporting this notion has accumulated over a decade through human and animal studies.

Several molecules known to be causative of or pathogenic for rheumatic diseases can activate inflammasomes, leading to the production of IL-1 β and IL-18. These include monosodium urate monohydrate and calcium pyrophosphate dihydrate (CPPD) crystals, which are responsible for gout and pseudogout, respectively (10), as well as double-stranded DNA (dsDNA) and U1 small nuclear RNP (U1 snRNP)–containing lupus immune complexes (Figure 2) (11,12). Also, monocytes and macrophages in patients with rheumatic diseases, especially SLE, have increased expression of inflammasome components and/or enhanced inflammasome activation (13,14), suggesting the existence of an intrinsic alteration in the intracellular inflammasome pathways. Of note, some polymorphisms of inflammasome-related genes have been shown to be associated with susceptibility, severity, and/or treatment response in rheumatic diseases, including SLE and RA (15–20). Improvement in disease activity was observed in murine models of SLE, RA, crystal-induced arthropathies, and Sjögren's syndrome (SS) when inflammasome activation was targeted genetically or chemically (see details below). In addition to the immune system, dysregulated inflammasome activation in rheumatic diseases likely affects multiple organ systems, including the kidneys, lungs, eyes, and cardiovascular system, contributing to morbidity and mortality (21,22). The links between inflammasomes and individual rheumatic diseases are discussed below.

The inflammasome and SLE

Possible dysregulation of inflammasome activation in lupus was identified as early as 3 decades ago. Those studies reported increased *IL1b* gene expression and IL-1 β production in the kidneys of lupus-prone mice and from human monocytes, respectively (23,24). Although the exact mechanisms for these findings were not clear at that time, the discovery of the inflammasome and its role in IL-1 β secretion revealed new insights into the pathogenesis of lupus. Unique to SLE, autoimmune features, such as immune complexes, can provoke the inflammatory response. Immune complexes containing dsDNA or U1 snRNP can activate the NLRP3 inflammasome in human monocytes, leading to the production of IL-1 β and IL-18 (11,12). Several pathways, including ROS, K⁺ efflux, and TLRs, are involved in this phenomenon, as evidenced by the fact that inhibition of ROS production, K⁺ efflux, and TLR activation suppressed cytokine production. IL-1 β released from such activated monocytes enhanced Th17 responses, which are increased in lupus, supporting the notion that inflammasome activation is implicated in dysregulated adaptive

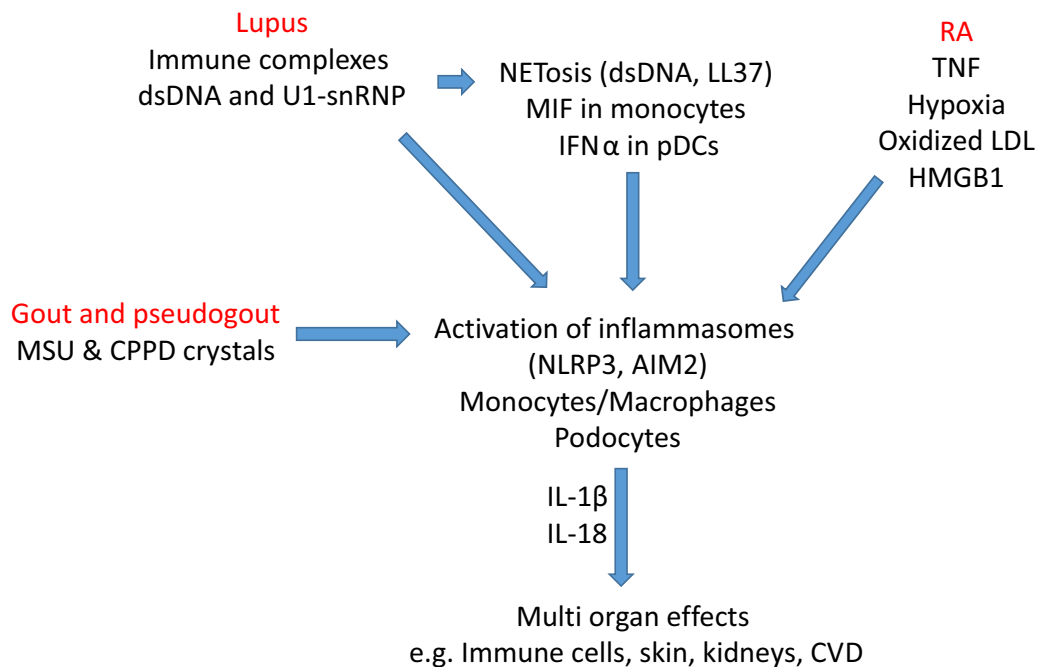


Figure 2. Schematic representation of the mechanisms of inflammasome activation in rheumatic diseases. Lupus immune complexes of double-stranded DNA (dsDNA) and U1 small nuclear RNP (U1 snRNP) affect inflammasome activation via inducing NETosis, macrophage migration inhibitory factor (MIF) in monocytes, and interferon- α (IFN α) in plasmacytoid dendritic cells (pDCs). In rheumatoid arthritis (RA), tumor necrosis factor (TNF), hypoxia, oxidized low-density lipoprotein (LDL), and high mobility group box chromosomal protein 1 (HMGB-1) affect NLRP3 expression and inflammasome activation. In gout and pseudogout, monosodium urate monohydrate (MSU) and calcium pyrophosphate dihydrate (CPPD) crystals activate the NLRP3 inflammasome. Monocytes, macrophages, and podocytes with activated inflammasome produce interleukin-1 β (IL-1 β) and IL-18, leading to inflammation and tissue damage in multiple organ systems. CVD = cardiovascular disease.

immune responses in lupus (12). Confirming this chronic inflammasome activation, patients with SLE demonstrate increased circulatory levels of IL-1 β and IL-18 (22,25).

Neutrophil extracellular traps (NETs) that contain self-DNA and other molecules such as the antibacterial protein LL-37 play a role in the pathogenesis of lupus. Both NETs and LL-37 activate the inflammasome in human and murine macrophages, leading to the release of IL-1 β and IL-18 (Figure 2) (13). The released IL-18 stimulates NETosis in human neutrophils, suggesting a feedforward inflammatory loop involving NET and inflammasome activation. Inflammasome activation and IL-18 production can be responsible in part for vascular dysfunction in SLE through impairment of vascular repair mechanisms; caspase 1 inhibition and IL-18 neutralization have been shown to improve dysfunctional SLE endothelial progenitor cell differentiation (22). Also, patients with SLE had increased AIM2 expression correlating with disease activity, and blocking AIM2 expression in lupus-prone mice reduced disease activity (26). The association of *IL1B*, *IL18*, and *NLRP1* polymorphisms with SLE has been demonstrated in patients of different ethnic backgrounds, supporting the possible genetic implication of certain inflammasome-related genes in SLE (15–17).

Monocytes and macrophages from patients with SLE appear to be more prone to inflammasome activation (13,14). Patients with SLE have enhanced inflammasome activation in monocyte-

derived macrophages upon NET and LL-37 stimulation (13). Also, freshly isolated monocytes from patients with SLE demonstrate increased expression of *NLRP3*, *AIM2*, and *CASP1* (14). The expression of these genes is correlated with IFN scores, and IFN α enhances caspase 1 expression via IFN regulatory factor 1 (Figure 2). These findings support the notion of a positive interaction between type I IFN and the inflammasome in lupus through priming of monocytes for robust inflammasome activation. Indeed, patients with SLE have increased levels of caspase 1 activation in monocytes that correlate with serum levels of IL-1 β , anti-dsDNA antibodies, and disease activity (25). Also, ATP-induced IL-1 β production has been shown to be increased in the macrophages of patients with SLE (27). Recently, the role of macrophage migration inhibitory factor (MIF) in up-regulating NLRP3 expression was demonstrated in human monocytes stimulated with the U1 snRNP lupus immune complex (4). Upon exposure to the latter, human monocytes produced MIF, and blocking MIF binding to its receptor CD74 suppressed NLRP3 expression and subsequent caspase 1 activation (4). The expression levels of MIF and CD74 correlated at the single cell level, supporting the autocrine and paracrine effects of MIF in regulating NLRP3. Of note, a separate study showed that MIF was implicated in activating the NLRP3 inflammasome through its interaction with NLRP3 (5). These findings support the notion that MIF plays a role in lupus pathogenesis, which is

further substantiated by human and animal studies showing the relationship of MIF genotypes to SLE and improvement in murine lupus upon blocking MIF, respectively (28,29).

Consistent with the results of human studies, animal studies indicate a pathogenic role for inflammasomes in lupus. In one study, mice lacking caspase 1 were protected against autoantibody production, type I IFN response, and glomerulonephritis upon pristane challenge (30). In the same lupus animal model, caspase 1 deficiency reduced vascular dysfunction, which is a major contributor to mortality in human lupus (30). Also, *Nlrp3-R258W* mice carrying the gain-of-function mutation exhibited significantly higher mortality and renal damage upon pristane challenge (31). Lupus-prone *MRL/lpr* mice have been shown to have increased expression of P2X₇, NLRP3, ASC, active caspase 1, and IL-1 β in the kidneys (32). Blockade of P2X₇ purinoceptor suppressed lupus nephritis in *MRL/lpr* mice by inhibiting NLRP3 inflammasome activation with decreased IL-1 β and IL-17 levels (32).

A recent study showed no effect of IL-1 β deficiency on lupus nephritis in NZM2328 mice injected with the TLR-7 agonist R848 (33). Given the role of inflammasomes in regulating multiple immune molecules, including IL-18, it is likely that targeting only IL-1 β may not be sufficient to suppress disease activity. The serine/threonine kinase glycogen synthase kinase 3 β (GSK-3 β) is a positive regulator of NF- κ B activation. Thiadiazolidinone 8 (TDZD-8), a selective inhibitor of GSK-3 β , inhibited caspase 1 activation and IL-1 β production and reduced anti-dsDNA antibody levels and renal disease in a study using *MRL/lpr* and NZB \times NZW F1 mice (34). This finding could be related to the suppressive effect of TDZD-8 on NF- κ B activation, which up-regulates NLRP3 expression (35). A20, encoded by TNF-induced protein 3, is a potent negative regulator of inflammation, and its gene polymorphisms are associated with autoimmunity, including SLE. A20 was found to suppress NF- κ B and caspase 1 activity (36), and its overexpression reduced nephritis in mice with pristane-induced lupus by inhibiting NF- κ B and NLRP3 (37).

The NLRP3 inflammasome contributes to the development of proteinuria in lupus nephritis by affecting podocyte function. NLRP3 inflammasome activation was detected in podocytes from patients with lupus nephritis and lupus-prone mice, and the selective NLRP3 inhibitor MCC950 ameliorated proteinuria and renal histologic lesions in lupus-prone mice (21). Pim-1, a member of the Pim family of serine/threonine kinases, promotes NLRP3 inflammasome activation in human podocytes in response to anti-dsDNA antibody-positive serum by increasing the intracellular calcium concentration, which regulates NLRP3 inflammasome activation (38). In contrast to the results of most studies, a few studies have shown decreased levels of inflammasome activation or related molecules in lupus. NZB mice that develop autoimmune hemolytic anemia express high levels of the AIM2 antagonist p202 and an *NLRP3* gene mutation, leading to impaired IL-1 β production, while lupus-prone (NZB \times NZW)F1 mice have been shown to have reduced NLRP3 and AIM2 inflammasome responses (39). Also, lupus-like autoimmunity became more

severe in C57BL/6-*lpr/lpr* mice deficient in *Nlrp3* and *Asc* (40). Another study identified decreased expression of *NLRP3* and *ASC* genes in peripheral blood mononuclear cells (PBMCs) from lupus patients but increased expression of *CASP1*, *IL1B*, and *IL18* in PBMCs (41). Nevertheless, a large set of animal and human data clearly support the notion that inflammasomes, especially the NLRP3 inflammasome, play a role in the pathogenesis of lupus.

The inflammasome and RA

Joint inflammation is initiated by inflammasome activation, as is seen in crystal arthropathies such as gout and CPPD crystal deposition disease. In RA, which is characterized by chronic inflammation and synovial activation that results in bony erosions, the role of the inflammasome may be of a more indirect nature. Interest in inflammasome biology in RA is longstanding, as anakinra, a soluble IL-1 receptor antagonist, was the first biologic agent approved for the treatment of RA. The success of anakinra as an RA therapy was modest at best (42); thus, the links between the inflammasome and RA continue to be a subject of debate and a topic for further research.

Genetic evidence provides hints, but no definitive links between RA and inflammasome biology. Polymorphisms and subsequent overexpression of NLRP1 have been linked to an increased risk of RA (18). Minor polymorphisms in both NLRP3 and CARD-8 (an inflammasome-regulating protein) have been shown to be associated with seropositivity and increased disease severity (43). Cytokine polymorphisms have not been definitive either. Polymorphisms of IL-1 β may be associated with the development of RA in certain ethnic populations (19), and IL-18 polymorphisms may also increase the risk of RA (20). Overall, the relationship between RA and the inflammasome may reflect the inflammatory activity in the joint itself, rather than a true genetic etiology of the disease.

Data from human studies support the notion that the inflammasome plays a role in RA. Expression of inflammasome-associated proteins in the joint is increased but varies with the cell population analyzed. Endothelial and inflammatory cells in the RA synovium express all components needed for inflammasome activation, but synovial fibroblasts do not express NLRP3 (44). Importantly, many RA-associated joint changes prime for inflammasome activation. TNF up-regulates key components of the inflammasome (45), partially through transforming growth factor β -activated kinase 1. Hypoxia, a feature of the inflamed synovium, induces IL-1 β protein and NLRP3 expression (46). Oxidized low-density lipoprotein, a modified lipid that is increased in RA patients, primes for inflammasome activation in macrophages, which results in increased IL-1 β release (47). High mobility group box chromosomal protein 1, an alarmin that is associated with the development of RA, primes for inflammasome activation as well (48). All of these features of RA lead to a state where the inflammasome is ready for activation (Figure 2).

Adaptive immune responses in RA are also regulated by the inflammasome. T cells from RA patients express elevated levels of active caspase 1 (49,50), which can be triggered by oxidized and nonoxidized mitochondrial DNA. Intriguingly, this inflammasome activation contributes to Th17 skewing in vitro (50). These data suggest that T cell inflammasome activation may also be an important target for RA treatment.

The cytokines produced by inflammasome activation contribute to the inflammatory phenotype in the RA joint. An imbalance of IL-1 β versus IL-1 receptor antagonist production was noted nearly 25 years ago in human RA synovial explants (51). IL-1 β activates synovial fibroblasts and induces the production of TNF, IL-6, and matrix metalloproteinases (52). IL-1 α , which is active in its full-length and 18-kd cleaved (by caspase 1) mature form, also has inflammatory effects on the joint. IL-1 α can promote the maturation of cathepsin B and cathepsin S and works in synergy to increase chondrocyte cathepsin B activation and secretion (52).

Murine models support the notion that the inflammasome plays a role in inflammatory arthritis, but most research has focused on infection or gout-related arthritis. In collagen-induced arthritis (CIA), a murine model with features of RA, inhibition of NLRP1 inflammasome activation is protective (53). Inhibition of P2X₇ purinoceptor is also protective in a rat streptococcal wall model of arthritis (54). Genetic data have not supported a role for either caspase 1 or NLRP3 in CIA, as absence of either protein was not protective; however, a functional ASC molecule was required for disease activity (55). Inhibitor data, however, have demonstrated a role for NLRP3 in CIA, since inhibition of NLRP3 via MCC950 is protective in a CIA model (56). Another orally available NLRP3 inhibitor, OLT1177, suppresses inflammation in zymosan-induced arthritis (57). Myeloid-specific deletion of *A20/Tnfrap3* causes erosive polyarthritis, similar to RA. In this model, NLRP3, caspase 1, and the IL-1 receptor are also required for full disease expression (58). A comparison of the role of the inflammasome in RA and its role in SLE is shown in Table 1.

The inflammasome and other rheumatic autoimmune diseases

Sjögren's syndrome. SS incorporates pathologic and clinical features of both SLE and RA; thus, it is not surprising to note that the inflammasome has been implicated in its pathogenesis as well. Circulating levels of IL-1 β and IL-18, as well as inflammasome components such as ASC, are elevated in SS patients (especially those with severe SS) compared to healthy controls (59,60). In addition, increased expression of NLRP3 inflammasome components is detectable in SS salivary gland macrophages in situ (59). Both AIM2 and NLRP3 inflammasomes may be involved in SS, as stimulation with DNA or NLRP3 agonists induces greater IL-1 β production in SS monocytes than control monocytes. In a murine model of autoimmune exocrinopathy, inhibition of P2X₇ purinoceptor is protective against induction of salivary gland inflammation

Table 1. Comparison of inflammasome involvement in SLE and RA*

	SLE	RA
Disease-associated polymorphisms	<i>NLRP1, IL1B, IL18</i>	<i>NLRP3, NLRP1, CARD8, IL1B, IL18</i>
Inflammasomes involved	NLRP1?, NLRP3, AIM2	NLRP3, NLRP1?
Murine models that improve with inflammasome inhibition	PIA, MRL/lpr, (NZB \times NZW)F1, NZM2328	CIA, A20/ <i>Tnfrap3</i> myeloid deletion
Triggers to prime/activate inflammasome response	Type I IFNs, MIF, dsDNA, RNP immune complexes	TNF, IL-6, Oxidized LDL, HMGB-1
Important pathogenic cells	Podocytes, monocytes, endothelial cells	Macrophages, endothelial cells

* SLE = systemic lupus erythematosus; RA = rheumatoid arthritis; PIA = pristane-induced arthritis; CIA = collagen-induced arthritis; type I IFNs = type I interferons; MIF = macrophage migration inhibitory factor; dsDNA = double-stranded DNA; TNF = tumor necrosis factor; IL-6 = interleukin-6; LDL = low-density lipoprotein; HMGB-1 = high mobility group box chromosomal protein 1.

(61). In addition, ocular dryness (as seen in primary or secondary SS) has been documented as a trigger for the NLRP3 inflammasome in murine models (62).

Celiac disease. IL-18 signaling has been linked to the development of celiac disease through genome-wide association studies (63), and this link has been validated in both pediatric and adult-onset celiac disease (64). There are data to support a role for inflammasome activation in both disruption of epithelial barriers and in more generalized inflammation in response to gluten. Similar to its inflammasome-promoting effects in SLE monocytes and endothelial cells (14,22), IFN can stimulate intestinal epithelial cells to promote inflammasome activation and disruption of epithelial barriers (65). In addition, circulating monocytes from patients with celiac disease mount a more robust NLRP3-dependent inflammatory response to gluten peptides than monocytes from healthy controls (66). Further research is required to determine whether the inflammasome is pathogenically activated in patients with celiac disease, contributes to disease phenotypes, and should be a target for treatment.

The inflammasome and complications of autoimmunity

Other complications of autoimmune disease are also influenced by inflammasome activation. NLRP3 may be involved in lung fibrosis, and increased circulating levels of IL-18 have been identified as a potential biomarker for interstitial lung disease in RA patients (67). Increased circulating levels of IL-1 β have been documented in patients with severe scleritis (68), and importantly, a recent small pilot trial has shown efficacy for anakinra in the

treatment of refractory scleritis associated with systemic inflammatory disorders (69). Many autoimmune diseases also lead to an increased risk of cardiovascular disease, and the inflammasome contributes to this risk through its known effects on plaque progression, destabilization of plaque (for review, see ref. 70), and promotion of endothelial dysfunction.

Therapeutic targeting of the inflammasome

Interest in inflammasome inhibition is high for many diseases. This has been most pronounced for the plethora of autoinflammatory syndromes linked to genetic causes of aberrant inflammasome activation. Pharmaceutical advances in cytokine and inflammasome inhibitors are beneficial for patients with autoimmune diseases, and they provide tools, as the science evolves, to link inflammasome activity to autoimmunity. Therapies can be classified into two categories: cytokine inhibition to block the end result of inflammasome activity, or inhibition of the inflammasome itself, which may be important for cytokine- and noncytokine-related functions of the inflammasome that contribute to disease.

Cytokine inhibition. IL-1 antagonism has been a long-standing biologic approach to the management of inflammatory diseases (for comprehensive review of drugs, see ref. 71) (Table 2). New developments in cytokine blockade include several drugs. Lutikizumab, which is a dual IL-1 α and IL-1 β antibody, is being evaluated in several diseases including erosive hand osteoarthritis (OA) (72) and knee OA (73). While trial results do not support use of IL-1 blockade in OA, the drug may have other indications. Bermekimab is a new human IL-1 α antibody that is in trials for cancer therapy (74). IL-18 inhibition is available via the drug tadekinig alfa, which is a recombinant human IL-18 binding protein that can bind IL-18 and inhibit its function. Tadekinig alfa is not approved by

the Food and Drug Administration, but it has orphan designation for the treatment of hemophagocytic lymphohistiocytosis as well as Breakthrough Therapy designation for NLRP4 macrophage activation syndrome and X-linked inhibitor of apoptosis protein deficiency (71). In addition, tadekinig alfa is being studied in adult-onset Still's disease (75).

Inflammasome inhibition. As research has progressed, inflammasome inhibition has been identified as a mechanism for several commonly used medications in the treatment of rheumatic diseases. Colchicine interrupts inflammasome activation by interfering with microtubule assembly (76). Hydroxychloroquine interferes with immune complex-triggered activation of the inflammasome in monocytes (11,12). Omega-3 fatty acids, which have been shown to be beneficial in RA (77) and possibly lupus (78), inhibit inflammasome activation through numerous mechanisms (79,80). Thalidomide, which has off-label therapeutic benefit in cutaneous lupus (81), inhibits inflammasome activation via repression of caspase 1 (82). Even nonsteroidal antiinflammatory drugs have been shown to have caspase-inhibiting properties. Caspase 4, but not caspase 1, is inhibited by ketorolac and ibuprofen (83). Whether inflammasome inhibition has direct links to the efficacy of these drugs in the autoimmune diseases they are used to treat remains to be determined.

Direct inhibitors of inflammasome activation are also being developed. MCC950, a specific inhibitor of the NLRP3 inflammasome (although the exact target has not been localized), inhibits inflammasome activation and protects against a myriad of inflammatory and autoimmune diseases in many murine models, including murine lupus nephritis (21) and CIA (56). CY-09 is another small molecule that binds to the ATP-binding motif of NLRP3 and can block inflammasome activation in murine models of type 2 diabetes mellitus and cryopyrin-associated periodic

Table 2. Strategies for targeting the inflammasome*

Drug	Mechanism	Target	Disease
Cytokine neutralization			
Anakinra	Soluble IL-1Ra	IL-1 α and IL-1 β	RA, CAPS, gout†
Canakinumab	Neutralizing IL-1 β antibody	IL-1 β	CAPS, colchicine-resistant FMF, MKD, TRAPS, systemic JIA
Rilonacept	Soluble IL-1R1/IL-1RACp	IL-1 α and IL-1 β	CAPS
Lutikizumab	Dual IL-1 α and IL-1 β antibody	IL-1 α and IL-1 β	Not yet FDA approved
Bermekimab	IL-1 α antibody	IL-1 α	Not FDA approved
Tadekinig alfa	Soluble IL-18 binding protein	IL-18	HLH,† MAS,† XIAP deficiency†
Inflammasome inhibition			
Colchicine	Interferes with microtubule assembly	NLRP3	Gout
Thalidomide	Inhibits caspase 1	Caspase 1	CLE
CY-09	Binds ATP-binding motif	NLRP3	Not FDA approved
MCC950	Mechanism unclear	NLRP3	Not FDA approved
β -sulfonyl nitrile	Inhibits inflammasome assembly	NLRP3	Not FDA approved

* IL-1Ra = interleukin-1 receptor antagonist; RA = rheumatoid arthritis; CAPS = cryopyrin-associated periodic syndromes; FMF = familial Mediterranean fever; MKD = mevalonate kinase deficiency; TRAPS = tumor necrosis factor receptor-associated periodic syndrome; JIA = juvenile idiopathic arthritis; IL-1RACp = IL-1R accessory protein; HLH = hemophagocytic lymphohistiocytosis; MAS = macrophage activation syndrome; XIAP = X-linked inhibitor of apoptosis protein; CLE = cutaneous lupus erythematosus; † Not approved by the Food and Drug Administration (FDA) for this indication.

syndromes (84). OLT1177, a β -sulfonyl nitrile compound, inhibits assembly of the NLRP3 inflammasome and has been shown to exert beneficial effects on zymosan-induced murine arthritis (57). Small molecule inhibitors of other inflammasomes have not yet been identified. Human trials of MCC950 or CY-09 have not been developed as of yet. Other methods of blocking inflammasome activation, including inhibiting upstream activators such as NF- κ B or increasing negative regulators such as Hsp70 (85), also work in murine models, but human trials are still pending.

Conclusions

The accelerating pace of inflammasome research has demonstrated important roles for inflammasome activation in many diseases, both autoinflammatory and autoimmune (Figure 2). While single cytokine inhibition of IL-1 β may not be overwhelmingly effective in autoimmune syndromes, further studies into the role of IL-18 blockade and general inflammasome inhibition may identify effective treatment strategies for diseases such as RA or SLE or may offer insight into mechanisms by which resulting complications of autoimmunity can be averted. Further research will continue to shed light on this ubiquitous inflammatory pathway in diseases of the immune system.

AUTHOR CONTRIBUTIONS

Drs. Kahlenberg and Kang drafted the article, revised it critically for important intellectual content, and approved the final version to be published.

REFERENCES

- Guo H, Callaway JB, Ting JP. Inflammasomes: mechanism of action, role in disease, and therapeutics. *Nat Med* 2015;21:677–87.
- Sharma D, Kanneganti TD. The cell biology of inflammasomes: mechanisms of inflammasome activation and regulation. *J Cell Biol* 2016;213:617–29.
- Mangan MS, Olhava EJ, Roush WR, Seidel HM, Glick GD, Latz E. Targeting the NLRP3 inflammasome in inflammatory diseases. *Nat Rev Drug Discov* 2018;17:588–606.
- Shin MS, Kang Y, Wahl ER, Park HJ, Lazova R, Leng L, et al. Macrophage migration inhibitory factor regulates U1 small nuclear RNP immune complex-mediated activation of the NLRP3 inflammasome. *Arthritis Rheumatol* 2019;71:109–20.
- Lang T, Lee JP, Elgass K, Pinar AA, Tate MD, Aitken EH, et al. Macrophage migration inhibitory factor is required for NLRP3 inflammasome activation. *Nat Commun* 2018;9:2223.
- He Y, Zeng MY, Yang D, Motro B, Núñez G. NEK7 is an essential mediator of NLRP3 activation downstream of potassium efflux [letter]. *Nature* 2016;530:354–7.
- Ito M, Shichita T, Okada M, Komine R, Noguchi Y, Yoshimura A, et al. Bruton's tyrosine kinase is essential for NLRP3 inflammasome activation and contributes to ischaemic brain injury. *Nat Commun* 2015;6:7360.
- Dinarello CA. Interleukin 1 and interleukin 18 as mediators of inflammation and the aging process. *Am J Clin Nutr* 2006;83:447S–55S.
- Lee WW, Kang SW, Choi J, Lee SH, Shah K, Eynon EE, et al. Regulating human Th17 cells via differential expression of IL-1 receptor. *Blood* 2010;115:530–40.
- Martinon F, Pétrilli V, Mayor A, Tardivel A, Tschopp J. Gout-associated uric acid crystals activate the NALP3 inflammasome. *Nature* 2006;440:237–41.
- Shin MS, Kang Y, Lee N, Kim SH, Kang KS, Lazova R, et al. U1-small nuclear ribonucleoprotein activates the NLRP3 inflammasome in human monocytes. *J Immunol* 2012;188:4769–75.
- Shin MS, Kang Y, Lee N, Wahl ER, Kim SH, Kang KS, et al. Self double-stranded (ds)DNA induces IL-1 β production from human monocytes by activating NLRP3 inflammasome in the presence of anti-dsDNA antibodies. *J Immunol* 2013;190:1407–15.
- Kahlenberg JM, Carmona-Rivera C, Smith CK, Kaplan MJ. Neutrophil extracellular trap-associated protein activation of the NLRP3 inflammasome is enhanced in lupus macrophages. *J Immunol* 2013;190:1217–26.
- Liu J, Berthier CC, Kahlenberg JM. Enhanced inflammasome activity in systemic lupus erythematosus is mediated via type I interferon-induced up-regulation of interferon regulatory factor 1. *Arthritis Rheumatol* 2017;69:1840–9.
- Pontillo A, Girardelli M, Kamada AJ, Pancotto JA, Donadi EA, Crovella S, et al. Polymorphisms in inflammasome genes are involved in the predisposition to systemic lupus erythematosus. *Autoimmunity* 2012;45:271–8.
- Umare V, Pradhan V, Rajadhyaksha A, Ghosh K, Nadkarni A. Predisposition of IL-1 β (-511 C/T) polymorphism to renal and hematologic disorders in Indian SLE patients. *Gene* 2018;641:41–5.
- Song GG, Choi SJ, Ji JD, Lee YH. Association between interleukin-18 polymorphisms and systemic lupus erythematosus: a meta-analysis. *Mol Biol Rep* 2013;40:2581–7.
- Sui J, Li H, Fang Y, Liu Y, Li M, Zhong B, et al. NLRP1 gene polymorphism influences gene transcription and is a risk factor for rheumatoid arthritis in Han Chinese. *Arthritis Rheum* 2012;64:647–54.
- Lee YH, Bae SC. Associations between interleukin-1 and IL-1 receptor antagonist polymorphisms and susceptibility to rheumatoid arthritis: a meta-analysis. *Cell Mol Biol (Noisy-le-grand)* 2015;61:105–11.
- Li LL, Deng XF, Li JP, Ning N, Hou XL, Chen JL. Association of IL-18 polymorphisms with rheumatoid arthritis: a meta-analysis. *Genet Mol Res* 2016;15.
- Fu R, Guo C, Wang S, Huang Y, Jin O, Hu H, et al. Podocyte activation of NLRP3 inflammasomes contributes to the development of proteinuria in lupus nephritis. *Arthritis Rheumatol* 2017;69:1636–46.
- Kahlenberg JM, Thacker SG, Berthier CC, Cohen CD, Kretzler M, Kaplan MJ. Inflammasome activation of IL-18 results in endothelial progenitor cell dysfunction in systemic lupus erythematosus. *J Immunol* 2011;187:6143–56.
- Boswell JM, Yui MA, Burt DW, Kelley VE. Increased tumor necrosis factor and IL-1 β gene expression in the kidneys of mice with lupus nephritis. *J Immunol* 1988;141:3050–4.
- Aotsuka S, Nakamura K, Nakano T, Kawakami M, Goto M, Okawa-Takatsuji M, et al. Production of intracellular and extracellular interleukin-1 α and interleukin-1 β by peripheral blood monocytes from patients with connective tissue diseases. *Ann Rheum Dis* 1991;50:27–31.
- Zhang H, Fu R, Guo C, Huang Y, Wang H, Wang S, et al. Anti-dsDNA antibodies bind to TLR4 and activate NLRP3 inflammasome in lupus monocytes/macrophages. *J Transl Med* 2016;14:156.
- Zhang W, Cai Y, Xu W, Yin Z, Gao X, Xiong S. AIM2 facilitates the apoptotic DNA-induced systemic lupus erythematosus via arbitrating macrophage functional maturation. *J Clin Immunol* 2013;33:925–37.
- Yang CA, Huang ST, Chiang BL. Sex-dependent differential activation of NLRP3 and AIM2 inflammasomes in SLE macrophages. *Rheumatology (Oxford)* 2015;54:324–31.

28. Sreih A, Ezzeddine R, Leng L, LaChance A, Yu G, Mizue Y, et al. Dual effect of the macrophage migration inhibitory factor gene on the development and severity of human systemic lupus erythematosus. *Arthritis Rheum* 2011;63:3942–51.
29. Leng L, Chen L, Fan J, Greven D, Arjona A, Du X, et al. A small-molecule macrophage migration inhibitory factor antagonist protects against glomerulonephritis in lupus-prone NZB/NZW F1 and MRL/lpr mice. *J Immunol* 2011;186:527–38.
30. Kahlenberg JM, Yalavarthi S, Zhao W, Hodgins JB, Reed TJ, Tsuji NM, et al. An essential role of caspase 1 in the induction of murine lupus and its associated vascular damage. *Arthritis Rheumatol* 2014;66:152–62.
31. Lu A, Li H, Niu J, Wu S, Xue G, Yao X, et al. Hyperactivation of the NLRP3 inflammasome in myeloid cells leads to severe organ damage in experimental lupus. *J Immunol* 2017;198:1119–29.
32. Zhao J, Wang H, Dai C, Wang H, Zhang H, Huang Y, et al. P2X₇ blockade attenuates murine lupus nephritis by inhibiting activation of the NLRP3/ASC/caspase 1 pathway. *Arthritis Rheum* 2013;65:3176–85.
33. Wolf SJ, Theros J, Reed TJ, Liu J, Grigorova IL, Martínez-Colón G, et al. TLR7-mediated lupus nephritis is independent of type I IFN signaling. *J Immunol* 2018;201:393–405.
34. Zhao J, Wang H, Huang Y, Zhang H, Wang S, Gaskin F, et al. Lupus nephritis: glycogen synthase kinase 3 β promotion of renal damage through activation of the NLRP3 inflammasome in lupus-prone mice. *Arthritis Rheumatol* 2015;67:1036–44.
35. Bauernfeind FG, Horvath G, Stutz A, Alnemri ES, MacDonald K, Speert D, et al. Cutting edge: NF- κ B activating pattern recognition and cytokine receptors license NLRP3 inflammasome activation by regulating NLRP3 expression. *J Immunol* 2009;183:787–91.
36. Duong BH, Onizawa M, Osés-Prieto JA, Advincula R, Burlingame A, Malynn BA, et al. A20 restricts ubiquitination of pro-interleukin-1 β protein complexes and suppresses NLRP3 inflammasome activity. *Immunity* 2015;42:55–67.
37. Li M, Shi X, Qian T, Li J, Tian Z, Ni B, et al. A20 overexpression alleviates pristane-induced lupus nephritis by inhibiting the NF- κ B and NLRP3 inflammasome activation in macrophages of mice. *Int J Clin Exp Med* 2015;8:17430–40.
38. Fu R, Xia Y, Li M, Mao R, Guo C, Zhou M, et al. Pim-1 as a therapeutic target in lupus nephritis. *Arthritis Rheumatol* 2019;71:1308–18.
39. Thygesen SJ, Takizawa KE, Robertson AA, Sester DP, Stacey KJ. Compromised NLRP3 and AIM2 inflammasome function in autoimmune NZB/W F1 mouse macrophages. *Immunol Cell Biol* 2019;97:17–28.
40. Lech M, Lorenz G, Kulkarni OP, Grosser MO, Stigrot N, Darisipudi MN, et al. NLRP3 and ASC suppress lupus-like autoimmunity by driving the immunosuppressive effects of TGF- β receptor signalling. *Ann Rheum Dis* 2015;74:2224–35.
41. Ma ZZ, Sun HS, Lv JC, Guo L, Yang QR. Expression and clinical significance of the NEK7-NLRP3 inflammasome signaling pathway in patients with systemic lupus erythematosus. *J Inflamm (Lond)* 2018;15:16.
42. Mertens M, Singh JA. Anakinra for rheumatoid arthritis. *Cochrane Database Syst Rev* 2009;CD005121.
43. Kastbom A, Verma D, Eriksson P, Skogh T, Wingren G, Söderkvist P. Genetic variation in proteins of the cryopyrin inflammasome influences susceptibility and severity of rheumatoid arthritis (the Swedish TIRA project). *Rheumatology (Oxford)* 2008;47:415–7.
44. Kolly L, Busso N, Palmer G, Talabot-Ayer D, Chobaz V, So A. Expression and function of the NALP3 inflammasome in rheumatoid synovium. *Immunology* 2010;129:178–85.
45. Franchi L, Eigenbrod T, Núñez G. Cutting edge: TNF- α mediates sensitization to ATP and silica via the NLRP3 inflammasome in the absence of microbial stimulation. *J Immunology* 2009;183:792–6.
46. Folco EJ, Sukhova GK, Quillard T, Libby P. Moderate hypoxia potentiates interleukin-1 β production in activated human macrophages. *Circ Res* 2014;115:875–83.
47. Rhoads JP, Lukens JR, Wilhelm AJ, Moore JL, Mendez-Fernandez Y, Kanneganti TD, et al. Oxidized low-density lipoprotein immune complex priming of the NLRP3 inflammasome involves TLR and FcyR cooperation and is dependent on CARD9. *J Immunol* 2017;198:2105–14.
48. Frank MG, Weber MD, Fonken LK, Hershman SA, Watkins LR, Maier SF. The redox state of the alarmin HMGB1 is a pivotal factor in neuroinflammatory and microglial priming: a role for the NLRP3 inflammasome. *Brain Behav Immun* 2016;55:215–24.
49. Li Y, Shen Y, Jin K, Wen Z, Cao W, Wu B, et al. The DNA repair nuclease MRE11A functions as a mitochondrial protector and prevents T cell pyroptosis and tissue inflammation. *Cell Metab* 2019;30:477–92.
50. Zhao C, Gu Y, Zeng X, Wang J. NLRP3 inflammasome regulates Th17 differentiation in rheumatoid arthritis. *Clin Immunol* 2018;197:154–60.
51. Chomarat P, Vannier E, Dechanet J, Rissoan MC, Banchereau J, Dinarello CA, et al. Balance of IL-1 receptor antagonist/IL-1 β in rheumatoid synovium and its regulation by IL-4 and IL-10. *J Immunol* 1995;154:1432–9.
52. Caglič D, Repnik U, Jedeszko C, Kosce G, Miniejew C, Kindermann M, et al. The proinflammatory cytokines interleukin-1 α and tumor necrosis factor α promote the expression and secretion of proteolytically active cathepsin S from human chondrocytes. *Biol Chem* 2013;394:307–16.
53. Li F, Guo N, Ma Y, Ning B, Wang Y, Kou L. Inhibition of P2X₄ suppresses joint inflammation and damage in collagen-induced arthritis. *Inflammation* 2014;37:146–53.
54. McInnes IB, Cruwys S, Bowers K, Braddock M. Targeting the P2X₇ receptor in rheumatoid arthritis: biological rationale for P2X₇ antagonism. *Clin Exp Rheumatol* 2014;32:878–82.
55. Ippagunta SK, Brand DD, Luo J, Boyd KL, Calabrese C, Stienstra R, et al. Inflammasome-independent role of apoptosis-associated speck-like protein containing a CARD (ASC) in T cell priming is critical for collagen-induced arthritis. *J Biol Chem* 2010;285:12454–62.
56. Guo C, Fu R, Wang S, Huang Y, Li X, Zhou M, et al. NLRP3 inflammasome activation contributes to the pathogenesis of rheumatoid arthritis. *Clin Exp Immunol* 2018;194:231–43.
57. Marchetti C, Swartzwelder B, Koenders MI, Azam T, Tengesdal IW, Powers N, et al. NLRP3 inflammasome inhibitor OLT1177 suppresses joint inflammation in murine models of acute arthritis. *Arthritis Res Ther* 2018;20:169.
58. Vande Walle L, Van Opdenbosch N, Jacques P, Fossoul A, Verheugen E, Vogel P, et al. Negative regulation of the NLRP3 inflammasome by A20 protects against arthritis [letter]. *Nature* 2014;512:69–73.
59. Vakrakou AG, Boiu S, Ziakas PD, Xingi E, Boleti H, Manoussakis MN. Systemic activation of NLRP3 inflammasome in patients with severe primary Sjögren's syndrome fueled by inflammagenic DNA accumulations. *J Autoimmun* 2018;91:23–33.
60. Kim SK, Choe JY, Lee GH. Enhanced expression of NLRP3 inflammasome-related inflammation in peripheral blood mononuclear cells in Sjögren's syndrome. *Clin Chim Acta* 2017;474:147–54.
61. Khalafalla MG, Woods LT, Camden JM, Khan AA, Limesand KH, Petris MJ, et al. P2X₇ receptor antagonism prevents IL-1 β release from salivary epithelial cells and reduces inflammation in a mouse model of autoimmune exocrinopathy. *J Biol Chem* 2017;292:16626–37.
62. Zheng Q, Ren Y, Reinach PS, She Y, Xiao B, Hua S, et al. Reactive oxygen species activated NLRP3 inflammasomes prime environment-induced murine dry eye. *Exp Eye Res* 2014;125:1–8.

63. Hunt KA, Zhernakova A, Turner G, Heap GA, Franke L, Bruinenberg M, et al. Newly identified genetic risk variants for celiac disease related to the immune response. *Nat Genet* 2008;40:395–402.
64. Pascual V, Medrano LM, López-Palacios N, Bodas A, Dema B, Fernández-Arquero M, et al. Different gene expression signatures in children and adults with celiac disease. *PLoS One* 2016;11:e0146276.
65. Jarry A, Malard F, Bou-Hanna C, Meurette G, Mohty M, Mosnier JF, et al. Interferon- α promotes Th1 response and epithelial apoptosis via inflammasome activation in human intestinal mucosa. *Cell Mol Gastroenterol Hepatol* 2016;3:72–81.
66. Palová-Jelínková L, Dáňová K, Drašarová H, Dvořák M, Funda DP, Fundová P, et al. Pepsin digest of wheat gliadin fraction increases production of IL-1 β via TLR4/MyD88/TRIF/MAPK/NF- κ B signaling pathway and an NLRP3 inflammasome activation. *PLoS One* 2013;8:e62426.
67. Matsuo T, Hashimoto M, Ito I, Kubo T, Uozumi R, Furu M, et al. Interleukin-18 is associated with the presence of interstitial lung disease in rheumatoid arthritis: a cross-sectional study. *Scand J Rheumatol* 2019;48:87–94.
68. Palexas GN, Puren A, Savage N, Welsh NH. Serum interleukin (IL-1 β) in patients with diffuse scleritis. *Scand J Immunol Suppl* 1992;11:171–2.
69. Bottin C, Fel A, Butel N, Domont F, Remond AL, Savey L, et al. Anakinra in the treatment of patients with refractory scleritis: a pilot study. *Ocul Immunol Inflamm* 2018;26:915–20.
70. Grebe A, Hoss F, Latz E. NLRP3 inflammasome and the IL-1 pathway in atherosclerosis. *Circ Res* 2018;122:1722–40.
71. Hausmann JS. Targeting cytokines to treat autoinflammatory diseases. *Clin Immunol* 2019;206:23–32.
72. Kloppenburg M, Peterfy C, Haugen IK, Kroon F, Chen S, Wang L, et al. Phase IIa, placebo-controlled, randomised study of lutikizumab, an anti-interleukin-1 α and anti-interleukin-1 β dual variable domain immunoglobulin, in patients with erosive hand osteoarthritis. *Ann Rheum Dis* 2019;78:413–20.
73. Fleischmann RM, Bliddal H, Blanco FJ, Schnitzer TJ, Peterfy C, Chen S, et al. A phase II trial of lutikizumab, an anti-interleukin-1 α / β dual variable domain immunoglobulin, in knee osteoarthritis patients with synovitis. *Arthritis Rheumatol* 2019;71:1056–69.
74. Kurzrock R, Hickish T, Wyrwicz L, Saunders M, Wu Q, Stecher M, et al. Interleukin-1 receptor antagonist levels predict favorable outcome after bermekimab, a first-in-class true human interleukin-1 α antibody, in a phase III randomized study of advanced colorectal cancer. *Oncoimmunology* 2018;8:1551651.
75. Gabay C, Fautrel B, Rech J, Spertini F, Feist E, Kötter I, et al. Open-label, multicentre, dose-escalating phase II clinical trial on the safety and efficacy of tadekinig alfa (IL-18BP) in adult-onset Still's disease. *Ann Rheum Dis* 2018;77:840–7.
76. Angelidis C, Kotsialou Z, Kossyvakis C, Vrettou AR, Zacharoulis A, Kolokathis F, et al. Colchicine pharmacokinetics and mechanism of action. *Curr Pharm Des* 2018;24:659–63.
77. Rajaei E, Mowla K, Ghorbani A, Bahadoram S, Bahadoram M, Dargahi-Malamir M. The effect of omega-3 fatty acids in patients with active rheumatoid arthritis receiving DMARDs therapy: double-blind randomized controlled trial. *Glob J Health Sci* 2015;8:18–25.
78. Arriens C, Hynan LS, Lerman RH, Karp DR, Mohan C. Placebo-controlled randomized clinical trial of fish oil's impact on fatigue, quality of life, and disease activity in systemic lupus erythematosus. *Nutr J* 2015;14:82.
79. Shen L, Yang Y, Ou T, Key CC, Tong SH, Sequeira RC, et al. Dietary PUFAs attenuate NLRP3 inflammasome activation via enhancing macrophage autophagy. *J Lipid Res* 2017;58:1808–21.
80. Garay-Lugo N, Dominguez-Lopez A, Miliar García A, Aguilar Barrera E, Gómez López M, Gómez Alcalá A, et al. N-3 fatty acids modulate the mRNA expression of the Nlrp3 inflammasome and Mtor in the liver of rats fed with high-fat or high-fat/fructose diets. *Immunopharmacol Immunotoxicol* 2016;38:353–63.
81. Chasset F, Tounsi T, Cesbron E, Barbaud A, Francès C, Arnaud L. Efficacy and tolerance profile of thalidomide in cutaneous lupus erythematosus: a systematic review and meta-analysis. *J Am Acad Dermatol* 2018;78:342–50.
82. Keller M, Sollberger G, Beer HD. Thalidomide inhibits activation of caspase-1. *J Immunol* 2009;183:5593–9.
83. Smith CE, Soti S, Jones TA, Nakagawa A, Xue D, Yin H. Non-steroidal anti-inflammatory drugs are caspase inhibitors. *Cell Chem Biol* 2017;24:281–92.
84. Jiang H, He H, Chen Y, Huang W, Cheng J, Ye J, et al. Identification of a selective and direct NLRP3 inhibitor to treat inflammatory disorders. *J Exp Med* 2017;214:3219–38.
85. Martine P, Chevriaux A, Derangère V, Apetoh L, Garrido C, Ghiringhelli F, et al. HSP70 is a negative regulator of NLRP3 inflammasome activation. *Cell Death Dis* 2019;10:256.

ACR PRESIDENTIAL ADDRESS

A Story to Tell, a Promise to Keep

Paula Marchetta

Hello everyone and welcome to the Annual Meeting of the American College of Rheumatology. I am Paula Marchetta, a rheumatologist from New York City, and I am the ACR President.

I stand here this evening to deliver the Presidential Address. But what I would rather do is tell a story—because I love stories and because as clinicians and scientists, we so often forget how important stories are to us. It has been said that “Medicine... begins with storytelling. Patients tell stories to describe illness; doctors tell stories to understand it. Science tells its own story to explain diseases.” (1). But this evening, I will tell a different kind of story—not a clinical story, not a story of scientific discovery, but a love story—and it is our story, the story of all of us here, the story of why we fell in love with rheumatology.

But I will preface this story by telling another story first—actually, the storyline of an old movie. It’s not a famous old movie, but rather a little-known contract movie filmed in 1944 during the Studio Era of Hollywood moviemaking and now preserved in the archives of Turner Classic Movies, which, as it so happens, is headquartered right here in Atlanta. So, I will press your patience a bit by sharing the plot of *The Impatient Years*, which begins with a young couple—she a housewife, he a serviceman on leave during World War II, appearing before a judge in divorce court. The judge, rather than granting the divorce they both want, orders the couple, who had been separated by the war after only one day of marriage, to return to San Francisco where they had first met and then hastily wed following a three-day whirlwind courtship. Here they must retrace all their steps, from the moment of their initial chance encounter in a coffee shop to the moment they married—to see whether they would rediscover why it was that they had fallen in love with each other.

This evening, as we gather at this Opening Ceremony to begin our Annual Meeting, we are, in a way, here to retrace our steps and rekindle our love for what we do—that spark which still endures at the heart of our own personal story. For each of us, the characters and the settings will be different, and our plots may hold some unexpected twists and turns, but where our stories all lead, how and why we all finally arrived at that moment of

epiphany—when we knew that rheumatology was “the one”—is remarkably the same for so many of us.

We fell in love with this specialty because of the complexity and range of diseases we diagnose and treat. We fell in love with the richness and nuance of their clinical presentations and the myriad ways they manifest and unfold over time. Our patients teach us our specialty—they don’t necessarily follow the textbook. Sir William Osler famously admonished, “Listen to your patients; they are telling you their diagnosis.” We in rheumatology have learned to listen well, and to observe carefully and, as clinicians and scientists, to measure and record. We develop long caring relationships with our patients—we look after the whole of them, with treatments that change lives in small everyday ways: getting out of bed, buttoning a shirt, lifting a child...simple tasks.

We cherish these rewards of our specialty. We also relish its challenges: the challenge of so many unsolved mysteries, of so much that is still undiscovered about the etiology and pathogenesis of our diseases and—so often, how little there is to guide us in evidence-based medical decision-making. We stand at the crossroads of the art and science of medicine, the divide between the unknown and the known, the turning point where we have put together just enough of the puzzle to get the picture despite missing so many pieces. We have been called the intellectuals of internal medicine. Like philosophers, we are thoughtful. We cannot make presumptions of certainty. We must deal with ambiguous clinical situations. We ponder; we deliberate; we collaborate. And we love the process as much as the accomplishments of our work and the progress we have made in understanding and treating our diseases.

Right now, all of us in rheumatology—and indeed all of us in health care—are embattled. We struggle to win the limited dollars available to fund innovative research that will advance our knowledge of the pathways to cure our diseases. We must fight so that our patients can receive necessary treatments which will spare them from pain, loss of function, and disability. We are shackled to electronic medical records and forced to be more engaged with a computer screen than with our patients. We decry the forces that

Presented at the 83rd Annual Meeting of the American College of Rheumatology, Atlanta, GA, November 9, 2019.

Paula Marchetta, MD, MBA: Concorde Medical Group, New York, New York; President, American College of Rheumatology, 2018–2019.

Address correspondence to Paula Marchetta, MD, MBA, 316 East 30th Street, New York, NY 10016. E-mail: pmarchettamd@concordemed.com.

Submitted for publication November 18, 2019; accepted November 19, 2019.

Which Physicians Are Most Burned Out?

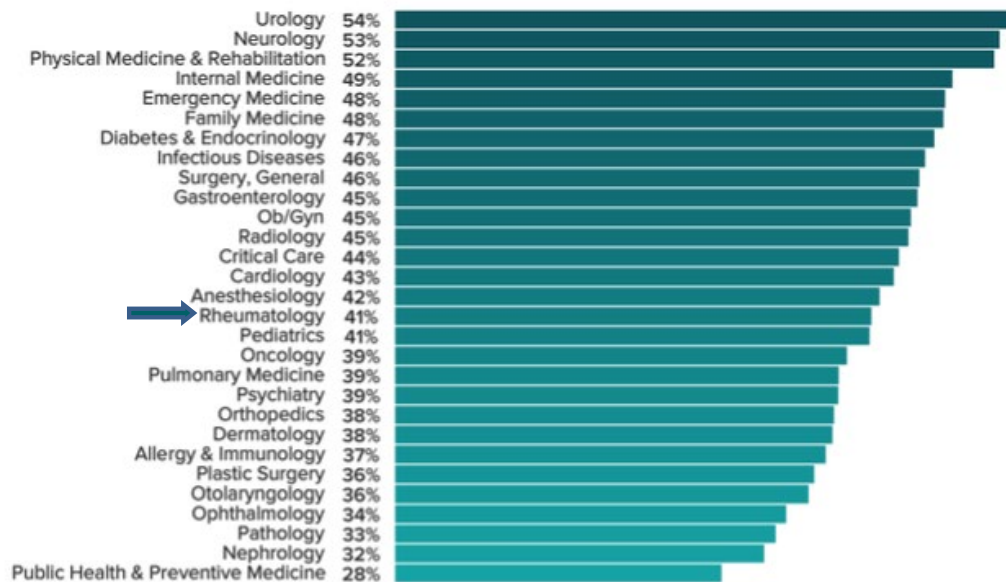


Figure 1. Results, Medscape survey on physician burnout by specialty (ref. 2). More than 15,000 physicians in over 29 specialties completed the survey.

threaten our autonomy as clinicians and as scientists. And at a time when access to rheumatologic care is more and more constrained by the workforce shortage, we must allocate our hours to burdensome administrative tasks that have little to do with why we chose rheumatology. We become physically exhausted and emotionally depleted by these battles, even as we recognize the importance of collecting our data, reporting our outcomes, and demonstrating the value of our specialty to those who still may ask: *What is rheumatology?*

These are some of the elements that have laid the groundwork for the well-documented rise in physician burnout throughout this country (2,3) (Figure 1). Much has been written now about burnout and the many factors that contribute to it (4–7). The direct adverse effects on doctors and other health professionals are widely described (4). Increasingly recognized as well are the negative downstream effects of physician burnout on patient safety, satisfaction, and the quality of care (8). Far less, however, is written about meaningful and sustainable solutions.

On this I speak with no real authority except as someone whose career has been spent in clinical practice and as witness to the changes that have taken place in our practice environment. And from this perspective, I was struck by one observation, so obvious that it is easy to overlook. It commanded my attention, as if written in boldface: **the disappearance of the doctors' lounge** (4,9–11) (Figure 2). This physical place has vanished from many if not most hospitals, a victim of greater work demands, productivity expectations, and the need to repurpose the space for other more efficient uses. Its insidious loss has been cited not only as one of the reasons for burnout,

but also as the underpinning of some of its most disheartening prodromal symptoms—professional loneliness, isolation, and disillusionment (12–14).

The doctors' lounge...beyond the four walls and serviceable furniture of some physical space, it really stands as a symbol—a symbol for a place where medical professionals can gather to share our common experiences—experiences unique to what we do, where a sense of community can be created and where collegiality is fostered and thrives. Without this place of interpersonal connection and exchange, we lose one of the most vital components of our professional fulfillment. We become battle-weary, serving as we do in the trenches of a system that does not necessarily seek to support us. We forget the powerful attraction that drew us to medicine and to rheumatology. We forget why we fell in love in the first place.

Drivers of Physician Burnout

- Increased workload demands
- Higher productivity expectations
- Less meaningful time spent with patients
- Loss of autonomy
- More administrative burdens
- Lack of enough support staff
- **Disappearance of the doctors' lounge**

Figure 2. Commonly cited factors contributing to physician burnout, as reported in *Mayo Clinic Proceedings* (ref. 4).

The Annual Meeting of the American College of Rheumatology is the single most important educational event of our specialty. We come here from around the world to learn about the latest scientific advances and best clinical practices for the diseases we treat. In 2019, we all know that education can be delivered in many innovative ways—ways that enable our learning to occur at a distance and be flexible, customizable, accessible, and available any time—all good things, and all made possible by technology and made necessary by the increasing demands of our work and the competing priorities of our daily lives. With so many virtual options, we may question whether a live meeting of this grand scale is still relevant in this changing world in which we must manage. Should we do without it? Or would we forgo something of such inestimable value to our professional well-being that we would suffer the consequences of its absence long before we realize what it is that we have truly lost—like the symbolic doctors' lounge—a place where time is purposely set aside for engagement with colleagues who understand the nature of what we do and the challenges that we face in a way no one else can, and where the solitary world of virtual connections and online knowledge acquisition can be vastly enriched by the power of simply being present, in the room where it happens.

At this year's Annual Meeting, we are shaking things up a bit in the "room where it happens" by introducing several pilots to enhance our learning and create a vibrant, dynamic, and more personalized experience. Among these innovations is a reconfiguration of the way some lectures will be delivered, changing them from their customary didactic format to TED-style presentations. TED talks are typically concise and centered on the speaker's passion and the breakthrough revelations that will transport the audience to a new level of understanding. These "In the Rheum" TED-style talks are not intended to replace the traditional learning platforms of the meeting, but to augment them by accommodating different learner preferences and stimulating interest in areas that can be more deeply explored in related sessions at this meeting and beyond. Another "room" we have created here is RheumConnect, a place where we can meet up with our friends and colleagues and where we can "Meet the Masters" of our field to hear their own compelling personal stories of career motivations and choices. Also new this year, we have introduced the concept of holding a "meeting within the meeting" with the launch of the Pediatric Community Lounge, which provides dedicated space for pediatric rheumatologists to congregate between sessions and is located close to the rooms where the pediatric sessions take place. If this pilot is successful, we foresee offering similar "meetings within the meeting" to other focused communities of learners within ACR.

The need for us to regain a sense of community in our professional lives—to recapture a feeling of belonging—has never been greater than now, when so many of the designated venues where we had once felt connected to and supported by our peers have disappeared. Our professional society cannot really replace the

lost doctors' lounge. But in some ways, it transcends it—because the ACR is home to all of us who reside within the house of rheumatology, from bench to translational researchers, academic to private practitioners, and 22 different types of rheumatology professionals within the Association of Rheumatology Professionals. This inclusivity—this bringing together of all these many diverse aspects of our profession into one organization—sets the ACR apart, and builds for us a level of support, collegiality, and respect for the views of others across our specialty in a way that lifts us all and helps to restore us.

The ACR has a brand promise, as do many service-based organizations. The Ritz-Carlton Hotel Company, for instance, conveys their brand promise through a simple motto: "We are ladies and gentlemen serving ladies and gentlemen."

At ACR, our promise is also simple: "We are here for you so that you can be there for your patients." *We* are here for you. *We*. It is not a singular pronoun. But who are the "we" making this promise? To borrow a line from the Ritz-Carlton: *We* are rheumatologists and rheumatology professionals serving rheumatologists and rheumatology professionals. The "we" of ACR is all of us. *We* are here for each other.

It has been my immense honor to work closely with so many dedicated, accomplished, and truly wonderful colleagues volunteering their time and talent to the ACR. I am especially grateful to the members of the Executive Committee for their friendship, their guidance, and the special synergy we have enjoyed in our work together—a synergy that developed not despite the differences in what we do but because of them. Likewise, our Board of Directors and our committee chairs have been remarkable in the insight, integrity, and equanimity they have brought individually and collectively to the table. Standing invisibly beside all of us and assisting us through all our many ministrations is the incredible ACR staff. They move stealthily behind the scenes, doing the hard day-to-day work of the College to advance our specialty, ensure its future, and empower us to excel. Their unwavering support for me personally through this momentous year has been both my rudder and my rock. There are no words that can completely express my gratitude to them, except to say that they are the embodiment of excellence and surpass the high bar set long ago by Aristotle: "Excellence is never an accident but always the result of high intention, sincere effort, and intelligent execution."

There are, of course, many others, both past and present, whom I must thank. I consider myself very fortunate to have attended New York University School of Medicine and to have done all my professional training at NYU-Bellevue, especially with its long and outstanding history as a pioneer in the study of rheumatic diseases. It was easy to fall in love with rheumatology there. I am so proud and so grateful to have had this privilege.

If someone had told me that one day I would serve as ACR President, I would have thought it as likely as lassoing the moon. We never really know when we look ahead what may be within

our reach or where our path may lead if we are willing to stay the course. We can see, though, when we look around, all of those who were there to help us prepare or to ease our way once we set out.


I see my late parents, and my immigrant Italian grandparents before them, from whom I learned through their words, and especially by their actions, the importance of always doing your best, of never shying away when there was work to be done, and of living a life of service to others. I see my dearest friends, Dr. Elizabeth Kitsis and Dr. Lenore Brancato, with whom I have walked in step since we met as rheumatology fellows at NYU. They have steadied my course during some of the steepest climbs. I have been blessed by their camaraderie, their generosity, and their unfailing loyalty and understanding. And then, I see my two Michaels—my son Michael, whose success in life matters more to me than whatever else I have done...and the other Michael, as my son calls him, who has joined me on this path and who has brought tremendous joy and needed perspective to my life and work.

Thank you.

REFERENCES

1. Mukherjee S. *The emperor of all maladies: a biography of cancer*. New York: Scribner; 2010.
2. Kane L. Medscape national physician burnout, depression & suicide report 2019. URL: <https://www.medscape.com/slideshow/2019-lifestyle-burnout-depression-6011056#13>.
3. Shanafelt TD, West CP, Sinsky C, Trockel M, Tutty M, Satele DV, et al. Changes in burnout and satisfaction with work-life integration in physicians and the general US working population between 2011 and 2017. *Mayo Clin Proc* 2019;94:1681–94.
4. Shanafelt TD, Noseworthy JH. Executive leadership and physician well-being: nine organizational strategies to promote engagement and reduce burnout. *Mayo Clinic Proc* 2017;92:129–46.
5. Friedberg MW, Chen PG, van Busum KR, Aunon F, Pham C, Caloyeras J, et al. Factors affecting physician professional satisfaction and their implications for patient care, health systems, and health policy. *Rand Health Q* 2014;3:1.
6. Kroth PJ, Morioka-Douglas N, Veres S, Babbott S, Poplau S, Qeadan F, et al. Association of electronic health record design and use factors with clinician stress and burnout. *JAMA Netw Open* 2019;2:e199609.
7. Pearl R. The 3 causes of physician burnout (and why there's no simple solution.) September 2019. URL: <https://www.forbes.com/sites/robertpearl/2019/09/09/burnout-3-causes/#2794702d6a09>.
8. Panagioti M, Geraghty K, Johnson J, Zhou A, Panagopoulou E, Chew-Graham C, et al. Association between physician burnout and patient safety, professionalism, and patient satisfaction a systematic review and meta-analysis. *JAMA Intern Med* 2018;178:1317–30.
9. Gunderman R. What happened to the doctor's lounge? 2013. URL: <https://www.theatlantic.com/health/archive/2013/11/what-happened-to-the-doctors-lounge/281112/>.
10. Brown S. Bringing back the doctors' lounge to help fight burnout. *CMAJ* 2019;191:E268–9.
11. Pearl R. Physician burnout: isolation, loneliness, and the loss of the American hospital. 2019. URL: <https://www.forbes.com/sites/robertpearl/2019/08/12/physician-burnout-isolation/#55a5839d58a0>.
12. Frey JJ III. Professional loneliness and the loss of the doctors' dining room. *Ann Fam Med* 2018;16:461–3.
13. Kulkarni A. Navigating loneliness in the era of virtual care. *N Engl J Med* 2019;380:307–9.
14. Wenzel RP. RVU medicine, technology, and physician loneliness. *N Engl J Med* 2019;380:305–7.

Impact of Cumulative Inflammation, Cardiac Risk Factors, and Medication Exposure on Coronary Atherosclerosis Progression in Rheumatoid Arthritis

George A. Karpouzas,  Sarah R. Ormseth, Elizabeth Hernandez, and Matthew J. Budoff

Objective. To explore incidence and progression of coronary atherosclerosis and identify determinants in patients with rheumatoid arthritis (RA). We specifically evaluated the impact of inflammation, cardiac risk factors, duration of medication exposure, and their interactions on coronary plaque progression.

Methods. One hundred one participants with baseline coronary computed tomography angiography findings underwent follow-up assessment a mean \pm SD of 83 ± 3.6 months after baseline. Plaque burden was reported as the segment involvement score (describing the number of coronary segments with plaque) and the segment stenosis score (characterizing the cumulative plaque stenosis over all evaluable segments). Plaque composition was classified as noncalcified, mixed, or calcified. Coronary artery calcium (CAC) was quantified using the Agatston method.

Results. Total plaque increased in 48% of patients, and progression was predicted by older age, higher cumulative inflammation, and total prednisone dose ($P < 0.05$). CAC progressors were older, more obese, hypertensive, and had higher cumulative inflammation compared to nonprogressors ($P < 0.05$). Longer exposure to biologics was associated with lower likelihood of noncalcified plaque progression, lesion remodeling, and constrained CAC change in patients without baseline calcification, independent of inflammation, prednisone dose, or statin exposure (all $P < 0.05$). Longer statin treatment further restricted noncalcified plaque progression and attenuated the effect of inflammation on increased plaque and CAC ($P < 0.05$). Stringent systolic blood pressure (BP) control further weakened the effect of inflammation on total plaque progression.

Conclusion. Inflammation was a consistent and independent predictor of coronary atherosclerosis progression in RA. It should therefore be specifically targeted toward mitigating cardiovascular risk. Biologic disease-modifying antirheumatic drugs, statins, and BP control may further constrain plaque progression directly or indirectly.

INTRODUCTION

Individuals with rheumatoid arthritis (RA) experience a higher rate of cardiovascular (CV) events compared to controls (1). We recently reported greater prevalence, severity, burden, and vulnerability of occult coronary plaque in patients with RA compared to age- and sex-matched individuals without autoimmunity (2). Increasing atherosclerosis burden on serial coronary computed tomography (CT) angiography is an independent predictor of acute coronary syndromes in both men and women without autoimmune disease (3,4). In contrast, stabilization in plaque size is associated with decreased risk of future CV events (5). Changes in coronary plaque load and composition in RA are largely unexplored. Two recent studies evaluated determinants of incident

coronary artery calcium (CAC) or prevalent CAC progression and described associations with age, higher blood pressure (BP), and triglyceride levels but not with disease-specific traits or treatments (6,7). However, CAC represents ~20% of total plaque burden both in patients with RA and in a general patient population, and may not be present in earlier disease (2,8). More importantly, having additional information on plaque burden and on stenotic severity and composition exclusively obtained by coronary CT angiography significantly improves upon predictive value of CAC for CV events in a general patient population (9).

In the present study, we explored incident coronary plaque rates, prevalent atherosclerosis progression, and changes in plaque composition in patients with RA who underwent coronary CT angiography at baseline and follow-up. We further identified

Supported by Pfizer through an investigator-initiated grant to Dr. Karpouzas (ASPIRE grant WI215017).

George A. Karpouzas, MD, Sarah R. Ormseth, PhD, Elizabeth Hernandez, MA, Matthew J. Budoff, MD: Harbor-UCLA Medical Center, Torrance, California. No potential conflicts of interest relevant to this article were reported.

Address correspondence to George A. Karpouzas, MD, 1124 West Carson Street, Building E4-R17, Torrance, CA 90502. E-mail: gkarpouzas@labiomed.org.

Submitted for publication March 19, 2019; accepted in revised form September 12, 2019.

determinants of increasing plaque and CAC burden, and specifically investigated the role of cumulative inflammation, cardiac risk factors, RA-specific or ancillary medications, and their interactions on plaque progression. We hypothesized that higher cumulative inflammation may predict greater coronary plaque load at follow-up, and we further posited that duration of exposure to RA-specific medications such as glucocorticoids, conventional synthetic and biologic disease-modifying antirheumatic drugs (DMARDs), traditional cardiac risk factors, and statin treatments may exert opposing effects on plaque growth or composition.

PATIENTS AND METHODS

Patient recruitment. One hundred one patients who participated in a prior coronary CT angiography study of subclinical coronary atherosclerosis in RA (2) underwent follow-up assessments after a mean \pm SD of 83 ± 3.6 months. Participants were prospectively followed up at our outpatient rheumatology clinic since their baseline visit (2010–2011). Inclusion and exclusion criteria have been previously described in detail (2). Briefly, patients were enrolled if they met the 2010 American College of Rheumatology/European League Against Rheumatism (EULAR) classification criteria for RA (10), were ≥ 18 years of age, and had no symptoms or history of CV disease at baseline. Major exclusion criteria were concomitant autoimmune syndromes (with the exception of Sjögren's syndrome), weight >325 pounds (147.7 kg), iodine allergy, glomerular filtration rate <60 ml/minute, malignancy, and chronic or active infections. The study was approved by the local institutional review board, and all participants provided written informed consent in accordance with the Declaration of Helsinki.

Predictor variables. Hypertension was defined as a systolic BP of ≥ 140 mm Hg or a diastolic BP of ≥ 90 mm Hg, or the use of an antihypertensive agent. Diabetes mellitus was defined as a glycosylated hemoglobin level of $>6.5\%$ or hypoglycemic medication use. Hyperlipidemia was defined as a fasting cholesterol level of >200 mg/dl, a low-density lipoprotein (LDL) level of >130 mg/dl, or statin use. Smoking was defined as cigarette consumption within 30 days from screening. The waist-to-height ratio was used to measure LDL central obesity (11). Screening for incident cardiac risk factors was conducted in accordance with the EULAR recommendations for CV risk assessment (12). Disease activity was evaluated using the Disease Activity Score in 28 joints (13) using the C-reactive protein level (DAS28-CRP) at every clinic visit. Cumulative inflammatory burden was calculated as a time-averaged CRP spanning all visits between baseline and follow-up scans (14). Medications were reconciled at every clinic visit, including use and doses of prednisone, conventional synthetic disease-modifying antirheumatic drugs (csDMARDs), biologic DMARDs, and statins. Total prednisone and methotrexate doses from baseline to follow-up were calculated, and the number of years of exposure to biologic DMARDs and statins were also estimated.

Laboratory evaluations. A complete blood cell count, comprehensive metabolic panels, erythrocyte sedimentation rate (ESR), and CRP levels were calculated on the day of each coronary CT angiography assessment, as well as at every clinic visit between scans. Fasting lipid evaluations were performed on the day of each scan, in accordance with the EULAR recommendations for CV risk assessment between scans (12).

Multidetector coronary CT angiography. Baseline scans were performed using a 64-multidetector row LightSpeed VCT scanner (GE Healthcare) between March 2010 and March 2011. Follow-up scans were performed using a 256-multidetector row scanner between March 2017 and March 2018. Baseline and follow-up images were analyzed in the same campaign and in random order by a single, blinded interpreter (MJB) (15). CAC was quantified by the Agatston method (16). Coronary arteries were evaluated on contrast-enhanced scans using a standardized 17-segment American Heart Association model (17). For longitudinal comparisons, baseline and follow-up coronary segments were coaligned using fixed anatomic landmarks as fiducial points. Each segment was scored for stenosis severity on a 0–4 scale based on grade of luminal restriction, where 0 = 0% (absence of plaque), 1 = 1–29% stenosis, 2 = 30–49% stenosis, 3 = 50–69% stenosis, and 4 = $>70\%$ stenosis (2). Plaque composition was defined as noncalcified, mixed, or calcified as previously reported (18). Subjects received 2 individual quantitative scores; the segment involvement score represented the total number of segments with plaque, and the segment stenosis score described the cumulative stenosis grade rendered by plaque in all evaluable segments. Reproducibility of these scoring measures at our institution has been previously reported (18).

Outcome measures. Changes in burden of total plaque, specific plaque types (noncalcified, mixed, and calcified), and CAC constituted the primary outcome measures. Atherosclerosis progression was defined as the number of new segments with any plaque per patient (segment involvement score increase, possible range 0–17) or rise in stenotic plaque severity in all evaluable coronary segments with plaque (segment stenosis score increase, possible range 0–68). CAC progression was expressed as the absolute difference between the follow-up measurement and the baseline measurement of CAC.

Statistical analysis. Continuous variables were expressed as the mean \pm SD, and categorical variables were expressed as the number and percentage. Negative binomial regression was used to assess continuous outcome measures (segment involvement score increase and segment stenosis score increase), robust logistic regression was used to assess categorical outcome measures (noncalcified, mixed, and calcified plaque progression), and generalized linear models with a Tweedie (Poisson-Gamma) error distribution and log link function were used to assess CAC change.

For each outcome measure, univariable models with candidate predictors were estimated, followed by multivariable models constructed via a backward elimination variable selection process. The backward selection process started with all predictors associated with the outcome in univariable analyses at a *P* value of < 0.20 and sequentially removed variables with a *P* value of >0.10, beginning with the least significant variable. For primary outcome measures, the possible presence of interactions between cumulative inflammation and traditional risk factors was tested by introducing into the adjusted multivariable models the product of time-averaged CRP and each CV risk factor, and the product of time-averaged CRP and

each medication exposure variable. Age and time between scans were included as covariates in all models. Odds ratios (ORs) with 95% confidence intervals (95% CIs) were calculated. Analyses were performed using SPSS software.

RESULTS

Participants were predominantly female with established, seropositive, erosive, and well-controlled disease (Table 1). Follow-up included an average of 19 visits over 7 years. Forty-eight patients were considered plaque progressors based on either

Table 1. Baseline clinical characteristics of progressors versus nonprogressors*

	No plaque progression (n = 53)	Plaque progression (n = 48)	Total sample (n = 101)
Age, years	48.07 ± 9.88	55.19 ± 9.49†	51.45 ± 10.29
Female, no. (%)	46 (86.79)	41 (85.42)	87 (86.14)
Follow-up duration, years	7.00 ± 0.33	6.94 ± 0.34	6.97 ± 0.33
No. of visits	18.83 ± 3.49	18.46 ± 4.18	18.65 ± 3.82
RA-related parameters			
RA duration, years	9.18 ± 6.28	11.36 ± 7.98	10.22 ± 7.19
RF-positive, no. (%)	48 (90.57)	43 (89.58)	91 (90.10)
ACPA-positive, no. (%)	47 (88.68)	40 (83.33)	87 (86.14)
Erosions, no. (%)	33 (62.26)	31 (64.58)	64 (63.37)
Time-averaged CRP, mg/dl	0.79 ± 0.53	0.99 ± 1.16	0.89 ± 0.89
Time-averaged SJC	1.83 ± 1.92	2.40 ± 2.84	2.10 ± 2.41
Time-averaged DAS28-CRP	2.69 ± 0.80	2.70 ± 0.90	2.69 ± 0.84
Cardiovascular risk factors			
Hypertension at baseline, no. (%)	16 (30.19)	29 (60.42)†	45 (44.55)
Time-averaged systolic BP, mm Hg	127.83 ± 13.11	133.08 ± 11.41†	130.32 ± 12.55
Time-averaged diastolic BP, mm Hg	71.97 ± 7.05	72.21 ± 6.56	72.08 ± 6.79
Dyslipidemia at baseline, no. (%)	25 (47.17)	26 (54.17)	51 (50.50)
Time-averaged LDL, mg/dl	101.78 ± 23.38	109.84 ± 35.30	105.61 ± 29.77
Diabetes at baseline, no. (%)	5 (9.43)	9 (18.75)	14 (13.86)
Current smoking, no. (%)	4 (7.55)	4 (8.33)	8 (7.92)
Waist-to-height ratio	57.82 ± 6.83	61.20 ± 7.78†	59.42 ± 7.46
Medication at baseline			
Prednisone use, no. (%)	12 (22.64)	19 (39.58)	31 (30.69)
No. of concomitant csDMARDs	1.90 ± 0.78	1.87 ± 0.79	1.89 ± 0.78
Biologic DMARD use, no. (%)	34 (64.15)	30 (62.50)	64 (63.37)
Statin use at baseline, no. (%)	20 (37.74)	21 (43.75)	41 (40.59)
Medication during follow-up			
Cumulative prednisone, gm‡	2.34 ± 4.49	4.12 ± 6.35	3.19 ± 5.50
Cumulative methotrexate, gm	36.01 ± 18.04	38.81 ± 18.52	37.34 ± 18.23
Biologic DMARD duration, years§	4.36 ± 2.88	4.24 ± 3.01	4.30 ± 2.93
Statin duration, years¶	1.83 ± 2.58	3.04 ± 2.82†	2.41 ± 2.75
Baseline plaque burden			
Total segment involvement score	0.94 ± 0.97	2.88 ± 2.76†	1.86 ± 2.24
Total segment stenosis score	1.04 ± 1.11	4.46 ± 5.11†	2.66 ± 3.98
Noncalcified plaque >0, no. (%)	29 (54.72)	31 (64.58)	60 (59.41)
Mixed plaque >0, no. (%)	4 (7.55)	20 (41.67)†	24 (23.76)
Calcified plaque >0, no. (%)	3 (5.66)	16 (33.33)†	19 (18.81)
CAC >0, no. (%)	5 (9.43)	26 (54.17)†	31 (30.69)
Agatston score	8.85 ± 53.49	135.29 ± 397.36†	68.94 ± 282.35

* Except where indicated otherwise, values are the mean ± SD. RA = rheumatoid arthritis; RF = rheumatoid factor; ACPA = anti-citrullinated protein antibody; CRP = C-reactive protein; SJC = swollen joint count; DAS28 = Disease Activity Score in 28 joints; BP = blood pressure; LDL = low-density lipoprotein; csDMARDs = conventional synthetic disease-modifying antirheumatic drugs; CAC = coronary artery calcium.

† *P* < 0.05 versus nonprogressors.

‡ Patients (n = 49) exposed to prednisone at any time between baseline and follow-up scans.

§ Patients (n = 78) exposed to biologic DMARDs at any time between baseline and follow-up scans.

¶ Patients (n = 59) exposed to statins at any time between baseline and follow-up scans.

displaying new coronary segments with plaque (segment involvement score change, range 0–6 among all patients) or increased stenotic severity in segments with prior plaque (segment stenosis score change, range 0–9 among all patients). Clinical characteristics of progressors and nonprogressors are presented in Table 1. RA-related parameters and treatments were similarly distributed across both groups, including use of csDMARDs, time receiving biologic DMARDs, and total prednisone and methotrexate doses. Although progressors were older, more obese, more likely to have hypertension, and had a higher time-averaged systolic BP compared to nonprogressors, those differences were no longer significant after adjustment for age. Progressors more commonly had plaque and CAC, as well as higher plaque and CAC scores at baseline ($P < 0.05$). Eight incident CV events (4 ischemic and 4 nonischemic) occurred throughout the observation period (see Supplementary Table 1, available on the *Arthritis & Rheumatology* web site at <http://onlinelibrary.wiley.com/doi/10.1002/art.41122/abstract>). All patients with CV events remained in the study and were included in the analysis.

Incident plaque rates, plaque progression, and calcification over time. Seventy patients (69.3%) displayed coronary plaque at baseline. The rate of incident plaque (segment involvement score >0 at follow-up in patients with a baseline segment involvement score of 0), was 4.7/100 person-years

(95% CI 2.2–8.6); in patients with prevalent atherosclerosis (baseline segment involvement score >0), plaque progressed at a rate of 7.8/100 person-years (95% CI 5.5–10.7). The rate of CAC progression was 6.0/100 person-years (95% CI 4.3–8.1); it increased at a median of 15.1 Agatston units/year in patients with prevalent CAC (95% CI 9.3–32.6). Patients with incident CAC demonstrated a median annualized progression rate of 1.7 units (95% CI 0.8–4.1). Quantitative changes for total plaque as well as all 3 plaque subtypes are shown in Supplementary Table 2 (available on the *Arthritis & Rheumatology* web site at <http://onlinelibrary.wiley.com/doi/10.1002/art.41122/abstract>). Overall, total plaque burden and coronary calcification scores increased ($P \leq 0.012$); additionally, progression of noncalcified plaque occurred in 9 patients, mixed plaque in 21, and calcified plaque in 35.

Changes in coronary plaque composition. At baseline, 187 coronary segments with plaque were identified in 70 patients. At follow-up, 97 new lesions appeared in segments without plaque initially; 15 new plaques were identified in 10 patients (9.9%) without plaque at baseline, while 82 new plaques were identified in 37 patients (36.6%) with prevalent plaque. Of the 97 incident plaques reported at follow-up, 20 were noncalcified, 21 were mixed, and 56 were calcified. Figure 1 delineates per-plaque composition changes from baseline to follow-up.

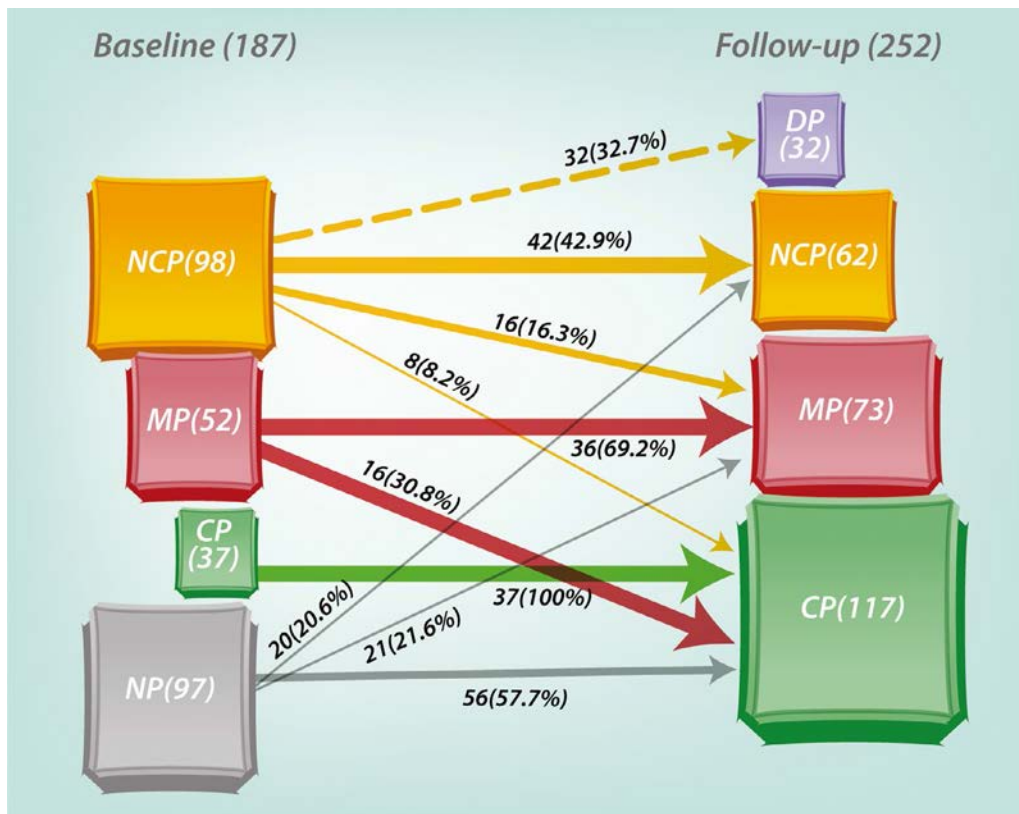


Figure 1. Change in plaque composition, new plaque (NP), and disappearing plaque (DP) from baseline to follow-up. NCP = noncalcified plaque; MP = mixed plaque; CP = calcified plaque.

Table 2. Predictors of total coronary plaque progression in patients with rheumatoid arthritis*

	Segment involvement score increase, estimate (95% CI)		Segment stenosis score increase, estimate (95% CI)		CAC increase, estimate (95% CI)	
	Univariable model	Multivariable model	Univariable model	Multivariable model	Univariable model	Multivariable model
Age, years	–	1.06 (1.03–1.09)†	–	1.05 (1.02–1.08)‡	–	1.17 (1.09–1.26)†
Male sex	1.05 (0.38–2.90)	–	1.04 (0.43–2.52)	–	1.05 (0.38–2.90)	–
Hypertension	1.74 (0.92–3.31)§	–	1.61 (0.90–2.90)	–	2.54 (1.19–5.42)‡	2.58 (0.99–6.78)§
Dyslipidemia	0.74 (0.41–1.33)	–	0.94 (0.54–1.62)	–	1.17 (0.59–2.32)	–
Diabetes	1.06 (0.45–2.51)	–	1.36 (0.63–2.94)	–	0.96 (0.39–2.37)	–
Waist-to-height ratio	1.03 (1.00–1.07)§	–	1.02 (0.98–1.06)	–	1.07 (1.03–1.11)‡	1.17 (1.02–1.34)¶
Time-averaged CRP, mg/dl	1.64 (1.36–1.98)†	1.42 (1.13–1.78)‡	1.52 (1.23–1.88)†	1.35 (1.08–1.70)‡	1.65 (1.34–2.03)†	1.64 (1.14–2.35)‡
Statin duration, years	1.05 (0.95–1.16)	–	1.04 (0.94–1.15)	–	1.14 (1.03–1.26)‡	–
Biologic DMARD duration, years	1.05 (0.97–1.14)	–	1.03 (0.94–1.12)	–	1.09 (0.96–1.23)	–
Cumulative methotrexate, gm	1.01 (0.99–1.02)	–	1.00 (0.99–1.02)	–	1.01 (0.99–1.03)	–
Cumulative prednisone, gm	1.09 (1.05–1.13)†	1.06 (1.02–1.10)‡	1.08 (1.05–1.12)†	1.06 (1.02–1.10)‡	1.07 (1.04–1.11)†	1.10 (1.01–1.21)¶

* 95% = 95% confidence interval; CAC = coronary artery calcium; CRP = C-reactive protein; DMARD = disease-modifying antirheumatic drug.

† $P < 0.001$.

‡ $P < 0.01$.

§ $P < 0.1$.

¶ $P < 0.05$.

Determinants of change in coronary atherosclerosis burden. Older age, higher time-averaged CRP, and greater total prednisone dose independently predicted both segment involvement score increase and segment stenosis score

increase in multivariate models (Table 2). The effect of time-averaged CRP on total plaque increase was modified by statin use, since time-averaged CRP predicted segment involvement score increase only in patients who were not exposed to statins

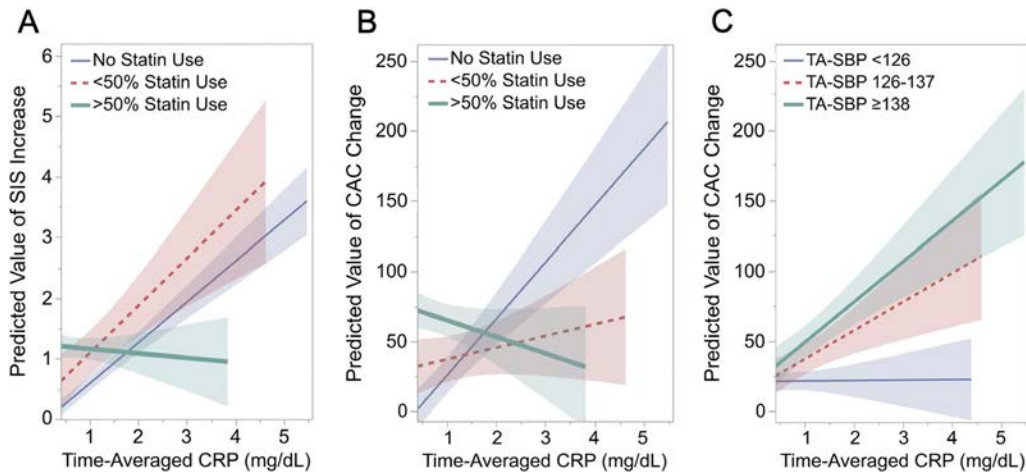


Figure 2. Duration of statin exposure and blood pressure control moderate the effect of cumulative inflammation on coronary plaque progression in rheumatoid arthritis. Relative risks (RRs) and odds ratios (ORs), with 95% confidence intervals (95% CIs), were calculated. **A**, Higher time-averaged C-reactive protein (CRP) yielded significant plaque progression in patients not receiving statins (RR 1.48 [95% CI 1.05–2.09], $P = 0.025$) and those receiving statins for <50% of the study period (RR 1.31 [95% CI 1.01–1.69], $P = 0.040$). No such risk was observed in patients with statin exposure for >50% of the study period (RR 1.07 [95% CI 0.93–1.22], $P = 0.35$, P for interaction = 0.017). **B**, Higher time-averaged CRP rendered high coronary artery calcium (CAC) progression risk in statin-naïve patients (OR 2.33 [95% CI 1.29–4.22], $P = 0.005$); in contrast, any statin exposure mitigated that risk (OR 1.17 [95% CI 0.81–1.68], $P = 0.410$; $P = 0.98$ for statin exposure <50% and OR 0.96 [95% CI 0.44–2.17], $P = 0.98$ for statin exposure >50%; P for interaction = 0.006). Both statin interaction models reported in **A** and **B** are adjusted for age, dyslipidemia, cumulative prednisone dose, total methotrexate dose, and biologic disease-modifying antirheumatic drug treatment duration. **C**, Higher time-averaged CRP significantly predicted CAC progression in patients in the middle and highest tertiles of time-averaged systolic blood pressure (TA-SBP) (OR 1.68 [95% CI 1.14–2.47], $P = 0.009$ and OR 2.39 [95% CI 1.52–3.77], $P < 0.001$, respectively), but not those in the lowest tertile (OR 1.03 [95% CI 0.61–1.74], $P = 0.92$). SIS = segment involvement score.

Table 3. Predictors of change in atherosclerosis burden by plaque type in patients with rheumatoid arthritis*

	Noncalcified plaque progression, OR (95% CI)		Mixed plaque progression, OR (95% CI)		Calcified plaque progression, OR (95% CI)	
	Model 1	Model 2	Model 1	Model 2	Model 1	Model 2
Age, years	–	1.00 (0.93–1.07)	–	1.06 (1.00–1.12)†	–	1.18 (1.09–1.27)‡
Male sex	1.17 (0.18–7.73)	–	1.34 (0.39–4.59)	–	1.78 (0.28–11.23)	–
Hypertension	0.25 (0.03–2.11)	–	1.68 (0.56–5.02)	–	4.30 (1.55–11.96)§	3.53 (1.00–12.53)¶
Dyslipidemia	0.40 (0.09–1.88)	–	0.50 (0.17–1.43)	–	1.49 (0.56–3.95)	–
Diabetes	0.72 (0.07–7.18)	–	1.36 (0.36–5.17)	–	2.42 (0.81–7.27)	–
Waist-height ratio	0.92 (0.82–1.04)	–	1.06 (0.99–1.13)	–	1.15 (1.08–1.22)‡	1.16 (1.07–1.25)‡
Time-averaged CRP, mg/dl	1.09 (0.64–1.87)	–	0.70 (0.24–2.02)	–	3.12 (1.92–5.05)‡	3.42 (1.85–6.35)‡
Statin duration, years	0.69 (0.55–0.88)§	0.72 (0.57–0.90)§	1.14 (0.94–1.39)	–	1.10 (0.93–1.31)	–
Biologic DMARD duration, years	0.76 (0.60–0.96)†	0.77 (0.61–0.98)†	1.12 (0.93–1.34)	–	1.07 (0.92–1.25)	–
Cumulative methotrexate, gm	1.03 (0.99–1.08)	–	1.01 (0.98–1.04)	–	1.00 (0.97–1.03)	–
Cumulative prednisone, gm	0.99 (0.92–1.07)	–	1.05 (0.96–1.13)	–	1.08 (0.99–1.18)¶	–

* Model 1 was adjusted for age and time between scans. Model 2 was adjusted as in model 1, and additionally for all variables in the final multivariable model selected using backward selection. OR = odds ratio; 95% CI = 95% confidence interval; CRP = C-reactive protein; DMARD = disease-modifying antirheumatic drug.

† $P < 0.05$.

‡ $P < 0.001$.

§ $P < 0.01$.

¶ $P < 0.1$.

or received statins for <50% of the study period, but not in those who received statins >50% of the time (P for interaction = 0.017) (Figure 2A).

CAC change was independently predicted by age, obesity, time-averaged CRP, and total prednisone dose (Table 2). Statin exposure also modified the effect of time-averaged CRP on CAC change. Specifically, higher time-averaged CRP was significantly associated with CAC change only in patients not exposed to statins, but not in patients who had any statin exposure during the study period (P for interaction = 0.006) (Figure 2B). Additionally, the effect of time-averaged CRP on CAC change was moderated by time-averaged systolic BP; specifically, time-averaged CRP significantly predicted CAC change in patients in the middle tertile (time-averaged systolic BP 126–137 mm Hg) and highest tertile (time-averaged systolic BP \geq 138 mm Hg), but not those in the lowest tertile of time-averaged systolic BP (P for interaction = 0.023) (Figure 2C).

CAC change was further assessed separately in patients with and those without detectable baseline CAC in a supplementary analysis, due to a significant interaction between baseline CAC and duration of biologic DMARD treatment (P for interaction = 0.001). In a model with adjustment for age, obesity, time-averaged CRP, and total prednisone dose, longer biologic DMARD exposure was negatively associated with CAC change in patients without CAC at baseline (OR 0.77 [95% CI 0.60–0.98]; $P = 0.031$), but not in those with prevalent CAC (OR 1.08 [95% CI 0.94–1.23]; $P = 0.28$). The presence of CAC at baseline did not modify the effects of the other primary predictors on CAC change (data not shown).

Determinants of plaque progression by subtype (noncalcified, mixed, calcified) are displayed in Table 3. Both a longer duration of biologic DMARD treatment and exposure to statins were independently associated with a decreased likelihood of noncalcified plaque progression. Inclusion of total prednisone and methotrexate dose in the model did not affect the results (data not shown). Older age was associated with both mixed plaque and calcified plaque progression. Increased calcified plaque burden was further associated with obesity and higher cumulative inflammation.

DISCUSSION

This is the first study to explore predictors of coronary plaque progression in a well-characterized, prospective cohort of patients with RA without known CV disease and with long-term follow-up. We specifically investigated the effects of cumulative inflammation, traditional cardiac risk factors, RA-specific and ancillary therapies and their interactions on total plaque progression, various plaque subtypes, and coronary calcification. Our findings complement previous reports on CAC progression in RA (6,7).

We report several novel findings. First, higher cumulative inflammation was a consistent and independent predictor of total coronary plaque progression in RA. This included new segments with plaque at follow-up, as well as greater stenosis severity in segments with plaque at baseline. This is consistent with 2 previous studies showing that higher inflammatory burden was associated with carotid plaque progression in RA (19,20). However, our observation is of unique significance, since the presence of carotid plaque in inflammatory joint diseases (including

RA) does not sufficiently identify patients with coronary artery disease and since quantitative measurements of carotid atherosclerosis do not correlate with the presence or burden of coronary plaque (21). We used time-averaged CRP as a surrogate for cumulative inflammation; in supplementary analyses, similar results were observed using time-averaged swollen joint counts as a predictor, but not when time-averaged tender joint counts, time-averaged patient global assessments, or composite indices such as the DAS28-CRP or the Clinical Disease Activity Index (22) were used. Importantly, higher cumulative inflammation in RA has been associated with a greater risk of a future CV event (23), while reduction in time-averaged inflammation yielded a lower risk of a CV event (24). Since atherosclerosis progression on serial coronary CT angiography independently predicted CV events in a general patient population (3,5), our observations collectively reaffirm that stringent and durable control of inflammation should be a primary objective in the quest to mitigate CV risk in RA.

Second, higher cumulative inflammation may also promote plaque remodeling and maturation, as evidenced by its strong association with CAC and calcified plaque progression. Indeed, 56 of 117 segments (48%) with calcified plaque at follow-up had no plaque at baseline. Ostensibly, incident plaques appeared in those segments as noncalcified plaques that grew and matured over periods of inflammation during disease flares; as inflammation subsided, they eventually transitioned to advanced, heavily calcified plaques. Support for this timeline was provided by supplementary analyses, where we demonstrated that the within-patient variability in CRP over time significantly predicted CAC progression independent of age, hypertension, obesity, and baseline CAC ($P = 0.018$). In accordance with this, previous reports confirmed that early atherogenesis inflammation drives and colocalizes with initial intimal calcification (25). In response to proinflammatory cytokine production by macrophages at sites of lipid accumulation, vascular smooth muscle cells (VSMCs) undergo apoptosis, release extracellular vesicles secondary to stress, or undergo phenotype transition to osteoblastic cells as a self-preservation strategy. All those events are associated with local calcification, which is initially undetectable using coronary CT angiography (25). If inflammation persists, macrophage infiltration and microcalcifications progress, eventually appearing as spotty calcifications on coronary CT angiography. If inflammation subsides and the VSMC repair system is not overwhelmed (cells do not die by apoptosis in the meantime), this process will lead to the development of calcified acellular plaque.

In advanced plaque, large, dense calcifications are spatially distinct from macrophages, inversely correlate with macrophage burden, and—like the calcific mummification of soft tissue infections—represent healing that stabilizes the arterial wall (25). Hence, higher burden of calcified plaque at follow-up may reflect the final stage in the plaque life cycle that appeared and evolved

in the context of a historically higher inflammatory load. However, this association between inflammation and calcification was not observed in prior studies of CAC progression in RA (6,7). Potential explanations may be the longer duration of follow-up (7 years compared to ≤ 3 years) and greater number of evaluation points (19 compared to 2 or 3) in our study, allowing for a more comprehensive assessment of inflammation variability as well as adequate time for plaque remodeling.

Our third novel finding is that longer biologic DMARD exposure may yield an atheroprotective effect in RA, independent of stringent control of systemic inflammation. Specifically, lengthier biologic DMARD treatment reduced the likelihood of noncalcified plaque progression, the earliest histologic atherosclerotic lesion discernible on coronary CT angiography. Biologic therapies were similarly shown to selectively influence lipid-rich, soft plaque volume in patients with psoriasis (26). Moreover, we showed that lengthier biologic DMARD exposure appeared to prevent maturation and remodeling of such plaques, as evidenced by the lower risk of progressive calcification independent of inflammation, duration of statin exposure, and total prednisone dose. In a similar manner, biologic DMARDs have been shown to inhibit radiographic progression in RA regardless of attainment of optimal disease control (27–29). In contrast, neither duration of exposure to csDMARDs nor total methotrexate dose in our study influenced coronary plaque progression.

Fourth, we established an independent coronary atheroprotective effect of statins in RA. Longer statin exposure was associated with lower risk of noncalcified plaque progression regardless of cumulative inflammation, total prednisone and methotrexate dose, or biologic DMARD duration. Indeed, stabilization or reduction in plaque size, particularly the noncalcified lipid core component, is well documented in response to high intensity statin therapy in general patient populations (30–33) and related to lower risk of CV events (5). However, the atheroprotective effect of statin in our study was not related to the treatment intensity, but rather the duration of the exposure. Our additional observation that the duration of statin exposure moderated the effect of cumulative inflammation on both plaque and CAC progression highlights potential local antiinflammatory effects of statins at the plaque level (34), independent of systemic inflammation as reflected by blood CRP levels (35).

Regrettably, sustained remission may be unrealistic for the majority of patients at the present time (36). Could RA-specific or other ancillary treatments mitigate coronary plaque progression in subjects who do not achieve stringent inflammation control? We observed that longer statin exposure also moderated the effect of inflammation on total plaque progression. In patients treated with statins for >50% of the observation time, higher time-averaged CRP failed to yield significant progression of either coronary plaque or CAC. We further noted that durable, aggressive systolic BP control throughout the observation period may be instrumental, particularly in the setting of chronic residual

inflammation. Time-averaged systolic BP at the lowest tertile (<126 mm Hg) attenuated the effect of higher cumulative inflammation on CAC progression, whereas higher measurements significantly accelerated it. Nevertheless, it is presently unclear whether atheroprotection in RA—specifically in the context of residual inflammation—requires adjustment of the recommendations for starting lipid-lowering therapy or adoption of more rigorous systolic BP targets than in general patient populations (37).

We also demonstrated that cumulative prednisone dose adversely affected total coronary plaque as well as CAC progression, independent of cumulative inflammation or cardiac risk factors. Despite the fact that physicians generally prescribe glucocorticoids to patients with higher disease activity, our observations highlight the true deleterious effect of glucocorticoids on the vascular wall, rather than confounding by indication. Importantly, the duration of statin exposure in our study did not moderate the effect of total prednisone dose on coronary plaque progression, as previously reported for carotid atherosclerosis (19). Since a higher cumulative prednisone dose has been linked to a greater incidence of CV events in RA (38), timely tapering and withdrawal may be warranted.

Our study has certain limitations. First, the absence of a control group hinders the ability to determine whether the observed magnitude and predictors of plaque change in RA are different from those in subjects without autoimmunity. However, at least for CAC, where there is a precedent for comparison (39), the observed CAC progression in our patients was significantly higher than predicted based on age, sex, and ethnicity-matched reference values (relative risk 2.21 [95% CI 1.39–3.52], $P = 0.001$). Second, our patients had low cumulative inflammatory burden; 47% had a time-averaged DAS28-CRP of <2.4, and 68% had a DAS28-CRP of <2.8. Moreover, all patients received rigorous screening and management of incident cardiac risk factors during their clinic visits. Additionally, patients with prevalent calcification or significant plaque burden on baseline coronary CT angiography received at least statin therapy, if not more aggressive treatment, for atherosclerosis, regardless of the presence or absence of clinical symptoms. Consequently, the likelihood of plaque progression may have been attenuated in patients who would otherwise have exhibited the greatest increase. Accordingly, the proportions, magnitude of plaque progression, and effect sizes of predictors may have been attenuated, compared to cohorts with higher disease activity or untreated risk factors.

Occult coronary atherosclerosis burden increased in a significant proportion of patients with RA. Cumulative inflammatory burden and total prednisone dose were disease-specific, independent determinants of plaque progression. Our findings confirm the importance of prioritizing and targeting durable control of inflammation in RA. Longer exposure to biologic DMARDs or statins, as well as rigorous control of systolic BP, may further moderate the effect of inflammation on atherosclerosis progression and yield additional coronary atheroprotective effects beyond optimal control of systemic inflammation.

ACKNOWLEDGMENTS

We wish to thank the study participants, Drs. Benedict Chou and Gopika Miller for their assistance with formalized clinical assessments, and Ms Lorena Ruiz for facilitation of study coordination.

AUTHOR CONTRIBUTIONS

All authors were involved in drafting the article or revising it critically for important intellectual content and all authors approved the final version to be published. Dr. Karpouzas had full access to all the data in the study and takes responsibility for the integrity of the data and the accuracy of the data analysis.

Study conception and design. Karpouzas, Budoff.

Acquisition of data. Karpouzas, Ormseth, Hernandez, Budoff.

Analysis and interpretation of the data. Karpouzas, Ormseth, Hernandez, Budoff.

ROLE OF THE STUDY SPONSOR




Pfizer provided funding for the study through an investigator-initiated grant. Pfizer was not involved in the study design, study-related procedures, or manuscript drafting. The authors independently collected the data, interpreted the results, and had the final decision to submit the manuscript for publication.

REFERENCES

- Naranjo A, Sokka T, Descalzo MA, Calvo-Alén J, Hørslev-Petersen K, Luukkainen RK, et al, and the QUEST-RA Group. Cardiovascular disease in patients with rheumatoid arthritis: results from the QUEST-RA study. *Arthritis Res Ther* 2008;10:R30.
- Karpouzas GA, Malpeso J, Choi TY, Li D, Munoz S, Budoff MJ. Prevalence, extent and composition of coronary plaque in patients with rheumatoid arthritis without symptoms or prior diagnosis of coronary artery disease. *Ann Rheum Dis* 2014;73:1797–804.
- Motoyama S, Ito H, Sarai M, Kondo T, Kawai H, Nagahara Y, et al. Plaque characterization by coronary computed tomography angiography and the likelihood of acute coronary events in mid-term follow-up. *J Am Coll Cardiol* 2015;66:337–46.
- Gu H, Gao Y, Wang H, Hou Z, Han L, Wang X, et al. Sex differences in coronary atherosclerosis progression and major adverse cardiac events in patients with suspected coronary artery disease. *J Cardiovasc Comput Tomogr* 2017;11:367–72.
- Inoue K, Motoyama S, Sarai M, Sato T, Harigaya H, Hara T, et al. Serial coronary CT angiography-verified changes in plaque characteristics as an end point: evaluation of effect of statin intervention. *JACC Cardiovasc Imaging* 2010;3:691–8.
- Chung CP, Giles JT, Kronmal RA, Post WS, Gelber AC, Petri M, et al. Progression of coronary artery atherosclerosis in rheumatoid arthritis: comparison with participants from the Multi-Ethnic Study of Atherosclerosis. *Arthritis Res Ther* 2013;15:R134.
- Udachkina HV, Novikova DS, Popkova TV, Kirillova IG, Markelova EI. Dynamic of changes in coronary artery calcification in early rheumatoid arthritis patients over 18 months. *Rheumatol Int* 2018;38:1217–24.
- Leschka S, Seitun S, Dettmer M, Baumüller S, Stolzmann P, Goetti R, et al. Ex vivo evaluation of coronary atherosclerotic plaques: characterization with dual-source CT in comparison with histopathology. *J Cardiovasc Comput Tomogr* 2010;4:301–8.
- Hou ZH, Lu B, Gao Y, Jiang SL, Wang Y, Li W, et al. Prognostic value of coronary CT angiography and calcium score for major adverse cardiac events in outpatients. *JACC Cardiovasc Imaging* 2012;5:990–9.
- Aletaha D, Neogi T, Silman AJ, Funovits J, Felson DT, Bingham CO III, et al. 2010 rheumatoid arthritis classification criteria: an American

- College of Rheumatology/European League Against Rheumatism collaborative initiative. *Arthritis Rheum* 2010;62:2569–81.
11. Swainson MG, Batterham AM, Tsakirides C, Rutherford ZH, Hind K. Prediction of whole-body fat percentage and visceral adipose tissue mass from five anthropometric variables. *PLoS One* 2017;12:e0177175.
 12. Peters MJ, Symmons DP, McCarey D, Dijkmans BA, Nicola P, Kvien TK, et al. EULAR evidence-based recommendations for cardiovascular risk management in patients with rheumatoid arthritis and other forms of inflammatory arthritis. *Ann Rheum Dis* 2010;69:325–31.
 13. Prevoo ML, van 't Hof MA, Kuper HH, van Leeuwen MA, van de Putte LB, van Riel PL. Modified disease activity scores that include twenty-eight-joint counts: development and validation in a prospective longitudinal study of patients with rheumatoid arthritis. *Arthritis Rheum* 1995;38:44–8.
 14. Matthews JN, Altman DG, Campbell MJ, Royston P. Analysis of serial measurements in medical research. *BMJ* 1990;300:230–5.
 15. Budoff MJ, Dowe D, Jollis JG, Gitter M, Sutherland J, Halamert E, et al. Diagnostic performance of 64-multidetector row coronary computed tomographic angiography for evaluation of coronary artery stenosis in individuals without known coronary artery disease: results from the prospective multicenter ACCURACY (Assessment by Coronary Computed Tomographic Angiography of Individuals Undergoing Invasive Coronary Angiography) trial. *J Am Coll Cardiol* 2008;52:1724–32.
 16. Agatston AS, Janowitz WR, Hildner FJ, Zusmer NR, Viamonte M Jr, Detrano R. Quantification of coronary artery calcium using ultrafast computed tomography. *J Am Coll Cardiol* 1990;15:827–32.
 17. Leipsic J, Abbara S, Achenbach S, Cury R, Earls JP, Mancini GJ, et al. SCCT guidelines for the interpretation and reporting of coronary CT angiography: a report of the Society of Cardiovascular Computed Tomography Guidelines Committee. *J Cardiovasc Comput Tomogr* 2014;8:342–58.
 18. Pagali SR, Madaj P, Gupta M, Nair S, Hamirani YS, Min JK, et al. Interobserver variations of plaque severity score and segment stenosis score in coronary arteries using 64 slice multidetector computed tomography: a substudy of the ACCURACY trial. *J Cardiovasc Comput Tomogr* 2010;4:312–8.
 19. Giles JT, Post WS, Blumenthal RS, Polak J, Petri M, Gelber AC, et al. Longitudinal predictors of progression of carotid atherosclerosis in rheumatoid arthritis. *Arthritis Rheum* 2011;63:3216–25.
 20. Im CH, Kwon SH, Eun JS, Kim NR, Nam EJ, Kang YM. Inflammatory burden predicts carotid plaque progression and subsequent cardiovascular events in rheumatoid arthritis: the 2-year prospective cohort study [abstract]. *Arthritis Rheum* 2013;65:S155.
 21. Svantesson M, Rollefstad S, Kløw NE, Hisdal J, Ikdahl E, Semb AG, et al. Associations between coronary and carotid artery atherosclerosis in patients with inflammatory joint diseases. *RMD Open* 2017;3:e000544.
 22. Aletaha D, Nell VP, Stamm T, Uffmann M, Pflugbeil S, Machold K, et al. Acute phase reactants add little to composite disease activity indices for rheumatoid arthritis: validation of a clinical activity score. *Arthritis Res Ther* 2005;7:R796–806.
 23. Innala L, Möller B, Ljung L, Magnusson S, Smedby T, Södergren A, et al. Cardiovascular events in early RA are a result of inflammatory burden and traditional risk factors: a five year prospective study. *Arthritis Res Ther* 2011;13:R131.
 24. Solomon DH, Reed GW, Kremer JM, Curtis JR, Farkouh ME, Harrold LR, et al. Disease activity in rheumatoid arthritis and the risk of cardiovascular events. *Arthritis Rheumatol* 2015;67:1449–55.
 25. Aikawa E, Nahrendorf M, Figueiredo JL, Swirski FK, Shtatland T, Kohler RH, et al. Osteogenesis associates with inflammation in early-stage atherosclerosis evaluated by molecular imaging in vivo. *Circulation* 2007;116:2841–50.
 26. Elnabawi YA, Dey AK, Goyal A, Groenendyk JW, Chung JH, Belur AD, et al. Coronary artery plaque characteristics and treatment with biologic therapy in severe psoriasis: results from a prospective observational study. *Cardiovasc Res* 2019;115:721–8.
 27. Døhn UM, Ejbjerg B, Boonen A, Hetland ML, Hansen MS, Knudsen LS, et al. No overall progression and occasional repair of erosions despite persistent inflammation in adalimumab-treated rheumatoid arthritis patients: results from a longitudinal comparative MRI, ultrasonography, CT and radiography study. *Ann Rheum Dis* 2011;70:252–8.
 28. Smolen JS, Avila JCM, Aletaha D. Tocilizumab inhibits progression of joint damage in rheumatoid arthritis irrespective of its anti-inflammatory effects: disassociation of the link between inflammation and destruction. *Ann Rheum Dis* 2012;71:687–93.
 29. Smolen JS, Han C, Bala M, Maini RN, Kalden JR, van der Heijde D, et al, for the ATTRACT Study Group. Evidence of radiographic benefit of treatment with infliximab plus methotrexate in rheumatoid arthritis patients who had no clinical improvement: a detailed sub-analysis of data from the Anti-tumor Necrosis Factor Trial in Rheumatoid Arthritis with Concomitant Therapy study. *Arthritis Rheum* 2005;52:1020–30.
 30. Nissen SE, Nicholls SJ, Sipahi I, Libby P, Raichlen JS, Ballantyne CM, et al, for the ASTEROID Investigators. Effect of very high-intensity statin therapy on regression of coronary atherosclerosis: the ASTEROID trial. *JAMA* 2006;295:1556–65.
 31. Nicholls SJ, Ballantyne CM, Barter PJ, Chapman MJ, Erbel RM, Libby P, et al. Effect of two intensive statin regimens on progression of coronary disease. *N Engl J Med* 2011;365:2078–87.
 32. Puri R, Nicholls SJ, Shao M, Kataoka Y, Uno K, Kapadia SR, et al. Impact of statins on serial coronary calcification during atheroma progression and regression. *J Am Coll Cardiol* 2015;65:1273–82.
 33. Räber L, Taniwaki M, Zaugg S, Kelbæk H, Roffi M, Holmvang L, et al. Effect of high-intensity statin therapy on atherosclerosis in non-infarct-related coronary arteries (IBIS-4): a serial intravascular ultrasonography study. *Eur Heart J* 2015;36:490–500.
 34. Martín-Ventura JL, Blanco-Colio LM, Gómez-Hernández A, Muñoz-García B, Vega M, Serrano J, et al. Intensive treatment with atorvastatin reduces inflammation in mononuclear cells and human atherosclerotic lesions in one month. *Stroke* 2005;36:1796–800.
 35. Tawakol A, Fayad ZA, Mogg R, Alon A, Klimas MT, Dansky H, et al. Intensification of statin therapy results in a rapid reduction in atherosclerotic inflammation: results of a multicenter fluorodeoxyglucose-positron emission tomography/computed tomography feasibility study. *J Am Coll Cardiol* 2013;62:909–17.
 36. Einarsson JT, Willim M, Ernestam S, Saxne T, Geborek P, Kapetanovic MC. Prevalence of sustained remission in rheumatoid arthritis: impact of criteria sets and disease duration, a nationwide study in Sweden. *Rheumatology (Oxford)* 2019;58:227–36.
 37. Hollan I, Dessein PH, Ronda N, Wasko MC, Svenungsson E, Agewall S, et al. Prevention of cardiovascular disease in rheumatoid arthritis. *Autoimmun Rev* 2015;14:952–69.
 38. Evans MR, Escalante A, Battafarano DF, Freeman GL, O'Leary DH, del Rincón I. Carotid atherosclerosis predicts incident acute coronary syndromes in rheumatoid arthritis. *Arthritis Rheum* 2011;63:1211–20.
 39. McClelland RL, Chung H, Detrano R, Post W, Kronmal RA. Distribution of coronary artery calcium by race, gender, and age: results from the Multi-Ethnic Study of Atherosclerosis (MESA). *Circulation* 2006;113:30–7.

Comparative Profiling of Serum Protein Biomarkers in Rheumatoid Arthritis–Associated Interstitial Lung Disease and Idiopathic Pulmonary Fibrosis

Daniel J. Kass,¹ Mehdi Nouraie,¹ Marilyn K. Glassberg,² Nitya Ramreddy,² Karen Fernandez,² Lisa Harlow,² Yingze Zhang,¹ Jean Chen,³ Gail S. Kerr,⁴ Andreas M. Reimold,⁵ Bryant R. England,⁶  Ted R. Mikuls,⁶  Kevin F. Gibson,¹ Paul F. Dellaripa,⁷ Ivan O. Rosas,⁷ Chester V. Oddis,¹ and Dana P. Ascherman¹ 

Objective. Interstitial lung disease (ILD) is a frequent complication of rheumatoid arthritis (RA), occurring in up to 40% of patients during the course of their disease. Early diagnosis is critical, particularly given the shared clinicoepidemiologic features between advanced rheumatoid arthritis–associated ILD (RA-ILD) and idiopathic pulmonary fibrosis (IPF). This study was undertaken to define the molecular basis of this overlap through comparative profiling of serum proteins in RA-ILD and IPF.

Methods. Multiplex enzyme-linked immunosorbent assays (ELISAs) were used to profile 45 protein biomarkers encompassing cytokines/chemokines, growth factors, and matrix metalloproteinases (MMPs) in sera obtained from RA patients with ILD and those without, individuals with IPF, and healthy controls. Levels of selected serum proteins were compared between patient subgroups using adjusted linear regression, principal component analysis (PCA), and least absolute shrinkage and selection operator (LASSO) modeling.

Results. Multiplex ELISA-based assessment of sera from 2 independent cohorts (Veterans Affairs [VA] and Non-VA) revealed a number of non-overlapping biomarkers distinguishing RA-ILD from RA without ILD (RA–no ILD) in adjusted regression models. Parallel analysis of sera from IPF patients also yielded a discriminatory panel of protein markers in models adjusted for age/sex/smoking, which showed differential overlap with profiles linked to RA-ILD in the VA cohort versus the Non-VA cohort. PCA revealed several distinct functional groups of RA-ILD–associated markers that, in the VA cohort, encompassed proinflammatory cytokines/chemokines as well as 2 different subsets of MMPs. Finally, LASSO regression modeling in the Non-VA and VA cohorts revealed distinct biomarker combinations capable of discriminating RA-ILD from RA–no ILD.

Conclusion. Comparative serum protein biomarker profiling represents a viable method for distinguishing RA-ILD from RA–no ILD and identifying population-specific mediators shared with IPF.

INTRODUCTION

Rheumatoid arthritis (RA) is a systemic inflammatory disease that affects ~1.3 million adults in the US (1). RA is commonly associated with extraarticular manifestations, including various

types of lung disease that represent major contributors to morbidity and mortality (2). Although prevalence estimates of RA-associated interstitial lung disease (RA-ILD) vary depending on the methods used for detection/classification, the development of clinically significant ILD is almost 9-fold higher in RA patients

The opinions and assertions contained herein are those of the authors and do not necessarily represent those of the Department of Veterans Affairs or the United States Government.

Supported in part by grant 1I01BX00788 from the Veterans Affairs Merit Review Office of Research and Development (to Dr. Ascherman), grants from the Rheumatology Research Foundation Within Our Reach program (to Drs. Ascherman and Oddis), and the Simmons Chair for Interstitial Lung Disease at the University of Pittsburgh.

¹Daniel J. Kass, MD, Mehdi Nouraie, MD, PhD, Yingze Zhang, PhD, Kevin F. Gibson, MD, Chester V. Oddis, MD, Dana P. Ascherman, MD; University of Pittsburgh School of Medicine, Pittsburgh, Pennsylvania; ²Marilyn K. Glassberg, MD, Nitya Ramreddy, MD, Karen Fernandez, MD, Lisa Harlow, BS; University of Miami Miller School of Medicine, Miami, Florida; ³Jean Chen, MD; First Xiamen University, Xiamen, China; ⁴Gail S.

Kerr, MD; Washington DC VA Health Care System; ⁵Andreas M. Reimold, MD; VA North Texas Health Care System, Dallas; ⁶Bryant R. England, MD, Ted R. Mikuls, MD, MSPH; VA Nebraska–Western Iowa Health Care System and University of Nebraska Medical Center, Omaha; ⁷Paul F. Dellaripa, MD, Ivan O. Rosas, MD; Brigham and Women's Hospital, Boston, Massachusetts.

Drs. Kass and Nouraie contributed equally to this work.

No potential conflicts of interest relevant to this article were reported.

Address correspondence to Dana P. Ascherman, MD, University of Pittsburgh School of Medicine, Division of Rheumatology and Clinical Immunology, Biomedical Science Tower South 723, 3500 Terrace Street, Pittsburgh, PA 15261. E-mail: DAscher@pitt.edu.

Submitted for publication June 21, 2019; accepted in revised form September 12, 2019.

compared to the general population, resulting in a standardized mortality ratio of 2.5–5 (3,4). Viewed differently, the 5-year mortality rate for RA patients with ILD and those without (RA–no ILD) is 39% versus 18.2%, respectively (5).

A number of genetic, environmental, clinical, and serologic factors contribute to the development of RA-ILD, which occurs more frequently in male patients (3,6) and typically manifests as nonspecific interstitial pneumonia (NSIP) or usual interstitial pneumonia (UIP) (7). Cigarette smoking serves as a major risk factor for RA, particularly in those individuals who also have the shared HLA–DRB1 epitope (8). This combination of environmental and genetic risk factors likely contributes to the development of RA-ILD as well, as smoking induces citrullination of lung antigens (8) that can promote a breach in immune tolerance. Consistent with this paradigm, a number of studies have demonstrated increased titers of anti-cyclic citrullinated peptide (anti-CCP) antibodies in patients with RA-ILD (9–12). Apart from high titers of anti-CCP antibodies and rheumatoid factor (RF) (13), several studies have shown associations between RA-ILD and alternative biomarkers (many of which are also associated with idiopathic pulmonary fibrosis [IPF] [14]), such as the epithelial cell–derived Krebs von den Lungen 6 (KL-6) antigen (15), matrix metalloproteinase 7 (MMP-7), pulmonary and activation-regulated chemokine (PARC), surfactant protein D (SP-D), and interferon- γ –inducible protein 10 (IP-10/CXCL10) (16,17).

As shown in a number of earlier studies (18,19), the disease course of clinically evident RA-ILD parallels that of IPF, a chronic progressive lung disease with a median survival of 3–5 years after diagnosis (20). The annual incidence of IPF is estimated to be between 4.6 and 16.3 cases per 100,000 people, resulting in a prevalence of 13–20 cases per 100,000 people (21). Like RA-ILD, IPF occurs predominantly in middle-aged to older men and is strongly associated with cigarette smoking as well as the presence of UIP on histopathologic examination (20, 22)—indicating that IPF may serve as an important comparator disease to better understand relevant/overlapping signaling pathways shared by advanced forms of RA-ILD.

Although many details of IPF pathogenesis remain undefined, dysregulated extracellular matrix remodeling is a key pathologic feature contributing to lung fibrosis, respiratory failure, and strikingly high mortality (23). Cigarette smoking and certain exposures (such as metal or wood dust) are key environmental triggers that can damage respiratory epithelium, promoting both innate and adaptive immune responses as well as profibrotic signaling pathways culminating in myofibroblast accumulation, differentiation, and activation (24,25). Autosomal-dominant genetic transmission occurs in ~0.5–3.7% of IPF patients (21), suggesting that genetic background may increase susceptibility to specified environmental insults. Intriguingly, polymorphisms in the promoter of MUC5B that are associated with both familial and sporadic forms of IPF (26) have recently been linked to RA-UIP (27).

Coupled with overlapping histopathologic and clinicoepidemiologic features, the existence of shared genetic risk factors

indicates that IPF and RA-UIP may involve common disease pathways. By extension, comparative profiling of serum protein biomarkers corresponding to relevant disease pathways represents a viable approach to more formally assess the putative mechanistic overlap between these disorders. Previous studies have shown, for example, that remodeling proteins such as MMP-1 and MMP-7 are overexpressed in IPF compared to other chronic lung diseases (28). While MMP-7 has also been linked to RA-ILD (16,17), less is known about other protein mediators previously implicated in IPF (such as MMP-1 and interleukin-8 [IL-8] [29]). Given that increased knowledge of these overlapping signals may clarify the pathogenesis of both diseases and thereby suggest novel therapeutic targets, this study was undertaken to more broadly define serum protein biomarker profiles in established cohorts of IPF and RA-ILD.

PATIENTS AND METHODS

Patient cohorts. In accordance with established protocols approved by each center's institutional review board, serum samples were obtained from patients who met the 1987 American College of Rheumatology (ACR) classification criteria for RA (30). The primary RA cohort encompassed US veterans recruited prospectively from 3 Veterans Affairs (VA) facilities (Miami, Florida; Washington, DC; and Dallas/North Texas) as well as a group of US veterans enrolled in the national Veterans Affairs RA (VARA) registry (31). A previously described group of RA patients recruited from the University of Pittsburgh and Brigham and Women's Hospital (16) served as a Non-VA comparator cohort for biomarker analyses. Patients meeting the American Thoracic Society (ATS) criteria for IPF (32) were enrolled from a database maintained through the Simmons Center for Interstitial Lung Disease at the University of Pittsburgh. Imaging studies, pulmonary function tests (PFTs), articular disease activity measurements (for RA patients), and serum samples were generally obtained within 3 months of enrollment, except where indicated.

Disease classification. Patients in the VA and Non-VA cohorts who met the criteria for RA were further classified into subcategories of no ILD, indeterminate ILD, subclinical ILD, or clinically evident ILD based on the presence versus absence of clinical features (cough, dyspnea), restrictive pulmonary function deficits (forced vital capacity [FVC] <80% of predicted, forced expiratory volume in 1 second [FEV₁]/FVC >80% of predicted), and/or imaging evidence of specified parenchymal lung abnormalities (defined below). While the indeterminate ILD subcategory encompassed individuals whose abnormalities on high-resolution computed tomography (HRCT) did not meet the threshold criteria for definite ILD (see below), subclinical ILD included patients with radiographic evidence of ILD who lacked symptoms of cough/dyspnea and had no known history of ILD. Patients who did not have radiographic evidence of defined interstitial lung abnormalities could not be classified as having RA-ILD; however, in a small number of VARA patients without HRCT data (16 of 67), definite chest radiographic evidence of interstitial lung

abnormalities allowed these patients to be classified as having RA-ILD. In accordance with ATS criteria (33), IPF patients had biopsy and/or radiographic evidence of UIP in the absence of underlying hypersensitivity pneumonitis, associated connective tissue disorder, or other known etiology.

Imaging. HRCT scans of the chest with cuts of 1–2 mm thickness were obtained at end inspiration for prospectively recruited patients in the VA cohort and Non-VA cohort, with a median (interquartile range [IQR]) time since serum sampling of 56 days (IQR 28–103) and 33 days (IQR 16–70), respectively. For individuals with previously diagnosed ILD, the scans obtained closest to the time of serum sampling were used for staging the radiographic pattern and severity of parenchymal lung abnormalities. HRCT classification (see below) was based on readings from at least 2 independent pulmonologists/radiologists (MKG, FKG) who were blinded with regard to patient disease characteristics. Radiographic features indicative of ILD included ground-glass opacification, septal thickening, reticulation, traction bronchiectasis, and/or honeycombing. Additional characterization utilized a published scale of interstitial lung abnormalities ranging from 0 to 3 (34,35), with 0 = no ILD, 1 = indeterminate ILD (presence of focal or unilateral ground-glass attenuation, focal or unilateral reticulation, or patchy ground-glass abnormality involving <5% of the lung), 2 = mild/moderate ILD (changes affecting >5% of any lobar region with nondependent ground-glass or reticular abnormalities, diffuse centrilobular nodularity, non-emphysematous cysts, honeycombing, or traction bronchiectasis), and 3 = advanced ILD (presence of bilateral fibrosis in multiple lobes associated with honeycombing and traction bronchiectasis in a subpleural distribution). For the purposes of this study, patients in interstitial lung abnormality categories 2 and 3 were considered to have RA-ILD.

Pulmonary function tests. PFTs obtained as part of enrollment protocols were assessed according to ATS recommendations (36). PFTs performed for clinical indications in individuals with known/suspected ILD were included if completed within 3 months of serum sampling. Among prospectively recruited patients from the VA cohort and the Non-VA cohort, the median time span between serum sampling and PFT assessment was 46 days (IQR 27–101) and 33 days (IQR 16–67), respectively. Reference values for FVC and FEV₁ were derived from the Third National Health and Nutrition Examination Survey (36). Percent predicted values for these parameters, as well as diffusing capacity for carbon monoxide (DL_{CO}) corrected for hemoglobin, were used to assess the severity of ventilatory/functional deficits.

Multiplex enzyme-linked immunosorbent assays (ELISAs). Serum levels of selected cytokines, chemokines, growth factors, and MMPs (Supplementary Table 1, available on the *Arthritis & Rheumatology* web site at <http://onlinelibrary.wiley.com/doi/10.1002/art.41123/abstract>) were measured using a

Luminex xMAP bead-based multiplex ELISA (EMD Millipore) in a 96-well format. With the exception of IPF samples, which were assessed in 2 batches, direct biomarker comparisons (e.g., VA RA-ILD versus VA RA-no ILD, Non-VA RA-ILD versus Non-VA RA-no ILD) were based on assays in which relevant sera were evaluated at the same time; nevertheless, technical replicates of representative samples were performed to ensure internal consistency as well as interassay reliability.

Statistical analysis. While categorical demographic data were compared using Fisher's exact test or chi-square test, continuous variables (including multiplex ELISA-derived serum protein levels) were compared between disease subgroups and relevant controls (e.g., RA-ILD versus RA-no ILD, IPF versus healthy controls) by 2-sample *t*-test (unequal variance). Regression models evaluating the relationship between individual biomarker levels and disease state were adjusted for potential confounding factors such as age, sex, Disease Activity Score in 28 joints (DAS28) (37), and smoking history. Medication profiles were not included as confounders because of concerns regarding misclassification, particularly with respect to timing of administration and dose. To avoid overfitting these models, we also excluded variables (such as race) that did not show statistically significant differences between disease subgroups. Finally, DAS28 was imputed for 14 of 71 patients in the Non-VA cohort using average DAS28 values in the appropriate subset of RA patients with or without ILD.

To demonstrate the strength of underlying biomarker associations with RA-ILD or IPF, volcano plots were constructed according to established methods, with adjustment of *P* values for multiple comparisons using the Benjamini-Hochberg correction (38) and a false discovery rate of 0.1. Principal component analysis (PCA) was used as a data reduction method to identify combinatorial signatures of serum proteins as well as potential functional groupings between signaling mediators associated with different disease subcategories (39). In each cohort, PCA was performed with logistic regression to discriminate between ILD and non-ILD control groups, using biomarkers that had uncorrected *P* values of less than 0.05 in age-, sex-, and DAS28-adjusted comparisons. Corresponding loading plots were generated using components with an eigenvalue of >1.0. Finally, least absolute shrinkage and selection operator (LASSO) modeling (40) was used as a penalized regression tool to develop a clinical prediction algorithm for detecting the presence of RA-ILD. For each cohort, we determined the lowest shrinkage parameter (λ) with which to select final protein biomarkers (and their coefficients) for predicting the probability of being diagnosed as having RA-ILD. Receiver operator characteristic (ROC) curves were then generated to assess the ability of algorithm-based predictions to discriminate between the presence versus absence of RA-ILD (as measured by area under the curve [AUC]). Statistical analyses were performed using Stata 15 and R package software. *P* values less than 0.05 were considered significant.

RESULTS

Cohort characteristics. In this analysis, we assessed a combined VA cohort of RA patients from a national database (the VARA registry) as well as prospectively enrolled patients recruited from 3 VA rheumatology centers. While patients enrolled from the VARA registry had diagnostic codes as well as imaging evidence of RA-ILD, prospectively recruited individuals in the VA cohort (all with an underlying diagnosis of RA) manifested different stages of ILD ranging from no ILD to UIP-like radiographic abnormalities. Overall, the frequency of subclinical ILD (absence of dyspnea, cough, or known history of ILD) was ~30% in prospectively recruited VA patients (those listed in Table 1 as well as additional patients who did not undergo biomarker assessment based on time of enrollment), which is consistent with prevalence values reported in non-VA cohorts (41–47).

Table 1 shows that the combined VA-derived cohort of RA patients predominantly consisted of white male ever smokers, though the prevalence of ever smoking versus never smoking was highly skewed in RA-ILD subgroups compared to subgroups with RA–no ILD (88% versus 41%, respectively;

$P = 0.0001$). Consistent with these differences in frequency of ever smoking, the prevalence of coexisting cardiovascular disease and/or chronic obstructive pulmonary disease (COPD) was much higher in the RA-ILD subgroup, with the prevalence of COPD reaching statistical significance ($P < 0.05$). In this cohort of RA patients, no statistically significant differences in articular disease activity (as measured by DAS28 scores) or prednisone usage emerged between individuals with ILD and those without ILD, but there were differences in the ever use of methotrexate and tumor necrosis factor inhibitors between these subgroups, with usage of both drugs found to be higher in the RA–no ILD subgroups ($P < 0.05$). Median anti-CCP-2 concentrations were higher in the RA-ILD subgroup compared to the RA–no ILD subgroup (147 units/ml [IQR 23–309] versus 28 units/ml [IQR 2–106]; $P = 0.01$); however, RF levels could not be directly compared due to use of alternative laboratory scales in different VA centers.

Broad comparison of the VA-RA and IPF cohorts demonstrated similar demographic characteristics, as IPF patients were also predominantly white men with a high rate of ever smoking (68%). Importantly, these characteristics differed from

Table 1. Cohort characteristics*

	VA RA–no ILD (n = 17)	VA RA-ILD (n = 86)	Non-VA RA–no ILD (n = 22)	Non-VA RA-ILD (n = 49)	Healthy controls (n = 36)	IPF (n = 100)
Demographics						
Age, median (IQR) years	57 (44–60)	64 (58–73)†	49 (44–55)	65 (58–75)†	65 (60–68)	70 (62–75)
Male sex, no. (%)	11 (65)	82 (95)†	5 (24)	18 (37)	23 (64)	67 (67)
White, no. (%)	9 (53)	61 (71)	15 (71)	37 (76)	31 (86)	95 (98)
RA duration, median (IQR) years	10 (4–16)	10 (3–16)	8 (2–11)	13 (5–20)	–	–
Smoking ever, no. (%)	7 (41)	76 (88)†	8 (42)	27 (55)	17 (52)	65 (68)
Comorbidities, no. (%)						
Cardiovascular disease	1 (6)	18 (21)	1 (5)	5 (10)	–	–
Diabetes mellitus	5 (29)	18 (21)	1 (5)	9 (18)	–	–
Chronic kidney disease	0 (0)	6 (7)	0 (0)	1 (2)	–	–
COPD	1 (6)	30 (35)†	0 (0)	5 (10)	–	–
Malignancy‡	1 (6)	12 (14)	0 (0)	3 (6)	–	–
RA parameters, median (IQR)						
RF by nephelometry	–	234 (69–498)	33 (22–66)	76 (22–329)	–	–
Anti-CCP-2, units/ml	28 (2–106)	147 (23–309)†	99 (30–280)	54 (9–316)	–	–
DAS28§	4.1 (3.2–4.2)	3.7 (2.8–4.6)	3.4 (2.2–4.5)	3.5 (2.7–4.3)	–	–
Medications ever, no. (%)						
Prednisone	14 (82)	58 (68)	15 (68)	28 (57)	–	–
Methotrexate	15 (88)	40 (47)†	14 (67)	30 (63)	–	–
Leflunomide	4 (24)	4 (22)	2 (9)	14 (29)	–	–
TNF α inhibitor	14 (82)	36 (42)†	2 (9)	9 (18)	–	–
Pulmonary function tests, median (IQR) % predicted						
FEV ₁	79 (67–90)	79 (71–87)	105 (95–112)	77 (65–90)†	–	85 (66–95)
FVC	84 (74–93)	83 (75–90)	104 (89–113)	71 (63–89)†	–	72 (57–82)
DLco	79 (74–86)	62 (55–70)†	83 (75–97)	50 (43–72)†	–	49 (38–60)

* For several of the variables, there were some missing data in ≥ 1 of the cohorts. See Patients and Methods for a description of the study groups. RA–no ILD = rheumatoid arthritis without interstitial lung disease; IPF = idiopathic pulmonary fibrosis; IQR = interquartile range; COPD = chronic obstructive pulmonary disease; RF = rheumatoid factor; anti-CCP-2 = anti-cyclic citrullinated peptide 2; TNF α = tumor necrosis factor α ; FEV₁ = forced expiratory volume in 1 second; FVC = forced vital capacity; DLco = diffusing capacity for carbon monoxide.

† $P < 0.05$ versus RA–no ILD group.

‡ Excludes nonmelanoma skin cancers; no active malignancy at time of serum sampling.

§ The Veterans Affairs (VA) cohort was assessed with the Disease Activity Score in 28 joints (DAS28), and the Non-VA cohort was assessed with the 3-variable DAS28 using the erythrocyte sedimentation rate (ESR), with ESR obtained >3 months from joint counts in 11 of 57 patients.

those of the Non-VA RA cohort, where the sex distribution (37% male) and smoking rates (55% ever smokers) among individuals with RA-ILD were more balanced than in the VA-RA cohort or IPF cohort (Table 1). In parallel with these observations, current smoking rates among RA-ILD patients in the VA cohort greatly exceeded those among RA-ILD patients in the Non-VA cohort (38.4% versus 12.2%; $P = 0.001$ [data not shown]). In contrast to these demographic discrepancies, composite PFT abnormalities were similar in the Non-VA and VA subgroups of RA-ILD (notwithstanding the lack of available

PFT data for the VARA registry component of the combined VA cohort), with mild restrictive deficits and moderate reduction in DLco that were generally less severe than corresponding deficits observed in the IPF cohort (Table 1).

Biomarker profiling. To establish peripheral blood biomarker profiles in individuals from the RA and IPF cohorts, we measured serum levels of 45 proteins consisting of cytokines, chemokines, growth factors, and remodeling proteins (MMPs) previously studied in IPF (28) and/or other forms of connective

Table 2. Distinguishing biomarkers in RA-ILD and IPF*

Cohort, protein	Age/sex/DAS28		Age/sex/DAS28/CS		Cohort, protein	Age/sex/DAS28		Age/sex/DAS28/CS	
	P†	Fold‡	P†	Fold‡		P†	Fold‡	P†	Fold‡
VA cohort					<i>(Non-VA cohort cont'd)</i>				
MMP-9	1.1×10^{-5}	2.12	-	-	Fractalkine	-	-	0.003	5.31
MMP-1	7.0×10^{-5}	2.24	-	-	IL-1β	-	-	0.010	11.3
MMP-10	7.7×10^{-5}	1.79	-	-	FGF2	-	-	0.011	4.82
Eotaxin	1.5×10^{-4}	1.53	-	-	IL-7	-	-	0.013	6.32
GRO1	0.001	1.51	-	-	VEGF	-	-	0.013	2.12
MIP-1β	0.001	2.69	-	-	Flt-3L	-	-	0.015	8.32
IL-8	0.004	61.2	-	-	IL-2	-	-	0.017	8.60
MCP-3	0.005	2.26	-	-	IL-15	-	-	0.017	7.12
MMP-7	0.007	1.46	-	-	IFNa2	-	-	0.018	7.23
MMP-2	0.014	1.17	-	-	IL-9	-	-	0.021	7.53
TGFα	0.016	3.07	-	-	GM-CSF	-	-	0.023	8.43
TNFα	0.024	2.12	-	-	TGFα	-	-	0.025	6.54
MMP-2	-	-	0.001	1.28	IL-12p70	-	-	0.025	5.73
MMP-10	-	-	0.003	1.86	MIP-1β	-	-	0.028	2.34
GRO1	-	-	0.003	1.53	IL-1α	-	-	0.030	5.28
MMP-9	-	-	0.004	1.85	IPF cohort§				
Eotaxin	-	-	0.004	1.40	MMP-2	1.2×10^{-16}	1.58	-	-
MMP-1	-	-	0.006	2.17	MDC	2.5×10^{-10}	1.50	-	-
IL-8	-	-	0.011	49.2	MCP-1	1.6×10^{-8}	1.53	-	-
MIP-1β	-	-	0.017	2.30	MMP-7	7.3×10^{-8}	1.70	-	-
MMP-7	-	-	0.018	1.43	Eotaxin	1.5×10^{-5}	1.39	-	-
Non-VA cohort					MMP-9	1.6×10^{-5}	1.45	-	-
Fractalkine	0.008	4.81	-	-	Flt-3L	5.7×10^{-4}	4.02	-	-
IL-1β	0.008	11.8	-	-	CXCL9	0.008	0.71	-	-
FGF2	0.008	5.07	-	-	IL-8	0.011	1.63	-	-
IL-7	0.009	6.19	-	-	MMP-2	-	-	3.0×10^{-15}	1.58
Flt-3L	0.009	8.84	-	-	MDC	-	-	3.9×10^{-10}	1.53
IL-15	0.009	7.65	-	-	MCP-1	-	-	4.0×10^{-8}	1.54
IL-2	0.010	9.32	-	-	MMP-7	-	-	3.6×10^{-7}	1.69
GM-CSF	0.012	9.37	-	-	MMP-9	-	-	1.1×10^{-5}	1.49
IL-9	0.013	8.06	-	-	Eotaxin	-	-	7.9×10^{-5}	1.37
IFNa2	0.013	7.38	-	-	Flt-3L	-	-	0.001	4.32
TNFα	0.016	2.36	-	-	CXCL9	-	-	0.010	0.71
IL-12p40	0.019	5.22	-	-	IL-8	-	-	0.011	1.70
IL-12p70	0.020	5.91	-	-					

* The VA cohort consisted of 17 RA-no ILD patients and 86 RA-ILD patients; the Non-VA cohort consisted of 22 RA-no ILD patients and 49 RA-ILD patients; the IPF cohort consisted of 100 IPF patients and 38 healthy controls. For several of the variables, there were some missing data in ≥1 of the cohorts. See Patients and Methods for a description of the study groups. CS = cigarette smoking; MMP-9 = matrix metalloproteinase 9; GRO1 = growth-related oncogene 1; MIP-1β = macrophage inflammatory protein 1β; IL-8 = interleukin-8; MCP-3 = monocyte chemoattractant protein 3; TGFα = transforming growth factor α; FGF2 = fibroblast growth factor 2; Flt-3L = Flt-3 ligand; GM-CSF = granulocyte-macrophage colony-stimulating factor; IFNa2 = interferon-α2; VEGF = vascular endothelial growth factor; MDC = macrophage-derived chemokine (see Table 1 for other definitions).

† P values (determined by 2-sample t-test) comparing serum protein levels in the RA-ILD versus RA-no ILD and the IPF versus healthy control subgroups.

‡ Ratio of mean serum protein levels in RA patients with ILD versus those without ILD, and in IPF patients versus healthy controls.

§ DAS28 not included in adjustment.

tissue disease-associated ILD (48) (Supplementary Table 1, available on the *Arthritis & Rheumatology* web site at <http://onlinelibrary.wiley.com/doi/10.1002/art.41123/abstract>). As shown in Supplementary Table 2 at <http://onlinelibrary.wiley.com/doi/10.1002/art.41123/abstract>, unadjusted analyses revealed a number of biomarkers with statistically significant differences between patients with RA-ILD and RA-no ILD patients in the VA cohort, even after correction for multiple comparisons. Adjustment for age, sex, DAS28, and smoking history in corresponding regression models of the VA cohort yielded a narrower range of distinguishing biomarkers that featured particularly strong associations between RA-ILD and eotaxin, growth-related oncogene 1 (GRO1)/CXCL1, MMP-1, MMP-2, MMP-9, and MMP-10 (Table 2; Supplementary Table 3, available on the *Arthritis & Rheumatology* web site at <http://onlinelibrary.wiley.com/doi/10.1002/art.41123/abstract>).

Parallel assessment of biomarker levels in the Non-VA cohort revealed a different profile of RA-ILD-associated mediators in models adjusted for age, sex, DAS28, and smoking, as fractalkine/CX3CL1, IL-1 α , IL-2, IL-7, IL-15, interferon- α 2 (IFN α 2), Flt-3 ligand (Flt-3L), fibroblast growth factor 2 (FGF-2), and vascular endothelial growth factor manifested the strongest associations with this disease subset (Table 2; Supplementary Table 3). In these models, we did not adjust for use of medications such as methotrexate, as biomarker levels in patients with RA-ILD did not differ significantly based on the use of this medication (data not shown).

Comparative analysis of IPF demonstrated a more restricted panel of elevated serum proteins (relative to healthy controls), many of which overlapped with the profile of mediators associated with RA-ILD (Table 2 and Supplementary Tables 3 and 4, <http://onlinelibrary.wiley.com/doi/10.1002/art.41123/abstract>). Of note, however, the range of markers shared with IPF in adjusted analyses differed between the VA and Non-VA subgroups of RA-ILD (Figure 1). While increased serum levels of eotaxin, IL-8, MMP-2, MMP-7, and MMP-9 characterized both IPF and the VA subgroup with RA-ILD, elevated concentrations of Flt-3L alone cosegregated with IPF in the Non-VA subgroup with RA-ILD. Macrophage-derived chemokine/CCL22 and monocyte chemoattractant protein 1 (MCP-1)/CCL2, however, were uniquely associated with IPF.

Strength of associations and functional correlations.

As shown in Table 2 and in volcano plots derived from adjusted models (Figure 2), a number of the serum proteins that were elevated in RA-ILD relative to RA-no ILD in the VA cohort retained statistical significance even after correction for multiple comparisons in the VA cohort. Importantly, 3 of the 6 most preferentially expressed markers were shared between this subset of RA-ILD and IPF (eotaxin, MMP-2, and MMP-9), although the fold amplification and significance levels were generally less than those seen in IPF (Figures 2A and C). Parallel assessment of the Non-VA RA-ILD cohort demonstrated more significant amplification of serum proteins encompassing a dif-

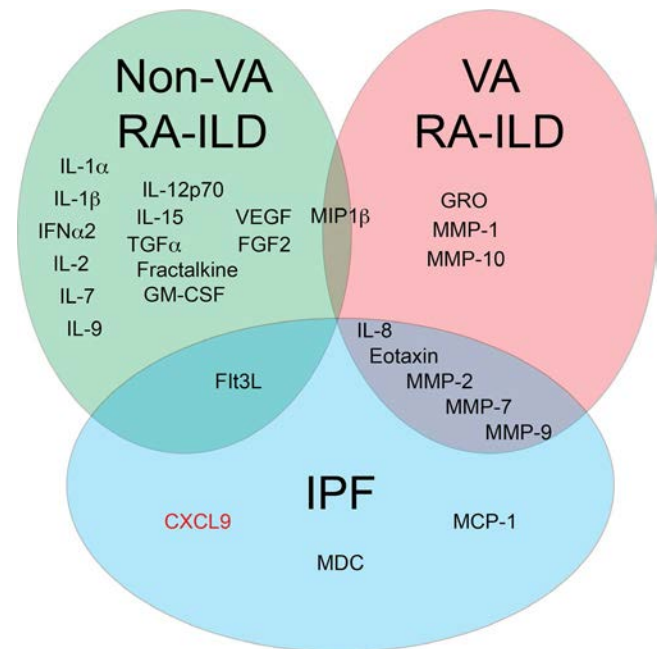


Figure 1. Differential overlap between idiopathic pulmonary fibrosis (IPF) and rheumatoid arthritis-associated interstitial lung disease (RA-ILD) in a Veterans Affairs (VA) cohort and Non-VA comparator cohort of RA patients. Partially overlapping expression profiles of different serum proteins are shown in a Venn diagram. Mediators depicted in this diagram include those that distinguish RA-ILD from RA without ILD (RA-no ILD) in the VA and Non-VA cohorts (after adjustment for age, sex, Disease Activity Score in 28 joints, and smoking history) and those that differentiate IPF from healthy controls (following adjustment for age, sex, and smoking history). Black font indicates increased expression relative to respective control groups, and red font indicates decreased levels relative to control groups. IL-1 α = interleukin-1 α ; IFN α 2 = interferon- α 2; TGF α = transforming growth factor α ; GM-CSF = granulocyte-macrophage colony-stimulating factor; VEGF = vascular endothelial growth factor; FGF2 = fibroblast growth factor 2; MIP-1 β = macrophage inflammatory protein 1 β ; GRO = growth-related oncogene/CXCL1; MMP-1 = matrix metalloproteinase 1; Flt-3L = Flt-3 ligand; MCP-1 = monocyte chemoattractant protein 1; MDC = macrophage-derived chemokine.

ferent array of markers (Figure 2B), only 1 of which was shared with the IPF cohort (Flt-3L).

To further address statistical issues associated with multiple comparisons and explore potential functional associations between signaling mediators, PCA was performed in the RA and IPF cohorts (Figures 3A–C). Of note, the odds ratios for RA-ILD exceeded 4 in the first 2 principal components (P1 and P2) of the fully adjusted model in the VA cohort ($P < 0.05$). Moreover, the corresponding loading plots (of component signaling mediators) for the VA-RA cohort (Figure 3D) demonstrated covariance/colocalization in 2 subgroups of MMPs (MMP-2 and MMP-7, versus MMP-1, MMP-9, and MMP-10) as well as a group of proinflammatory/profibrotic mediators associated with macrophage activation that included macrophage inflammatory protein 1 β (MIP-1 β), MCP-3, and tumor necrosis factor α (TNF α). Compari-

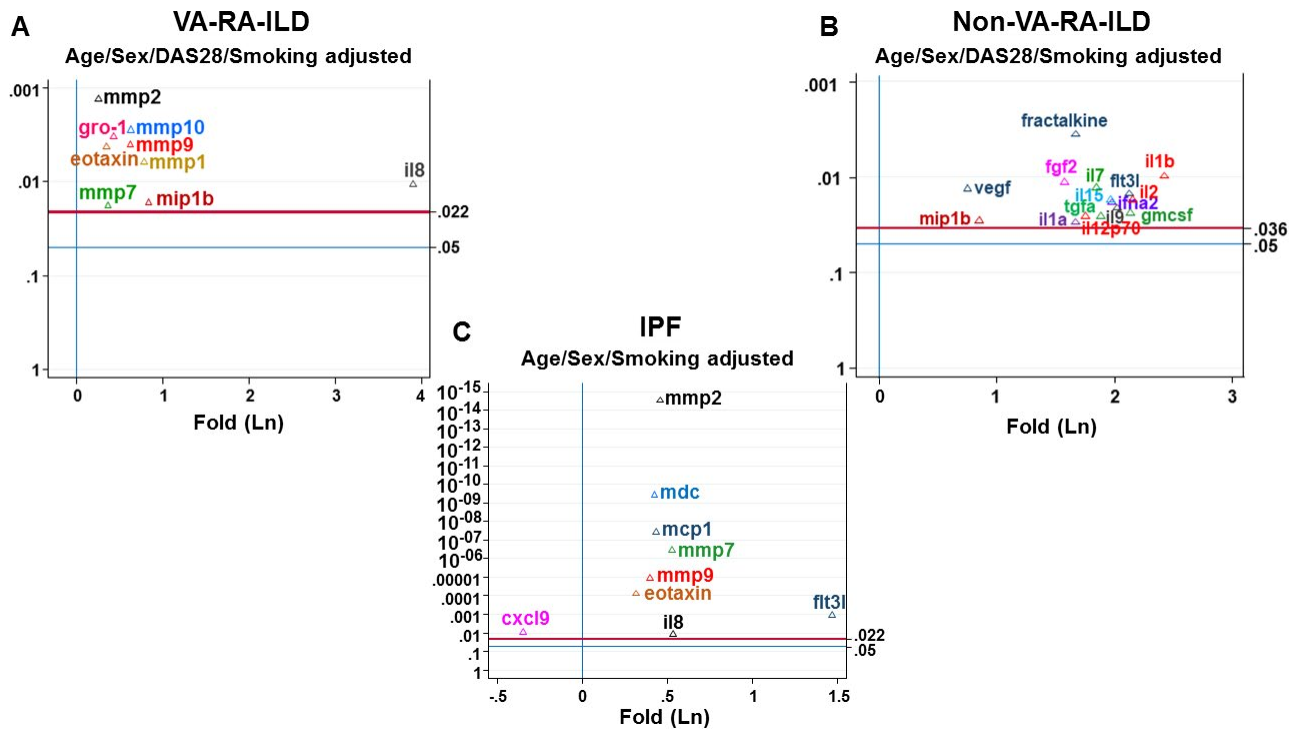


Figure 2. Strength and significance of serum protein biomarker associations. Volcano plots depict amplification (x-axis) versus *P* value (y-axis) of designated serum proteins in RA-ILD patients (A and B) and IPF patients (C) relative to RA–no ILD patients and healthy controls, respectively. Individual plots correspond to adjusted analyses, as indicated. Red lines show *P* values that correspond to a Benjamini-Hochberg *q* cutoff value of 0.1. DAS28 = Disease Activity Score in 28 joints; Ln = natural logarithm (see Figure 1 for other definitions).

son of the loading and PCA plots for the VA cohort (Figures 3A and D) indicated that these putative functional groups drive differences between RA-ILD and RA–no ILD in P2 and P1, respectively. In contrast, most of the variance in the Non-VA cohort was encompassed by a single principal component (which had a statistically significant odds ratio of 5.3 for RA-ILD [Figure 3B]), precluding meaningful analysis of loading plots for functional grouping of mediators.

Clinical prediction. To develop complementary clinical prediction tools capable of distinguishing RA-ILD from RA–no ILD in the VA and Non-VA cohorts, we applied LASSO modeling—a machine learning–based, penalized regression method designed to minimize data complexity and maximize precision. This analysis demonstrated that a 7 biomarker signature consisting of MMP-1, MMP-2, MMP-7, MMP-9, IL-1 receptor antagonist, soluble CD40L, and CXCL9 effectively differentiated RA-ILD from RA–no ILD with high sensitivity and specificity in the VA cohort, yielding an AUC of 0.93 (Figure 4 and Supplementary Figure 1, available on the *Arthritis & Rheumatology* web site at <http://onlinelibrary.wiley.com/doi/10.1002/art.41123/abstract>). Comparison of these protein mediators with functional groupings determined by PCA revealed significant overlap, particularly among the MMPs (MMP-1, MMP-2, MMP-7, and MMP-9). Although the P1-dominated PCA analysis did not allow for similar comparisons in the Non-VA cohort, LASSO modeling also yielded a highly discriminatory

regression model incorporating normalized serum levels of FGF-2, soluble CD40L, IP-10, MCP-1, MMP-2, MMP-7, and MMP-9 (Figure 4). In both the VA and Non-VA cohorts, AUC values derived from serum protein–based LASSO algorithms greatly exceeded those obtained from parallel ROC analysis (data not shown) of serologic markers such as CCP-2 antibody levels, with AUC LASSO versus AUC CCP-2 values of 0.93 and 0.71, respectively, in the VA cohort and 0.93 versus 0.46, respectively, in the Non-VA cohort.

DISCUSSION

Through multiplex ELISA–based assays and a series of complementary statistical models, we have shown that a number of serum protein biomarkers are associated with the presence of ILD in independent cohorts of RA patients. Even after adjustment for potential confounders such as age, sex, DAS28 score, and smoking history, resulting models demonstrated that selected markers, which fall into the broader categories of proinflammatory cytokines/chemokines (eotaxin, GRO-1, MIP-1 β , and IL-8) and MMPs (MMP-1, MMP-2, MMP-7, MMP-9, and MMP-10), reliably differentiate RA-ILD from RA–no ILD in the VA cohort. Importantly, PCA and covariance of selected protein mediators in associated loading plots suggested particular inflammatory and remodeling pathways that may be operative in this cohort of RA-ILD characterized by the predominance of male smokers. At the same

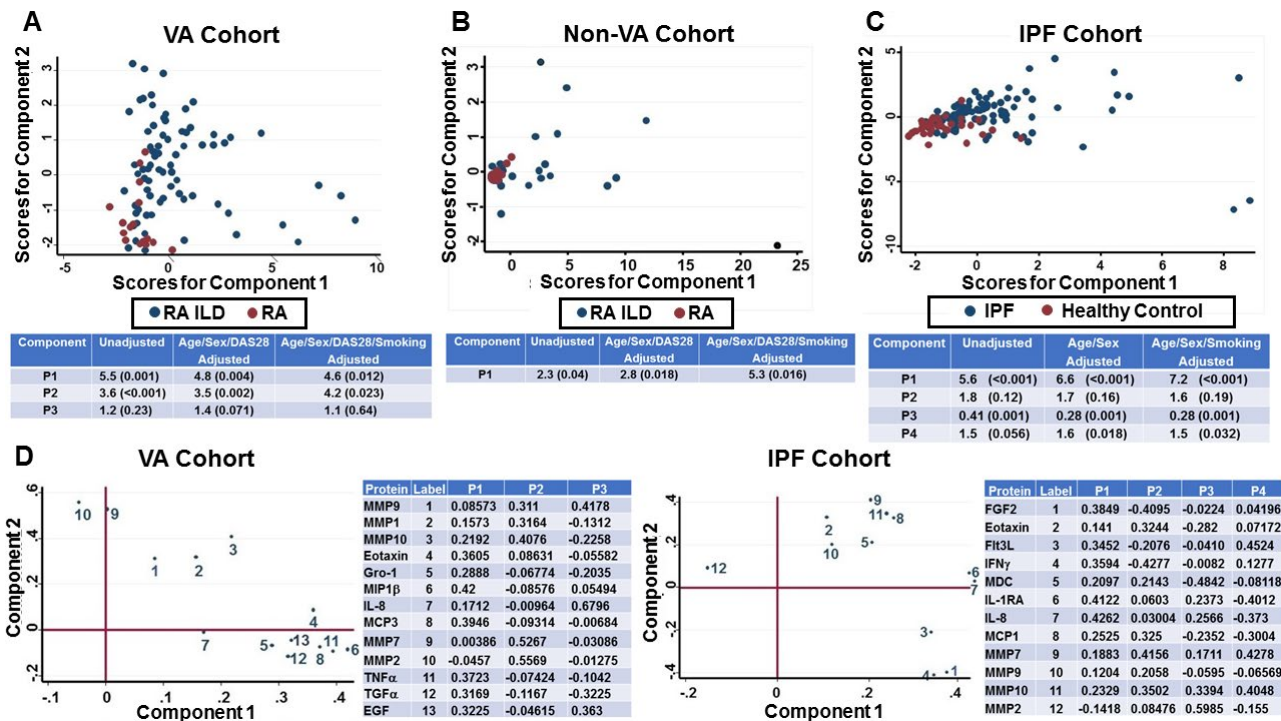


Figure 3. Principal component analysis (PCA) of the RA-ILD and IPF cohorts. **A**, PCA of the VA cohort of RA patients with and those without ILD (17 RA-no ILD patients and 68 RA-ILD patients with evaluable data). **B**, Parallel analyses of the Non-VA RA cohort (22 RA-no ILD patients and 49 RA-ILD patients). **C**, PCA of 95 IPF patients versus 36 healthy controls. Accompanying tables in **A–C** include odds ratios for the RA-ILD and IPF cohorts and *P* values for each of the principal components derived from serum proteins identified as significant discriminators in adjusted regression models. **D**, Loading plots that correspond to principal components 1 and 2 for the VA RA cohort and IPF cohort. Accompanying tables include eigenvectors (loadings) for designated mediators in each of the specified PCs. The percents of variance encompassed by principal components contributing to these models in the RA and IPF cohorts are as follows: VA cohort P1 = 38%, P2 = 14%, and P3 = 11%; Non-VA cohort P1 = 92%; and IPF cohort P1 = 30%, P2 = 17%, P3 = 12%, and P4 = 9%. TNF α = tumor necrosis factor α ; EGF = epidermal growth factor α ; IL-1Ra = IL-1 receptor antagonist (see Figure 1 for other definitions).

time, LASSO modeling demonstrated that different combinations of serum proteins, which include a number of MMPs as well as the proinflammatory chemokine CXCL9, can reliably discriminate between RA-ILD and RA-no ILD in the VA cohort and are important molecular biomarkers of this damaging extraarticular disease manifestation.

Intriguingly, comparative analyses demonstrated that the range of biomarkers associated with RA-ILD in fully adjusted models is quite different between the VA and Non-VA cohorts included in this study (Figure 1). In particular, our results failed to identify IP-10/CXCL10 as an important functional/clinical indicator of RA-ILD in the VA cohort, contrasting with earlier studies that have implicated this CXCR3-binding chemokine in other (non-VA) US and Chinese RA-ILD cohorts (16). Conversely, the preferential association between eotaxin and RA-ILD in the VA cohort suggests that activation of fibroblasts, as well as recruitment of eosinophils and neutrophils (all of which express CCR3, the receptor for eotaxin/CCL11 [49,50]), may play a more prominent role in selected subsets of RA-ILD represented by the VA cohort. Consistent with this notion, the remaining mediators that are uniquely associated with RA-ILD in the VA cohort (IL-8, GRO-1/CXCL1, MMP-1, MMP-2, MMP-7, MMP-9, and MMP-10) have collectively been

linked to neutrophil chemotaxis, macrophage activation, and tissue remodeling—processes that also occur in IPF (24,25). As shown in Figure 1, this overall “profibrotic” profile contrasts with the predominance of proinflammatory cytokines (e.g., IL-1 α , IL-1 β , IL-2, IL-7, IL-9, IL-12p70, IL-15, and IFN α 2) associated with RA-ILD in the Non-VA cohort.

Viewed more broadly, the observed discrepancies between these RA-ILD subpopulations undoubtedly highlight unique characteristics of our VA cohort, including its predominance of male patients and high prevalence of ever smoking (>80%). Of note, these demographic features resemble those of patients with IPF, potentially explaining the significant degree of overlap in selected biomarkers (particularly remodeling proteins and profibrotic chemokines) that emerged from parallel assessment of the VA cohort and this alternative pulmonary-focused disorder. By extension, the differential overlap in mediators between IPF and the VA versus the Non-VA subgroups of RA-ILD (Figures 1–3) emphasizes the potential importance of sex as well as smoking and other environmental exposures unique to the VA population (such as Agent Orange, burn pits, etc.) in shaping critical signaling networks/disease pathways involved in the development of different RA-ILD phenotypes.

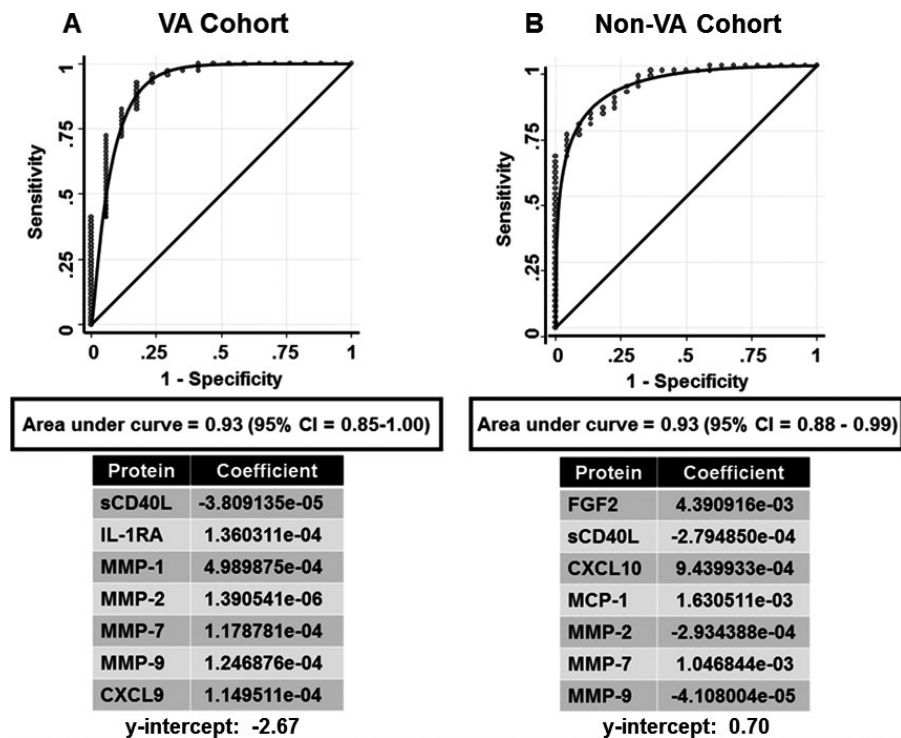


Figure 4. Least absolute shrinkage and selection operator (LASSO) modeling in the identification of RA-ILD. Application of machine learning-based LASSO regression modeling revealed a panel of serum protein biomarkers capable of predicting the presence of RA-ILD in the combined VA cohort (A) as well as the Non-VA cohort of RA patients with ILD and those without ILD (B). Tables show regression coefficients for specific serum proteins as well as y-intercepts for corresponding regression models. The accompanying receiver operator characteristic curves reflect performance characteristics of these models, as indicated by area under the curve values. 95% CI = 95% confidence interval; sCD40L = soluble CD40L; IL-1Ra = IL-1 receptor antagonist (see Figure 1 for other definitions).

Counterbalancing the partial overlap in protein markers linked to both RA-ILD and IPF, a number of other proinflammatory signaling molecules correlated more closely with RA-ILD (again, with differential associations in the VA and Non-VA cohorts). These observations likely reflect interactions between ILD and the underlying systemic autoimmune disease (RA) as well as potentially overlapping processes such as COPD, an important smoking-related disorder that is highly prevalent in the VA population (and in our VA RA-ILD cohort, as shown in Table 1) and has been linked to many of the non-IPF biomarkers associated with RA-ILD in this study (51).

The potential interaction between smoking and underlying disease state is highlighted by the frequently discordant relationship between smoking history and biomarker level in RA patients with versus those without ILD (Supplementary Figure 2, available on the *Arthritis & Rheumatology* web site at <http://online.library.wiley.com/doi/10.1002/art.41123/abstract>)—suggesting that smoking does not independently drive biomarker alterations but, instead, mediates effects through dysregulation of pathways that are primarily operative in the context of RA-ILD and/or other coexisting conditions such as COPD. Furthermore, while the levels of numerous biomarkers in RA-ILD subgroups are preferentially elevated among smokers (particularly in the VA cohort), notable exceptions include the CXCR3-binding

chemokines MIG/CXCL9, IP-10/CXCL10, and I-TAC/CXCL11, whose mean serum concentrations are much higher in non-smokers compared to smokers with RA-ILD (indicating that the impact of smoking is biomarker- and disease-dependent; Supplementary Figure 2). Collectively, these observations suggest that overall differences in biomarker profile between the VA and Non-VA cohorts could reflect differences in environmental exposures (both measured and unmeasured) that ultimately translate into activation of distinct signaling pathways corresponding to subsets of RA-ILD that cannot be characterized/classified by radiographic abnormalities alone.

Beyond these considerations, differences in the predominant histopathologic subtype of ILD in IPF (UIP) and the RA cohorts (which are marked by a paucity of histologically or radiographically documented RA-UIP) may also impact molecular signatures. In fact, subset analysis of RA-ILD patients with radiographic evidence of probable UIP (as defined in ref. 33) indicates even greater overlap in biomarker profiles with IPF (data not shown), though the small number of RA-ILD patients meeting radiographic criteria for probable UIP (13 patients in the VA cohort and 8 patients in the Non-VA cohort) precludes adequate assessment of statistical significance. Ultimately, intercohort comparisons involving additional RA populations with different histopathologic subtypes

and varied rates of smoking will be critical in defining the relative modulatory effects of disease state and environmental exposures (such as smoking) on peripheral blood biomarker profiles/molecular subphenotypes.

While our results are provocative, this study does have limitations. Because both the VA cohort and the Non-VA cohort are partly retrospective and heavily skewed toward clinically evident RA-ILD, for example, the clinical prediction models may be less applicable to those patients with subclinical RA-ILD (though the remarkable sensitivity of LASSO-derived algorithms, even among patients with subclinical RA-ILD, indicates that selected biomarker signatures can serve as effective screening tools to identify individuals who require additional diagnostic assessment with chest HRCT and/or PFTs). Moreover, the relatively small comparator groups of RA–no ILD may have introduced additional bias, limiting our capacity to account for other potential confounders such as COPD (particularly in the VA cohort) or determine whether differences in current versus ever smoking prevalence are more directly linked to the development of RA-ILD. By extension, the presence of clinical/demographic features that may be unique to our VA cohort (and that cannot be fully “controlled” in adjusted models) indicates that the observed biomarker profiles must be validated in other non-VA cohorts to fully assess the generalizability of our findings. Meticulous phenotypic and radiographic classification will be critical to this effort, as the development of well-characterized, appropriately sized subgroups encompassing all stages of RA-ILD (including indeterminate ILD) will be necessary to fully control for variables such as current versus former smoking (note that, with few exceptions, subgroup analysis of RA-ILD patients enrolled from the VARA registry did not reveal significant differences between biomarker levels in current versus ever smokers [data not shown]), alternative environmental exposures, medication usage, and comorbid illnesses.

Beyond these issues, the derivation of pathogenically relevant signaling pathways from PCA is inherently limited by the inability of such methods to prove causality—emphasizing the need for future *in vitro* experimental studies to confirm mediator networks suggested by this type of statistical analysis. At the same time, the lack of complete PFT data in the VA cohort (Table 1) precludes meaningful functional correlations with observed biomarker profiles that could further support the pathogenic and clinical relevance of selected mediators/pathways.

Despite these potential shortcomings, our study clearly shows that peripheral blood biomarker profiling represents a viable approach for 1) determining candidate signaling networks worthy of additional investigation and 2) developing clinically useful prediction tools capable of identifying “at-risk” individuals in whom more detailed screening for subclinical/early stage RA-ILD is needed. As such, this work establishes the foundation for prospective/longitudinal studies geared toward the development of additional models predictive of disease onset and/or progression. Equally important, elucidating signaling pathways that contribute to disease patho-

genesis in different RA-ILD cohorts will further define the impact of key environmental exposures (such as smoking), clarify mechanistic overlap with IPF, and suggest novel therapeutic targets for this potentially devastating extraarticular disease manifestation of RA.

AUTHOR CONTRIBUTIONS

All authors were involved in drafting the article or revising it critically for important intellectual content, and all authors approved the final version to be published. Dr. Ascherman had full access to all of the data in the study and takes responsibility for the integrity of the data and the accuracy of the data analysis.


Study conception and design. Kass, Glassberg, Chen, Rosas, Ascherman.
Acquisition of data. Nouraie, Glassberg, Ramreddy, Fernandez, Harlow, Zhang, Kerr, Reimold, Gibson, Dellaripa, Rosas, Oddis, Ascherman.
Analysis and interpretation of data. Kass, Nouraie, Ramreddy, Fernandez, Harlow, England, Mikuls, Oddis, Ascherman.

REFERENCES

- Hunter TM, Boytsov NN, Zhang X, Schroeder K, Michaud K, Araujo AB. Prevalence of rheumatoid arthritis in the United States adult population in healthcare claims databases, 2004–2014. *Rheumatol Int* 2017;37:1551–7.
- Shaw M, Collins BF, Ho LA, Raghu G. Rheumatoid arthritis-associated lung disease. *Eur Respir Rev* 2015;24:1–16.
- Bongartz T, Nannini C, Medina-Velasquez YF, Achenbach SJ, Crowson CS, Ryu JH, et al. Incidence and mortality of interstitial lung disease in rheumatoid arthritis: a population-based study. *Arthritis Rheum* 2010;62:1583–91.
- Brown KK. Rheumatoid lung disease. *Proc Am Thorac Soc* 2007;4:443–8.
- Raimundo K, Solomon JJ, Olson AL, Kong AM, Cole AL, Fischer A, et al. Rheumatoid arthritis-interstitial lung disease in the United States: prevalence, incidence, and healthcare costs and mortality. *J Rheumatol* 2019;46:360–9.
- Solomon JJ, Brown KK. Rheumatoid arthritis-associated interstitial lung disease. *Open Access Rheumatol* 2012;4:21–31.
- Vivero M, Padera RF. Histopathology of lung disease in the connective tissue diseases. *Rheum Dis Clin North Am* 2015;41:197–211.
- Klareskog L, Stolt P, Lundberg K, Källberg H, Bengtsson C, Grunewald J, et al. A new model for an etiology of rheumatoid arthritis: smoking may trigger HLA–DR (shared epitope)–restricted immune reactions to autoantigens modified by citrullination. *Arthritis Rheum* 2006;54:38–46.
- Alexiou I, Germeis A, Koutroumpas A, Kontogianni A, Theodoridou K, Sakkas LI. Anti-cyclic citrullinated peptide-2 (CCP2) autoantibodies and extra-articular manifestations in Greek patients with rheumatoid arthritis. *Clin Rheumatol* 2008;27:511–3.
- Aubart F, Crestani B, Nicaise-Roland P, Tubach F, Bollet C, Dawidowicz K, et al. High levels of anti-cyclic citrullinated peptide autoantibodies are associated with co-occurrence of pulmonary diseases with rheumatoid arthritis. *J Rheumatol* 2011;38:979–82.
- Kelly CA, Saravanan V, Nisar M, Arthanari S, Woodhead FA, Price-Forbes AN, et al. Rheumatoid arthritis-related interstitial lung disease: associations, prognostic factors and physiological and radiological characteristics—a large multicentre UK study. *Rheumatology (Oxford)* 2014;53:1676–82.
- Yang JA, Lee JS, Park JK, Lee EB, Song YW, Lee EY. Clinical characteristics associated with occurrence and poor prognosis of interstitial lung disease in rheumatoid arthritis. *Korean J Intern Med* 2019;34:434–41.
- Doyle TJ, Lee JS, Dellaripa PF, Lederer JA, Matteson EL, Fischer A, et al. A roadmap to promote clinical and translational research

- in rheumatoid arthritis-associated interstitial lung disease. *Chest* 2014;145:454–63.
14. Raghu G, Richeldi L, Jagerschmidt A, Martin V, Subramaniam A, Ozoux ML, et al. Idiopathic pulmonary fibrosis: prospective, case-controlled study of natural history and circulating biomarkers. *Chest* 2018;154:1359–70.
 15. Lee JS, Lee EY, Ha YJ, Kang EH, Lee YJ, Song YW. Serum KL-6 levels reflect the severity of interstitial lung disease associated with connective tissue disease. *Arthritis Res Ther* 2019;21:58.
 16. Chen J, Doyle TJ, Liu Y, Aggarwal R, Wang X, Shi Y, et al. Biomarkers of rheumatoid arthritis-associated interstitial lung disease. *Arthritis Rheumatol* 2015;67:28–38.
 17. Doyle TJ, Patel AS, Hatabu H, Nishino M, Wu G, Osorio JC, et al. Detection of rheumatoid arthritis-interstitial lung disease is enhanced by serum biomarkers. *Am J Respir Crit Care Med* 2015;191:1403–12.
 18. Kim EJ, Elicker BM, Maldonado F, Webb WR, Ryu JH, Van Uden JH, et al. Usual interstitial pneumonia in rheumatoid arthritis-associated interstitial lung disease. *Eur Respir J* 2010;35:1322–8.
 19. Solomon JJ, Ryu JH, Tazelaar HD, Myers JL, Tuder R, Cool CD, et al. Fibrosing interstitial pneumonia predicts survival in patients with rheumatoid arthritis-associated interstitial lung disease (RA-ILD). *Respir Med* 2013;107:1247–52.
 20. Spagnolo P, Rossi G, Cavazza A. Pathogenesis of idiopathic pulmonary fibrosis and its clinical implications [review]. *Expert Rev Clin Immunol* 2014;10:1005–17.
 21. King TE Jr, Pardo A, Selman M. Idiopathic pulmonary fibrosis. *Lancet* 2011;378:1949–61.
 22. Ryu JH, Moua T, Daniels CE, Hartman TE, Yi ES, Utz JP, et al. Idiopathic pulmonary fibrosis: evolving concepts. *Mayo Clin Proc* 2014;89:1130–42.
 23. White ES, Xia M, Murray S, Dyal R, Flaherty CM, Flaherty KR, et al. Plasma surfactant protein-D, matrix metalloproteinase-7, and osteopontin index distinguishes idiopathic pulmonary fibrosis from other idiopathic interstitial pneumonias. *Am J Respir Crit Care Med* 2016;194:1242–51.
 24. Wynn TA. Cellular and molecular mechanisms of fibrosis. *J Pathol* 2008;214:199–210.
 25. Drakopanagiotakis F, Wujak L, Wygrecka M, Markart P. Biomarkers in idiopathic pulmonary fibrosis. *Matrix Biol* 2018;68–9:404–21.
 26. Seibold MA, Wise AL, Speer MC, Steele MP, Brown KK, Loyd JE, et al. A common MUC5B promoter polymorphism and pulmonary fibrosis. *N Engl J Med* 2011;364:1503–12.
 27. Juge PA, Lee JS, Ebstein E, Furukawa H, Dobrinskikh E, Gazal S, et al. MUC5B promoter variant and rheumatoid arthritis with interstitial lung disease. *N Engl J Med* 2018;379:2209–19.
 28. Rosas IO, Richards TJ, Konishi K, Zhang Y, Gibson K, Lokshin AE, et al. MMP1 and MMP7 as potential peripheral blood biomarkers in idiopathic pulmonary fibrosis. *PLoS Med* 2008;5:e93.
 29. Guiot J, Moermans C, Henket M, Corhay JL, Louis R. Blood biomarkers in idiopathic pulmonary fibrosis. *Lung* 2017;195:273–80.
 30. Arnett FC, Edworthy SM, Bloch DA, McShane DJ, Fries JF, Cooper NS, et al. The American Rheumatism Association 1987 revised criteria for the classification of rheumatoid arthritis. *Arthritis Rheum* 1988;31:315–24.
 31. Mikuls TR, Kazi S, Copher D, Hooker R, Kerr GS, Richards JS, et al. The association of race and ethnicity with disease expression in male US veterans with rheumatoid arthritis. *J Rheumatol* 2007;34:1480–4.
 32. Raghu G, Remy-Jardin M, Myers JL, Richeldi L, Ryerson CJ, Lederer DJ, et al, on behalf of the American Thoracic Society, European Respiratory Society, Japanese Respiratory Society, and Latin American Thoracic Society. Diagnosis of idiopathic pulmonary fibrosis: an official ATS/ERS/JRS/ALAT clinical practice guideline. *Am J Respir Crit Care Med* 2018;198:e44–68.
 33. Raghu G, Collard HR, Egan JJ, Martinez FJ, Behr J, Brown KK, et al. An official ATS/ERS/JRS/ALAT statement: idiopathic pulmonary fibrosis—evidence-based guidelines for diagnosis and management. *Am J Respir Crit Care Med* 2011;183:788–824.
 34. Doyle TJ, Dellaripa PF, Batra K, Frits ML, Iannaccone CK, Hatabu H, et al. Functional impact of a spectrum of interstitial lung abnormalities in rheumatoid arthritis. *Chest* 2014;146:41–50.
 35. Hunninghake GM, Hatabu H, Okajima Y, Gao W, Dupuis J, Latourelle JC, et al. MUC5B promoter polymorphism and interstitial lung abnormalities. *N Engl J Med* 2013;368:2192–200.
 36. Culver BH, Graham BL, Coates AL, Wanger J, Berry CE, Clarke PK, et al. Recommendations for a standardized pulmonary function report: an official American Thoracic Society technical statement. *Am J Respir Crit Care Med* 2017;196:1463–72.
 37. Prevoo ML, van 't Hof MA, Kuper HH, van Leeuwen MA, van de Putte LB, van Riel PL. Modified disease activity scores that include twenty-eight-joint counts: development and validation in a prospective longitudinal study of patients with rheumatoid arthritis. *Arthritis Rheum* 1995;38:44–8.
 38. Benjamini Y, Hochberg Y. Controlling the false discovery rate: a practical and powerful approach to multiple testing. *J Royal Stat Soc B* 1995;57:289–300.
 39. Giuliani A. The application of principal component analysis to drug discovery and biomedical data. *Drug Discov Today* 2017;22:1069–76.
 40. Tibshirani R. Regression shrinkage and selection via the lasso. *J Royal Stat Soc B* 1996;58:267–88.
 41. Chen J, Shi Y, Wang X, Huang H, Ascherman D. Asymptomatic pre-clinical rheumatoid arthritis-associated interstitial lung disease. *Clin Dev Immunol* 2013;2013:406927.
 42. Dawson JK, Fewins HE, Desmond J, Lynch MP, Graham DR. Fibrosing alveolitis in patients with rheumatoid arthritis as assessed by high resolution computed tomography, chest radiography, and pulmonary function tests. *Thorax* 2001;56:622–7.
 43. Demir R, Bodur H, Tokoğlu F, Olcay I, Uçan H, Borman P. High resolution computed tomography of the lungs in patients with rheumatoid arthritis. *Rheumatol Int* 1999;19:19–22.
 44. Gabbay E, Tarala R, Will R, Carroll G, Adler B, Cameron D, et al. Interstitial lung disease in recent onset rheumatoid arthritis. *Am J Respir Crit Care Med* 1997;156:528–35.
 45. Georgiadis AN, Metafratzi ZM, Drosos AA. Pulmonary abnormalities in patients with early and longstanding rheumatoid arthritis [letter]. *J Rheumatol* 2009;36:444–5.
 46. Gochuico BR, Avila NA, Chow CK, Novero LJ, Wu HP, Ren P, et al. Progressive preclinical interstitial lung disease in rheumatoid arthritis. *Arch Intern Med* 2008;168:159–66.
 47. Mori S, Cho I, Koga Y, Sugimoto M. A simultaneous onset of organizing pneumonia and rheumatoid arthritis, along with a review of the literature. *Mod Rheumatol* 2008;18:60–6.
 48. Richards TJ, Eggebeen A, Gibson K, Yousem S, Fuhrman C, Gochuico BR, et al. Characterization and peripheral blood biomarker assessment of anti-Jo-1 antibody-positive interstitial lung disease. *Arthritis Rheum* 2009;60:2183–92.
 49. Huax F, Gharaee-Kermani M, Liu T, Morel V, McGarry B, Ullenbruch M, et al. Role of eotaxin-1 (CCL₁₁) and CC chemokine receptor 3 (CCR₃) in bleomycin-induced lung injury and fibrosis. *Am J Pathol* 2005;167:1485–96.
 50. Puxeddu I, Bader R, Piliponsky AM, Reich R, Levi-Schaffer F, Berkman N. The CC chemokine eotaxin/CCL₁₁ has a selective profibrogenic effect on human lung fibroblasts. *J Allergy Clin Immunol* 2006;117:103–10.
 51. Pinto-Plata V, Toso J, Lee K, Park D, Bilello J, Mullerova H, et al. Profiling serum biomarkers in patients with COPD: associations with clinical parameters. *Thorax* 2007;62:595–601.

Mediating Role of Bone Marrow Lesions, Synovitis, Pain Sensitization, and Depressive Symptoms on Knee Pain Improvement Following Substantial Weight Loss

S. Reza Jafarzadeh,¹  Tuhina Neogi,¹ Joshua J. Stefanik,² Jing-Sheng Li,³ Ali Guermazi,¹ Caroline M. Apovian,⁴ and David T. Felson⁵

Objective. Massive weight loss leads to marked knee pain reduction in individuals with knee pain, but the reason for the reduction in pain is unknown. This study was undertaken to quantify the contribution of magnetic resonance imaging (MRI)–evidenced changes in pain-sensitive structures, bone marrow lesions (BMLs), and synovitis, and changes in pain sensitization or depressive symptoms, to knee pain improvement after substantial weight loss.

Methods. Morbidly obese patients with knee pain on most days were evaluated before bariatric surgery or medical weight management and at 1-year follow-up for BMLs and synovitis seen on MRI, the pressure pain threshold (PPT) at the patella and the right wrist, depressive symptoms (using the Center for Epidemiologic Studies Depression scale [CES-D]), and Western Ontario and McMaster Universities Osteoarthritis Index (WOMAC) pain survey. Natural-effects models were used to quantify the extent that achieving a minimum clinically important difference (MCID) of $\geq 18\%$ on the WOMAC pain scale could be mediated by weight loss–induced changes in BMLs, synovitis, PPT, and depressive symptoms.

Results. Of 75 participants, 53.3% lost $\geq 20\%$ of weight by 1 year. Of these, 75% attained the MCID for pain improvement, compared with 34.3% in those who had $< 20\%$ weight loss. Mediation analyses suggested that, in those with at least 20% weight loss, the odds of pain improvement increased by 62%, 15%, and 22% through changes in patella PPT, wrist PPT, and CES-D, respectively, but pain improvement was not mediated by MRI changes in BMLs or synovitis.

Conclusion. Weight loss–induced knee pain improvement is partially mediated by changes in pain sensitization and depressive symptoms but is independent of MRI changes in BMLs and synovitis.

INTRODUCTION

Osteoarthritis (OA) is the most common cause of arthritis, which is estimated to affect 91.2 million adults in the US (1), making it a leading cause of disability. While pain is the most prominent cause of OA-related disability, the association between pain and structural features of joints affected by OA is incompletely understood. These structural features often include bone marrow

lesions (BMLs) and synovitis visualized by magnetic resonance imaging (MRI). Some studies have suggested an association of BMLs with pain (2–8) and synovitis (4,7–10), while others have suggested no association (11–14). In addition to structural features, there are reports of other factors that affect knee pain. For example, pain sensitization is associated with pain severity in knee OA (15), and a recent study suggested an improvement in pain sensitization following bariatric surgery (16). Further, sustained

Supported by the NIH (National Institute of Arthritis and Musculoskeletal and Skin Diseases grants P60AR047785 and K24AR070892 and National Institute on Aging grant R03AG060272). Dr. Felson's work was supported by the NIHR Biomedical Research Centre (paid to the University of Manchester).

¹S. Reza Jafarzadeh, DVM, MPVM, PhD, Tuhina Neogi, MD, PhD, Ali Guermazi, MD, PhD: Boston University School of Medicine, Boston, Massachusetts; ²Joshua J. Stefanik, MSPT, PhD: Boston University School of Medicine and Northeastern University, Boston, Massachusetts; ³Jing-Sheng Li, MS: The Boston University College of Health and Rehabilitation Sciences: Sargent College, Boston, Massachusetts; ⁴Caroline M. Apovian, MD: Boston Medical Center, Boston, Massachusetts; ⁵David T. Felson, MD, MPH: Boston University School of Medicine, Boston, Massachusetts, and University of

Manchester, NIHR Manchester Biomedical Research Centre, and Manchester University NHS Foundation Trust, Manchester, UK.

Dr. Guermazi owns stock or stock options in Boston Imaging Core Lab, LLC. Dr. Apovian has received consulting fees from Novo Nordisk, Eisai, Zafgen, Orexigen Therapeutics, EnteroMedics, GI Dynamics, Gelesis, Bariatrix, Xeno Pharmaceuticals, Biosciences, Rhythm Pharmaceuticals, and Scientific Intake (less than \$10,000 each) and owns stock or stock options in Science-Smart, LLC. No other disclosures relevant to this article were reported.

Address correspondence to S. Reza Jafarzadeh, DVM, MPVM, PhD, Boston University School of Medicine, Section of Rheumatology, Department of Medicine, 650 Albany Street, Suite X200, Boston, MA 02118. E-mail: srjafarz@bu.edu.

Submitted for publication March 28, 2019; accepted in revised form September 24, 2019.

depressive symptoms that often co-occur with OA (17) have been reported to be associated with pain severity (18).

Obesity is a major risk factor for OA (19), and is also associated with pain and depressive symptoms. Several studies have shown considerable improvement in knee pain following bariatric surgery (16,20,21), which results in substantial weight loss. However, no study to our knowledge has evaluated the extent to which changes in BMLs, synovitis, pain sensitization, or depressive symptoms contribute to pain improvement in individuals who experience substantial weight loss. A cause-specific assessment for the pain improvement would provide insight into the causes of knee pain in obese persons and might provide clues to effective pain-relieving treatments.

Our study focused on BMLs and synovitis assessed by longitudinal MRI evaluations, pain sensitization, and depressive symptoms measured pre- and postintervention, in morbidly obese subjects who experienced substantial weight loss after bariatric surgery or medical weight management. Specifically, we quantified the extent to which changes in BMLs, synovitis, pain sensitization, or depressive symptoms that may occur with substantial weight loss could mediate the effect of weight loss on knee pain improvement.

PATIENTS AND METHODS

Setting. Study participants were recruited from the Nutrition and Weight Management Center at Boston Medical Center. The study was approved by the Institutional Review Board at the Boston University Medical Campus. All participants provided written informed consent.

The eligible study participants included obese patients between 25 and 60 years of age who had a body mass index (BMI) of ≥ 35 kg/m² with a weight-related comorbidity or a BMI of ≥ 40 kg/m². In addition, subjects had to have experienced knee pain on most days for the past month and had to be able to undergo a knee MRI evaluation. If both knees were affected, the more painful knee was evaluated by MRI. Patients with a history of knee surgery or inflammatory arthritis were not eligible.

Following the baseline assessment, study participants received either medical weight management treatment or bariatric surgery. The medical weight management group received dietary recommendations with or without prescription medications that included phentermine (with or without topiramate), lorcaserin, bupropion (with or without naltrexone), or liraglutide. Dietary guidance consisted of 1,200–1,500 and 1,500–1,800 kcal/day high-protein, low-fat diets with or without meal replacements for women and men, respectively. In the bariatric surgery group, patients underwent either a laparoscopic Roux-en-Y gastric bypass or laparoscopic sleeve gastrectomy. It was recommended to the subjects in both treatment groups that they walk for a minimum of 30 minutes/day and perform resistance exercise twice weekly. The follow-up study visit occurred ~1 year after bariatric surgery or the baseline visit in the medical weight management group.

Measurements. All study participants underwent 3T MRI (Philips Achieva) and pulse sequences, including sagittal WATSc and 3-dimensional fat-saturation Spectral Attenuated Inversion Recovery. Semiquantitative MRI assessments consisted of paired readings of baseline and follow-up images by an experienced musculoskeletal radiologist using the MRI Osteoarthritis Knee Score (MOAKS) for BMLs and synovitis. The radiologist was blinded with regard to the treatment received and the weight loss experienced. For BMLs and synovitis in a knee, we examined the maximum (i. e., worst) score and the sum of scores for BMLs and synovitis, as previously described (22).

Pain sensitization was assessed by measuring pressure pain thresholds (PPTs) with a handheld algometer applied at a rate of 0.5 kg/second as the point at which the pressure first changed to slight pain. The PPT was obtained at the index patella and right wrist. The average of 3 consecutive PPT measurements was determined. Low patella and wrist PPTs are suggestive of greater pain sensitization. Depressive symptoms were assessed using the 20-item Center for Epidemiologic Studies Depression scale (CES-D) (23).

Knee-specific pain severity was assessed using the Western Ontario and McMaster Universities Osteoarthritis Index (WOMAC) pain subscale (24). We defined the minimum clinically important difference (MCID) for WOMAC pain as a reduction of $\geq 18\%$ in the WOMAC pain subscale score, as previously described (25).

Analytical approach. Characteristics of the study sample were represented by frequencies for binary and categorical covariates and by distribution summaries for continuous covariates. As in a prior study (22) and based on a cutoff determined using the approximate median distribution of weight loss, these descriptive statistics were stratified based on whether participants lost $\geq 20\%$ of weight by the 1-year follow-up visit. Changes in the mean PPT at the patella and wrist, and changes in the mean CES-D score between baseline and 1-year follow-up were evaluated by linear mixed-effects models, with random effects specified for subjects to account for the correlation due to repeated measurements on the same knees across visits (26).

We performed a causal mediation analysis to quantify the extent to which specific causal pathways allow weight loss to exert its effects on pain improvement. These potential causal pathways included an indirect effect, which is the extent of pain improvement attributable to weight loss–induced changes in BMLs, synovitis, patella and wrist PPTs, and CES-D score. The direct effect quantified any remaining effect not mediated by changes in BMLs, synovitis, patella and wrist PPTs, and CES-D score (Figure 1).

To estimate indirect and direct effects, we fit a natural-effects model (27), which is a flexible and robust method to decompose the overall total effect into specific potential causal pathways, without reliance on a restrictive linear parametric statistical model (28). These indirect and direct effects are defined based on the counterfactual framework for causal inference, which is the effect

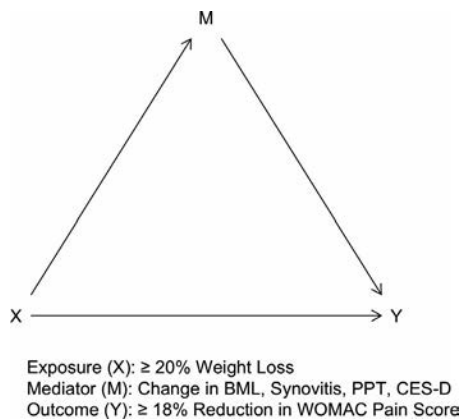


Figure 1. Directed acyclic graph representing the natural indirect effect (mediated by changes in bone marrow lesions [BMLs], synovitis, pain sensitization according to the patella and wrist pressure pain threshold [PPT], or depressive symptoms according to the Center for Epidemiologic Studies Depression scale [CES-D]; X to Y pathway through M) and the natural direct effect (not mediated; X to Y pathway not passing through M) of weight loss on knee pain improvement. WOMAC = Western Ontario and McMaster Universities Osteoarthritis Index.

that would have been observed if the exposure or mediator were absent in contrast to the observed data (29).

Mediated interaction. We assessed mediated interaction, which is the effect modification of natural effects between the exposure, weight loss, and the mediators, i. e., we assessed whether weight loss and BMLs, synovitis, patella or wrist PPTs, or CES-D score interact in their effect on pain improvement. In this effect decomposition, both indirect and direct effects are decomposed into pure indirect and pure direct effects in addition to the interactive effect, as previously described (30).

Interpretation of natural effects. Modern causal mediation analysis approaches rely on modeling techniques to estimate mediated/indirect effects under the counterfactual framework (for technical details, see ref. 31). These sets of parametric models or nonparametric (i. e., model-free) approaches allow an estimate of effect by changing treatment assignment (e. g., exposure level of $\geq 20\%$ and $<20\%$ weight loss) along specific pathways, but not along other pathways. A natural-effects model is one such approach that allows for model-free decomposition of exposure effect into indirect and direct effects. Identifying indirect and direct effects depends on 3 causal assumptions: exchangeability (e. g., those with $\geq 20\%$ weight loss, had they lost $<20\%$ of weight, would have experienced the same average outcome as those with $<20\%$ weight loss); consistency (e. g., the observed outcome for each subject with $\geq 20\%$ weight loss equals the counterfactual outcome if the subject lost $\geq 20\%$ of weight, and same for those with $<20\%$ weight loss); and positivity (e. g., there is a nonzero positive probability that each subject could lose $\geq 20\%$ or $<20\%$ of weight). Consequently, this counterfactual framework under

which causal mediating effects are estimated does not rely on other assumptions such as hypothesis testing to assess the statistical significance of the association between mediators and exposure (i. e., weight loss).

The natural direct effect was defined by Robins and Greenland (32) as the expected effect of an exposure on an outcome, while retaining the mediator constant at the level that would have naturally occurred in the absence of the exposure. The natural indirect effect provides an estimate for the effect of an exposure on an outcome if all subjects were exposed by setting the mediator to a level that would have occurred in the absence of the exposure. Note that in estimating the natural indirect effect, the exposure status remains constant, whereas the mediator level is held constant in the natural direct effect estimate (28).

Computation. We used the imputation-based approach developed by Vansteelandt et al (33) to estimate the parameters of the natural-effects model. In this approach, no model is specified for the distribution of the mediator; thus, unlike a competing approach that uses weighting, it is not sensitive to the potential misspecification of the mediator model, especially if the mediator is continuous (34). Nonetheless, in a sensitivity analysis, we calculated our effect measures using both imputation- and weighting-based approaches. Effects measures for our binary outcome

Table 1. Baseline characteristics of the study population (n = 75) stratified by weight loss at 1-year follow-up*

	<20% weight loss (n = 35)	$\geq 20\%$ weight loss (n = 40)
Age, years	47.3 \pm 8.3 (49.0)	42.5 \pm 9.6 (49.0)
Female, no. (%)	30 (85.7)	39 (97.5)
African American, no. (%)	27 (77.1)	19 (47.5)
Bariatric surgery, no. (%)	8 (22.9)	39 (97.5)
BMI, kg/m ²	40.9 \pm 4.5 (40.0)	42.3 \pm 4.5 (41.6)
College/graduate education, no. (%)	15 (42.9)	14 (35.0)
Employed, no. (%)	9 (25.7)	9 (22.5)
K/L grade, no. (%)		
0	6 (17.1)	8 (20.0)
1	11 (31.4)	11 (27.5)
2	8 (22.9)	14 (35.0)
3	9 (25.7)	7 (17.5)
4	1 (2.9)	0 (0.0)
WOMAC pain (0–24 scale)	12.5 \pm 4.9 (13.0)	11.8 \pm 4.2 (12.0)
BML worst score >0, no. (%)	24 (68.6)	24 (60.0)
Synovitis worst score >0, no. (%)	18 (51.4)	24 (60.0)
Patella PPT	429.6 \pm 198.1 (412.2)	345.4 \pm 158.0 (318.1)
Wrist PPT	346.4 \pm 150.0 (299.5)	351.7 \pm 144.9 (326.0)
CES-D	19.3 \pm 11.6 (17.5)	14.4 \pm 9.2 (11.5)

* Except where indicated otherwise, values are the mean \pm SD (median). BMI = body mass index; K/L = Kellgren/Lawrence; WOMAC = Western Ontario and McMaster Universities Osteoarthritis Index; BML = bone marrow lesion; PPT = pressure pain threshold; CES-D = Center for Epidemiologic Studies Depression scale.

were expressed as odds ratios (ORs), with corresponding 95% confidence intervals (95% CIs) calculated using the bootstrap technique. All analyses were implemented using R software version 3.4.0 (35) and the medflex library version 0.6-1 (36).

Sensitivity analyses. We examined weight loss of $\geq 20\%$ versus $< 20\%$ in our primary analyses. We additionally performed sensitivity analyses using a threshold of $\geq 10\%$ versus $< 10\%$ for weight loss, and another analysis in which we limited the analyses to subjects with BMLs or synovitis at baseline as well as a sensitivity analysis in which we compared mediating effects in bariatric surgery patients versus those in the medical weight management group regardless of percent weight loss.

RESULTS

Baseline data. Baseline characteristics of the study participants are presented in Table 1. There were 75 participants: 47 (63%) in the bariatric surgery group and 28 (37%) in the medical weight management group. Nearly half of the study

participants (40 [53%]) lost $\geq 20\%$ body weight by the 1-year follow-up visit; 39 of the 40 (97.5%) were from the bariatric surgery group.

On baseline MRI assessment, 64% (48 of 75) and 56% (42 of 75) of the participants had BMLs and synovitis, respectively, based on MOAKS scores of ≥ 1 (Table 1). Among patients who eventually experienced $\geq 20\%$ weight loss over the follow-up period, 60% (24 of 40) had BMLs and 60% had synovitis at baseline, compared with 68.6% (24 of 35) and 51.4% (18 of 35) who had baseline BMLs and synovitis, respectively, among patients who did not achieve $\geq 20\%$ weight loss by 1-year follow-up.

At baseline, neither patella PPT (mean difference -84.2 [95% CI $-2.9, 171.2$]) nor wrist PPT (mean difference 5.3 [95% CI $-75.4, 64.6$]) were significantly different among participants who had lost $\geq 20\%$ of weight by follow-up, compared with those with $< 20\%$ weight loss. The mean CES-D at baseline was lower in subjects with $\geq 20\%$ weight loss by 1-year follow-up, compared with those who did not experience weight loss (mean difference -4.9 [95% CI $0.0, 9.8$]) (Table 1 and Figure 2).

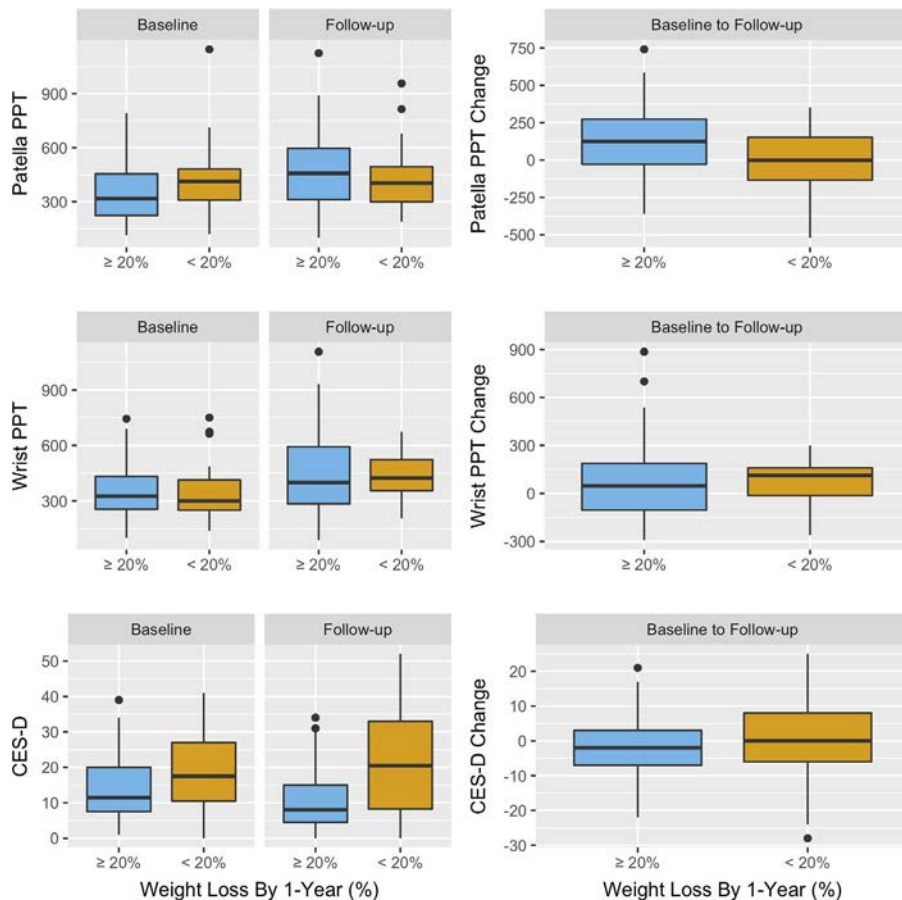


Figure 2. Box plots of baseline and follow-up measures of the pressure pain threshold (PPT) at the patella and the right wrist, and the Center for Epidemiologic Studies Depression scale (CES-D), stratified by weight loss at 1 year. Each box represents the 25th to 75th percentiles. Lines inside the boxes represent the median. Whiskers represent 1.5 times the upper and lower interquartile ranges. Circles indicate outliers.

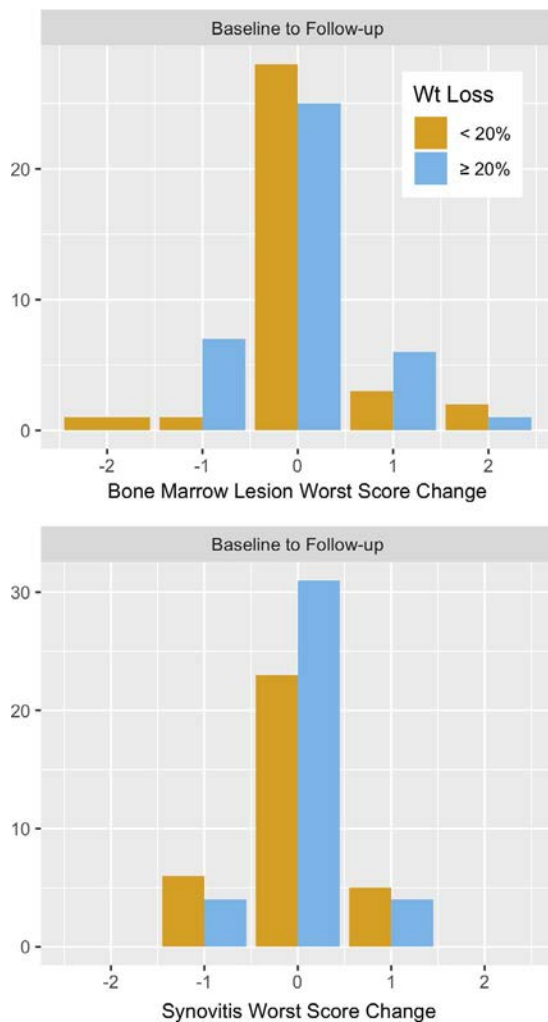


Figure 3. Longitudinal changes in bone marrow lesion and synovitis worst scores, measured semiquantitatively by magnetic resonance imaging, stratified by weight (Wt) loss from baseline to 1-year follow-up.

Change in mediators: BMLs, synovitis, pain sensitization, and depressive symptoms. Change in the worst score from baseline to follow-up in patients with BMLs (coefficient for mean difference [coef.] 0.1 [95% CI -0.2, 0.4]) and synovitis (coef. 0.1 [95% CI -0.3, 0.2]) was not significantly different between the group of patients with $\geq 20\%$ weight loss, compared with patients who had $< 20\%$ weight loss (Figure 3). Similarly, when the sum of MRI scores was considered for each structural feature, changes in BMLs (coef. 0.2 [95% CI -0.7, 1.2]) and synovitis (coef. 0.1 [95% CI -0.5, 0.2]) were not significantly different between patients with $\geq 20\%$ weight loss and those with $< 20\%$ weight loss.

The mean PPT increased significantly from baseline to follow-up for both the patella (coef. 68.4 [95% CI 10.8, 125.9]) and the wrist (coef. 88.5 [95% CI 38.1, 138.0]) for all subjects, suggesting less pain sensitization across visits. However, the change in mean PPT for the patella (coef. -11.3 [95% CI -84.6, 62.6]) and the wrist (coef. 18.0 [95% CI -48.0, 87.6]) was not significantly

different between patients with and those without $\geq 20\%$ weight loss. The mean CES-D score decreased from baseline to follow-up for all subjects (coef. -0.8 [95% CI -3.1, 1.67]), and was significantly lower (coef. -6.2 [95% CI -11.0, -1.4]) in those who lost $\geq 20\%$ of weight compared with those who had $< 20\%$ loss of weight (Figure 2).

Pain improvement. Among participants who lost $\geq 20\%$ body weight, 75% (30 of 40) experienced the MCID improvement in WOMAC pain. In contrast, 35% of those with $< 20\%$ weight loss (12 of 35) experienced the MCID improvement in WOMAC pain.

Mediated effects. Estimates for the natural indirect effect suggested that the effect of weight loss on pain improvement was not mediated by the BML score (for worst BMLs, OR 1.01 [95% CI 0.78, 1.28]) or synovitis (OR 1.03 [95% CI 0.73, 1.45]). Results were similar for the sum of BMLs or synovitis scores. However, there was 62% and 15% increased odds of attaining the MCID in pain improvement by changes in the patella PPT (OR 1.62 [95% CI 0.89, 2.75]) and the wrist PPT (OR 1.15 [95% CI 0.77, 1.77]), respectively, in participants who lost $\geq 20\%$ body weight compared with those who had $< 20\%$ loss of body weight (Table 2). Further, the estimate of the natural indirect effect for CES-D score suggested 22% increased odds (OR 1.22 [95% CI 0.77, 1.87]) of pain improvement in subjects with $\geq 20\%$ weight loss compared with those with $< 20\%$ weight loss.

Unmediated effects. Estimates for the natural direct effect, not mediated through changes in the worst scores for BMLs and synovitis, suggested a 5.39-fold increase (95% CI 1.43, 16.99) and a 5.07-fold increase (95% CI 1.38, 15.33), respectively, in the odds of pain improvement in patients with $\geq 20\%$ weight loss compared with those without such weight loss. Natural direct effect estimates not mediated through the patella PPT and the wrist PPT also suggested a 2.47-fold increase (95% CI 0.73, 7.71) and a 3.82-fold increase (95% CI 1.10, 11.30), respectively, in the odds

Table 2. Estimates of the natural indirect effect (mediated) and natural direct effect (not mediated) of $\geq 20\%$ weight loss on knee pain improvement*

	Natural indirect effect, OR (95% CI)	Natural direct effect, OR (95% CI)
BML		
Worst score	1.01 (0.78, 1.28)	5.39 (1.43, 16.99)
Sum of scores	1.01 (0.72, 1.30)	4.70 (1.35, 15.22)
Synovitis		
Worst score	1.03 (0.73, 1.45)	5.07 (1.38, 15.33)
Sum of scores	0.98 (0.73, 1.33)	4.87 (1.44, 13.82)
PPT		
Patella	1.62 (0.89, 2.75)	2.47 (0.73, 7.71)
Wrist	1.15 (0.77, 1.77)	3.82 (1.10, 11.30)
CES-D	1.22 (0.77, 1.87)	4.08 (1.08, 13.17)

* OR = odds ratio; 95 % CI = 95% confidence interval (bootstrap method); BML = bone marrow lesion; PPT = pressure pain threshold; CES-D = Center for Epidemiologic Studies Depression scale.

of pain improvement in subjects who lost $\geq 20\%$ body weight compared with those who did not. The estimate for the natural direct effect not mediated through changes in CES-D score suggested a 4.08-fold increase (95% CI 1.08, 13.17) in the odds of pain improvement in patients with $\geq 20\%$ weight loss compared with those with $< 20\%$ weight loss (Table 2).

Mediated interaction. Estimates for the mediated interaction between weight loss and worst BML or synovitis scores suggested no evidence of effect modification between the effect of weight loss and BMLs (OR 0.95 [95% CI 0.32, 3.75]) or synovitis (OR 0.88 [95% CI 0.50, 1.40]) on pain improvement. Results were similar for the sum of BML or synovitis scores. Mediated interaction effect measures for the patella PPT (OR 0.81 [95% CI 0.44, 1.35]), the wrist PPT (OR 0.89 [95% CI 0.51, 1.86]), and CES-D score (OR 1.05 [95% CI 0.59, 1.95]) also suggested no effect modification between the effect of weight loss and the patella or wrist PPTs and CES-D score on pain improvement.

Sensitivity analyses. In sensitivity analyses, the effect sizes for the natural effects were similar when the analysis was restricted to those with BMLs and synovitis at baseline, or when a weight loss of $\geq 10\%$, rather than $\geq 20\%$, was considered. They were also similar when subjects who had bariatric surgery were compared with those who underwent medical weight management regardless of weight loss percentage at follow-up visit, although all patients, with the exception of 1, who lost $\geq 20\%$ body weight by 1-year follow-up were in the bariatric surgery group (see Supplementary Table 1, available on the *Arthritis & Rheumatology* web site at <http://onlinelibrary.wiley.com/doi/10.1002/art.41125/abstract>).

DISCUSSION

We found that clinically meaningful improvement in knee pain that occurred in morbidly obese patients following $\geq 20\%$ weight loss over a 1-year follow-up period was not explained by changes in BMLs and synovitis. However, changes in pain sensitization assessed as the patella and wrist PPTs, and depressive symptoms quantified by CES-D, partially explained the effects of weight loss on pain reduction. No effect modification on knee pain improvement was found between these mediated effects and weight loss levels.

As expected, subjects with knee pain undergoing bariatric surgery experienced a marked reduction in pain. To our knowledge, there have been no studies examining factors potentially mediating the effect of weight loss on knee pain. The inclusion of patients undergoing substantial weight loss and knee pain reduction offered us a unique opportunity to explore potential mechanisms of pain reduction. While our goal was to report the effect sizes for natural direct and indirect effects, the uncertainty around our reported effect sizes, expressed by bootstrap CIs,

slightly overlapped the null, partially attributable to the study sample size (37,38). Our inference focused more on effect sizes than on the results of hypothesis testing and corresponding *P* values. While we hoped that we could achieve a narrower CI around our calculated estimates, power analysis for the main study outcome (i. e., pain improvement) assumed a satisfactory sample size. Power analysis for a mediation analysis, however, is more complex and much less developed in the statistical literature, and, to the best of our knowledge, there is no statistical development for imputation-based (and nonparametric) natural-effects models. However, the width of confidence bounds that we calculated by bootstrap resampling (for increased accuracy) appears reasonable. As we noted above in the interpretation of natural direct and indirect effects and assessment of mediating roles, the status of BMLs or synovitis has to stay at a level that naturally occurs for a given level of weight loss. This means that the natural levels of BMLs and synovitis scores could be the same across exposure levels (i. e., $\geq 20\%$ and $< 20\%$ weight loss levels), regardless of the significance of their mediating role.

Beyond our initial study objective, we also tested a mediation hypothesis to examine how much pain improvement due to bariatric surgery was potentially mediated by weight loss. The results of this new mediation hypothesis suggested that compared with patients undergoing medical weight management, the direct (not mediated) effect of bariatric surgery on pain improvement was 39% greater (OR for natural direct effect 1.39 [95% CI 0.14, 12.13]). Further, there was a 2.75-fold increase in the odds of pain improvement with bariatric surgery, which was mediated by weight loss (OR for natural indirect effect 2.75 [95% CI 0.42, 16.98]). These effect sizes suggest that the effect of bariatric surgery on pain improvement is mostly mediated by weight loss; however, the sample size for this secondary mediation hypothesis was small.

In an earlier study, we assessed cartilage both semiquantitatively and quantitatively in the same study sample (22) and reported no effect of weight loss on this measure over a year, although morphologic changes in cartilage would be unusual in this time frame. BMLs and synovitis have both been shown to change within a few weeks (2,5,39). Our longitudinal MRI assessments revealed non-statistically significant changes in BMLs and synovitis scores within 1 year, despite massive weight loss. Similarly, Gudbergson et al (14) reported a lack of improvement in BMLs in response to rapidly decreasing body weight following a weight loss intervention, and also concluded that there was no association between changes in BMLs and clinical symptoms, including pain. However, no formal assessment of a potential mediating role (i. e., an estimate for indirect effect) was presented (14). Further, results of the Cartilage in Obese Knee Osteoarthritis Patients trial on the influence of weight loss therapy on cartilage in obese subjects with knee OA have similarly suggested nonsignificant changes in synovitis at 1-year follow-up after the intervention, but showed increased BMLs only in those who lost weight by exercise compared with those who experienced

weight loss by diet or a no-attention group (40). Moreover, in the Intensive Diet and Exercise for Arthritis trial in which subjects who experienced 10% weight loss by the 18-month follow-up through diet and exercise, solely by diet, or solely through exercise were studied, no significant changes in structural features such as BMLs and synovitis were found, despite improvement in knee pain (41).

While previous studies have both supported (2,4–8,10) and not supported (11–14) the association of BMLs and synovitis with pain in OA, few studies have explored the underlying causal mechanisms by which these structural features could be related to pain. Exceptions were found in studies that attributed chronic pain in OA to changes in central sensitization during OA development and progression (15,42). A strength of our study was the assessment of these mediating effects in a population who lost a lot of weight (i. e., $\geq 20\%$) in contrast to previous studies that assessed lesser degrees of weight loss (14,40,41). Another strength was the use of modern approaches to causal mediation that allow assessment of intermediate variables on a causal pathway to quantify knee pain reduction mediated by these factors as part of the effect of weight loss.

There are some limitations to our study as well. Our study participants were almost entirely women, despite efforts to recruit men. The sample size was relatively small, resulting in limited precision manifested by relatively wide CIs. While MRI is an ideal instrument for quantifying the changes in structural features of OA compared with plain radiography, the semiquantitative nature of the MOAKS scoring method does not allow a volumetric measurement for quantifying the size of these structural features. Future studies should assess other potential causal pathways through which substantial weight loss could exert its effect on knee pain improvement, such as changes in biomechanical or inflammatory factors.

In conclusion, pain is a complex phenomenon in knee OA. Our findings suggest that changes in pain sensitization and in depressive symptoms mediate, in part, knee pain improvement experienced by those undergoing substantial weight loss, especially following bariatric surgery. This suggests that pain sensitization and depressive symptoms could be a promising target for future intervention studies in those with chronic knee pain.

AUTHOR CONTRIBUTIONS

All authors were involved in drafting the article or revising it critically for important intellectual content, and all authors approved the final version to be published.

Study conception and design. Jafarzadeh, Felson, Neogi, Stefanik.

Acquisition of data. Felson, Neogi, Stefanik, Guermazi, Li, Apovian.

Analysis and interpretation of data. Jafarzadeh, Felson, Neogi.

REFERENCES

- Jafarzadeh SR, Felson DT. Updated estimates suggest a much higher prevalence of arthritis in United States adults than previous ones. *Arthritis Rheumatol* 2018;70:185–92.
- Felson DT, Chaisson CE, Hill CL, Totterman SM, Gale ME, Skinner KM, et al. The association of bone marrow lesions with pain in knee osteoarthritis. *Ann Intern Med* 2001;134:541–9.
- Zhai G, Blizzard L, Srikanth V, Ding C, Cooley H, Cicuttini F, et al. Correlates of knee pain in older adults: Tasmanian Older Adult Cohort Study. *Arthritis Rheum* 2006;55:264–71.
- Torres L, Dunlop DD, Peterfy C, Guermazi A, Prasad P, Hayes KW, et al. The relationship between specific tissue lesions and pain severity in persons with knee osteoarthritis. *Osteoarthritis Cartilage* 2006;14:1033–40.
- Felson DT, Niu J, Guermazi A, Roemer F, Aliabadi P, Clancy M, et al. Correlation of the development of knee pain with enlarging bone marrow lesions on magnetic resonance imaging. *Arthritis Rheum* 2007;56:2986–92.
- Davies-Tuck ML, Wluka AE, Wang Y, English DR, Giles GG, Cicuttini F. The natural history of bone marrow lesions in community-based adults with no clinical knee osteoarthritis. *Ann Rheum Dis* 2009;68:904–8.
- Lo GH, McAlindon TE, Niu J, Zhang Y, Beals C, Dabrowski C, et al. Bone marrow lesions and joint effusion are strongly and independently associated with weight-bearing pain in knee osteoarthritis: data from the osteoarthritis initiative. *Osteoarthritis Cartilage* 2009;17:1562–9.
- Zhang Y, Nevitt M, Niu J, Lewis C, Torner J, Guermazi A, et al. Fluctuation of knee pain and changes in bone marrow lesions, effusions, and synovitis on magnetic resonance imaging. *Arthritis Rheum* 2011;63:691–9.
- Hill CL, Gale DG, Chaisson CE, Skinner K, Kazis L, Gale ME, et al. Knee effusions, popliteal cysts, and synovial thickening: association with knee pain in osteoarthritis. *J Rheumatol* 2001;28:1330–7.
- Hill CL, Hunter DJ, Niu J, Clancy M, Guermazi A, Genant H, et al. Synovitis detected on magnetic resonance imaging and its relation to pain and cartilage loss in knee osteoarthritis. *Ann Rheum Dis* 2007;66:1599–603.
- Sowers MF, Hayes C, Jamadar D, Capul D, Lachance L, Jannausch M, et al. Magnetic resonance-detected subchondral bone marrow and cartilage defect characteristics associated with pain and x-ray-defined knee osteoarthritis. *Osteoarthritis Cartilage* 2003;11:387–93.
- Link TM, Steinbach LS, Ghosh S, Ries M, Lu Y, Lane N, et al. Osteoarthritis: MR imaging findings in different stages of disease and correlation with clinical findings. *Radiology* 2003;226:373–81.
- Kornaat PR, Kloppenburg M, Sharma R, Botha-Scheepers SA, Le Graverand MP, Coene LN, et al. Bone marrow edema-like lesions change in volume in the majority of patients with osteoarthritis: associations with clinical features. *Eur Radiol* 2007;17:3073–8.
- Gudbergensen H, Boesen M, Christensen R, Bartels EM, Henriksen M, Danneskiold-Samsøe B, et al. Changes in bone marrow lesions in response to weight-loss in obese knee osteoarthritis patients: a prospective cohort study. *BMC Musculoskelet Disord* 2013;14:106.
- Neogi T, Guermazi A, Roemer F, Nevitt MC, Scholz J, Arendt-Nielsen L, et al. Association of joint inflammation with pain sensitization in knee osteoarthritis: the Multicenter Osteoarthritis Study. *Arthritis Rheumatol* 2016;68:654–61.
- Stefanik JJ, Felson DT, Apovian CM, Niu J, Clancy MM, LaValley MP, et al. Changes in pain sensitization after bariatric surgery. *Arthritis Care Res (Hoboken)* 2018;70:1525–8.
- Stubbs B, Aluko Y, Myint PK, Smith TO. Prevalence of depressive symptoms and anxiety in osteoarthritis: a systematic review and meta-analysis. *Age Ageing* 2016;45:228–35.
- Rathbun AM, Stuart EA, Shardell M, Yau MS, Baumgarten M, Hochberg MC. Dynamic effects of depressive symptoms on osteoarthritis knee pain. *Arthritis Care Res (Hoboken)* 2018;70:80–8.

19. Felson DT, Anderson JJ, Naimark A, Walker AM, Meenan RF. Obesity and knee osteoarthritis: the Framingham Study. *Ann Intern Med* 1988;109:18–24.
20. Speck RM, Bond DS, Sarwer DB, Farrar JT. A systematic review of musculoskeletal pain among bariatric surgery patients: implications for physical activity and exercise. *Surg Obes Relat Dis* 2014;10:161–70.
21. King WC, Chen JY, Belle SH, Courcoulas AP, Dakin GF, Elder KA, et al. Change in pain and physical function following bariatric surgery for severe obesity. *JAMA* 2016;315:1362–71.
22. Jafarzadeh SR, Clancy M, Li JS, Apovian CM, Guermazi A, Eckstein F, et al. Changes in the structural features of osteoarthritis in a year of weight loss. *Osteoarthritis Cartilage* 2018;26:775–82.
23. Radloff LS. The CES-D scale: a self-report depression scale for research in the general population. *Appl Psychol Meas* 1977;1:385–401.
24. Bellamy N, Buchanan WW, Goldsmith CH, Campbell J, Stitt LW. Validation study of WOMAC: a health status instrument for measuring clinically important patient relevant outcomes to antirheumatic drug therapy in patients with osteoarthritis of the hip or knee. *J Rheumatol* 1988;15:1833–40.
25. Angst F, Aeschlimann A, Michel BA, Stucki G. Minimal clinically important rehabilitation effects in patients with osteoarthritis of the lower extremities. *J Rheumatol* 2002;29:131–8.
26. Bates D, Mächler M, Bolker BM, Walker SC. Fitting linear mixed-effects models using lme4. *J Stat Softw* 2015;67.
27. Lange T, Vansteelandt S, Bekaert M. A simple unified approach for estimating natural direct and indirect effects. *Am J Epidemiol* 2012;176:190–5.
28. Loeys T, Moerkerke B, De Smet O, Buysse A, Steen J, Vansteelandt S. Flexible mediation analysis in the presence of nonlinear relations: beyond the mediation formula. *Multivariate Behav Res* 2013;48:871–94.
29. Vansteelandt S. Understanding counterfactual-based mediation analysis approaches and their differences. *Epidemiology* 2012;23:889–91.
30. VanderWeele TJ. A three-way decomposition of a total effect into direct, indirect, and interactive effects. *Epidemiology* 2013;24:224–32.
31. Shpitser I, Tchetgen ET. Causal inference with a graphical hierarchy of interventions. *Ann Stat* 2016;44:2433–66.
32. Robins JM, Greenland S. Identifiability and exchangeability for direct and indirect effects. *Epidemiology* 1992;3:143–55.
33. Vansteelandt S, Bekaert M, Lange T. Imputation strategies for the estimation of natural direct and indirect effects. *Epidemiologic Methods* 2012;1:131–58.
34. Steen J, Loeys T, Moerkerke B, Vansteelandt S. Medflex: an R package for flexible mediation analysis using natural effect models. *J Stat Softw* 2017;76.
35. R Core Team, R Foundation for Statistical Computing. R: a language and environment for statistical computing. 2014. URL: <http://www.r-project.org>.
36. Steen J, Loeys T, Moerkerke B, Vansteelandt S, Meys J, Lange T, et al. Medflex: flexible mediation analysis using natural effect models. 2018. URL: <https://cran.r-project.org/package=medflex>.
37. Wasserstein RL, Lazar NA. The ASA's statement on p-values: context, process, and purpose [editorial]. *Am Stat* 2016;70:129–33.
38. Greenland S, Senn SJ, Rothman KJ, Carlin JB, Poole C, Goodman SN, et al. Statistical tests, P values, confidence intervals, and power: a guide to misinterpretations. *Eur J Epidemiol* 2016;31:337–50.
39. O'Neill TW, Parkes MJ, Maricar N, Marjanovic EJ, Hodgson R, Gait AD, et al. Synovial tissue volume: a treatment target in knee osteoarthritis (OA). *Ann Rheum Dis* 2016;75:84–90.
40. Henriksen M, Christensen R, Hunter DJ, Gudbergson H, Boesen M, Lohmander LS, et al. Structural changes in the knee during weight loss maintenance after a significant weight loss in obese patients with osteoarthritis: a report of secondary outcome analyses from a randomized controlled trial. *Osteoarthritis Cartilage* 2014;22:639–46.
41. Hunter DJ, Beavers DP, Eckstein F, Guermazi A, Loeser RF, Nicklas BJ, et al. The Intensive Diet and Exercise for Arthritis (IDEA) trial: 18-month radiographic and MRI outcomes. *Osteoarthritis Cartilage* 2015;23:1090–8.
42. Gwilym SE, Keltner JR, Warnaby CE, Carr AJ, Chizh B, Chessell I, et al. Psychophysical and functional imaging evidence supporting the presence of central sensitization in a cohort of osteoarthritis patients. *Arthritis Rheum* 2009;61:1226–34.

BRIEF REPORT

Altered Cytotoxicity Profile of CD8+ T Cells in Ankylosing Spondylitis

Eric Gracey,¹  Yuchen Yao,² Zoya Qaiyum,³ Melissa Lim,³ Michael Tang,³ and Robert D. Inman¹

Objective. Ankylosing spondylitis (AS) is an inflammatory arthritis in which men have a higher risk of developing progressive axial disease than women. Transcriptomic studies have shown reduced expression of cytotoxic cell genes in the blood of AS patients. HLA-B27 contributes the greatest risk for AS, suggesting a role for CD8+ T cells. This study was undertaken to profile AS patient cytotoxic cells with the hypothesis that an alteration in CD8+ T cells might explain the aberrant cytotoxic profile observed in patients.

Methods. Whole blood was examined for *GZM* and *PRF1* gene expression by quantitative polymerase chain reaction. Serum and synovial fluid (SF) were examined for granzyme and perforin 1 expression by bead array, and blood and SF mononuclear cells were examined for granzyme and perforin 1 expression by fluorescence-activated cell sorting (FACS).

Results. *GZM* and *PRF1* gene expression were both reduced in AS patients compared to healthy controls, especially in men. Perforin 1, but not granzyme, protein levels were reduced in AS patient serum. Granzymes were elevated in AS SF, but not in rheumatoid arthritis or osteoarthritis SF. FACS revealed a reduction in granzyme-positive and perforin 1–positive lymphocytes, but not an intrinsic defect in CD8+ T cell granzyme or perforin 1 production. CD8+ T cell frequency was reduced in the blood and increased in the SF of AS patients.

Conclusion. Our findings indicate that AS patients have an altered cytotoxic T cell profile. These data suggest that CD8+ T cells with a cytotoxic phenotype are recruited to the joints, where they exhibit an activated phenotype. Thus, a central role for CD8+ T cells in AS may have been overlooked and deserves further study.

INTRODUCTION

Ankylosing spondylitis (AS) is an inflammatory disease of axial and peripheral joints in which men have a higher risk of developing progressive axial disease than women. Inflammation-associated erosive changes in the target joints coexist with new bone formation, resulting in complete ankylosis of the spine in severe cases.

How the immune system is altered in AS, and how these changes mediate arthritis, are not fully understood. Basic human research, animal studies, clinical trials, and genome-wide association studies have indicated a role for interleukin-17 (IL-17)–producing CD4+ T (Th17) cells (1). Those same genetic studies also linked AS with a large number of CD8+ T cell–related factors,

such as *TBX21*, *EOMES*, and *RUNX3*, and with antigen processing and presentation factors, including *ERAP1*, *ERAP2*, *NPEPPS*, and HLA-B27 (2,3). HLA-B27, a major histocompatibility complex (MHC) class I allele, contributes the greatest risk for AS and is present in >80% of AS patients, but in <8% of healthy individuals. Despite being such a strong risk factor for AS, a mechanistic role for MHC class I–restricted CD8+ T cells has yet to be defined (4), leading many to conclude that CD8+ T cells may play a limited role in AS.

We recently performed a gene expression analysis on AS patients and healthy controls (5), in which we observed a down-regulation of cytotoxic cell–related genes, such as granzymes A, B, and K and granulysin in whole blood from AS patients. In the

Supported by a grant from the Institute of Musculoskeletal Health and Arthritis, Canadian Institutes of Health Research (201803) and an unrestricted grant from AbbVie.

¹Eric Gracey, PhD (current address: Ghent University, Ghent, Belgium), Robert D. Inman, MD: University of Toronto, Krembil Research Institute, Toronto Western Hospital, and University Health Network, Toronto, Ontario, Canada; ²Yuchen Yao, MSc: University of Toronto, Krembil Research Institute, and University Health Network, Toronto, Ontario, Canada; ³Zoya Qaiyum, MSc, Melissa Lim, MSc, Michael Tang, PhD: Krembil Research Institute,

Toronto Western Hospital, and University Health Network, Toronto, Ontario, Canada.

Dr. Gracey and Mr. Yao contributed equally to this work.

No potential conflicts of interest relevant to this article were reported.

Address correspondence to Eric Gracey, PhD, VIB-UGent Center for Inflammation Research, MRB Building 2, Corneel Heymanslaan 10, Ghent 9000, Belgium. E-mail: Roberteric.gracey@ugent.be.

Submitted for publication January 25, 2019; accepted in revised form October 1, 2019.

present study, we confirm this finding in an independent cohort of patients, and further show that this loss of cytotoxic factor expression is driven by a reduction in CD8+ T cell frequency in the peripheral blood. We show that CD8+ T cells are enriched in the synovial fluid (SF) of AS patients, providing evidence that CD8+ T cells may play an overlooked role in the pathogenesis of AS.

MATERIALS AND METHODS

Patient cohorts. Patients with AS, patients with rheumatoid arthritis (RA), and patients with osteoarthritis (OA) were recruited from the rheumatology clinics at Toronto Western Hospital and Mt. Sinai Hospital (Toronto, Ontario, Canada). All AS patients fulfilled the modified New York criteria (6), and all RA patients fulfilled the American College of Rheumatology/European League Against Rheumatism 2010 criteria (7). Healthy controls were recruited from hospital staff and volunteers with no clinical autoimmune disease or recent infections. All patients and controls completed a University Health Network Research Ethics Board–approved consent form to participate. Cohort demographics and details on specimen processing are given in Supplementary Tables 1–4 and the Supplementary Meth-

ods, respectively, available on the *Arthritis & Rheumatology* web site at <http://onlinelibrary.wiley.com/doi/10.1002/art.41129/abstract>.

Gene expression. Quantitative polymerase chain reaction (qPCR) was performed using Power SYBR Green (ABI) on an ABI 7900HT system. A list of primers used is shown in Supplementary Table 5, and detailed methods are provided in the Supplementary Methods, available on the *Arthritis & Rheumatology* web site at <http://onlinelibrary.wiley.com/doi/10.1002/art.41129/abstract>.

Cytokine bead array. A customized LEGENDplex kit was obtained from BioLegend. Samples were analyzed by standard LEGENDplex protocol using Data Analysis Software version 7.0.

Flow cytometric analysis. Single-cell suspensions were first stained with a Live/Dead fixable cell stain (L/D NIR [Invitrogen] or FVS780 [BD]) according to the recommendations of the manufacturer. Cells were blocked with FcX (BioLegend) prior to staining with surface antibodies. For experiments in which granzyme A, granzyme B, and perforin 1 were stained, cells were fixed with a paraformaldehyde buffer and permeabilized with intracellular staining

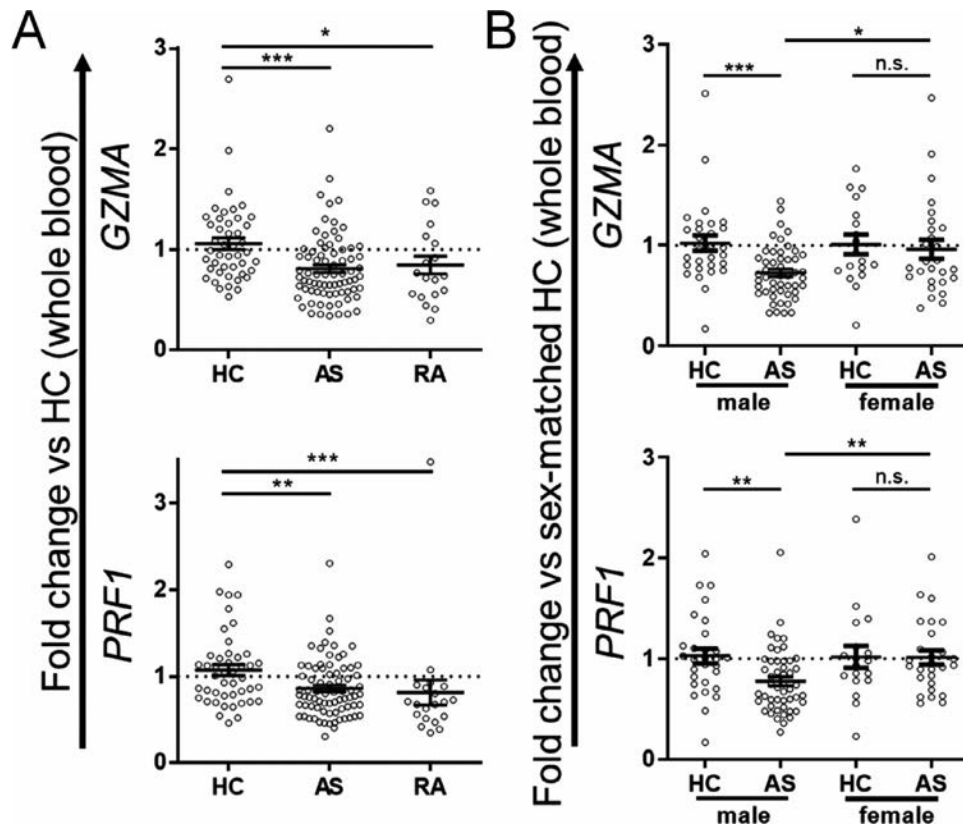


Figure 1. Reduced *GZMA* and *PRF1* gene expression in the whole blood of male patients with ankylosing spondylitis (AS). **A**, *GZMA* and *PRF1* expression in patients with AS and patients with rheumatoid arthritis (RA), normalized to the average expression in healthy controls (HCs) (dotted lines), determined by quantitative polymerase chain reaction (qPCR). **B**, *GZMA* and *PRF1* expression in male patients with AS and female patients with AS, normalized to the average expression in sex-matched healthy controls (dotted lines), determined by qPCR. Fold change in *GZMA* expression was calculated using the $\Delta\Delta C_t$ method, and fold change in *PRF1* expression was calculated using the Pfaffl method. *HPRT* was used as a housekeeping gene. Circles represent individual patients; horizontal lines and error bars show the mean \pm SEM. * = $P < 0.05$; ** = $P < 0.01$; *** = $P < 0.001$, by Kruskal-Wallis test with Dunn's post hoc test in **A**; by Mann-Whitney test in **B**. NS = not significant.

buffer (BioLegend). Antibodies used are listed in Supplementary Table 6, available on the *Arthritis & Rheumatology* web site at <http://onlinelibrary.wiley.com/doi/10.1002/art.41129/abstract>. Data were acquired on a FACS Aria III, Fortessa X20, or FACSCanto II system (BD) and analyzed with FlowJo.

Statistical analysis. All statistical analyses were performed using GraphPad Prism software. Data were tested for normality before the statistical test was selected. Except where indicated otherwise, values are presented as the mean \pm SEM. Two-tailed statistical tests were used, with specific tests indicated in the figure legends. Multiple regression analyses, using IBM SPSS Statistics version 22.0.0, were performed to investigate the influence of various clinical parameters on the expression of *GZMA*, *PRF1*, and serum perforin 1 and CD8⁺ T cell frequency. *P* values less than 0.05 were considered significant.

RESULTS

Reduced expression of cytotoxic cell genes in patients with AS. In a previously published microarray study (5), we identified a sex-dependent cytotoxic gene expression profile in AS patients. In the present study, we assembled an independent cohort of AS patients to confirm these results in whole blood by qPCR. RA patients were analyzed as disease controls. We confirmed that *GZMA* expression was reduced in AS patients compared to healthy controls and found that *PRF1* expression was also reduced in AS patients (Figure 1A). In addition, the expression of both of these genes was reduced in RA patients compared to healthy controls. We reanalyzed the data by sex, normalizing AS patient data to that for sex-matched healthy controls (Figure 1B), which confirmed that the reduced *GZMA* and *PRF1* expression in AS patients displays sexual dimorphism. To examine the effect of clinical parameters within the AS patient cohort, we performed regression analysis. While treatment type (e.g., tumor necrosis factor [TNF] inhibitors and nonsteroidal antiinflammatory drugs) and systemic inflammation (e.g., C-reactive protein level and erythrocyte sedimentation rate) did not predict *GZMA* and *PRF1* expression, the Bath Ankylosing Spondylitis Disease Activity Index (BASDAI) (8) was a significant negative predictor ($P < 0.05$) (Supplementary Tables 7 and 8, available on the *Arthritis & Rheumatology* web site at <http://onlinelibrary.wiley.com/doi/10.1002/art.41129/abstract>).

Elevation of granzyme, but not perforin, levels in AS SF.

To gain insight into secreted cytotoxic cell products at the protein level, we used a fluorescence-activated cell sorting (FACS)-based bead array to examine the levels of granzyme A, granzyme B, granulysin, perforin 1, and selected cytokines. In these experiments we found that only perforin 1 was down-regulated in the serum of AS patients compared to healthy controls (Figure 2A). Granzyme A, granzyme B, and granulysin levels were significantly higher in AS SF compared to AS serum, whereas perforin 1 levels were further

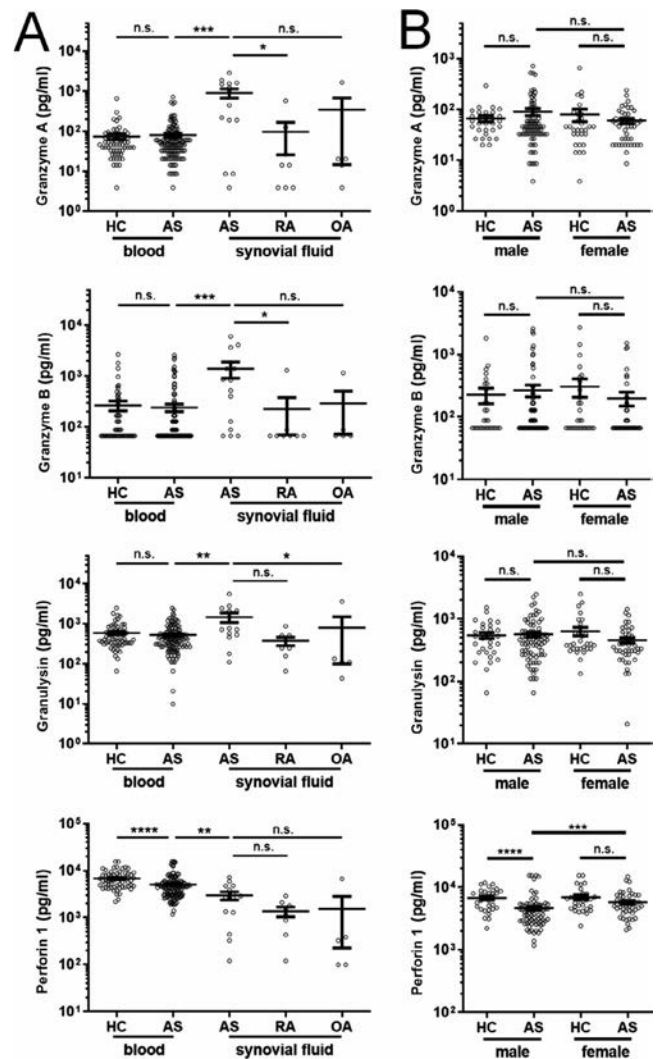


Figure 2. Altered granzyme and perforin 1 expression in the synovial fluid (SF) of patients with ankylosing spondylitis (AS). **A**, Serum levels of granzyme A, granzyme B, granulysin, and perforin 1 protein in healthy controls (HCs) and AS patients and SF levels in patients with AS, patients with rheumatoid arthritis (RA), and patients with osteoarthritis (OA), determined by fluorescence-activated cell sorting (FACS)-based bead array. **B**, Serum levels of granzyme A, granzyme B, granulysin, and perforin 1 protein in healthy controls and patients with AS stratified by sex, determined by FACS-based bead array. Circles represent individual patients; horizontal lines and error bars show the mean \pm SEM. * = $P < 0.05$; ** = $P < 0.01$; *** = $P < 0.001$; **** = $P < 0.0001$, by Mann-Whitney test for healthy control versus AS blood and for AS blood versus AS SF and by Kruskal-Wallis test with Dunn's post hoc test for AS SF versus RA SF and OA SF in **A**; by Mann-Whitney test in **B**. NS = not significant.

decreased in AS SF versus AS serum. Further, the elevation of granzyme A, granzyme B, and granulysin levels in the SF appeared to be specific to AS, although the limited numbers of RA SF and OA SF controls preclude a conclusive comparator statement for this observation. Given the sex-specific gene expression changes in *PRF1* and *GZMA*, we stratified the patients by sex and assessed serum protein levels (Figure 2B). We found that perforin 1 levels

were lower in male AS patients. Regression analysis of clinical parameters in AS patients found only sex to be a close predictor of serum perforin 1 level ($P = 0.056$) (Supplementary Table 9, available on the *Arthritis & Rheumatology* web site at <http://onlinelibrary.wiley.com/doi/10.1002/art.41129/abstract>).

Our bead array also included a range of disease-relevant cytokines. IL-1 β , IL-17A, IL-17F, IL-22, IL-23, and IL-33 levels were below the detection limit in most serum and SF samples. There was a trend toward higher IL-6 and TNF levels in the serum of AS patients compared to healthy controls (Supplementary Figure 1A, available on the *Arthritis & Rheumatology* web site at <http://onlinelibrary.wiley.com/doi/10.1002/art.41129/abstract>); however, the levels were close to the detection limit in many samples. In contrast, robust expression of IL-8 was detected in all serum samples and was significantly higher in AS patients than in healthy controls. While IL-6 and IL-8 levels were significantly elevated in AS SF versus AS serum, this finding did not appear to be disease specific, as both RA SF and OA SF also had elevated levels. TNF levels were low or undetectable in the SF in all disease groups. As we previously reported (5), serum IL-6 and TNF levels were significantly higher in male AS patients than in sex-matched healthy controls (Supplementary Figure 1B). In contrast, the elevation of serum IL-8 levels was independent of patient sex.

These results revealed a prominent cytotoxic cell profile in the SF of AS patients, suggesting a strong recruitment of cytotoxic cells. These findings further showed a dissociation between perforin 1 and the granzymes in AS patients, which we next investigated at the cellular level using FACS.

Correlation of reduced granzyme expression with reduced CD8+ T cell frequency in AS. Using flow cytometry, we were able to detect intracellular granzyme A, granzyme B, and perforin 1 without the need to restimulate peripheral blood mononuclear cells (PBMCs). Granzyme A-positive and perforin 1-positive lymphocytes were reduced in the PBMCs of AS patients compared to healthy controls (Figure 3A), which is consistent with our gene expression results. Moreover, examination of paired blood and SF samples showed a paradoxical enrichment of granzyme A-positive lymphocytes and reduction in perforin 1-positive lymphocytes in SF; however, our cohort was not sufficiently powered for statistical analysis owing to limited sample availability.

Natural killer (NK) and CD8+ T cells account for the majority of cytotoxic molecule-producing cells in PBMCs (Supplementary Figure 2A, available on the *Arthritis & Rheumatology* web site at <http://onlinelibrary.wiley.com/doi/10.1002/art.41129/abstract>). Therefore, we investigated whether there was an intrinsic reduction in granzyme A, granzyme B, or perforin 1 expression in CD8+ T or NK cells in the blood. This analysis yielded negative results (Figure 3B and Supplementary Figure 2B). Despite this finding, we observed a clear enrichment of granzyme A-positive CD8+ T cells (Figure 3B), but not granzyme A-positive NK cells (Supplementary Figure 2B), in the SF of AS patients. We therefore

considered whether an alteration to CD8+ T or NK cell frequency might explain the reduction in total granzyme A-positive/perforin 1-positive blood lymphocytes. NK cell frequency was significantly lower in RA, but not AS, patients compared to healthy controls (Supplementary Figure 2C). In contrast, CD8+ T cell frequency was significantly lower in both RA and AS patients than in healthy controls when analyzed as a frequency of either total lymphocytes (Supplementary Figure 2C) or T cells (Figure 3C). Notably, the reduction in CD8+ T cell frequency compared to sex-matched healthy controls was restricted to male AS patients. Regression analysis of clinical parameters in AS patients further revealed that the BASDAI score was a significant negative predictor of CD8+ T cell frequency ($P = 0.009$) (Supplementary Table 10, available on the *Arthritis & Rheumatology* web site at <http://onlinelibrary.wiley.com/doi/10.1002/art.41129/abstract>). In support of the notion of a CD8+ T cell-driven loss of cytotoxic gene expression, we observed that *GZMA* gene expression strongly correlated with the frequency of granzyme A-positive lymphocytes and CD8+ T cells, but weakly with NK cells (Supplementary Figure 2D).

We next sought to explain what might be contributing to the reduced frequency of CD8+ T cells in AS patient blood. Our first line of inquiry was to explore CD8+ T cell maturity, since AS patients have accelerated thymic output and premature senescence compared to healthy controls (9). We ran a concurrent FACS panel to examine CD8+ naive T (CD45RA+CCR7+) cell, central memory (CD45RA-CCR7+) cell, effector memory (CD45RA-CCR7-) cell, and T effector memory CD45RA+ (CD45RA+CCR7-) cell subsets. (The gating strategy is shown in Supplementary Figure 3A, available on the *Arthritis & Rheumatology* web site at <http://onlinelibrary.wiley.com/doi/10.1002/art.41129/abstract>.) We found no difference in the CD8+ T cell composition between AS patients and healthy controls (Figure 3D and Supplementary Figure 3B); however, we did observe a reduction in naive CD8+ T cell frequency in RA patients. Since naive CD8+ T cell frequency is reduced dramatically with age (Supplementary Figure 3C), it is likely that age and not disease status of our RA controls explains their loss of naive CD8+ T cells and thus reduction in CD8+ T cell frequency. Although we were not able to directly assess granzyme or perforin 1 expression in CD8+ T cell subsets, we were able to correlate our 2 FACS panels. This analysis suggested that granzyme or perforin 1 are mostly produced by mature T cells, specifically the effector memory subset (Figure 3E and Supplementary Figure 3D). Thus, CD8+ T cell maturation status could not explain the lower granzyme and perforin 1 expression in AS patients.

We examined SF to address the hypothesis that CD8+ T cell recruitment to sites of inflammation may be responsible for the low CD8+ T cell frequency in the blood of AS patients. (The gating strategy is shown in Supplementary Figure 4, available on the *Arthritis & Rheumatology* web site at <http://onlinelibrary.wiley.com/doi/10.1002/art.41129/abstract>.) We confirmed the reduced frequency of CD8+ T cells in AS patient blood, and found a significant elevation in the proportion of CD8+ T cells in AS

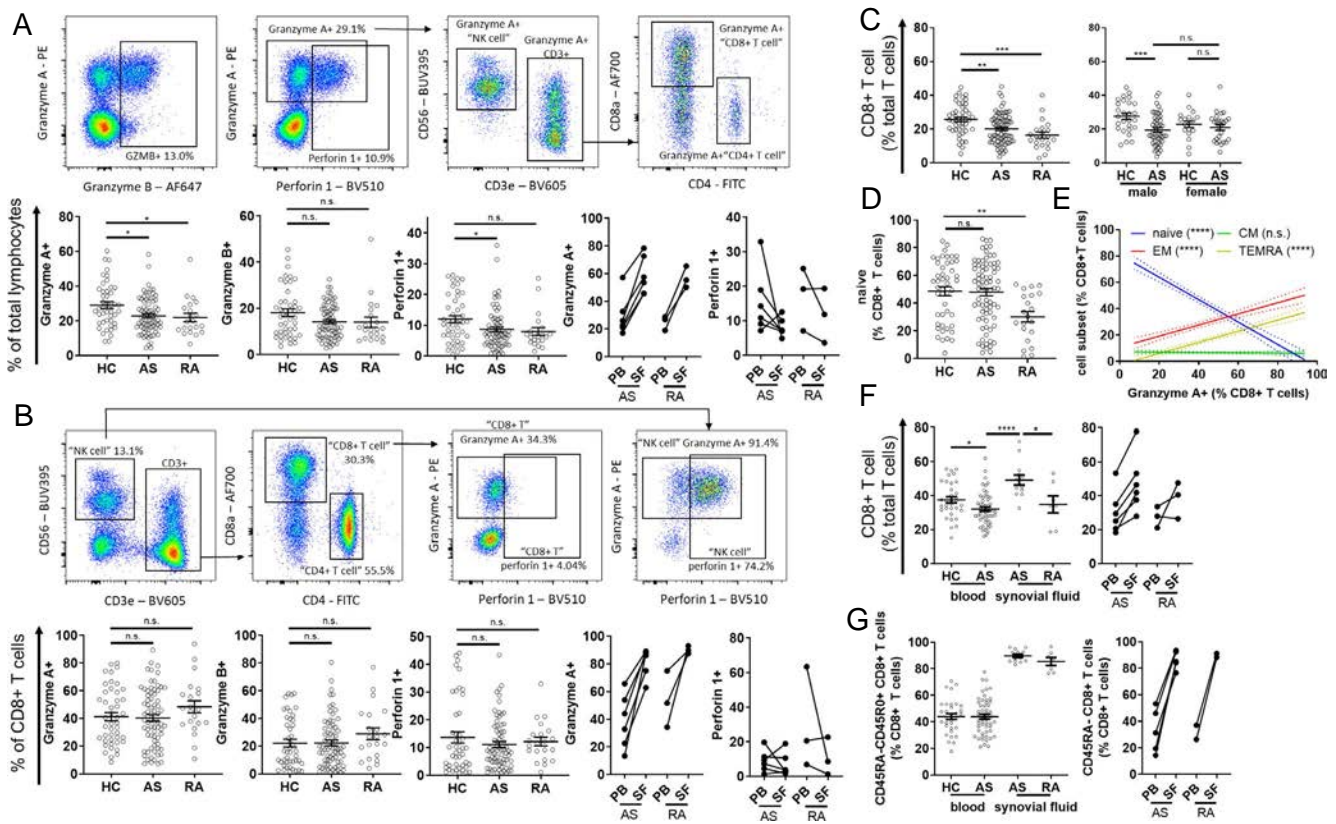


Figure 3. Correlation of reduced granzyme and perforin 1 expression in ankylosing spondylitis (AS) patient blood with reduced CD8+ T cell frequency in blood and enrichment in synovial fluid (SF). Unstimulated peripheral blood mononuclear cells (PBMCs) and synovial fluid mononuclear cells (SFMCs) were examined by flow cytometry. **A**, Expression of granzyme and perforin 1 in lymphocytes from healthy controls (HCs), patients with AS, and patients with rheumatoid arthritis (RA). Granzyme- and perforin 1-expressing cells were identified in total live lymphocytes, followed by gating on the indicated cell subsets to identify dominant granzyme- and perforin 1-expressing populations. Granzyme and perforin 1 expression levels in paired PB and SF samples from patients with AS and patients with RA are shown. **B**, Cell type-specific alterations in granzyme and perforin 1 expression in natural killer (NK) and CD8+ T cells from healthy controls, patients with AS, and patients with RA. Cell-intrinsic alterations in granzyme and perforin 1 were assessed by first identifying lymphocyte populations and then gating on granzyme/perforin 1-positive cells. Granzyme and perforin 1 expression levels in paired PB and SF samples from patients with AS and patients with RA are shown. **C**, CD8+ T cell frequency in PB from healthy controls, patients with AS, and patients with RA, and in healthy controls and patients with AS stratified by sex. **D**, Naive CD8+ T cell frequency in PBMCs from healthy controls, patients with AS, and patients with RA. **E**, Correlation of CD8+ T cell subset frequency (naive, effector memory [EM], central memory [CM], and T effector memory CD45RA+ [TEMRA] cells) with CD8+ T cell granzyme A expression in PBMCs. All patients and controls were pooled and analyzed as a single cohort. Data were examined by linear regression analysis. Dotted lines show the 95% confidence interval. **F**, CD8+ T cell frequency in blood from healthy controls and patients with AS and in SF from patients with AS and patients with RA. Cell frequencies in paired PB and SF samples from patients with AS and patients with RA are shown. **G**, Mature CD8+ T cell frequency in blood from healthy controls and patients with AS and in SF from patients with AS and patients with RA. Cell frequencies in paired PB and SF samples from patients with AS and patients with RA are shown. In **A**, **B**, **C**, **D**, **F**, and **G**, circles represent individual patients; horizontal lines and error bars show the mean \pm SEM. * = $P < 0.05$; ** = $P < 0.01$; *** = $P < 0.001$; **** = $P < 0.0001$, by Kruskal-Wallis test with Dunn's post hoc test in **A**, **B**, **D**, **G**, and for non-sex-stratified data in **C**; by Spearman's test in **E**, and by Mann-Whitney test in **F** and for sex-stratified data in **C**. PE = phycoerythrin; AF647 = Alexa Fluor 647; FITC = fluorescein isothiocyanate; NS = not significant.

SF compared to blood, which was confirmed in a limited number of paired blood and SF samples (Figure 3F). Most notable was that almost all CD8+ T cells in SF were of a mature phenotype (Figure 3G).

DISCUSSION

To date, studies of AS have shown a limited role for CD8+ T cells, despite the high risk imposed by HLA-B27 for the

development of disease and the enrichment of CD8+ T cell-related genes in genome-wide association studies. Of note, the literature does report that CD8+ T cells restricted by HLA-B27 presented self and non-self peptides in SpA patients (10,11). It has also been reported that AS-associated *TBX21* variants alter T-bet expression in CD8+ T cells, which impacts CD8+ T cell function (12). Further, AS patients have an increase in CD28-CD8+ T cells (13), which have a dual cytotoxic and regulatory

phenotype. Finally, it has been observed that HLA-B27+ AS patients may have an expansion of CD8+ T cell clones as assessed by T cell receptor β (TCR β) CDR3 sequencing (14), and a unique population of mature CD103+CD49a+ cells was recently identified in the SF of AS patients by our laboratory (15). Taken together, these findings provide mounting evidence that CD8+ T cells play a role in AS.

Herein we provide detailed observational data that AS patients have a bona fide alteration in their CD8+ T cell component. The initial goal of this study was to validate previously published results, in which we observed a lower cytotoxic gene expression in the whole blood of AS patients (5). We confirmed this observation in an independent cohort of patients, and we also found lower *PRF1* expression in AS patients, which was not detected in our original microarray. Importantly, we confirmed that the loss of *GZMA* and *PRF1* expression appears to be specific to male AS patients. We evaluated 2 hypotheses to explain this loss of cytotoxic gene expression in AS patients: 1) a cell-intrinsic defect in cytotoxic cells or 2) recruitment of cytotoxic cells to the inflamed joints in AS patients.

The first step we took to address these hypotheses was to examine the expression of extracellular cytotoxic proteins in the blood and SF. As we report, most cytotoxic factors were unchanged in the serum of AS patients. Notably, perforin 1 expression was slightly lower in AS patients, revealing a dissociation between perforin and granzyme. This dissociation was accentuated in the SF, with granzyme and granulysin being uniquely elevated in AS SF compared to RA and OA disease controls; in contrast, perforin 1 expression was lower in SF than in serum. The strong granzyme/granulysin profile in the SF supports the hypothesis of cytotoxic cell activity in the inflamed joint. Unlike perforin 1, granulysin readily forms pores in cholesterol-poor microbial membranes (16), hinting at an antimicrobial function of synovial cytotoxic cells.

Our FACS analysis supports the notion that the loss of *GZMA* expression in AS patient blood is due to cytotoxic cell recruitment to the inflamed joint. While granzyme-positive cells were reduced in frequency in PBMCs, we found no evidence that this reduction was due to an intrinsic defect in CD8+ T or NK cells, since the frequency of granzyme-positive CD8+ T or NK cells was equivalent between patients and controls. Since we saw reduced CD8+ T, but not NK, cell frequency in AS patients, we concluded that the loss of cytotoxic cell gene expression must be due to a reduction in the absolute number of CD8+ T cells in the blood. Our observation of an enrichment of CD8+ T cells in the SF of AS patients suggests that CD8+ T cells are preferentially recruited to the inflamed joints in AS patients. We hypothesize that they are the cells responsible for the high levels of granzyme and granulysin observed in AS SF. The recruitment of CD8+ T cells to the inflamed joint may be due in part to IL-8, which we show is elevated in the SF, and which has been reported to recruit highly cytotoxic CD8+ T cells (17). Last, the negative correlation of both *GZMA* and *PRF1* expression and CD8+ T cell frequency with BASDAI is suggestive of a relationship

between CD8+ T cell recruitment to the joint and disease activity in AS patients, a hypothesis worthy of future study.

Many questions remain. First, we have not been able to identify a mechanism to account for the loss of perforin 1 expression in the blood and joint. It is possible that this may reflect the impact of AS risk factors such as T-bet, EOMES, or RUNX3, which are known to control *PRF1* expression (18). Second, it is worth pointing out that a loss of perforin is central to macrophage activation syndrome, which can manifest as inflammatory arthritis (19). Perforin 1 loss causes CD8+ T cell overactivation through “frustrated killing,” which results in release of interferon- γ (IFN γ) and granzymes (19). Indeed, AS patients do have an elevation in systemic IFN γ (5). Third, granzymes are generally viewed as being intracellular activators of apoptosis. We do not know yet whether extracellular granzyme is pathogenic in AS, but extracellular granzyme does have proinflammatory effects (20). Finally, it is of extreme interest to know if these granzyme-producing, joint-recruited CD8+ T cells are HLA-B27 restricted. If this were the case, it would lend support for the arthritogenic peptide hypothesis (21).

There are some limitations to this study. We lacked tissue from the axial skeleton and from synovial tissue, so we had to extrapolate from SF recovered from peripheral joints. Additionally, while the inclusion of disease controls is informative, it is not practical to include age- and sex-matched RA or OA controls owing to the demographics of the diseases. Therefore, comparison of AS and disease controls must be done carefully.

In conclusion, we provide gene, protein, and cellular data showing that AS patients have a reduced cytotoxic CD8+ T cell profile in their peripheral blood, and an enrichment in the inflamed joint. We propose that CD8+ T cells play a significant role in chronic joint inflammation, which is the hallmark of AS and should be the focus of next-generation, multi-omics research. The identification of pathogenic CD8+ T cells would allow for the discovery of autoreactive TCR clones and arthritogenic peptides, and the generation of novel animal models to truly understand the pathogenesis of AS. This knowledge could lay the groundwork for innovative, curative therapies.

AUTHOR CONTRIBUTIONS

All authors were involved in drafting the article or revising it critically for important intellectual content, and all authors approved the final version to be published. Dr. Gracey had full access to all of the data in the study and takes responsibility for the integrity of the data and the accuracy of the data analysis.

Study conception and design. Gracey, Inman.

Acquisition of data. Gracey, Yao, Qaiyum, Lim, Tang.


Analysis and interpretation of data. Gracey, Qaiyum, Tang, Inman.

REFERENCES

1. Ranganathan V, Gracey E, Brown MA, Inman RD, Haroon N. Pathogenesis of ankylosing spondylitis—recent advances and future directions [review]. *Nat Rev Rheumatol* 2017;13:359–67.
2. International Genetics of Ankylosing Spondylitis Consortium (IGAS). Identification of multiple risk variants for ankylosing spondylitis

- through high-density genotyping of immune-related loci. *Nat Genet* 2013;45:730–8.
3. Ellinghaus D, Jostins L, Spain SL, Cortes A, Bethune J, Han B, et al. Analysis of five chronic inflammatory diseases identifies 27 new associations and highlights disease-specific patterns at shared loci. *Nat Genet* 2016;48:510–8.
 4. Colbert RA, Navid F, Gill T. The role of HLA-B*27 in spondyloarthritis. *Best Pract Res Clin Rheumatol* 2007;31:797–815.
 5. Gracey E, Yao Y, Green B, Qaiyum Z, Baglaenko Y, Lin A, et al. Sexual dimorphism in the Th17 signature of ankylosing spondylitis. *Arthritis Rheumatol* 2016;68:679–89.
 6. Van der Linden S, Valkenburg HA, Cats A. Evaluation of diagnostic criteria for ankylosing spondylitis: a proposal for modification of the New York criteria. *Arthritis Rheum* 1984;27:361–8.
 7. Aletaha D, Neogi T, Silman AJ, Funovits J, Felson DT, Bingham CO III, et al. 2010 rheumatoid arthritis classification criteria: an American College of Rheumatology/European League Against Rheumatism collaborative initiative. *Arthritis Rheum* 2010;62:2569–81.
 8. Garrett S, Jenkinson T, Kennedy LG, Whitelock H, Gaisford P, Calin A. A new approach to defining disease status in ankylosing spondylitis: the Bath Ankylosing Spondylitis Disease Activity Index. *J Rheumatol* 1994;21:2286–91.
 9. Fessler J, Raicht A, Husic R, Ficjan A, Duftner C, Schwinger W, et al. Premature senescence of T-cell subsets in axial spondyloarthritis. *Ann Rheum Dis* 2016;75:748–54.
 10. Fiorillo MT, Maragno M, Butler R, Dupuis ML, Sorrentino R. CD8(+) T-cell autoreactivity to an HLA-B27-restricted self-epitope correlates with ankylosing spondylitis. *J Clin Invest* 2000;106:47–53.
 11. Hermann E, Yu DT, Meyer zum Büschenfelde KH, Fleischer B. HLA-B27-restricted CD8 T cells derived from synovial fluids of patients with reactive arthritis and ankylosing spondylitis. *Lancet* 1993;342:646–50.
 12. Lau MC, Keith P, Costello ME, Bradbury LA, Hollis KA, Thomas R, et al. Genetic association of ankylosing spondylitis with TBX21 influences T-bet and pro-inflammatory cytokine expression in humans and SKG mice as a model of spondyloarthritis. *Ann Rheum Dis* 2017;76:261–9.
 13. Schirmer M, Goldberger C, Würzner R, Duftner C, Pfeiffer KP, Clausen J, et al. Circulating cytotoxic CD8⁺ CD28⁻ T cells in ankylosing spondylitis. *Arthritis Res* 2002;4:71–6.
 14. Faham M, Carlton V, Moorhead M, Zheng J, Klinger M, Pepin F, et al. Discovery of T Cell receptor β motifs specific to HLA-B27-positive ankylosing spondylitis by deep repertoire sequence analysis. *Arthritis Rheumatol* 2017;69:774–84.
 15. Qaiyum Z, Gracey E, Yao Y, Inman RD. Integrin and transcriptomic profiles identify a distinctive synovial CD8⁺ T cell subpopulation in spondyloarthritis. *Ann Rheum Dis* 2019;78:1566–75.
 16. Dotiwala F, Mulik S, Polidoro RB, Ansara JA, Burleigh BA, Walch M, et al. Killer lymphocytes use granzysin, perforin and granzymes to kill intracellular parasites. *Nat Med* 2016;22:210–6.
 17. Hess C, Means TK, Autissier P, Woodberry T, Altfeld M, Addo MM, et al. IL-8 responsiveness defines a subset of CD8 T cells poised to kill. *Blood* 2004;104:3463–71.
 18. Cruz-Guilloty F, Pipkin ME, Djuretic IM, Levanon D, Lotem J, Lichtenheld MG, et al. Runx3 and T-box proteins cooperate to establish the transcriptional program of effector CTLs. *J Exp Med* 2009;206:51–9.
 19. Voskoboinik I, Trapani JA. Perforinopathy: a spectrum of human immune disease caused by defective perforin delivery or function. *Front Immunol* 2013;4:441.
 20. Buzza MS, Bird PI. Extracellular granzymes: current perspectives. *Biol Chem* 2006;387:827–37.
 21. Colbert RA, Tran TM, Layh-Schmitt G. HLA-B27 misfolding and ankylosing spondylitis. *Mol Immunol* 2014;57:44–51.

Polyfunctional, Proinflammatory, Tissue-Resident Memory Phenotype and Function of Synovial Interleukin-17A+CD8+ T Cells in Psoriatic Arthritis

Kathryn J. A. Steel,¹ Ushani Srenathan,¹ Michael Ridley,¹ Lucy E. Durham,¹ Shih-Ying Wu,¹ Sarah E. Ryan,¹ Catherine D. Hughes,² Estee Chan,³ Bruce W. Kirkham,³ and Leonie S. Taams¹ 

Objective. Genetic associations imply a role for CD8+ T cells and the interleukin-23 (IL-23)/IL-17 axis in psoriatic arthritis (PsA) and other spondyloarthritides (SpA). IL-17A+CD8+ (Tc17) T cells are enriched in the synovial fluid (SF) of patients with PsA, and IL-17A blockade is clinically efficacious in PsA/SpA. This study was undertaken to determine the immunophenotype, molecular profile, and function of synovial Tc17 cells in order to elucidate their role in PsA/SpA pathogenesis.

Methods. Peripheral blood (PB) and SF mononuclear cells were isolated from patients with PsA or other types of SpA. Cells were phenotypically, transcriptionally, and functionally analyzed by flow cytometry (n = 6–18), T cell receptor β (TCR β) sequencing (n = 3), RNA-Seq (n = 3), quantitative reverse transcriptase–polymerase chain reaction (n = 4), and Luminex or enzyme-linked immunosorbent assay (n = 4–16).

Results. IL-17A+CD8+ T cells were predominantly TCR $\alpha\beta$ + and their frequencies were increased in the SF versus the PB of patients with established PsA ($P < 0.0001$) or other SpA ($P = 0.0009$). TCR β sequencing showed that these cells were polyclonal in PsA (median clonality 0.08), while RNA-Seq and deep immunophenotyping revealed that PsA synovial Tc17 cells had hallmarks of Th17 cells (*RORC/IL23R/CCR6/CD161*) and Tc1 cells (granzyme A/B). Synovial Tc17 cells showed a strong tissue-resident memory T (Trm) cell signature and secreted a range of proinflammatory cytokines. We identified CXCR6 as a marker for synovial Tc17 cells, and increased levels of CXCR6 ligand CXCL16 in PsA SF ($P = 0.0005$), which may contribute to their retention in the joint.

Conclusion. Our results identify synovial Tc17 cells as a polyclonal subset of Trm cells characterized by polyfunctional, proinflammatory mediator production and CXCR6 expression. The molecular signature and functional profiling of these cells may help explain how Tc17 cells can contribute to synovial inflammation and disease persistence in PsA and possibly other types of SpA.

INTRODUCTION

Psoriatic arthritis (PsA) is part of an umbrella group of inflammatory diseases, termed spondyloarthritides (SpA), that share common patterns of joint inflammation (peripheral and axial);

skin, gut, and eye manifestations; genetic components; and the absence of diagnostic autoantibodies (seronegativity). In addition to PsA, SpA includes ankylosing spondylitis (AS)/nonradiographic axial spondylitis, reactive arthritis, enteropathic arthritis, and undifferentiated SpA, with a combined prevalence of 1–2% (1).

Supported in part by King's Health Partners R&D Challenge Fund (R140808), Research Councils UK Medical Research Council (grant MR/P018904/1), Novartis Pharma AG, Versus Arthritis (grant 21139), and the NIHR Biomedical Research Centre at Guy's and St. Thomas' NHS Foundation Trust and King's College London. The views expressed are those of the authors and not necessarily those of the NHS, the NIHR, or the Department of Health.

¹Kathryn J. A. Steel, PhD, Ushani Srenathan, PhD, Michael Ridley, PhD, Lucy E. Durham, MBBS, Shih-Ying Wu, MSc, Sarah E. Ryan, MRes, Leonie S. Taams, PhD: King's College London, London, UK; ²Catherine D. Hughes, MBChB, MSc, MRCP: King's College London, Guy's Hospital, and St. Thomas' Hospital, London, UK; ³Estee Chan, BHB, MBChB, FRACP, Bruce W. Kirkham, MD, FRCP, FRACP: Guy's Hospital and St. Thomas' Hospital, London, UK.

Drs. Srenathan and Ridley contributed equally to this work. Drs. Kirkham and Taams contributed equally to this work.

Dr. Kirkham has received consulting fees, speaking fees, and/or honoraria from AbbVie, Eli Lilly, Gilead, Janssen, and Novartis (less than \$10,000 each) and research support from Eli Lilly and Novartis. Dr. Taams has received consulting fees, speaking fees, and/or honoraria from Cytokine Signalling Forum (less than \$10,000), speaking fees from UCB and Novartis (less than \$10,000 each), and research support from those companies. No other disclosures relevant to this article were reported.

Address correspondence to Leonie S. Taams, PhD, King's College London, Centre for Inflammation Biology and Cancer Immunology (CIBCI), Department of Inflammation Biology, School of Immunology & Microbial Sciences, New Hunt's House First Floor, Guy's Campus, London SE1 1UL, UK. E-mail: leonie.taams@kcl.ac.uk.

Submitted for publication June 10, 2019; accepted in revised form October 31, 2019.

It is increasingly recognized that the interleukin-23 (IL-23)/IL-17 pathway plays a major role in PsA/SpA immunopathogenesis (2,3). Therapies targeting IL-17A show clinical efficacy in patients with PsA and those with AS (4,5), while several genetic loci implicated in the IL-17/IL-23 axis, including *IL12B* (IL-12p40), *IL23R*, and *TRAF3IP2* (Act1) are associated with PsA and AS susceptibility (6,7). To date, the majority of studies have focused on identifying IL-17A-producing CD4+ T (Th17) cells or group 3 innate lymphoid cells in the inflamed joints of patients with PsA/SpA, yet the strong association of major histocompatibility complex (MHC) class I and other CD8+ T cell/MHC class I-related loci (*RUNX3*, *ERAP1/2*) suggests that CD8+ T cells play an important role in PsA/SpA (7–9). We previously demonstrated the enrichment of IL-17A-expressing CD8+ T (Tc17) cells in the synovial fluid (SF) of patients with PsA (10); Tc17 cells have also been observed in the SF of patients with juvenile idiopathic arthritis (JIA) (11) and at the site of inflammation in other immune-mediated inflammatory diseases (for review, see refs. 2 and 12). Recent murine models and transcriptional analysis of healthy human spleen Tc17 cells have shed light on the function of Tc17 cells (13,14). However, functional and molecular analysis of human synovial Tc17 cells is essential to elucidate the role of synovial Tc17 cells in PsA/SpA pathogenesis.

The enrichment of Tc17 in the inflamed joint raises the question of whether these cells migrate into the joint or are persistently present. Recently, a novel subset of CD8+ effector T cells enriched in tissue compartments without significant presence in the blood has been described (15). These tissue-resident memory T (Trm) cells are characterized by expression of CD69 and CD103, defined by a core transcriptional signature (16), and have the potential to produce proinflammatory cytokines including IL-17A, IL-22, and interferon- γ (IFN γ), as well as granzymes and perforin (for review, see refs. 17 and 18). In humans, Trm cells have been observed in skin, lung, gut, and brain tissue, and a recent study demonstrated the presence of CD8+ T cells with a tissue-resident memory phenotype in the SF of patients with JIA (11). As such, Trm cells are hypothesized to contribute to the immunopathogenesis of human immune-mediated inflammatory disease. However, if and how Tc17 and Trm cells relate to each other is not well established.

To enhance our understanding of the function and molecular biology of human IL-17A+CD8+ T cells, we performed extensive phenotypic, molecular, and functional profiling of human Tc17 cells derived from PsA SF. Using flow cytometry, T cell receptor (TCR) sequencing, Luminex, and RNA-Seq analysis, we demonstrated that PsA synovial IL-17A+CD8+ T cells have a polyclonal TCR repertoire, a polyfunctional, proinflammatory cytokine profile, and many hallmarks of Trm cells. These features position Tc17 cells as relevant contributors to the initiation or perpetuation of chronic inflammation in PsA, and possibly other SpA or IL-17A/HLA class I-associated inflammatory diseases.

MATERIALS AND METHODS

Study subjects. Peripheral blood (PB) and SF samples were obtained from patients with PsA or other types of peripheral SpA (AS/nonradiographic axial SpA, reactive arthritis, and enteropathic arthritis) who were seen in the Rheumatology Department of Guy's Hospital. Patients fulfilled the Classification of Psoriatic Arthritis Study Group or American College of Rheumatology/European League Against Rheumatism 2010 criteria (19,20). The demographic and clinical characteristics of patients are shown in Supplementary Table 1, available on the *Arthritis & Rheumatology* web site at <http://onlinelibrary.wiley.com/doi/10.1002/art.41156/abstract>. All subjects provided written informed consent. Ethics approval was obtained from Bromley Research Ethics Committee (06/Q0705/20) and Harrow Research Ethics Committee (17/LO/1940).

Cell isolation. Mononuclear cells (PB mononuclear cells [PBMCs] and SF mononuclear cells [SFMCs]) were isolated using Lymphoprep (Axis-Shield) and washed in culture medium (RPMI 1640 supplemented with 10% fetal calf serum [FCS] + 1% penicillin/streptomycin/L-glutamine). Cells were cryopreserved and stored in liquid nitrogen in culture medium supplemented with 50% FCS and 10% dimethyl sulfoxide (all from ThermoFisher).

Flow cytometric analysis. Thawed cells were rested for 1 hour at 37°C in an atmosphere of 5% CO₂. For intracellular staining, samples were stimulated with phorbol myristate acetate (PMA; 50 ng/ml) and ionomycin (750 ng/ml) (both from Sigma-Aldrich) in the presence of GolgiStop (BD Biosciences) for 3 hours at 37°C in an atmosphere of 5% CO₂. Cells were stained with eFluor 780 Viability Dye (eBioscience), and surface staining was performed at 4°C. Cells were fixed with 2% paraformaldehyde and permeabilized using 0.5% saponin (Sigma-Aldrich). Antibodies are listed in Supplementary Table 2, available on the *Arthritis & Rheumatology* web site at <http://onlinelibrary.wiley.com/doi/10.1002/art.41156/abstract>. Samples were acquired using an LSRFortessa system (BD Biosciences). Data were analyzed using FlowJo (version 10; Tree Star).

TCR β sequencing. Extracted DNA (Qiagen) was subjected to bias-controlled amplification of V–D–J rearrangements followed by high-throughput sequencing (immunoSEQ; Adaptive Biotech). Data from productive reads (sequence level) were analyzed using an immunoSEQ analysis platform (Adaptive Biotech). Clonality was defined as $1 - \text{Pielou's evenness}$ and ranged from 0 (indicating a highly polyclonal repertoire) to 1 (indicating a monoclonal repertoire). Overlap was determined using the Morisita index, with possible scores ranging from 0 (indicating no similarity between 2 populations) to 1 (indicating complete similarity between 2 populations).

Cell sorting. For Trm cell sorting, SFMCs were stained with eFluor 780 and CD3, CD4, CD8, CD14, CD69, and CD103 antibodies (Supplementary Table 2, available on the *Arthritis & Rheumatology*

web site at <http://onlinelibrary.wiley.com/doi/10.1002/art.41156/abstract>). After sorting, CD8+ Trm subsets were stimulated, fixed, and permeabilized before intracellular cytokine staining for IL-17A and IFN γ . For sorting of cytokine-producing cells, magnetically

isolated (Miltenyi Biotec) CD3+ T cells were stimulated for 1.5 hours at 37°C with PMA (50 ng/ml) and ionomycin (750 ng/ml) before staining using an IL-17A and, where indicated, IFN γ cytokine secretion assay (Miltenyi). To identify cytokine-producing T cell subsets,

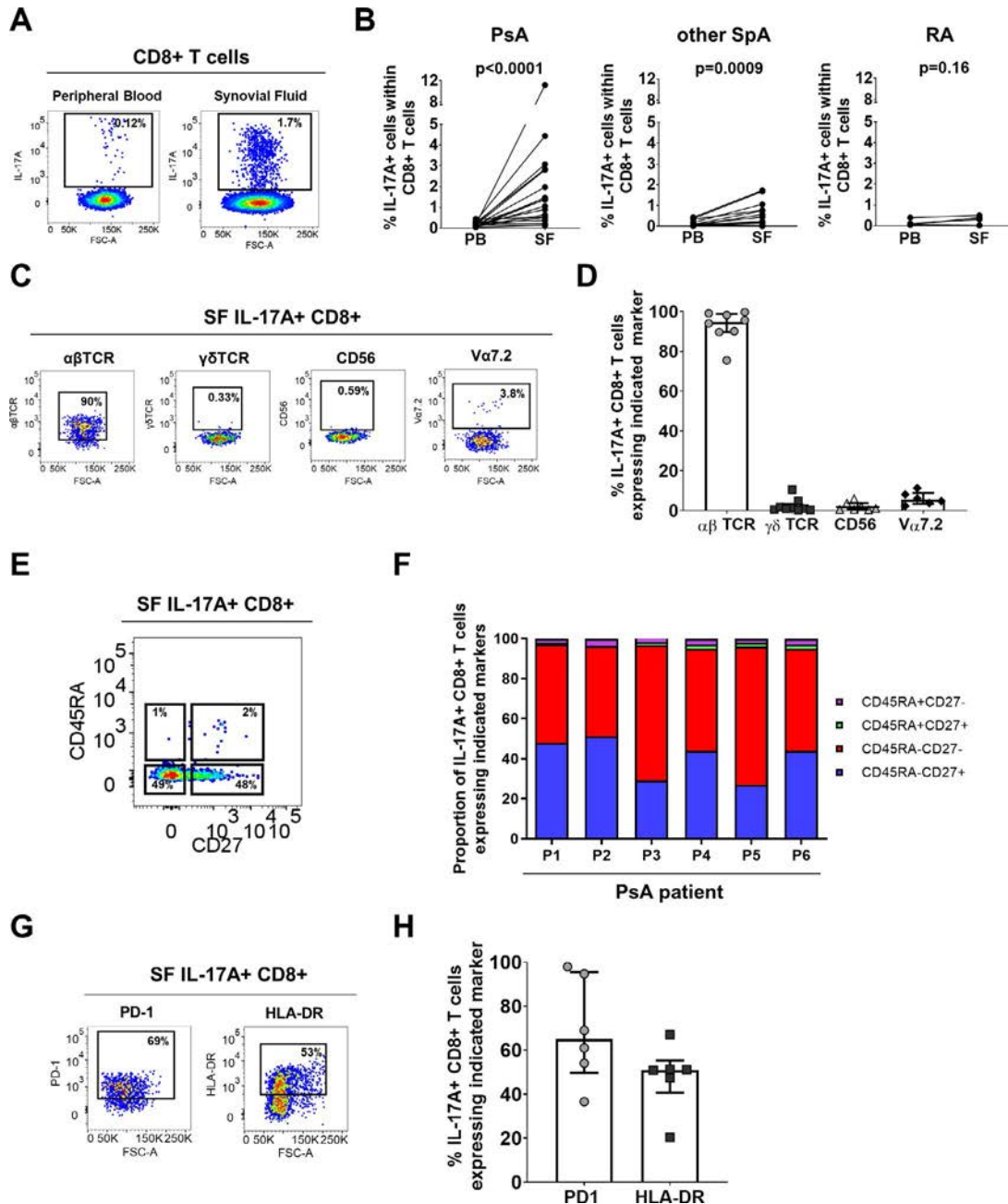


Figure 1. Enrichment of T cells positive for interleukin-17A (IL-17A) and T cell receptor $\alpha\beta$ (TCR $\alpha\beta$) in the synovial fluid (SF) of patients with spondyloarthritis (SpA). **A** and **B**, Representative staining (**A**) and cumulative data (**B**) showing the frequencies of IL-17A+ cells among CD3+CD8+ T cells in paired peripheral blood mononuclear cells (PBMCs) and SF mononuclear cells (SFMCs) from patients with psoriatic arthritis (PsA; $n = 18$), other peripheral SpA ($n = 14$), or rheumatoid arthritis (RA; $n = 6$) after 3 hours of stimulation in the presence of phorbol myristate acetate, ionomycin, and GolgiStop. P values were determined by Wilcoxon's matched pairs signed rank test. **C** and **D**, Representative staining (**C**) and cumulative data (**D**) showing the frequencies of IL-17A+CD8+ T cells expressing TCR $\alpha\beta$ ($n = 8$), TCR $\gamma\delta$ ($n = 9$), CD56 ($n = 7$), and V α 7.2 ($n = 6$) in PsA SF (stimulated as described in **A** and **B**). **E** and **F**, Representative staining (**E**) and frequencies (**F**) of IL-17A+CD8+ T cells expressing CD45RA and/or CD27 in PsA SFMCs ($n = 6$) (stimulated as described in **A** and **B**). **G** and **H**, Representative staining (**G**) and cumulative data (**H**) showing the frequencies of IL-17A+CD8+ T cells expressing programmed death 1 (PD-1) or HLA-DR in PsA patients ($n = 6$). In **D** and **H**, symbols represent individual patients, bars show the median and interquartile range. Color figure can be viewed in the online issue, which is available at <http://onlinelibrary.wiley.com/doi/10.1002/art.41156/abstract>.

cells were counterstained with eFluor 780, and anti-CD3, CD8, CD14, and CD4 antibodies. Cells were sorted using a BD FACSAria and acquired using an LSRFortessa system (BD Biosciences).

RNA sequencing and quantitative reverse transcriptase-polymerase chain reaction (qRT-PCR). Libraries were prepared by Genewiz and sequenced on a HiSeq 2500 platform (Illumina) at a depth of 28–40M reads. Low-quality bases and adapters (phred score <20) were trimmed using TrimGalore!, and reads were aligned (hg38) using RNA STAR. Paired reads were quantified using featureCounts. Principal components analysis and statistical comparison of gene expression were performed using DESeq2. RNAseq data are available via GSE137510.

For qRT-PCR, total RNA was extracted from sorted cell subsets (Qiagen). Complementary DNA (cDNA) was generated using a high-capacity cDNA reverse transcription kit (ThermoFisher). RT-PCR was performed using a SensiFAST SYBR kit (BioLine) and primers from Integrated DNA Technologies (listed in Supplementary Table 3, available on the *Arthritis & Rheumatology* web site at <http://onlinelibrary.wiley.com/doi/10.1002/art.41156/abstract>).

Luminex assay and CXCL16 enzyme-linked immunosorbent assay (ELISA). Supernatants were obtained from sorted T cell subsets cultured for 24 hours in culture media. A custom magnetic Luminex (Bio-Techne) was analyzed on a Luminex FlexMap 3D platform. Serum and SF were analyzed using a CXCL16 ELISA (Bio-Techne).

Graphics and statistical analysis. Statistical analysis and graphic illustration were performed using either GraphPad Prism (version 7) or ggplot2 (R version 3.5.2). Results are expressed as the median and interquartile range. Wilcoxon's matched pairs signed rank test or Friedman's multiple comparisons test were performed.

RESULTS

Tc17 cells are polyclonal TCR $\alpha\beta$ + memory cells enriched in PsA/SpA joints. To determine whether synovial Tc17 cells are enriched only in PsA or are also enriched in other SpA types, we stimulated paired PBMCs and SFMCs from patients with PsA, patients with other types of SpA, and patients with rheumatoid arthritis (RA) ex vivo with PMA/ionomycin and assessed the frequency of IL-17A+CD8+ T cells by flow cytometry (Figures 1A and B). (The gating strategy is shown in Supplementary Figure 1, available on the *Arthritis & Rheumatology* web site at <http://onlinelibrary.wiley.com/doi/10.1002/art.41156/abstract>.) Low frequencies of Tc17 cells were detected in PBMCs from patients with PsA, those with other types of SpA, and those with RA (median 0.1%), with no significant differences observed between these groups. The frequencies of Tc17 cells were significantly increased in SFMCs compared to PBMCs in patients with PsA ($P < 0.0001$) and

those with other types of SpA ($P = 0.0009$), but not those with RA ($P = 0.16$). The frequencies of Th17 cells were similar between the 3 disease groups (Supplementary Figure 1B).

Synovial Tc17 cells predominantly comprised TCR $\alpha\beta$ + cells, with small proportions of mucosal-associated invariant T cells (V α 7.2+), TCR $\gamma\delta$, and natural killer T cells (Figures 1C and D). Over 98% of synovial Tc17 cells exhibited a memory phenotype (CD45RA–CD27+/- or CD45RA+CD27-) (Figures 1E and F), while a considerable proportion of Tc17 cells expressed the immunoinhibitory receptor programmed death 1 (PD-1; median 65%) and activation marker HLA–DR (median 51%), suggesting that these cells previously experienced antigen stimulation (Figures 1G and H).

The presence of clonally restricted memory CD8+ T cells with features of antigen-specific expansion has been described in the SF, synovial tissue, and skin of patients with PsA (21–23). To investigate whether synovial Tc17 cells are also clonally restricted in PsA, bulk memory (CD45RA–CD27+/- and CD45RA+CD27-), IL-17A+IFN γ +/- (Tc17), and IL-17A–IFN γ + (Tc1) memory CD8+ T cells were sorted from the SF of PsA patients. (The gating strategy is shown in Supplementary Figure 2, available on the *Arthritis & Rheumatology* web site at <http://onlinelibrary.wiley.com/doi/10.1002/art.41156/abstract>.) TCR β sequencing showed that synovial Tc17 cells have a diverse TCR repertoire (Figure 2A) with a low clonality score (Pielou's evenness), which was similar to that for synovial Tc1 and bulk memory CD8+ T cells (Figures 2A and B). For 2 patients, a substantial proportion of the clones found in synovial Tc17 cells were also present in the synovial Tc1 population, resulting in a Morisita overlap index >0.9 (Figures 2C and D). The third patient had a lower number of productive templates, which may have resulted in a low Morisita score.

Molecular analysis of synovial Tc17 cells reveals commonalities in transcriptional profile with Th17 and Tc1 cells. Recent transcriptional analysis of healthy human spleen Tc17 cells revealed a distinct molecular profile compared to IL-17–CD8+ T cells or Th17 cells (14). To determine the molecular profile of Tc17 cells from the inflamed PsA joint, we sorted highly pure Tc17, Tc1, and Th17 cells from the SFMCs of patients with PsA for RNA sequencing. (The gating strategy is shown in Supplementary Figure 3, available on the *Arthritis & Rheumatology* web site at <http://onlinelibrary.wiley.com/doi/10.1002/art.41156/abstract>.) Accurate sorting was confirmed by the normalized gene counts of *IL17A* and *IFNG* for each of the populations (Supplementary Figure 3B).

Principal components analysis showed a degree of gene expression heterogeneity between synovial Tc17 cells from different patients. In 2 of 3 patients, the synovial Tc17 cells clustered separately from the Th17 cells but close to the Tc1 cells (Figures 3A and B), suggesting that a proportion of the transcriptional profile is shared between synovial Tc17 and Tc1 cells. In total, 80 genes were differentially expressed between the synovial Tc17 and Tc1 subsets ($\leq 1\%$ false discovery rate; fold change >2). MA plots indicating the 10 genes up-regulated to the greatest

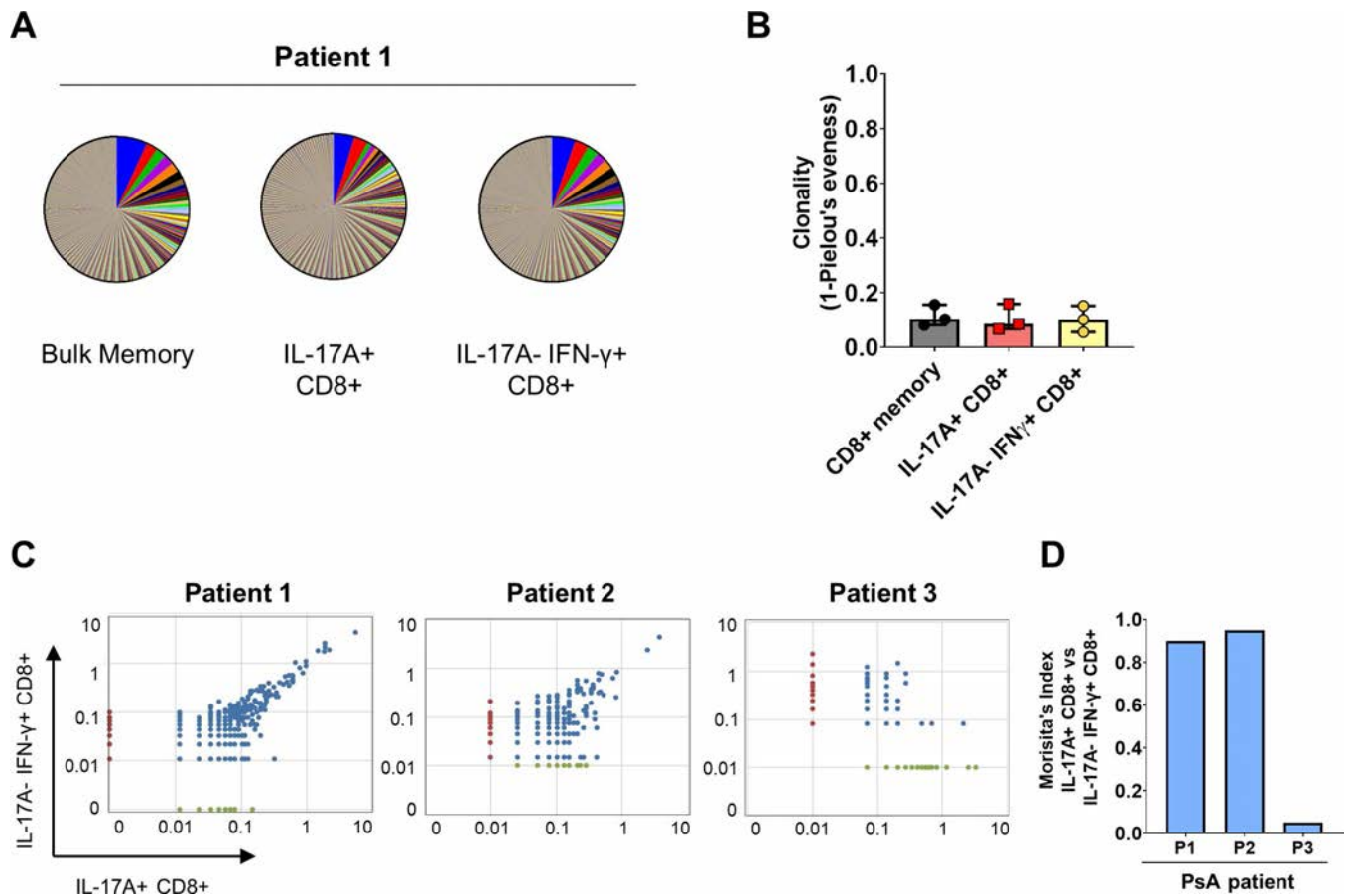


Figure 2. Diverse T cell receptor (TCR) repertoire in synovial Tc17 cells. **A**, Representative pie charts with segments representing the frequencies of all TCR β sequences in bulk memory CD8+ T cells, CD8+ T cells positive for interleukin-17A (IL-17A), and CD8+ T cells negative for IL-17A and positive for interferon- γ (IFN γ) in a patient with psoriatic arthritis (PsA). **B**, Clonality score (defined as 1 – Pielou's evenness) for bulk memory CD8+, IL-17A+CD8+, and IL-17A–IFN γ +CD8+ T cells in PsA synovial fluid samples ($n = 3$). Symbols represent individual patients; bars show the median and interquartile range. **C** and **D**, Dot plots (**C**) and Morisita's index (**D**) showing the degree of clonal overlap between IL-17A+CD8+ and IL-17A–IFN γ +CD8+ T cells in 3 patients with PsA. Color figure can be viewed in the online issue, which is available at <http://onlinelibrary.wiley.com/doi/10.1002/art.41156/abstract>.

degree and the 10 genes down-regulated to the greatest degree are shown in Figure 3C. Several genes relating to a type 17 T cell response (*IL17A*, *IL17F*, *RORC*, *IL23R*, *CCR6*, and *KLRB1*) were elevated in synovial Tc17 cells compared to synovial Tc1 cells (Figures 3C and E). When synovial Tc17 cells were compared to synovial Th17 cells, 145 genes were found to be differentially expressed (Figure 3D). Genes that were up-regulated in synovial Tc17 cells compared to Th17 cells included *CD8A* and *CD8B*, confirming our gating strategy, plus genes associated with cytolytic activity (*GRZA*, *GRZB*, and *PRF1*) (Figures 3D and F). Expression levels of *TCF7* (encoding T cell factor 1), recently identified as a transcription regulator of mouse Tc17 cells through repression of MAF BZIP transcription factor and retinoic acid receptor–related orphan nuclear receptor γ t (14), were low in synovial Tc17 cells (Supplementary Figure 3C).

We confirmed the transcription data for the type 17 T cell markers CCR6 and CD161 at the protein level by flow cytometry. A high frequency of synovial Tc17 cells coexpressed CCR6

or CD161, at levels comparable to those in synovial Th17 cells. In contrast, only limited proportions of synovial IL-17A–CD8+ or IFN γ +CD8+ T cells expressed these molecules (Figures 4A and B). A viSNE analysis showed that CCR6 and CD161 were coexpressed by Tc17 cells (Figure 4C) (results are representative of those for 7 patients). Notably, this analysis also revealed that expression of CCR6 and CD161 was not restricted to the IL-17A+ population, i.e., these markers do not exclusively define IL-17A expression in synovial CD8+ T cells. Quantitative RT-PCR analysis further confirmed that transcript levels of *RORC* and *IL23R* in the synovial Tc17 population were comparable to those in Th17 cells, and higher than those in IL-17A–CD8+ T cells (which contains IFN γ +CD8+ T cells) (Figure 4D).

Frequencies of Tc17 cells expressing granzyme A, granzyme B, CD107a, or perforin were variable but enhanced compared to synovial Th17 cells, while they were comparable to those among synovial Tc1 cells (Figures 4E and F). It should be noted, however, that limited expression of perforin

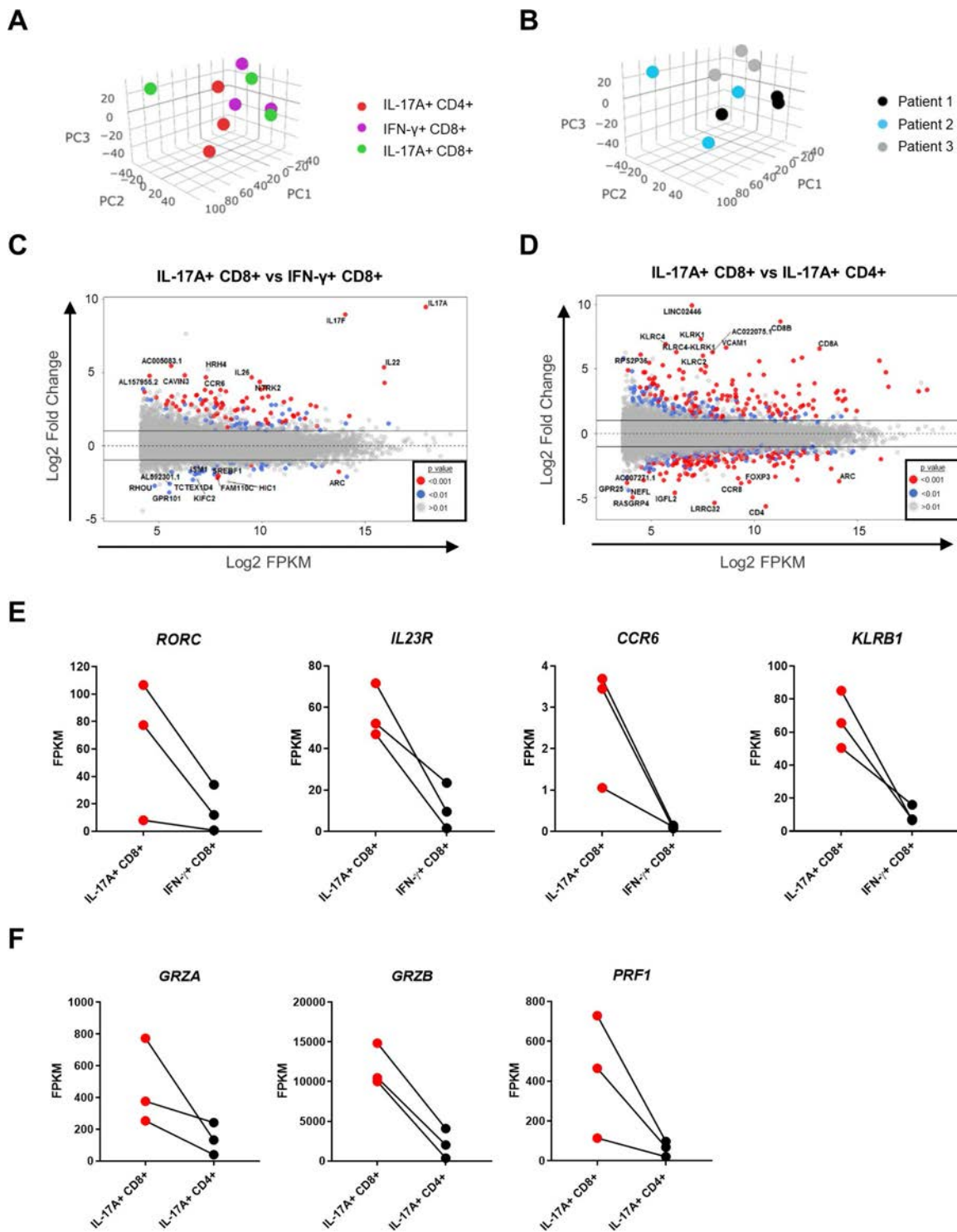


Figure 3. Transcriptional profile of synovial Tc17 cells compared to Tc1 cells and Th17 cells. **A** and **B**, Principal components analysis of the transcriptome of IL-17A+CD8+, IFN γ +CD8+, and IL-17A+CD4+ T cells from the synovial fluid of PsA patients ($n = 3$) by cell type (**A**) and by patient (**B**). **C** and **D**, MA plots showing genes that were significantly up-regulated or down-regulated in synovial IL-17A+CD8+ T cells compared to IFN γ +CD8+ T cells or IL-17A+CD4+ T cells ($n = 3$). **E** and **F**, Selected gene expression profiles shown as average gene expression values (fragments per kilobase million [FPKM]) in synovial IL-17A+CD8+ compared to IFN γ +CD8+ T cells or CD4+IL-17A+ T cells ($n = 3$). PC1 = principal component 1 (see Figure 2 for other definitions).

and lysosomal-associated membrane protein 1 (LAMP-1)/CD107a was observed in synovial Tc17 cells, suggesting that these cells may not have full cytotoxic capability.

Tc17 cells have hallmarks of Trm cells. The observation that Tc17 cells with a memory phenotype are enriched in the joint, but not the blood, in PsA patients prompted us to investigate

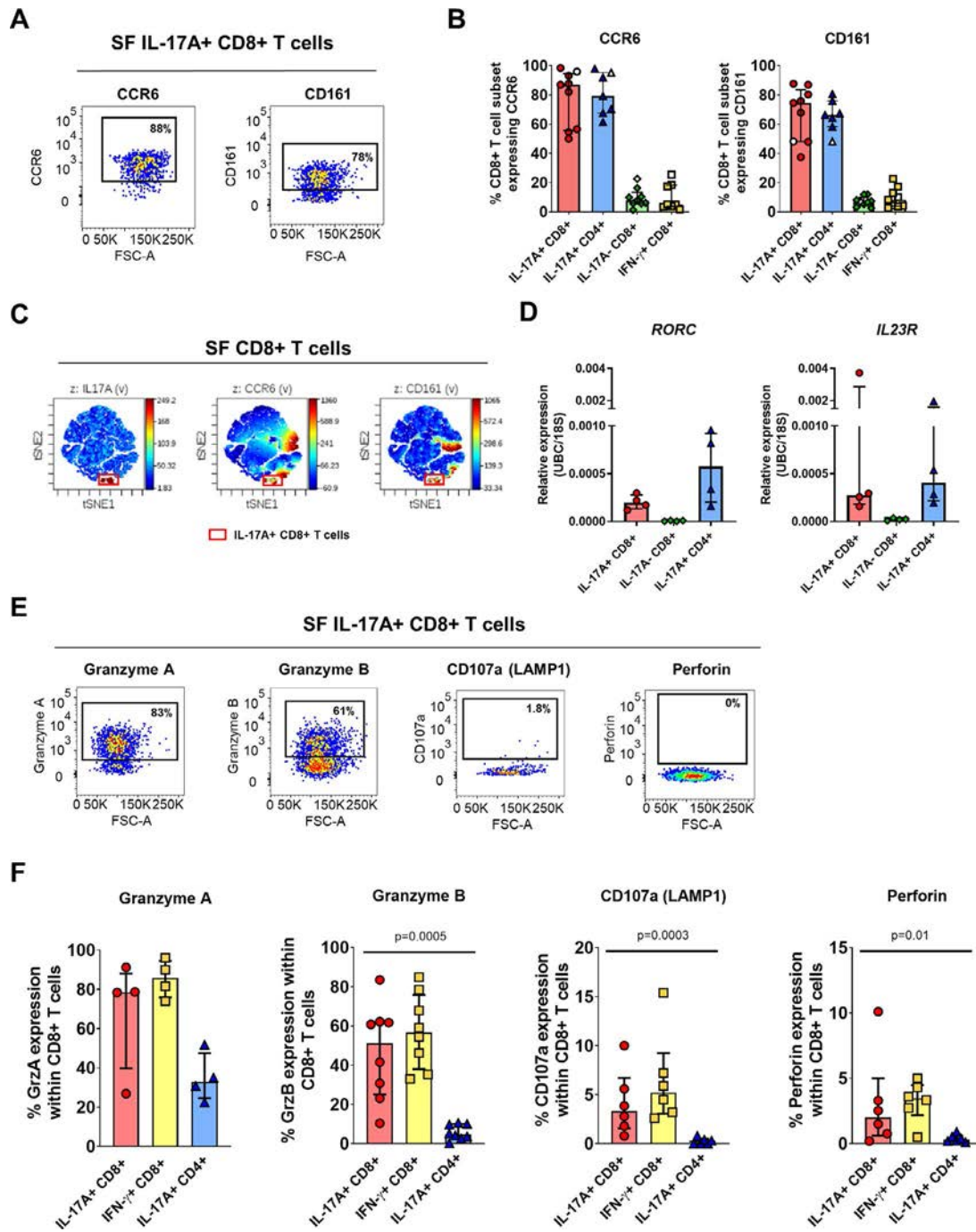


Figure 4. Synovial Tc17 cells have functional hallmarks of Th17 and Tc1 cells. **A** and **B**, Representative staining (**A**) and cumulative data (**B**) showing the frequencies of IL-17A+CD8+, IL-17A+CD4+, IL-17A-CD8+, and IFN γ +CD8+ T cells expressing CCR6 and CD161 in synovial fluid mononuclear cells (SFMCs) from patients with PsA (solid symbols) and patients with other types of spondyloarthritis (open symbols) ($n = 7-9$). **C**, Representative viSNE plot showing concomitant expression of IL-17A, CCR6, and CD161 among CD8+ T cells in PsA SFMCs. Representative results from 1 of 7 patients are shown. **D**, Gene expression levels of *RORC* and *IL23R*, normalized to the average values for *UBC* and *18S* in sorted IL-17A+CD8+, IL-17A-CD8+, and IL-17A+CD4+ T cells from PsA SFMCs ($n = 4$). **E** and **F**, Representative staining (**E**) and cumulative data (**F**) showing the frequencies of IL-17A+CD8+, IFN γ +CD8+, and IL-17A+CD4+ T cells expressing granzyme A (GrzA; $n = 4$), granzyme B (GrzB; $n = 9$), CD107a/lysosomal-associated membrane protein 1 (LAMP-1; $n = 6$), and perforin ($n = 6$) in PsA SFMCs. *P* values were determined by Friedman's multiple comparisons test. In **B**, **D**, and **F**, symbols represent individual patients; bars show the median and interquartile range. See Figure 2 for other definitions. Color figure can be viewed in the online issue, which is available at <http://onlinelibrary.wiley.com/doi/10.1002/art.41156/abstract>.

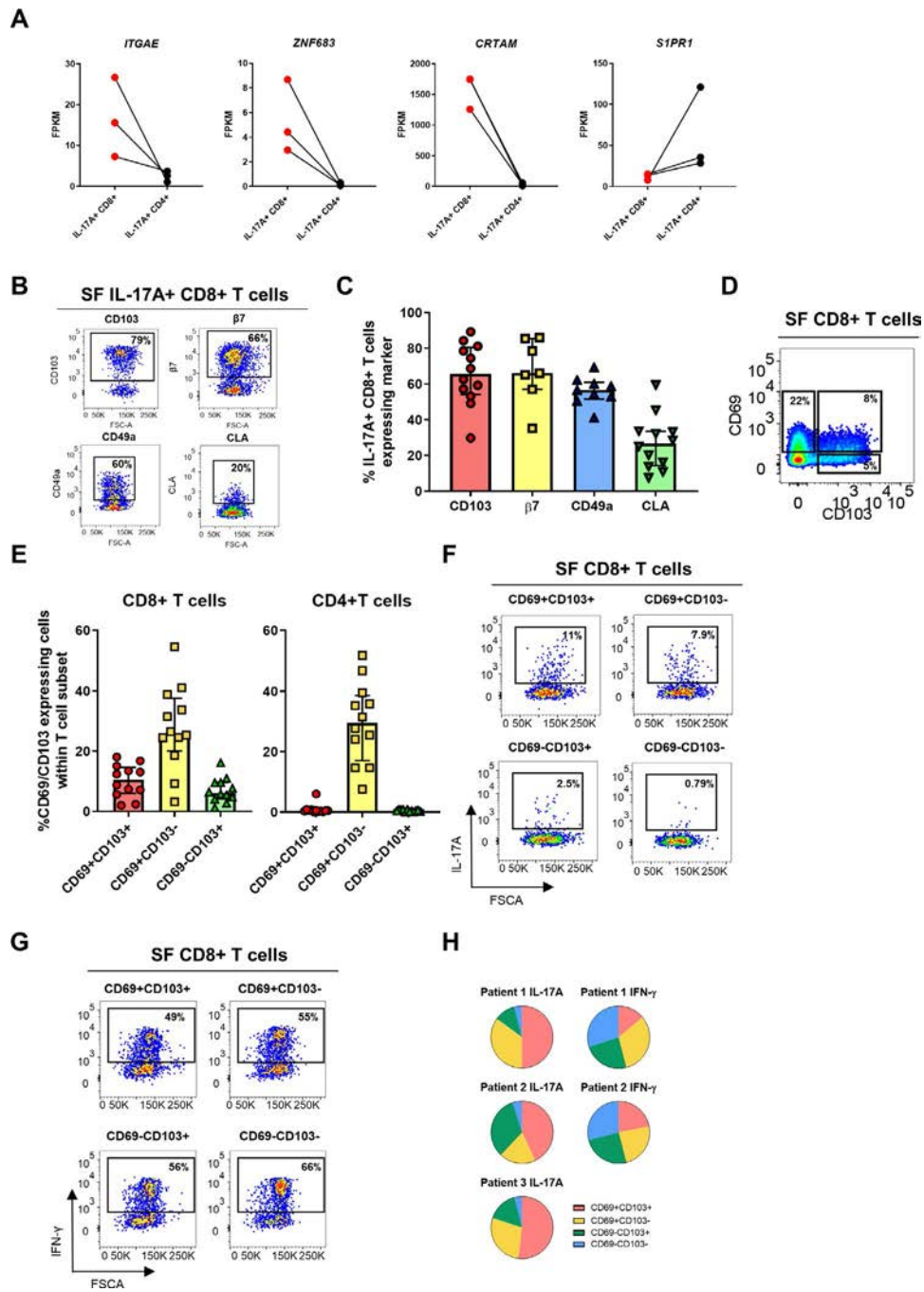


Figure 5. Synovial Tc17 cells form part of the synovial tissue-resident T cell compartment. **A**, Selected tissue-resident memory T (Trm) cell-associated gene expression profiles of sorted synovial IL-17A+CD8+ T cells compared to IL-17A+CD4+ T cells ($n = 3$). **B** and **C**, Representative staining (**B**) and cumulative data (**C**) showing the frequencies of IL-17A+CD8+ T cells expressing CD103/ α E integrin ($n = 12$), β 7 integrin ($n = 7$), CD49a/very late activation antigen 1 ($n = 9$), or cutaneous lymphocyte antigen (CLA; $n = 12$) in PsA synovial fluid mononuclear cells (SFMCs), after 3 hours of stimulation in the presence of phorbol myristate acetate (PMA), ionomycin, and GolgiStop. **D** and **E**, Representative staining (**D**) and cumulative data (**E**) showing the frequencies of CD69+CD103+, CD69+CD103-, and CD69-CD103+ Trm cells among synovial CD3+CD8+ and CD3+CD4+ T cells ($n = 12$). **F-H**, PsA SF cells ($n = 3$) were sorted into CD69+CD103+, CD69+CD103-, CD69-CD103+, and CD69-CD103- CD8+ T cells. Sorted subsets were stimulated with PMA and ionomycin in the presence of GolgiStop for 3 hours. **F** and **G**, Representative staining showing IL-17A (**F**) and IFN γ (**G**) expression within the 4 sorted subsets. **H**, Proportion of IL-17A+ cells (left; $n = 3$) and IFN γ + cells (right; $n = 2$) in each Trm subset, as a fraction of total IL-17A-expressing or IFN γ -expressing cells. In **C** and **E**, symbols represent individual patients; bars show the median and interquartile range. FPKM = fragments per kilobase million (see Figure 2 for other definitions). Color figure can be viewed in the online issue, which is available at <http://onlinelibrary.wiley.com/doi/10.1002/art.41156/abstract>.

whether synovial Tc17 cells from the inflamed joint expressed markers of tissue residency. Molecular profiling revealed that genes reported to be transcriptional hallmarks of T_{rm} cells (e.g., *ITGAE*

[encoding CD103], *ZNF683* [encoding HOBIT], *CRTAM*, and low levels of *S1PR1*) (16) were differentially expressed between synovial Tc17 and Th17 cells (Figure 5A). We confirmed the

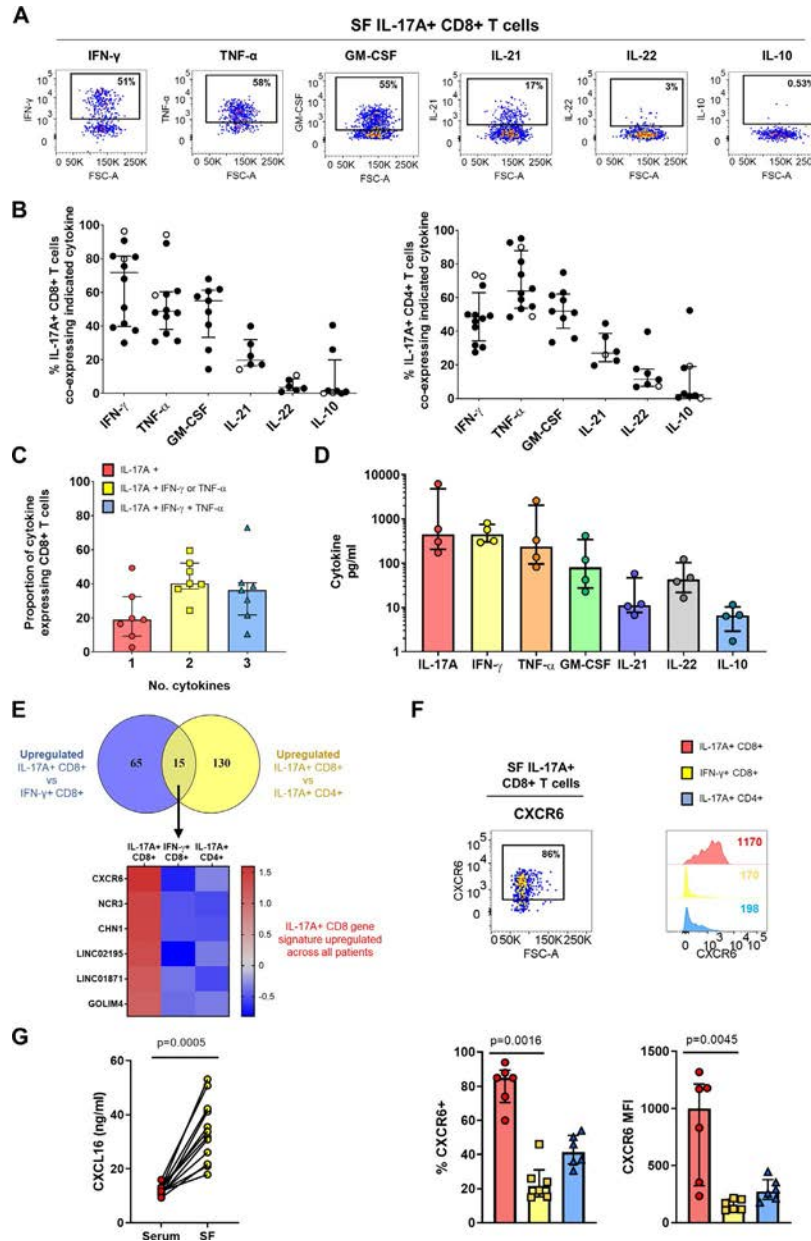


Figure 6. Synovial Tc17 cells are polyfunctional proinflammatory cells characterized by high expression of CXCR6. **A** and **B**, Representative staining (**A**) and cumulative data (**B**) showing the frequencies of IL-17A+CD8+ (left) and IL-17A+CD4+ (right) T cells expressing IFN γ (n = 12), tumor necrosis factor (TNF; n = 12), granulocyte–macrophage colony-stimulating factor (GM-CSF; n = 9), IL-21 (n = 6), IL-22 (n = 6), and IL-10 (n = 8) in synovial fluid mononuclear cells (SFMCs) from patients with PsA (solid symbols) or other types of spondyloarthritis (open symbols). **C**, Proportion of IL-17A+CD8+ T cells expressing IL-17A alone, IL-17A plus IFN γ and TNF, and IL-17A plus IFN γ and TNF. **D**, IL-17A, IFN γ , GM-CSF, IL-21, IL-22, and IL-10 secretion by sorted synovial IL-17A+CD8+ T cells (n = 4). **E**, Top, Venn diagram showing the number of significantly up-regulated genes ($P < 0.01$) in IL-17A+CD8+ T cells versus IFN γ +CD8+ T cells and in IL-17A+CD8+ T cells versus IL-17A+CD4+ T cells. Bottom, Heatmap showing genes that were consistently up-regulated in all patients. **F**, Representative dot plot and histograms (top) and cumulative data (bottom) showing the percentage of CXCR6+ cells and CXCR6 expression levels in PsA synovial IL-17A+CD8+ T cells, IFN γ +CD8+ T cells, and IL-17A+CD4+ T cells (n = 6). P values were determined by Friedman’s multiple comparisons test. **G**, CXCL16 levels in paired PsA serum and SF samples (n = 12) as measured by enzyme-linked immunosorbent assay. P value was determined by Wilcoxon’s matched pairs signed rank test. In **C** and **D**, bars show the median and interquartile range. MFI = mean fluorescence intensity (see Figure 2 for other definitions). Color figure can be viewed in the online issue, which is available at <http://onlinelibrary.wiley.com/doi/10.1002/art.41156/abstract>.

expression of the T_{rm} cell marker CD103 (α E integrin) on a high proportion of joint-derived Tc17 cells by flow cytometry (Figures 5B and C). CD69, which is also commonly used as a T_{rm} marker, is up-regulated upon PMA/ionomycin stimulation and was therefore not evaluated. Since Tc17 cells have been identified in the gut and the skin (24–27), sites that can also be affected in PsA/SpA, we assessed markers for the gut-related molecule β 7 integrin (which is normally coexpressed with α E integrin) and the skin-related adhesion/homing molecules cutaneous lymphocyte antigen (CLA) and CD49a (very late activation antigen [VLA-1]). Considerable proportions of synovial Tc17 cells coexpressed β 7 integrin, CD49a/VLA-1, and to a lesser extent CLA (Figures 5B and C).

Based on these findings, we examined the presence of T_{rm} cells using the markers CD69 and/or CD103 in unstimulated SFMCs from PsA patients (Figures 5D and E). Within the CD8+ T cell population, on average 11% of cells were CD69+CD103+ (range 2–16%), 26% of cells were CD69+CD103– (range 3.2–54%), and 6% of cells were CD69–CD103+ (range 1.29–16%). In the CD4+ compartment, 26% of the cells were CD69+CD103–, while CD103 expression was negligible (expressed by <1% of CD4+ T cells). These data indicate that CD103+ T_{rm} cells in the inflamed PsA joint are typically CD8+ T cells.

To directly demonstrate that CD8+ T_{rm} cells contain IL-17A-producing cells, we sorted synovial CD8+ T cells from PsA patients into highly pure CD69+CD103+, CD69+CD103–, CD69–CD103+, and CD69–CD103– subsets. (The gating strategy is shown in Supplementary Figure 4, available on the *Arthritis & Rheumatology* web site at <http://onlinelibrary.wiley.com/doi/10.1002/art.41156/abstract>.) The sorted cells were then stimulated *ex vivo* and stained for IL-17A and IFN γ (Figures 5F and G). After normalizing for total cytokine expression, we observed that the CD69+CD103+CD8+ T cell population contained the highest frequency of IL-17A+ cells, followed by cells expressing either CD69 or CD103 only, while CD69–CD103–CD8+ T cells contained minimal IL-17A+ cells (Figure 5H). In contrast, frequencies of IFN γ + cells were distributed more equally among the 4 sorted cell subsets. We also found a significant correlation between the presence of IL-17A+CD8+ T cells and CD69+CD103+ T_{rm} cells in the SF, further supporting a relationship between these 2 cell populations (Supplementary Figure 5, available on the *Arthritis & Rheumatology* web site at <http://onlinelibrary.wiley.com/doi/10.1002/art.41156/abstract>). Taken together, these data indicate that synovial T_{rm} cells are enriched for IL-17A expression and that Tc17 cells form part of the T_{rm} cell pool in the inflamed synovial joints in PsA.

Synovial Tc17 cells are polyfunctional inflammatory cells characterized by high expression of CXCR6.

Finally, we sought to determine the functional potential of synovial Tc17 cells. For this, we assessed the coexpression and secretion of proinflammatory and antiinflammatory cytokines by flow cytometry and Luminex assay. A substantial proportion of synovial Tc17 cells coexpressed proinflammatory IFN γ , TNF, and

granulocyte–macrophage colony-stimulating factor (GM-CSF), while IL-21 was coexpressed by <20% of Tc17 cells. IL-22 and antiinflammatory IL-10 were found to be either absent or expressed by only a small proportion of Tc17 cells (Figures 6A and B). IL-17F was found to be coexpressed by only a small proportion of Tc17 cells (Supplementary Figure 6B, available on the *Arthritis & Rheumatology* web site at <http://onlinelibrary.wiley.com/doi/10.1002/art.41156/abstract>). The cytokine coexpression profile of synovial Tc17 cells closely resembled the cytokine profile of synovial Th17 cells (Figure 6B), while this profile was not shared by synovial IL-17A–CD8+ or IFN γ +CD8+ T cell subsets (Supplementary Figure 6A). Overall, synovial Tc17 cells displayed a polyfunctional cytokine profile with a sizable proportion of cells (median 36%) expressing IL-17A, IFN γ , and TNF concomitantly (Figure 6C). This concomitant cytokine production was also observed in the Luminex analysis: sorted IL-17A+CD8+ T cells from the SF of patients with PsA produced IL-17A, IFN γ , TNF, GM-CSF, and IL-22, with low levels of IL-21 and IL-10, during a 24-hour culture (Figure 6D). (The gating strategy is shown in Supplementary Figure 7, available on the *Arthritis & Rheumatology* web site at <http://onlinelibrary.wiley.com/doi/10.1002/art.41156/abstract>.)

Finally, we investigated whether Tc17 cells from the inflamed PsA joint express a unique set of markers. For this analysis, we compared the transcriptional profile of synovial Tc17 cells to the profiles of both synovial Tc1 and Th17 cells, to determine which markers are uniquely up-regulated in synovial Tc17 cells. Bioinformatics analysis revealed that 15 genes were up-regulated in both comparisons, suggesting that synovial Tc17 cells have a small unique transcriptional profile in comparison to synovial Tc1 and Th17 cells (Figure 6E). Of these 15 genes, 6 were found to be consistently up-regulated in all 3 patients: *CXCR6*, *NCR3*, *CHN1*, *LINC02195*, *LINC01871*, and *GOLIM4*. Since *CXCR6* is part of the T_{rm} gene signature (16), we validated *CXCR6* at the protein level and found that PsA synovial Tc17 cells indeed expressed *CXCR6* at the highest level and contained the highest proportion of *CXCR6*-expressing cells as compared to their synovial Tc1 and Th17 counterparts (Figure 6F). In addition, levels of CXCL16, the ligand for *CXCR6*, were significantly increased in PsA SF versus paired serum samples (Figure 6G).

DISCUSSION

We previously described an enrichment of IL-17A+CD4– (the majority of which were CD8+) T cells in the SF, compared to the PB, in patients with PsA (10). In this study we showed that frequencies of IL-17A+CD8+ T cells were also increased in the SF of patients with other types of SpA, and confirmed that these cells were not increased in patients with RA (10). These findings add to the growing evidence that CD8+ T cells and the IL-17/IL-23 axis are relevant to the immunopathogenesis of PsA/SpA (2). We demonstrated that the vast majority of PsA synovial Tc17 cells are

memory cells, indicated by a CD45RA–PD-1+HLA–DR+ profile, as well as TCR $\alpha\beta$ bearing, suggesting that these cells are MHC class I restricted and antigen-experienced.

Previous studies demonstrated oligoclonal expansion of joint-derived bulk T cells in PsA (21–23). Our TCR β sequencing of synovial Tc17 cells, although limited in sample size, showed that while some T cell clones occupied >5% of the total TCR repertoire, the majority of Tc17 cells, as well as of the bulk memory CD8+ T cells and Tc1 cells, had a polyclonal TCR repertoire. One reason for the differences observed between the previous studies and our own could be patient disease activity. A previous study investigating the clonality of psoriatic skin-derived CD8+ T cells showed that the TCR repertoire is polyclonal in active disease, while in resolved disease only a few dominant clones persist (28). We obtained SF effusions from joints with active inflammation, which could explain the polyclonal repertoire observed. It would be of interest to investigate whether a polyclonal repertoire is also observed in joints in which PsA has resolved; however, this would require a synovial biopsy study design since noninflamed joints rarely contain sufficient SF for aspiration.

A notable observation in our analysis was the extensive sharing of T cell clones between the synovial Tc17 and Tc1 populations. Our RNA-Seq analysis also showed significant overlap in transcriptional profile between Tc17 and Tc1 cells. A possible explanation for these findings is that synovial Tc17 and Tc1 cells may have shared ancestry, which raises the question of plasticity between these subsets. Adoptive transfer of in vitro generated Tc17 cells into recipient mice showed that Tc17 cells can switch to an IL-17A–negative Tc1 profile (29–31). A direct demonstration of this phenomenon came from an elegant IL-17A fate-mapping study using reporter donor IL-17^{Cre}Rosa26^{eYFP} (13). That study showed that Tc17 cells developed early after allogeneic stem cell transplantation in both lymphoid tissue and graft-versus-host disease target organs. However, their production of IL-17A was transient, while IFN γ production was largely maintained, a process defined by the surrounding cytokine milieu. A similar capacity to transition to IFN γ production and Th1 phenotype had previously been shown for mouse Th17 cells (32). These fate-mapping data, taken together with our findings on shared TCR and transcriptional profiles and the observation that a high frequency of synovial Tc17 cells express IFN γ , suggest that synovial Tc17 cells can transition to a Tc1-like cytokine profile, as was previously suggested for Th17 and Th1 cells in the joints of patients with JIA (33). If this scenario is indeed the case, then one implication of this finding would be that the percentage of IL-17A+CD8+ T cells detected by flow cytometry may underrepresent the contribution that Tc17 cells make or have made to the synovial T cell compartment.

In addition to Tc17/Tc1 overlap, we observed a phenotypic and molecular overlap between Tc17 and Th17 cells in PsA, as evaluated by RNA-Seq, qRT-PCR, and flow cytometry. Two markers typically expressed by Th17 cells, CCR6 and CD161 (34–36), are coexpressed by a large proportion of synovial Tc17 cells.

Furthermore, expression of *IL23R* by synovial Tc17 cells indicates that IL-23 may be involved in the generation or maintenance of these cells, while elevated *RORC* transcript expression suggests that ROR γ t may at least play a part in IL-17A regulation in these cells. These data indicate that Tc17 cells may be regulated by similar pathways as Th17 cells.

The relatively limited sample sizes in the TCR and RNA-Seq analysis could be considered a limitation of our study. However, given the challenges in obtaining sufficient numbers from small populations of immune cells, this number of samples ($n = 3$) is not uncommon in studies of human tissue-derived cells. Additionally, many of our RNA-Seq results were independently validated at the protein or RNA level. A further limitation of our study is that we did not have access to synovial tissue samples from patients with PsA. Nonetheless, the work presented here provides an important basis for future studies aimed at comparing the phenotype and molecular profile of SF- and synovial tissue-derived Tc17 cells.

A key novel finding of our study is that synovial Tc17 cells are part of the Trm cell compartment and express molecules that prevent egress from the inflamed tissue into the blood. Trm cells are rapidly emerging as potential contributors to inflammation in several immune-mediated inflammatory diseases (17,37). To our knowledge, this is the first study to show that Tc17 cells form part of the synovial Trm pool, and only the second description of Trm-like cells in the context of human immune-mediated arthritis (11). Our data also show that a high proportion of synovial Tc17 cells express markers typically associated with homing to the skin or gut. This finding could indicate that synovial Tc17 cells have tropism for these tissues as well as for the synovial compartment, and indeed, the presence of Tc17 cells has been described in both the skin and the gut (24,25,27). An alternative explanation could be that synovial Tc17 cells expressing these markers have enhanced adherence to the surrounding joint tissue, as both CLA and CD49a ligands (E-selectin and type IV collagen, respectively) are present in the synovial tissue (38,39). β 7 integrin, which is expressed by a large proportion of synovial Tc17 cells, can form a heterodimer with the Trm cell marker CD103 (α E integrin), which is expressed by Tc17 cells. The product, α E β 7 integrin, exclusively binds E-cadherin, a structural protein expressed in the synovial joint and fluid in patients with inflammatory arthritis (39,40). Interaction of synovial Tc17 cells with the surrounding tissue and extracellular matrix in the fluid combined with lack of response to exit cues (e.g., S1P1) could represent one way in which Tc17 cells are retained in the synovial joint and contribute to perpetuation or re-initiation of inflammation.

Residence of synovial Tc17 cells in the inflamed tissue may be further enhanced by their high expression of CXCR6, a marker of Trm cells (16), in combination with the increased levels of CXCL16 in the PsA synovial joint. CXCL16 has chemotactic and angiogenic properties and can be produced as a soluble mediator or as a transmembrane-bound chemokine by monocytes, macrophages, and dendritic cells. Evidence of increased CXCL16

and CXCR6 expression at the site of inflammation was reported previously in the context of RA and psoriasis, and CXCL16 was shown to enhance recruitment of inflamed tissue-derived CXCR6-expressing T cells (41–43). Furthermore, CXCL16 blockade or CXCR6 deficiency led to reduced arthritis scores and lower IFN γ /IL-17 production in an experimental model of arthritis (42,44). Taken together, these data suggest that the increased CXCR6 expression on synovial Tc17 cells may contribute to their recruitment and persistence in the inflamed PsA joint.

Functionally, our data indicate that synovial Tc17 cells are polyfunctional and actively secrete several proinflammatory cytokines (IFN γ , TNF, GM-CSF, IL-21, and IL-22) in parallel with IL-17A, but little IL-10 or IL-17F. IFN γ , TNF, and GM-CSF have all been shown to act synergistically with IL-17A to promote inflammation. In a recent study by Wade et al, polyfunctional CD8 $^+$ T cells were also found to be enriched in the PsA synovium, although enrichment was not observed for single cytokine-producing T cells, including IL-17A+CD8 $^+$ T cells (45). Concordant with their proinflammatory cytokine production, Tc17 cells coexpressed cytolytic molecules granzyme A and granzyme B at levels comparable to those in synovial Tc1 cells. However, Tc17 cells lacked significant expression of other cytolytic machinery (perforin and LAMP-1). Most studies to date in both mice and humans have shown that Tc17 cells lack cytolytic function (29,31,46,47), although some evidence for cytotoxic function has been reported (24,48). An interesting alternative interpretation of our data is that the secretion of granzymes is not cytolytic but leads to extracellular matrix degradation or promotion of inflammation (49,50). Taken together, these data show that Tc17 cells are armed with an array of proinflammatory mediators, which could act directly on surrounding cells to promote inflammation in the synovial joint.

In summary, our findings reveal that synovial Tc17 cells from the PsA joint bear hallmarks of T_{RM} cells, and express high levels of CXCR6, which may enhance retention of these cells in the inflamed joint. Our analysis of the transcriptional profile and TCR repertoire of these cells highlights several commonalities between Tc17 and Tc1 cells in the PsA joint. Combined with the observed polyfunctional proinflammatory mediator production, we hypothesize that Tc17 cells exert heterogeneous effector responses that contribute to the initiation and persistence of PsA.

ACKNOWLEDGMENTS

The authors would like to thank Sylvine Lahnunhlimi (King's College London) for help in processing some of the patient samples; Celine Trouillet, Yasmin Haque, and the BRC Flow Core staff for their help in flow sorting; and Dr. Esperanza Perucha (King's College London) for critical reading of the manuscript.

AUTHOR CONTRIBUTIONS

All authors were involved in drafting the article or revising it critically for important intellectual content, and all authors approved the final version to be

published. Dr. Taams had full access to all of the data in the study and takes responsibility for the integrity of the data and the accuracy of the data analysis.

Study conception and design. Steel, Kirkham, Taams.

Acquisition of data. Steel, Srenathan, Durham, Wu, Ryan, Hughes, Kirkham, Taams.

Analysis and interpretation of data. Steel, Srenathan, Ridley, Durham, Wu, Ryan, Chan, Kirkham, Taams.

ROLE OF THE STUDY SPONSOR


Novartis Pharma AG had no role in the study design or in the collection, analysis, or interpretation of the data, the writing of the manuscript, or the decision to submit the manuscript for publication. Publication of this article was not contingent upon approval by Novartis Pharma AG.

REFERENCES

1. Stolwijk C, Boonen A, van Tubergen A, Reveille JD. Epidemiology of spondyloarthritis. *Rheum Dis Clin North Am* 2012;38:441–76.
2. Taams LS, Steel KJ, Srenathan U, Burns LA, Kirkham BW. IL-17 in the immunopathogenesis of spondyloarthritis. *Nat Rev Rheumatol* 2018;14:453–66.
3. Gravallesse EM, Schett G. Effects of the IL-23-IL-17 pathway on bone in spondyloarthritis. *Nat Rev Rheumatol* 2018;14:631–40.
4. Mease PJ, McInnes IB, Kirkham B, Kavanaugh A, Rahman P, van der Heijde D, et al. Secukinumab inhibition of interleukin-17A in patients with psoriatic arthritis. *N Engl J Med* 2015;373:1329–39.
5. Baeten D, Sieper J, Braun J, Baraliakos X, Dougados M, Emery P, et al. Secukinumab, an interleukin-17A inhibitor, in ankylosing spondylitis. *N Engl J Med* 2015;373:2534–48.
6. International Genetics of Ankylosing Spondylitis Consortium (IGAS), Cortes A, Hadler J, Pointon JP, Robinson PC, Karaderi T, et al. Identification of multiple risk variants for ankylosing spondylitis through high-density genotyping of immune-related loci. *Nat Genet* 2013;45:730–8.
7. Bowes J, Budu-Aggrey A, Huffmeier U, Uebe S, Steel K, Hebert HL, et al. Dense genotyping of immune-related susceptibility loci reveals new insights into the genetics of psoriatic arthritis. *Nat Commun* 2015;6:6046.
8. Winchester R, Minevich G, Steshenko V, Kirby B, Kane D, Greenberg DA, et al. HLA associations reveal genetic heterogeneity in psoriatic arthritis and in the psoriasis phenotype. *Arthritis Rheum* 2012;64:1134–44.
9. Cortes A, Pulit SL, Leo PJ, Pointon JJ, Robinson PC, Weisman MH, et al. Major histocompatibility complex associations of ankylosing spondylitis are complex and involve further epistasis with ERAP1. *Nat Commun* 2015;6:7146.
10. Menon B, Gullick NJ, Walter GJ, Rajasekhar M, Garrood T, Evans HG, et al. IL-17+CD8 $^+$ T-cells are enriched in the joints of patients with psoriatic arthritis and correlate with disease activity and joint damage progression. *Arthritis Rheumatol* 2014;66:1272–81.
11. Petrelli A, Mijnheer G, Hoytema van Konijnenburg DP, van der Wal MM, Giovannone B, Mocholi E, et al. PD-1+CD8 $^+$ T cells are clonally expanding effectors in human chronic inflammation. *J Clin Invest* 2018;128:4669–81.
12. Srenathan U, Steel K, Taams LS. IL-17+ CD8 $^+$ T cells: differentiation, phenotype and role in inflammatory disease. *Immunol Lett* 2016;178:20–6.
13. Gartlan KH, Markey KA, Varelias A, Bunting MD, Koyama M, Kuns RD, et al. Tc17 cells are a proinflammatory, plastic lineage of pathogenic CD8 $^+$ T cells that induce GVHD without antileukemic effects. *Blood* 2015;126:1609–20.
14. Mielke LA, Liao Y, Clemens EB, Firth MA, Duckworth B, Huang Q, et al. TCF-1 limits the formation of Tc17 cells via repression of the MAF-ROR γ t axis. *J Exp Med* 2019;216:1682–99.

15. Sathaliyawala T, Kubota M, Yudanin N, Turner D, Camp P, Thome JJ, et al. Distribution and compartmentalization of human circulating and tissue-resident memory T cell subsets. *Immunity* 2013;38:187–97.
16. Kumar BV, Ma W, Miron M, Granot T, Guyer RS, Carpenter DJ, et al. Human tissue-resident memory T cells are defined by core transcriptional and functional signatures in lymphoid and mucosal sites. *Cell Rep* 2017;20:2921–34.
17. Masopust D, Soerens AG. Tissue-resident T cells and other resident leukocytes. *Annu Rev Immunol* 2019;37:521–46.
18. Clark RA. Resident memory T cells in human health and disease. *Sci Transl Med* 2015;7:269rv1.
19. Taylor W, Gladman D, Helliwell P, Marchesoni A, Mease P, Mielants H, and the CASPAR Study Group. Classification criteria for psoriatic arthritis: development of new criteria from a large international study. *Arthritis Rheum* 2006;54:2665–73.
20. Aletaha D, Neogi T, Silman AJ, Funovits J, Felson DT, Bingham CO III, et al. 2010 rheumatoid arthritis classification criteria: an American College of Rheumatology/European League Against Rheumatism collaborative initiative. *Arthritis Rheum* 2010;62:2569–81.
21. Tassioulas I, Duncan SR, Centola M, Theofilopoulos AN, Boumpas DT. Clonal characteristics of T cell infiltrates in skin and synovium of patients with psoriatic arthritis. *Hum Immunol* 1999;60:479–91.
22. Costello PJ, Winchester RJ, Curran SA, Peterson KS, Kane DJ, Bresnihan B, et al. Psoriatic arthritis joint fluids are characterized by CD8 and CD4 T cell clonal expansions appear antigen driven. *J Immunol* 2001;166:2878–86.
23. Curran SA, FitzGerald OM, Costello PJ, Selby JM, Kane DJ, Bresnihan B, et al. Nucleotide sequencing of psoriatic arthritis tissue before and during methotrexate administration reveals a complex inflammatory T cell infiltrate with very few clones exhibiting features that suggest they drive the inflammatory process by recognizing autoantigens. *J Immunol* 2004;172:1935–44.
24. Ortega C, Fernández-A S, Carrillo JM, Romero P, Molina IJ, Moreno JC, et al. IL-17-producing CD8⁺ T lymphocytes from psoriasis skin plaques are cytotoxic effector cells that secrete Th17-related cytokines. *J Leukoc Biol* 2009;86:435–43.
25. Res PC, Piskin G, de Boer OJ, van der Loos CM, Teeling P, Bos JD, et al. Overrepresentation of IL-17A and IL-22 producing CD8 T cells in lesional skin suggests their involvement in the pathogenesis of psoriasis. *PLoS One* 2010;5:e14108.
26. Hijnen D, Knol EF, Gent YY, Giovannone B, Beijm SJ, Kupper TS, et al. CD8⁺ T cells in the lesional skin of atopic dermatitis and psoriasis patients are an important source of IFN- γ , IL-13, IL-17, and IL-22. *J Invest Dermatol* 2013;133:973–9.
27. Tom MR, Li J, Ueno A, Fort Gasia M, Chan R, Hung DY, et al. Novel CD8⁺ T-cell subsets demonstrating plasticity in patients with inflammatory bowel disease. *Inflamm Bowel Dis* 2016;22:1596–608.
28. Matos TR, O'Malley JT, Lowry EL, Hamm D, Kirsch IR, Robins HS, et al. Clinically resolved psoriatic lesions contain psoriasis-specific IL-17-producing $\alpha\beta$ T cell clones. *J Clin Invest* 2017;127:4031–41.
29. Yen HR, Harris TJ, Wada S, Grosso JF, Getnet D, Goldberg MV, et al. Tc17 CD8 T cells: functional plasticity and subset diversity. *J Immunol* 2009;183:7161–8.
30. Hinrichs CS, Kaiser A, Paulos CM, Cassard L, Sanchez-Perez L, Heemskerck B, et al. Type 17 CD8⁺ T cells display enhanced antitumor immunity. *Blood* 2009;114:596–9.
31. Flores-Santibáñez F, Cuadra B, Fernández D, Roseblatt MV, Núñez S, Cruz P, et al. In vitro-generated Tc17 cells present a memory phenotype and serve as a reservoir of Tc1 cells in vivo. *Front Immunol* 2018;9:209.
32. Hirota K, Duarte JH, Veldhoen M, Hornsby E, Li Y, Cua DJ, et al. Fate mapping of IL-17-producing T cells in inflammatory responses. *Nat Immunol* 2011;12:255–63.
33. Nistala K, Adams S, Cambrook H, Ursu S, Olivito B, de Jager W, et al. Th17 plasticity in human autoimmune arthritis is driven by the inflammatory environment. *Proc Natl Acad Sci U S A* 2010;107:14751–6.
34. Maggi L, Santarlasci V, Capone M, Peired A, Frosali F, Crome SQ, et al. CD161 is a marker of all human IL-17-producing T-cell subsets and is induced by RORC. *Eur J Immunol* 2010;40:2174–81.
35. Cosmi L, Cimaz R, Maggi L, Santarlasci V, Capone M, Borriello F, et al. Evidence of the transient nature of the Th17 phenotype of CD4⁺CD161⁺ T cells in the synovial fluid of patients with juvenile idiopathic arthritis. *Arthritis Rheum* 2011;63:2504–15.
36. Annunziato F, Cosmi L, Liotta F, Maggi E, Romagnani S. Defining the human T helper 17 cell phenotype. *Trends Immunol* 2012;33:505–12.
37. Park CO, Kupper TS. The emerging role of resident memory T cells in protective immunity and inflammatory disease. *Nat Med* 2015;21:688–97.
38. Klimiuk PA, Sierakowski S, Latosiiewicz R, Cylwik JP, Cylwik B, Skowronski J, et al. Soluble adhesion molecules (ICAM-1, VCAM-1, and E-selectin) and vascular endothelial growth factor (VEGF) in patients with distinct variants of rheumatoid synovitis. *Ann Rheum Dis* 2002;61:804–9.
39. Steenvoorden MM, Tolboom TC, van der Pluijm G, Löwik C, Visser CP, DeGroot J, et al. Transition of healthy to diseased synovial tissue in rheumatoid arthritis is associated with gain of mesenchymal/fibroblastic characteristics. *Arthritis Res Ther* 2006;8:R165.
40. Melis L, Van Praet L, Pircher H, Venken K, Elewaut D. Senescence marker killer cell lectin-like receptor G1 (KLRG1) contributes to TNF- α production by interaction with its soluble E-cadherin ligand in chronically inflamed joints. *Ann Rheum Dis* 2014;73:1223–31.
41. Van der Voort R, van Lieshout AW, Toonen LW, Slöetjes AW, van den Berg WB, Figdor CG, et al. Elevated CXCL16 expression by synovial macrophages recruits memory T cells into rheumatoid joints. *Arthritis Rheum* 2005;52:1381–91.
42. Nanki T, Shimaoka T, Hayashida K, Taniguchi K, Yonehara S, Miyasaka N. Pathogenic role of the CXCL16–CXCR6 pathway in rheumatoid arthritis. *Arthritis Rheum* 2005;52:3004–14.
43. Günther C, Carballido-Perrig N, Kaesler S, Carballido JM, Biedermann T. CXCL16 and CXCR6 are upregulated in psoriasis and mediate cutaneous recruitment of human CD8⁺ T cells. *J Invest Dermatol* 2012;132:626–34.
44. Slauenwhite D, Gebremeskel S, Doucette CD, Hoskin DW, Johnston B. Regulation of cytokine polarization and T cell recruitment to inflamed paws in mouse collagen-induced arthritis by the chemokine receptor CXCR6. *Arthritis Rheumatol* 2014;66:3001–12.
45. Wade SM, Canavan M, McGarry T, Low C, Wade SC, Mullan RH, et al. Association of synovial tissue polyfunctional T-cells with DAPSA in psoriatic arthritis. *Ann Rheum Dis* 2019;78:350–4.
46. Hamada H, Garcia-Hernandez Mde L, Reome JB, Misra SK, Strutt TM, McKinstry KK, et al. Tc17, a unique subset of CD8 T cells that can protect against lethal influenza challenge. *J Immunol* 2009;182:3469–81.
47. Cheuk S, Schlums H, Gallais Sérézal I, Martini E, Chiang SC, Marquardt N, et al. CD49a expression defines tissue-resident CD8⁺ T cells poised for cytotoxic function in human skin. *Immunity* 2017;46:287–300.
48. Yeh N, Glosson NL, Wang N, Guindon L, McKinley C, Hamada H, et al. Tc17 cells are capable of mediating immunity to vaccinia virus by acquisition of a cytotoxic phenotype. *J Immunol* 2010;185:2089–98.
49. Wensink AC, Hack CE, Bovenschen N. Granzymes regulate proinflammatory cytokine responses. *J Immunol* 2015;194:491–7.
50. Santiago L, Mena C, Arias M, Martin P, Jaime-Sánchez P, Metkar S, et al. Granzyme A contributes to inflammatory arthritis in mice through stimulation of osteoclastogenesis. *Arthritis Rheumatol* 2017;69:320–34.

Hydroxychloroquine Blood Levels Predict Hydroxychloroquine Retinopathy

Michelle Petri,¹  Marwa Elkhalfifa,² Jessica Li,¹ Laurence S. Magder,³ and Daniel W. Goldman¹

Objective. In 2016, the American Academy of Ophthalmology (AAO) changed the recommended daily dose of hydroxychloroquine (HCQ) from 6.5 mg/kg to <5 mg/kg. However, it is not clear that the lower prescribed dose of HCQ will have the same efficacy for systemic lupus erythematosus (SLE) activity or the same role in protecting against cardiovascular risk factors and thrombosis. This study was undertaken to address the frequency of HCQ retinopathy and the role of HCQ blood levels in identifying those individuals who are at a greater future risk of retinopathy.

Methods. HCQ blood levels in 537 patients with SLE from a large clinical cohort were repeatedly measured, and patients were tested for HCQ retinopathy. We assessed the risk of retinopathy according to clinical characteristics and blood levels of HCQ.

Results. The overall frequency of retinopathy was 4.3% (23 of 537 patients). There was a 1% risk of retinopathy in the first 5 years of HCQ treatment, 1.8% from 6 to 10 years, 3.3% from 11 to 15 years, 11.5% from 16 to 20 years, and 8.0% after 21 years of use. We found that older age ($P < 0.0001$), higher body mass index (P for trend = 0.0160), and longer duration of HCQ intake ($P = 0.0024$ and P for trend = 0.0006) were associated with a higher risk of HCQ toxicity. Higher blood levels of HCQ predicted later HCQ retinopathy ($P = 0.0124$ and $P = 0.0340$ for mean and maximum HCQ blood levels, respectively).

Conclusion. Our data prove the utility of assessing blood levels of HCQ in the prediction of retinopathy. This would allow clinicians to either decrease the dose or increase monitoring in those patients with high HCQ blood levels.

INTRODUCTION

Hydroxychloroquine (HCQ) is one of only 4 medications approved by the US Food and Drug Administration for use in the treatment of systemic lupus erythematosus (SLE) (1,2). It is the only medication proven to improve survival (2–4), and has been demonstrated to reduce SLE flares by half (5). HCQ is particularly effective in the treatment of cutaneous disease (6) and arthritis (7). It has antithrombotic (8–10), antidiabetic (11,12), and lipid-lowering effects (13,14). In lupus nephritis, HCQ is an independent predictor of complete renal remission in patients treated with mycophenolate mofetil (15). HCQ has been shown to improve pregnancy outcomes in SLE (16,17), reduce the risk of congenital heart block in women with positive anti-Ro/SSA antibody (18,19), and delay the onset of SLE in individuals with undifferentiated connective tissue disease (20). All these benefits of HCQ were proven using previous dosing regimens (21,22).

The most important long-term side effect of HCQ treatment is HCQ retinopathy involving the photoreceptors with secondary disruption of the retinal pigment epithelium (23; for review, see ref. 24). The hydroxyl group in HCQ reduces its capability of crossing the blood–retinal barrier, which explains the lower retinal toxicity compared to chloroquine (25). Risk factors that increase the risk of HCQ retinopathy include a daily dose of >400 mg or >6.5 mg/kg ideal/lean body weight for short individuals, a cumulative dose of >1000 gm, a duration of use of >5 years, renal or hepatic dysfunction, obesity, age >60 years, and preexisting retinal disease or maculopathy (21).

The American Academy of Ophthalmology (AAO) 2011 recommendations on screening for HCQ retinopathy advised weight-based HCQ dosing of 6.5 mg/kg/day with a maximum dose of 400 mg/day (21). Exceptions were individuals of short stature and obese patients, for whom the AAO advised calculating dosage based on ideal body weight (21). The incidence of HCQ

Presented in part at the 82nd Annual Scientific Meeting of the American College of Rheumatology, Chicago, IL, October 2018.

The Hopkins Lupus Cohort is supported by the NIH (National Institute of Arthritis and Musculoskeletal and Skin Diseases grant R01-AR-069572).

¹Michelle Petri, MD, MPH, Jessica Li, MPH, Daniel W. Goldman, PhD, MCS: Johns Hopkins University School of Medicine, Baltimore, Maryland; ²Marwa Elkhalfifa, MD, PhD: Alexandria University School of Medicine, Alexandria,

Egypt; ³Laurence S. Magder, PhD, MPH: University of Maryland School of Medicine, Baltimore.

No potential conflicts of interest relevant to this article were reported.

Address correspondence to Michelle Petri, MD, MPH, Johns Hopkins University School of Medicine, Division of Rheumatology, Baltimore, MD 21286. E-mail: mpetri@jhmi.edu.

Submitted for publication April 8, 2019; accepted in revised form September 12, 2019.

retinopathy in clinical practice was originally reported in several studies as demonstrating the presence of little or no toxicity among thousands of patients (1,26). In a systematic review of 6 studies comprising 2,043 patients taking HCQ for a mean duration of >10 years, only 2 patients (0.1%) were diagnosed as having definite retinal toxicity and 6 patients (0.3%) were diagnosed as having probable HCQ retinal toxicity (1). A meta-analysis performed by Yam and Kwok on studies of retinopathy published between 1960 and 2005 showed that HCQ retinopathy was rare, with only 12 of 4,415 patients developing retinopathy (27). Wolfe and Marmor, in a study of 3,995 patients with rheumatoid arthritis or SLE receiving HCQ, found definite or probable toxicity of HCQ in 0.65% of patients with lifetime use, but only in 1% of patients after 5–7 years of use (28).

However, in a later retrospective review of 2,361 Kaiser Permanente patients who had received HCQ, Melles and Marmor reported toxicity in <1% of patients at 5 years, <2% of patients up to 10 years, but almost 20% of patients after 20 years (29). This led to, in 2016, revised AAO recommendations that the maximum daily dose of HCQ should be <5.0 mg/kg real weight, which was thought to possibly correlate better with risk compared to dosing based on ideal weight (22).

These dosing recommendations were made without evidence that the lower dose of HCQ would have the same efficacy for SLE activity or the same protective role against cardiovascular risk factors and thrombosis. In the study of Kaiser Permanente patients (29), Melles and Marmor did not analyze prescribed dose, but pharmacy-dispensed medication. While pharmacy-dispensed medication likely gives a better estimate of actual dosing than prescribed dosing, the issue of nonadherence confounds our ability to truly know HCQ intake (30). Genetic

differences in HCQ metabolism might also contribute to our inability to estimate effective dosing (31–33).

HCQ blood levels can be quantified by high-performance liquid chromatography (34), which is a widely available method of measuring drug concentrations. It is also possible to measure serum levels, but because of pharmacokinetic stability and reliability, whole blood is preferable (35). Monitoring HCQ blood levels has proven to be an effective tool to improve medication adherence in patients with SLE (30). Herein, we present the first prospective study on HCQ blood levels and HCQ retinopathy.

PATIENTS AND METHODS

Patients. Patients with SLE were enrolled from the Hopkins Lupus Cohort, a prospective study on predictors of flare, atherosclerosis, and health status in SLE. SLE patients met the Systemic Lupus International Collaborating Clinics (SLICC) Criteria for SLE (36). Enrolled subjects were followed up quarterly, or more frequently if clinically necessary. The Hopkins Lupus Cohort has been approved yearly by the Johns Hopkins University School of Medicine Institutional Review Board and complied with the Helsinki Declaration. All patients gave informed, written consent to participate in the study.

Clinical evaluation. Beginning in 2013, blood levels of HCQ were measured at each visit for cohort patients who had been prescribed HCQ. HCQ blood levels were measured by liquid chromatography tandem mass spectrometry, as previously described by Füzéry et al (34). For patients with retinopathy, all HCQ blood levels measured prior to the diagnosis date were included. For those without retinopathy, HCQ blood levels prior to

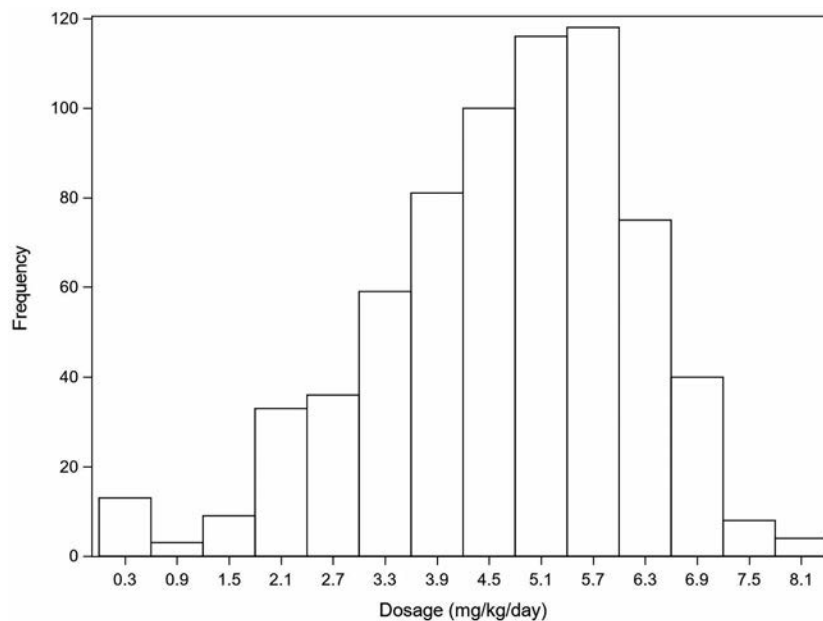


Figure 1. Distribution of hydroxychloroquine dosage among the study subjects.

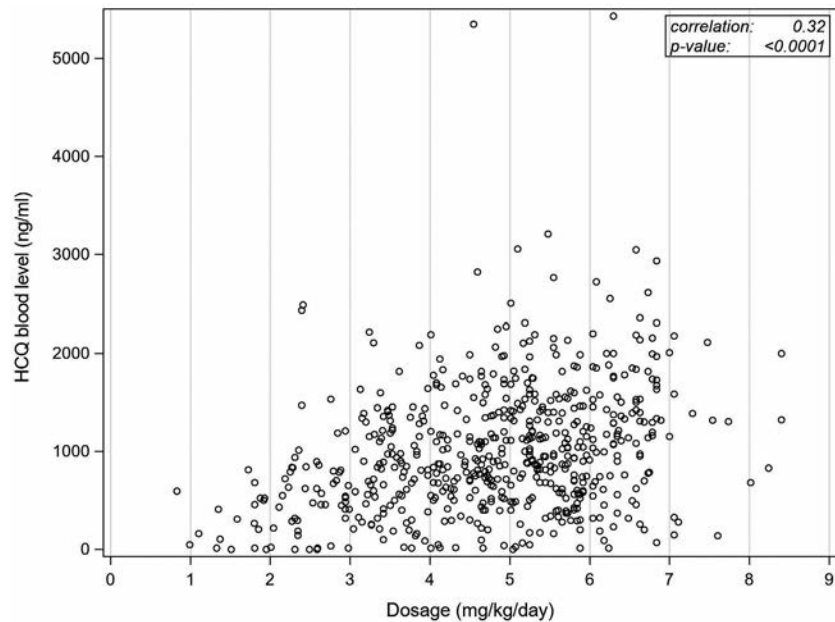


Figure 2. Hydroxychloroquine (HCQ) dosage versus HCQ blood levels. Each symbol represents an individual data point.

the final retina assessment were included to calculate the mean and maximum HCQ blood levels.

SLE patients receiving HCQ therapy were examined by retina specialists at the Johns Hopkins Wilmer Eye Institute with a fundus examination and ≥ 1 of the newer retinal screening tests: spectral-domain optical coherence tomography (SD-OCT), multifocal electroretinography, microperimetry, and fundus autofluorescence. In our analysis, HCQ toxicity was defined dichotomously by the retina specialist, with patients who were assigned a value of “no” or “possible” categorized as not having HCQ toxicity, and patients who were assigned a “yes” categorized as having HCQ toxicity. The risk of HCQ toxicity was then assessed in tertiles defined by the mean or maximum HCQ blood levels.

Statistical analysis. The risk of retinopathy was calculated in subgroups that were defined by demographic and clinical variables and by tertiles of HCQ blood concentration. *P* values were calculated using Fisher’s exact test, chi-square test, or Cochran-Armitage test for trend, and the intraclass correlation coefficient (ICC) was calculated using the “proc mixed” procedure in SAS, version 9.4.

RESULTS

Our study included 537 patients with SLE who underwent retinal testing, of whom 494 (92%) were female. The majority of patients were white (46.9%) or African American (41.5%). Figure 1 shows the distribution of HCQ dosing in the cohort.

HCQ blood levels were measured in 492 of the 537 SLE patients, with 1–25 measurements recorded per patient (median 7 measurements). Figure 2 shows the relationship between prescribed dosing and HCQ blood levels at the same visit. Patients

showed a variation in their HCQ blood levels over time. The ICC compares the variability of different measurements of HCQ blood levels in the same patient to the total variation across all measurements and all patients. The ICC for HCQ blood levels was 0.51. To provide a frame of reference, the ICCs of systolic

Table 1. Risk of hydroxychloroquine toxicity according to demographic and clinical variables

Variable	No toxicity, no. (%) (n = 514)	Toxicity, no. (%) (n = 23)	<i>P</i>
Sex			0.1029
Female	475 (96.2)	19 (3.8)	
Male	39 (90.7)	4 (9.3)	
Ethnicity			0.3804
White	238 (94.4)	14 (5.6)	
African American	215 (96.4)	8 (3.6)	
Other	61 (98.4)	1 (1.6)	
Age, years			<0.0001*
<45	215 (99.5)	1 (0.5)	
45–59	175 (95.6)	8 (4.4)	
60+	124 (89.9)	14 (10.1)	
Body mass index, kg/m ²			0.1701†
<20	50 (98.0)	1 (2.0)	
20–<25	171 (97.7)	4 (2.3)	
25–<30	159 (95.2)	8 (4.8)	
30–<35	76 (95.0)	4 (5.0)	
35+	58 (90.6)	6 (9.4)	
Smoking ever			0.6463
Yes	154 (95.1)	8 (4.9)	
No	357 (96.0)	15 (4.0)	
Hypertension ever			0.0020
Yes	276 (93.2)	20 (6.8)	
No	238 (98.8)	3 (1.2)	

* *P* for trend < 0.0001.

† *P* for trend = 0.0160.

Table 2. Hydroxychloroquine toxicity by duration of use*

Duration of use, years	No. of patients	Toxicity, no. (%)
≤5	103	1 (0.97)
6–10	109	2 (1.83)
11–15	91	3 (3.30)
16–20	96	11 (11.46)
≥21	75	6 (8.00)

* $P = 0.0024$; P for trend = 0.0006.

blood pressure and weight were also calculated, and were 0.47 and 0.94, respectively. Weight was the most consistent variable between visits in patients while HCQ blood levels showed more variation, similar to that of systolic blood pressure.

The overall prevalence of confirmed HCQ toxicity was 4.3% (23 patients). Table 1 shows the risk of HCQ toxicity according to patient demographic and clinical subsets. Men exhibited a higher frequency of toxicity than women (9.3% versus 3.8%; $P = 0.1029$). Compared to patients of other ethnicities, white patients had a higher frequency of toxicity (5.6%), but the increase was not significant. Greater age was significantly associated with HCQ toxicity. Of patients <45 years of age, 0.5% had HCQ toxicity, while for patients ages 45–59 years and patients age ≥60 years, the prevalence of HCQ toxicity was 4.4% and 10.1%, respectively. Patients with a high body mass index (BMI) had a higher risk of HCQ toxicity (P for trend = 0.0160).

Table 2 shows the risk of HCQ toxicity according to duration of HCQ intake. The duration of HCQ usage ranged from 0 to 48 years and was categorized into 5 categories by distribution. Patients with a longer duration of HCQ intake had more HCQ toxicity after 16 years of use ($P = 0.0024$; P for trend = 0.0006). Both the mean ($P = 0.0124$) and maximum ($P = 0.034$) HCQ blood levels predicted later HCQ retinopathy (Table 3). There was no difference in the risk of HCQ toxicity between white patients and African American patients. Although the mean daily dosage (mg/kg) of HCQ was significantly lower among African American patients compared to white patients (4.46 versus 4.84; $P = 0.0022$ by t -test), this did not result in significant differences in blood levels or rate of retinal toxicity (Table 4).

Some patients in our study were screened multiple times with the newer screening tests, often with more than one test at the same visit. A total of 926 retina assessments were performed,

Table 4. Comparison of HCQ blood levels and rate of HCQ retinopathy between African American patients and white patients*

	African American, no. (%)	White, no. (%)
Mean HCQ level, tertile		
0–741 ng/ml	82 (39.2)	71 (30.9)
741.5–1,176.5 ng/ml	63 (30.2)	77 (33.5)
1,177+ ng/ml	64 (30.6)	82 (35.6)
Maximum HCQ level, tertile		
0–1,182 ng/ml	74 (35.4)	73 (31.7)
1,183–1,752 ng/ml	66 (31.6)	66 (28.7)
1,753+ ng/ml	69 (33.0)	91 (39.6)
HCQ retinopathy		
Yes	8 (3.6)	14 (5.6)
No	215 (96.4)	238 (94.4)

* There were no significant differences between African American and white patients according to hydroxychloroquine (HCQ) blood level or rate of HCQ retinopathy.

with up to 8 retina examinations and a median of 1 examination completed per patient. Three hundred patients underwent 1 retina assessment, 149 patients underwent 2 assessments, and 88 patients had ≥3 assessments. Whether we examined the prevalence of HCQ retinopathy by number of ophthalmology visits completed by each patient or by number of tests done at each patient’s last assessment, there was no association between number of examinations and toxicity (P not significant).

DISCUSSION

This investigation represents the first prospective cohort study of HCQ blood levels and retinopathy. The prevalence of HCQ retinopathy was 4.3% as determined by the use of fundus examination and ≥1 of the following newer retinal screening tests: SD-OCT (the most commonly used assessment), multifocal electroretinography, fundus autofluorescence, and microperimetry. Most earlier studies on the prevalence of HCQ retinopathy were retrospective and depended on the presence of severe toxicity and bull’s eye maculopathy apparent on fundus examination (1,26–28).

In the recent large retrospective study by Melles and Marmor, they reported the overall prevalence of HCQ retinopathy to be 7.5%, evaluated by SD-OCT and visual field testing. The risk of toxicity was <1% in the first 5 years and <2% in the first 10 years but increased to almost 20% after 20 years (29). We found

Table 3. Hydroxychloroquine (HCQ) toxicity in each HCQ blood level tertile

	No toxicity, no. (%)	Toxicity, no. (%)	P	P for trend
Maximum HCQ level, tertile			0.0340	0.0143
0–1,182 ng/ml	161 (98.8)	2 (1.2)		
1,183–1,752 ng/ml	157 (95.2)	8 (4.8)		
1,753–6,281 ng/ml	153 (93.3)	11 (6.7)		
Mean HCQ level, tertile			0.0124	0.0027
0–741 ng/ml	162 (98.8)	2 (1.2)		
741.5–1,176.5 ng/ml	158 (96.3)	6 (3.7)		
1,177–3,513 ng/ml	151 (92.1)	13 (7.9)		

that the frequency of HCQ retinopathy was less than this, with the overall prevalence being 4.3%. The risk of retinopathy was 1% in the first 5 years of use, 1.8% from 6 to 10 years, 3.3% from 11 to 15 years, 11.5% from 16 to 20 years, and 8.0% after 21 years.

Our data indicate that the prevalence of HCQ retinopathy, with the use of newer screening technologies, is much higher than previously reported. Importantly, we have shown that the risk increases after 16 years of use. Even after 20 years, however, the risk of retinopathy in our study was less than half of that reported in the study of Kaiser Permanente patients (29). This may reflect our local practice, wherein a daily maximum dosing limit of 400 mg was utilized, and in which dose reductions were made for patients with renal insufficiency and elderly patients (30).

We found that older age, high BMI, and duration of HCQ intake were associated with a higher risk of HCQ retinopathy. The results on high BMI were particularly concerning, as we capped the dosage of HCQ at 400 mg daily, no matter how high the BMI. In accordance with our findings, the AAO considered the duration of HCQ usage and age as risk factors for development of HCQ retinopathy (22). However, the AAO went far beyond emphasizing the need to adopt more sensitive screening tests, recommending a cap at <5 mg/kg. Figure 2 shows that this cap, in fact, still leads to a broad distribution of HCQ blood levels.

The Kaiser Permanente study found that age and chronic kidney disease (CKD) were predictors of retinopathy risk (29). We also found age to be a predictor. Many causes of retinopathy, including common ones such as macular degeneration, which is diagnosed after age 55, increase with age. Diabetic retinopathy increases with duration of diabetes (and thus with age). One of the stronger predictors in the Kaiser Permanente study was CKD (29). As we always reduce the dose in patients with CKD (as well as following blood levels), it is not surprising that we have never found an association with CKD.

The equal proportion of white patients and African American patients in our cohort allowed us to examine ethnic differences. We did not find any differences between the African American patients and white patients with respect to HCQ blood levels or retinal toxicity, despite the lower mean dosing in African American patients.

Monitoring HCQ blood levels is an important step in improving medication adherence in patients with SLE (30). In this report, we introduce the concept of HCQ blood level monitoring to reduce the chances of prescribed dosages being too high. Although both the mean and maximum blood levels predict risk, we believe mean blood levels provide a better measure than maximum levels in the assessment of risk due to the issues of patient nonadherence (30,37,38) and due to the variation we observed even when the patient was adherent. Correlation of HCQ blood levels with skin pigmentation (39) and gastrointestinal side effects has been reported (35). Figure 2 shows the large variance between HCQ blood levels and prescribed dosage. It should not be surprising that blood levels vary. Genetic polymorphisms are known to affect HCQ levels (31–33). However, the demonstrated nonadherence of patients receiving HCQ (30) and changes in adherence over time (37) are the

major reasons for variations in blood levels. Monitoring serum/blood level targets is routine in other areas of rheumatology (such as monitoring uric acid levels, rather than allopurinol doses, in gout) and in other specialties (such as monitoring antiepileptic levels, rather than antiepileptic doses, in neurology). We think our data clearly indicate the benefit of blood level monitoring in SLE management.

In our study, the prevalence of HCQ retinopathy was found to be 4.3% using fundus examination and ≥ 1 of the newer retinal screening tests. The risk of retinopathy increased after year 16, but remained much lower than that reported in the retrospective Kaiser Permanente study (29). The risk of retinopathy was numerically higher in men and in white patients, and statistically significantly higher in older patients and patients with a higher BMI. Importantly, no patients had blindness.

Our data show, for the first time, the utility of HCQ blood level monitoring in predicting retinopathy risk. Other prospective studies are needed to substantiate our results. The present findings suggest that clinicians should consider either decreasing the dosage of HCQ or increasing monitoring in patients whose HCQ blood levels are in the highest tertile.

ACKNOWLEDGMENTS

The authors thank the Johns Hopkins Wilmer Eye Institute, Retina Division. In particular, we thank Dr. Mandeep Singh for evaluating patients for retinopathy and Dr. Hendrik Scholl for implementing retinopathy screening protocols at Johns Hopkins Hospital.

AUTHOR CONTRIBUTIONS

All authors were involved in drafting the article or revising it critically for important intellectual content, and all authors approved the final version to be published. Dr. Petri had full access to all of the data in the study and takes responsibility for the integrity of the data and the accuracy of the data analysis.

Study conception and design. Petri, Elkhalfa, Magder.

Acquisition of data. Petri, Elkhalfa.

Analysis and interpretation of data. Petri, Elkhalfa, Li, Magder, Goldman.

REFERENCES

1. Ruiz-Irastorza G, Ramos-Casals M, Brito-Zeron P, Khamashta MA. Clinical efficacy and side effects of antimalarials in systemic lupus erythematosus: a systematic review. *Ann Rheum Dis* 2010;69:20–8.
2. Alarcón GS, McGwin G, Bertoli AM, Fessler BJ, Calvo-Alén J, Bastian HM, et al. Effect of hydroxychloroquine on the survival of patients with systemic lupus erythematosus: data from LUMINA, a multiethnic US cohort (LUMINA L). *Ann Rheum Dis* 2007;66:1168–72.
3. Fessler BJ, Alarcón GS, McGwin G Jr, Roseman J, Bastian HM, Friedman AW, et al, for the LUMINA Study Group. Systemic lupus erythematosus in three ethnic groups. XVI. Association of hydroxychloroquine use with reduced risk of damage accrual. *Arthritis Rheum* 2005;52:1473–80.
4. Sutton EJ, Davidson JE, Bruce IN. The Systemic Lupus International Collaborating Clinics (SLICC) damage index: a systematic literature review. *Semin Arthritis Rheum* 2013;43:352–61.
5. The Canadian Hydroxychloroquine Study Group. A randomized study of the effect of withdrawing hydroxychloroquine sulfate in systemic lupus erythematosus. *N Engl J Med* 1991;324:150–4.

6. Kuhn A, Ruland V, Bonsmann G. Cutaneous lupus erythematosus: update of therapeutic options. Part I. *J Am Acad Dermatol* 2011;65:e179–93.
7. Williams HJ, Egger MJ, Singer JZ, Willkens RF, Kalunian KC, Clegg DO, et al. Comparison of hydroxychloroquine and placebo in the treatment of the arthropathy of mild systemic lupus erythematosus. *J Rheumatol* 1994;21:1457–62.
8. Wallace DJ. Does hydroxychloroquine sulfate prevent clot formation in systemic lupus erythematosus? [letter]. *Arthritis Rheum* 1987;30:1435–6.
9. Ruiz-Irastorza G, Egurbide MV, Pijoan JI, Garmendia M, Villar I, Martinez-Berriotxoa A, et al. Effect of antimalarials on thrombosis and survival in patients with systemic lupus erythematosus. *Lupus* 2006;15:577–83.
10. Petri M. Use of hydroxychloroquine to prevent thrombosis in systemic lupus erythematosus and in antiphospholipid antibody-positive patients. *Curr Rheumatol Rep* 2011;13:77–80.
11. Gerstein HC, Thorpe KE, Taylor DW, Haynes RB. The effectiveness of hydroxychloroquine in patients with type 2 diabetes mellitus who are refractory to sulfonyleureas: a randomized trial. *Diabetes Res Clin Pract* 2002;55:209–19.
12. Wasko MC, Hubert HB, Lingala VB, Elliott JR, Luggen ME, Fries JF, et al. Hydroxychloroquine and risk of diabetes in patients with rheumatoid arthritis. *JAMA* 2007;298:187–93.
13. Kerr G, Aujero M, Richards J, Sayles H, Davis L, Cannon G, et al. Associations of hydroxychloroquine use with lipid profiles in rheumatoid arthritis: pharmacologic implications. *Arthritis Care Res (Hoboken)* 2014;66:1619–26.
14. Durcan L, Winegar DA, Connelly MA, Otvos JD, Magder LS, Petri M. Longitudinal evaluation of lipoprotein variables in systemic lupus erythematosus reveals adverse changes with disease activity and prednisone and more favorable profiles with hydroxychloroquine therapy. *J Rheumatol* 2016;43:745–50.
15. Kasitanon N, Fine DM, Haas M, Magder LS, Petri M. Hydroxychloroquine use predicts complete renal remission within 12 months among patients treated with mycophenolate mofetil therapy for membranous lupus nephritis. *Lupus* 2006;15:366–70.
16. Petri M, Howard D, Repke J. Frequency of lupus flare in pregnancy: the Hopkins Lupus Pregnancy Center experience. *Arthritis Rheum* 1991;34:1538–45.
17. Mekinian A, Lazzaroni MG, Kuzenko A, Alijotas-Reig J, Ruffatti A, Levy P, et al, on the behalf of the SNFMI and the European Forum on Antiphospholipid Antibodies. The efficacy of hydroxychloroquine for obstetrical outcome in anti-phospholipid syndrome: data from a European multicenter retrospective study [review]. *Autoimmun Rev* 2015;14:498–502.
18. Izmirly PM, Kim MY, Llanos C, Le PU, Guerra MM, Askanase AD, et al. Evaluation of the risk of anti-SSA/Ro-SSB/La antibody-associated cardiac manifestations of neonatal lupus in fetuses of mothers with systemic lupus erythematosus exposed to hydroxychloroquine. *Ann Rheum Dis* 2010;69:1827–30.
19. Izmirly PM, Costedoat-Chalumeau N, Pisoni CN, Khamashta MA, Kim MY, Saxena A, et al. Maternal use of hydroxychloroquine is associated with a reduced risk of recurrent anti-SSA/Ro-antibody-associated cardiac manifestations of neonatal lupus. *Circulation* 2012;126:76–82.
20. James JA, Kim-Howard XR, Bruner BF, Jonsson MK, McClain MT, Arbuckle MR, et al. Hydroxychloroquine sulfate treatment is associated with later onset of systemic lupus erythematosus. *Lupus* 2007;16:401–9.
21. Marmor MF, Kellner U, Lai TY, Lyons JS, Mieler WF. Revised recommendations on screening for chloroquine and hydroxychloroquine retinopathy. *Ophthalmology* 2011;118:415–22.
22. Marmor MF, Kellner U, Lai TY, Melles RB, Mieler WF, for the American Academy of Ophthalmology. Recommendations on screening for chloroquine and hydroxychloroquine retinopathy (2016 revision). *Ophthalmology* 2016;123:1386–94.
23. Marmor MF. Comparison of screening procedures in hydroxychloroquine toxicity. *Arch Ophthalmol* 2012;130:461–9.
24. Jorge A, Ung C, Young LH, Melles RB, Choi HK. Hydroxychloroquine retinopathy—implications of research advances for rheumatology care [review]. *Nat Rev Rheumatol* 2018;14:693–703.
25. Raines MF, Bhargava SK, Rosen ES. The blood-retinal barrier in chloroquine retinopathy. *Invest Ophthalmol Vis Sci* 1989;30:1726–31.
26. Levy GD, Munz SJ, Paschal J, Cohen HB, Pince KJ, Peterson T. Incidence of hydroxychloroquine retinopathy in 1,207 patients in a large multicenter outpatient practice. *Arthritis Rheum* 1997;40:1482–6.
27. Yam J, Kwok A. Ocular toxicity of hydroxychloroquine. *Hong Kong Med J* 2006;12:294–304.
28. Wolfe F, Marmor MF. Rates and predictors of hydroxychloroquine retinal toxicity in patients with rheumatoid arthritis and systemic lupus erythematosus. *Arthritis Care Res (Hoboken)* 2010;62:775–84.
29. Melles RB, Marmor MF. The risk of toxic retinopathy in patients on long-term hydroxychloroquine therapy. *JAMA Ophthalmol* 2014;132:1453–60.
30. Durcan L, Clarke WA, Magder LS, Petri M. Hydroxychloroquine blood levels in systemic lupus erythematosus: clarifying dosing controversies and improving adherence. *J Rheumatol* 2015;42:2092–7.
31. Lee JY, Vinayagamoorthy N, Han K, Kwok SK, Ju JH, Park KS, et al. Association of polymorphisms of cytochrome P450 2D6 with blood hydroxychloroquine levels in patients with systemic lupus erythematosus. *Arthritis Rheumatol* 2016;68:184–90.
32. Shroyer NF, Lewis RA, Lupski JR. Analysis of the ABCR (ABCA₄) gene in 4-aminoquinoline retinopathy: is retinal toxicity by chloroquine and hydroxychloroquine related to Stargardt disease? *Am J Ophthalmol* 2001;131:761–6.
33. Grassmann F, Bergholz R, Mändl J, Jäggle H, Ruether K, Weber BH. Common synonymous variants in ABCA4 are protective for chloroquine induced maculopathy (toxic maculopathy). *BMC Ophthalmol* 2015;15:18.
34. Füzéry AK, Breaud AR, Emezienna N, Schools S, Clarke WA. A rapid and reliable method for the quantitation of hydroxychloroquine in serum using turbulent flow liquid chromatography-tandem mass spectrometry. *Clin Chim Acta* 2013;421:79–84.
35. Munster T, Gibbs JP, Shen D, Baethge BA, Botstein GR, Caldwell J, et al. Hydroxychloroquine concentration-response relationships in patients with rheumatoid arthritis. *Arthritis Rheum* 2002;46:1460–9.
36. Petri M, Orbai AM, Alarcón GS, Gordon C, Merrill JT, Fortin PR, et al. Derivation and validation of the Systemic Lupus International Collaborating Clinics classification criteria for systemic lupus erythematosus. *Arthritis Rheum* 2012;64:2677–86.
37. Feldman CH, Collins J, Zhang Z, Subramanian SV, Solomon DH, Kawachi I, et al. Dynamic patterns and predictors of hydroxychloroquine nonadherence among Medicaid beneficiaries with systemic lupus erythematosus. *Semin Arthritis Rheum* 2018;48:205–13.
38. Costedoat-Chalumeau N, Houssiau F, Izmirly P, Le Guern V, Navarra S, Jolly M, et al. A prospective international study on adherence to treatment in 305 patients with flaring SLE: assessment by drug levels and self-administered questionnaires. *Clin Pharmacol Ther* 2018;103:1074–82.
39. Jallouli M, Francès C, Piette JC, Huong DL, Moguelet P, Factor C, et al. Hydroxychloroquine-induced pigmentation in patients with systemic lupus erythematosus: a case control study. *JAMA Dermatol* 2013;149:935–40.

Improved Mitochondrial Metabolism and Reduced Inflammation Following Attenuation of Murine Lupus With Coenzyme Q10 Analog Idebenone

Luz P. Blanco,¹ Hege L. Pedersen,¹ Xinghao Wang,¹ Yaíma L. Lightfoot,¹ Nickie Seto,¹ Carmelo Carmona-Rivera,¹ Zu-Xi Yu,² Victoria Hoffmann,³ Peter S. T. Yuen,⁴ and Mariana J. Kaplan¹

Objective. A role for mitochondrial dysfunction has been proposed in the immune dysregulation and organ damage characteristic of systemic lupus erythematosus (SLE). Idebenone is a coenzyme Q10 synthetic quinone analog and an antioxidant that has been used in humans to treat diverse diseases in which mitochondrial function is impaired. This study was undertaken to assess whether idebenone ameliorates lupus in murine models.

Methods. Idebenone was administered orally to MRL/lpr mice at 2 different doses (1 gm/kg or 1.5 gm/kg idebenone-containing diet) for 8 weeks. At peak disease activity, clinical, immunologic, and metabolic parameters were analyzed and compared to those in untreated mice (n = 10 per treatment group). Results were confirmed in the lupus-prone NZM2328 mouse model.

Results. In MRL/lpr mice, idebenone-treated mice showed a significant reduction in mortality incidence ($P < 0.01$ versus untreated mice), and the treatment attenuated several disease features, including glomerular inflammation and fibrosis (each $P < 0.05$ versus untreated mice), and improved renal function in association with decreased renal expression of interleukin-17A (IL-17A) and mature IL-18. Levels of splenic proinflammatory cytokines and inflammasome-related genes were significantly decreased (at least $P < 0.05$ and some with higher significance) in mice treated with idebenone, while no obvious drug toxicity was observed. Idebenone inhibited neutrophil extracellular trap formation in neutrophils from lupus-prone mice ($P < 0.05$) and human patients with SLE. Idebenone also improved mitochondrial metabolism (30% increase in basal respiration and ATP production), reduced the extent of heart lipid peroxidation (by one-half that of untreated mice), and significantly improved endothelium-dependent vasorelaxation ($P < 0.001$). NZM2328 mice exposed to idebenone also displayed improvements in renal and systemic inflammation, reducing the kidney pathology score ($P < 0.05$), IgG/C3 deposition ($P < 0.05$), and the gene expression of interferon, proinflammatory, and inflammasome-related genes (at least $P < 0.05$ and some with higher significance).

Conclusion. Idebenone ameliorates murine lupus disease activity and the severity of organ damage, supporting the hypothesis that agents that modulate mitochondrial biologic processes may have a therapeutic role in human SLE.

INTRODUCTION

An important role for mitochondrial dysfunction in the pathogenesis of systemic lupus erythematosus (SLE) has been described by our group and by others (for review, see ref. 1). Enhanced synthesis of mitochondrial reactive oxygen species

(mROS) by lupus neutrophil subsets is associated with enhanced formation of neutrophil extracellular traps (NETs) that are enriched in oxidized mitochondrial DNA (mDNA). This oxidized mDNA promotes type I interferon (IFN) responses through activation of the cyclic GMP-AMP synthase/stimulator of IFN genes pathway (2). Mitochondrial dysfunction has also been reported to develop

Supported by the Alliance for Lupus Research (Target Identification in Lupus grant) and the Intramural Research Program of the NIH (National Institute of Arthritis and Musculoskeletal and Skin Diseases grant ZIA-AR-041199).

¹Luz P. Blanco, PhD, Hege L. Pedersen, PhD, Xinghao Wang, BSc, Yaíma L. Lightfoot, PhD, Nickie Seto, BSc, Carmelo Carmona-Rivera, PhD, Mariana J. Kaplan, MD: National Institute of Arthritis and Musculoskeletal and Skin Diseases, NIH, Bethesda, Maryland; ²Zu-Xi Yu, MD, PhD: National Heart, Lung, and Blood Institute, NIH, Bethesda, Maryland; ³Victoria Hoffmann, VMD: Office of the Director, Division of Veterinary Resources,

Diagnostic and Research Services Branch, NIH, Bethesda, Maryland; ⁴Peter S. T. Yuen, PhD: National Institute of Diabetes and Digestive and Kidney Diseases, NIH, Bethesda, Maryland.

No potential conflicts of interest relevant to this article were reported.

Address correspondence to Mariana J. Kaplan, MD, NIH, National Institute of Arthritis and Musculoskeletal and Skin Diseases, 9000 Rockville Pike, Bethesda, MD 20892. E-mail: mariana.kaplan@nih.gov.

Submitted for publication November 19, 2018; accepted in revised form September 26, 2019.

in lupus-prone mice at an early age, manifesting before overt immune dysregulation and tissue damage become apparent (3). Furthermore, in vivo administration of mROS scavengers ameliorates murine lupus (2). These observations indicate that drugs aimed at improving mitochondrial homeostasis may have therapeutic benefits in SLE.

Idebenone (2,3-dimethoxy-5-methyl-6-[10-hydroxydecyl]-1,4-benzoquinonenoben) is a drug previously tested in clinical trials and already approved in some countries for the treatment of certain diseases associated with mitochondrial dysfunction (4–7), including Leber's hereditary optic neuropathy and Duchenne's muscular dystrophy. It is a synthetic quinone analog compound of coenzyme Q10 with a shorter aliphatic chain, and is considered a potent antioxidant that protects cells against enhanced ROS toxicity (8,9). Idebenone improves electron transfer chain function by bypassing deficient complex I activity and enhancing the amount of ATP synthesized, thereby improving mitochondrial physiology (10). The potential therapeutic benefit of idebenone has been tested in various murine models of disease (11–13). We hypothesized that idebenone could modulate the pathologic development and progression of SLE through regulation of mitochondrial function and ROS synthesis. To test this, we evaluated the effect of this drug in 2 murine models of lupus.

MATERIALS AND METHODS

Animal procedures and diet. The National Institute of Arthritis and Musculoskeletal and Skin Diseases (NIAMS) Animal Care and Use Committee approved all animal procedures for these experiments (protocol no. A016-05-26). Female lupus-prone MRL/MpJ-Fas^{lpr}/J mice (MRL/lpr; stock no. 000485) and female nonautoimmune MRL/MpJ mice (control MpJ; stock no. 000486) were purchased from The Jackson Laboratory (n = 10 mice per group per experiment). The control diet was the standard NIH-31 diet (14), while the idebenone (Cayman Chemical)–supplemented diet (Envigo) contained either 1 gm/kg (low dose) or 1.5 gm/kg (high dose) idebenone-containing NIH-31 diet, in conjunction with a blue dye (FD&C Green #3, CAS no. 2353-45-9; chemical formula C₃₇H₃₄N₂Na₂O₁₀S₃) to monitor intake. MRL/lpr mice started the idebenone diet at age 9 weeks. MRL/lpr mice were kept on the diet for ~2 months until disease manifestations peaked, followed by euthanasia.

All experiments compared the high- and low-dose idebenone groups to the control diet group. In addition, a more limited set of experiments (assessing the effects of dietary intake on mitochondrial complex II activity) were performed comparing only the low dose of idebenone to the control diet group (see details in Supplementary Figures 1–6, available on the *Arthritis & Rheumatology* web site at <http://onlinelibrary.wiley.com/doi/10.1002/art.41128/abstract>).

In addition, a more limited set of experiments in NZM2328 lupus-prone mice (breeding pair originally obtained by Dr. Shu-

Man Fu, University of Virginia, Charlottesville) was performed to assess treatment efficacy beyond a single mouse model. NZM2328 mice were treated from week 10 to week 38 with the low-dose idebenone-containing diet (1.0 gm/kg diet) or normal control NIH-31 diet (n = 10 mice per group).

Anti-double-stranded DNA (anti-dsDNA), anti-nuclear RNP (anti-nRNP), and anti-SSA quantification. Serum concentrations of autoantibodies were calculated as previously described (2) using commercially available enzyme-linked immunosorbent assay (ELISA) kits (catalog nos. 5110, 5410, and 5710; Alpha Diagnostic). Briefly, serum was diluted (1:125) in NSB buffer, and ELISAs were carried out in accordance with the manufacturer's instructions.

Assessment of kidney function and histologic features. Slides containing kidney sections from the mice were evaluated in a blinded manner by a veterinary pathologist (Z-XY and VH) for disease severity, fibrosis, inflammation, and glomerulosclerosis, and each histologic score was calculated using previously described scoring systems (15). Renal immune complex deposition was quantified as previously described (2), using an Alexa Fluor 594–conjugated F(ab')₂ goat anti-mouse IgG (catalog no. A11020; ThermoFisher) and a fluorescein isothiocyanate–conjugated anti-murine C3 antibody (catalog no. GC3-90F-Z; Immunology Consultants Laboratories). Frozen kidney sections were also stained with Alexa Fluor 488–conjugated rat anti-mouse interleukin-17A (IL-17A) antibodies (BD Biosciences). Nuclei were stained with Hoechst dye (1:500; Life Technologies).

For quantification, 3 random images were obtained from each stained frozen kidney section. The images were analyzed with ImageJ software (NIH), selecting the glomerular compartment to quantify the mean pixels for each fluorescence channel used.

To quantify serum creatinine levels and eliminate the influence of chromogens (which interfere with the classic Jaffe method for creatinine detection) in the mouse serum, a high-performance liquid chromatography assay was used, as previously described (16). Briefly, 5 μ l serum was treated with 0.5 ml acetonitrile and then centrifuged at 4°C at 13,000g for 20 minutes, and supernatants were dried using a Speed-Vac and resuspended in mobile phase (5 mM sodium acetate, pH 5.1). Duplicates were run on a 100 \times 4.1–mm PRP-X200 column (Hamilton) and isocratically eluted at 2 ml/minute in an Agilent 1100 system, with ultraviolet detection at 234 nm. Absolute quantitation was determined with a standard curve of 2–50 ng creatinine ($r^2 = 0.999$).

Determination of endothelium-dependent vasorelaxation. Endothelium-dependent vasorelaxation of the thoracic aorta was accomplished using a method previously described by our group (15). Clean aorta rings were mounted in a

myograph DMV device and allowed to stabilize under 7 mN isometric conditions. After exposure to potassium buffer, aortic rings were precontracted with phenylephrine, followed by the addition of increasing amounts of acetylcholine. Vasorelaxation was then measured as the percentage of contraction.

Assessment of proinflammatory gene expression.

Messenger RNA (mRNA) was isolated from frozen spleens, and quantification of proinflammatory and IFN-regulated genes was performed as previously described (2). Briefly, spleen tissue was homogenized in RLT lysis buffer, and RNA was isolated with an RNA Easy kit (Qiagen), following the manufacturer's instructions. Complementary DNA was synthesized with 1 μ g of RNA, using a Bio-Rad iScript kit and an ABI thermocycler. Quantitative reverse transcription-polymerase chain reaction was performed using Bio-Rad reagents and instructions, and a CFX96 Bio-Rad real-time thermocycler.

The fold change in gene expression for each gene was calculated using *Actb* (β -actin) as a housekeeping gene and threshold cycle (C_t) values derived from tissue from mice receiving the control diet, which was used for the $2^{-\Delta\Delta C_t}$ calculations. The following primers were used: for *Actb*, forward 5'-CCA-ACC-GCG-AGA-AGA-TGA-3' and reverse 5'-CCA-GAG-GCG-TAC-AGG-GAT-AG-3'; for *Iffa1*, forward 5'-AAG-GAC-AGG-CAG-GAC-TTT-GGA-TTC-3' and reverse 5'-GAT-CTC-GCA-GCA-CAG-GGA-TGG-3'; for *Iffb*, forward 5'-AAG-AGT-TAC-ACT-GCC-TT-GCC-ATC-3' and reverse 5'-CAC-TGT-CTG-CTG-GTG-GAG-TTC-ATC-3'; for *IIf6*, forward 5'-TGG-CTA-AGG-ACC-AAG-ACC-ATC-CAA-3' and reverse 5'-AAC-GCA-CTA-GGT-TTG-CCG-AGT-AGA-3'; for *Mx1*, forward 5'-GAT-CCG-ACT-TCA-CTT-CCA-GAT-GG-3' and reverse 5'-CAT-CTC-AGT-GGT-AGT-CAA-CCC-3'; for *Tnf*, forward 5'-CCC-TCA-CAC-TCA-GAT-CAT-CTT-CT-3' and reverse 5'-GCT-ACG-ACG-TGG-GCT-ACA-G-3'; for *IIf1b*, forward 5'-CCC-TGC-AGC-TGG-AGA-GTG-TGG-A-3' and reverse 5'-CTG-AGC-GAC-CTG-TCT-TGG-CCG-3'; for *IIf12b*, forward 5'-AGA-AGA-GTC-CGT-TCC-TCG-TAG-3' and reverse 5'-AGC-CAA-CC-A-AGC-AGA-AGA-CAG-3'; for *Pycard*, forward 5'-AAC-CCA-AGC-AAG-ATG-CGG-AAG-3' and reverse 5'-TTA-GGG-CCT-GGA-GGA-GCA-AG-3'; for *Nlrp3*, forward 5'-CTT-CTC-TGA-TGA-GGC-CCA-AG-3' and reverse 5'-GCA-GCA-AAC-TGG-AAA-GGA-AG-3'; for *IIf10*, forward 5'-CCA-GTT-TTA-CCT-GGT-AGA-AGT-GAT-G-3' and reverse 5'-TGT-CTA-GGT-CCT-GGA-GTC-CAG-CAG-AG-3'; for *Mpo*, forward 5'-TGC-TCT-CGA-ACA-AAG-AGG-GT-3' and reverse 5'-CTC-CTC-ACC-AAC-CGC-TCC-3'; and for *IIf18*, forward 5'-ACT-GTA-CAA-CCG-CAG-TAA-TAC-GC-3' and reverse 5'-AGT-GAA-CAT-TAC-AGA-TTT-ATC-CC-3'. The mitochondrial:nuclear transcription ratio was measured using the following primers: *16S* or *Mmr2* (forward 5'-CTA-GAA-ACC-CCG-AAA-CCA-AA-3' and reverse 5'-CCA-GCT-ATC-ACC-AAG-CTC-GT-3') and β_2 -microglobulin *B2m* (forward 5'-ATG-GGA-AGC-CGA-ACA-TAC-TG-3' and reverse 5'-CAG-TCT-CAG-TGG-GGG-TGA-AT-3').

Quantification of NETs and mROS in bone marrow (BM)-derived neutrophils.

The isolation of BM-derived neutrophils and quantification of NETs and mROS were performed as previously described by us (2). Briefly, hind-limb bone marrow neutrophils were purified by Percoll gradient. Cells were seeded in a 96-well plate (200,000 cells/100 μ l/well) in triplicate for each dye, and allowed to form NETs in the presence of Sytox (externalized DNA, 1 μ M final concentration), Quant-It Picogreen (total DNA, stock solution diluted 250 times), and MitoSox (mROS final concentration 200 ng/ml) (all from ThermoFisher). Fluorescence was measured at different time points for each dye, at 485/520 at the earliest time point (for Picogreen), at 510/580 at 1 hour (for MitoSox), and at 485/520 at 2 hours (for Sytox), using a FLUOstar Omega BMG Labtech plate reader. Picogreen measurement was used for determining the initial number of cells or total DNA.

Phenotyping of splenocytes by flow cytometry.

After euthanasia, splenocytes were isolated from the mice, and following red blood lysis using ACK lysing buffer (Gibco-Life Technologies), single-cell suspensions were stained with Live/Dead Aqua (ThermoFisher) diluted in phosphate buffered saline (PBS) on ice for 15 minutes, and then washed with fluorescence-activated cell sorting (FACS) buffer (PBS + 2% fetal bovine serum). Cells were then incubated with TruStain FcX (BioLegend) on ice for 10 minutes, before staining with the following antibodies (all from BioLegend) on ice for 15 minutes: allophycocyanin (APC)-conjugated CD8a (53-6.7), fluorescein isothiocyanate-conjugated CD19 (6D5), PerCP-Cy5.5-conjugated CD45 (30-F11), phycoerythrin (PE)-conjugated CD62L (MEL-14), BV421-conjugated CD4 (GK1.5), APC-Cy7-conjugated CD44 (IM7), and PE-Cy7-conjugated CD3 (17A2). Cells were washed twice in FACS buffer and immediately collected on an LSRFortessa flow cytometer (BD Biosciences). Data were analyzed using FlowJo software (Tree Star).

Isolation of human neutrophils and characterization of NET formation.

Human peripheral blood neutrophils were isolated in a manner as previously described (2) from subjects who fulfilled the American College of Rheumatology revised criteria for SLE (17). All subjects gave informed consent to participate in the NIAMS/National Institute of Diabetes and Digestive and Kidney Diseases Institutional Review Board-approved protocol.

Peripheral blood was obtained by venipuncture, and normal-density neutrophils were purified from sedimented red blood cells (RBCs) following Ficoll gradient, using 10% dextran solution. RBCs were lysed using sodium chloride hypo- and hypertonic solutions. Lupus low-density granulocytes (LDGs) were isolated by negative selection from the peripheral blood mononuclear cell layer following Ficoll gradient, as previously described by our group (18). NETs were detected by immunofluorescence, as described previously (2). Neutrophils seeded in coverslips or coverslip chambers

were incubated for 90 minutes at 37°C with or without idebenone (10 μ M), fixed with 4% paraformaldehyde, and permeabilized with 0.2% Triton X-100, followed by 0.5% gelatin for 20 minutes. Cells were stained with antibodies directed against human neutrophil elastase (1:1,000, ab21595; Abcam), Hoechst 33342 (1:1,000; Life Technologies), and secondary antibodies (1:500, Alexa Fluor 488 [A31570]; Life Technologies). After mounting (Prolong; Life Technologies), cells were visualized and imaged using a Zeiss LSM780 confocal microscope.

Mitochondrial metabolism analysis. BM-derived neutrophils or splenocytes were plated on Cell-Tak-coated Seahorse culture plates (300,000 cells/well) in Seahorse XF RPMI medium (pH 7.4). XF analysis of mitochondrial activity was performed at 37°C in the absence of CO₂, using an XF-96e analyzer (Agilent) in accordance with the manufacturer's instructions.

A mitochondrial stress test assay was performed using Seahorse XF RPMI medium (pH 7.4) supplemented with 25 mM

glucose, 1 mM sodium pyruvate, and 2 mM L-glutamine. Cells were treated serially with oligomycin (5 μ M), FCCP (1 μ M), rotenone (100 nM), and antimycin A (10 μ M), and the oxygen consumption rate was measured over time. The cell numbers at assay completion were normalized to DNA content using CyQuant dye (ThermoFisher). Seahorse Wave (Agilent), Excel (Microsoft), and GraphPad Prism software packages were used to analyze the data. To calculate significant differences between groups, the Mann-Whitney U test was performed.

Measurement of cardiac lipid peroxidation. Lipid peroxidation was measured in halved sections of the mouse hearts using a previously described method (19). Briefly, heart sections were homogenized in Tris HCl buffer (0.1M, pH 7.4) and incubated with 10% trichloroacetic acid for 15 minutes on ice. After centrifugation at 2,200g for 15 minutes, supernatants and standard solutions were mixed with an equal volume of thiobarbituric acid (0.67% weight/volume) and incubated for 10 minutes at 95°C. Standard was prepared using base-2 serial dilutions with

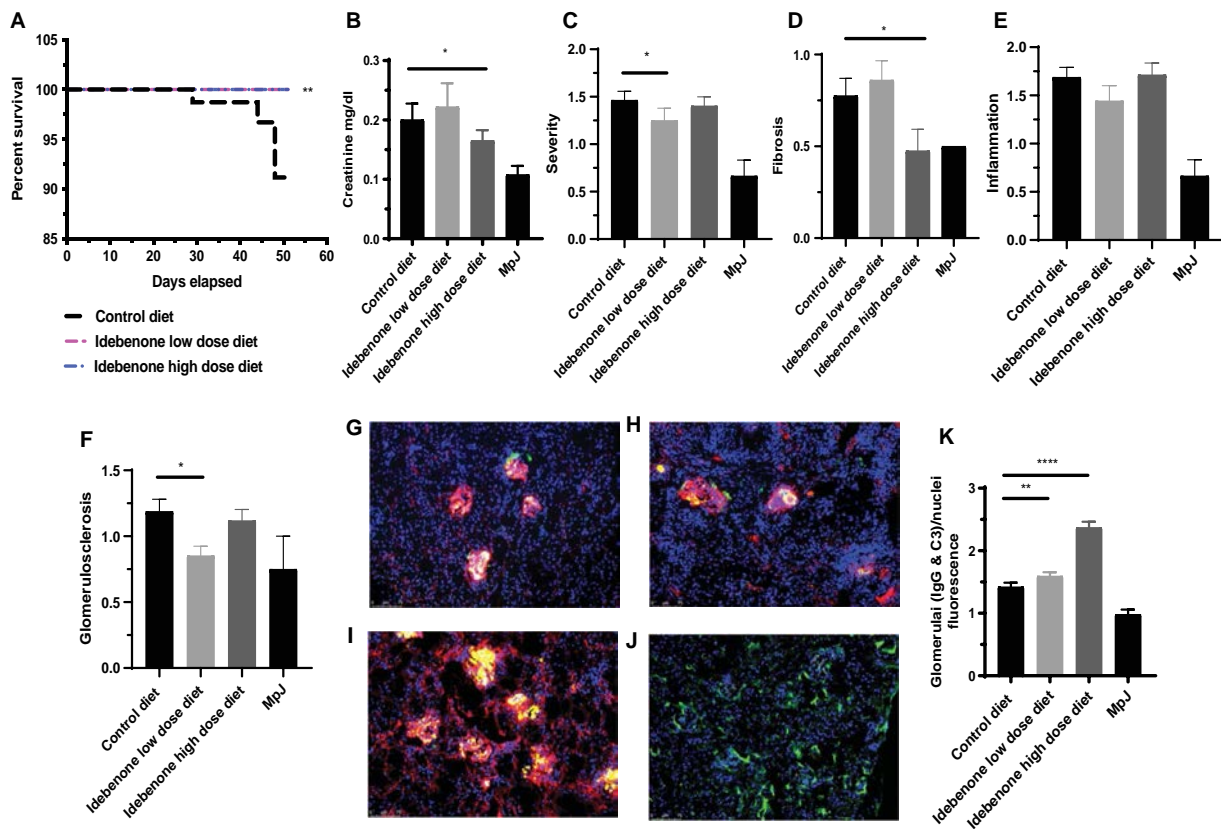


Figure 1. Idebenone improves renal disease in murine lupus. **A**, Kaplan-Meier survival curves for MRL/lpr mice receiving either low- or high-dose idebenone or the control diet ($n = 10$ mice/group). $** = P < 0.01$ by log rank (Mantel-Cox) test. **B**, Serum creatinine levels at euthanasia in MRL/lpr mice or nonautoimmune control MpJ mice ($n = 40$ MRL/lpr mice/group and $n = 5$ MpJ mice). **C–F**, Scores for the severity of kidney disease (**C**), fibrosis (**D**), inflammation (**E**), and glomerulosclerosis (**F**) at euthanasia in MRL/lpr or control MpJ mice ($n = 20$ MRL/lpr mice/group and $n = 3$ MpJ mice). **G–J**, Representative images at euthanasia of renal IgG (red) and C3 (green) deposition in the kidneys of an MRL/lpr mouse fed the control diet (**G**), low-dose idebenone (**H**), or high-dose idebenone (**I**) or a control MpJ mouse (**J**). Nuclei were stained with Hoechst (blue). **K**, Quantification of glomerular immune complex (IgG and C3) deposition in each group of mice. In **B–F** and **K**, results are the mean \pm SEM. $* = P < 0.05$; $** = P < 0.01$; $**** = P < 0.0001$, by Mann-Whitney U test.

tetramethoxypropane solution, starting from 500 μM in water. Absorbance was measured at 532 nm. The protein concentration in the homogenized tissue was measured using a BCA protein assay (ThermoFisher) in accordance with the manufacturer's instructions.

Kidney expression of mature IL-18. Protein detection in renal tissue preserved at -80°C was performed as previously described (20). Briefly, 50 μg of total protein was resolved in a 4–12% NuPAGE Bis-Tris gradient gel (Invitrogen). Proteins were immobilized onto a nitrocellulose membrane (Invitrogen) and blocked with 10% bovine serum albumin for 30 minutes at room temperature. Thereafter, the membrane was incubated with rabbit anti-mouse IL-18 clone H-173 (1:500; Santa Cruz Biotechnology) or anti-tubulin (1:1,000; Cell Signaling Technology) overnight at 4°C . After 3 washes with PBS–Tween, the membrane was probed with secondary IRDye800 goat anti-mouse or IRDye800 goat anti-rabbit antibodies (1:10,000; Li-Cor Biosciences) for 1 hour at room temperature. Proteins were detected using a Li-Cor Biosciences Odyssey Infrared Imaging System, in accordance with the manufacturer's instructions.

RESULTS

Assessment of intake and tolerability of the idebenone-supplemented diet. The mice displayed adequate intake of the idebenone-containing diet, as measured by incorporation of blue dye into feces and intestinal lumen (see Supplementary Figures 1A–C [http://onlinelibrary.wiley.com/doi/10.1002/art.41128/abstract]). MRL/*lpr* mice started the idebenone diet at age 9 weeks. Two doses of idebenone were tested. Assuming each 20-gm mouse consumes ~ 3 –5 gm diet per day, the dose received per mouse was in the range of 150 mg (low dose) to 375 mg (high dose) per day per kg. Mice tolerated the diet well without any obvious signs of toxicity. At euthanasia, the weight of the idebenone-treated mice was slightly higher than that of the mice fed the control diet (see Supplementary Figure 1D).

Better survival and improvement in renal histopathologic features following idebenone treatment in murine lupus. Mice were not kept alive beyond age 17 weeks, in order to follow institutional regulations of animal care designed to prevent discomfort from neck lymphadenopathy in this animal model. Nevertheless, we observed that mice in both the low-dose and the high-dose idebenone diet groups survived through week 17, while several early deaths occurred in the control group, as shown by the Kaplan-Meier survival curve (Figure 1A).

One of the most prominent features of lupus is the development of glomerulonephritis. To explore the effect of ide-

benone on kidney function, we quantified serum creatinine levels and found that MRL/*lpr* mice fed high-dose idebenone displayed significantly lower serum creatinine concentrations compared to the other groups (Figure 1B), similar to the levels in the nonautoimmune control MpJ mouse strain. In contrast, serum creatinine levels in the mice receiving low-dose idebenone did not significantly differ from those in mice receiving the control diet.

Histologic analysis of the kidneys (for representative images, see Supplementary Figure 2 [http://onlinelibrary.wiley.com/doi/10.1002/art.41128/abstract]) revealed that low-dose idebenone significantly reduced the severity of glomerulonephritis (Figure 1C) and glomerulosclerosis (Figure 1F). High-dose idebenone was associated with significant reductions in the glomerular fibrosis score (Figure 1D). No reductions in the inflammation score were observed with either dose of idebenone compared

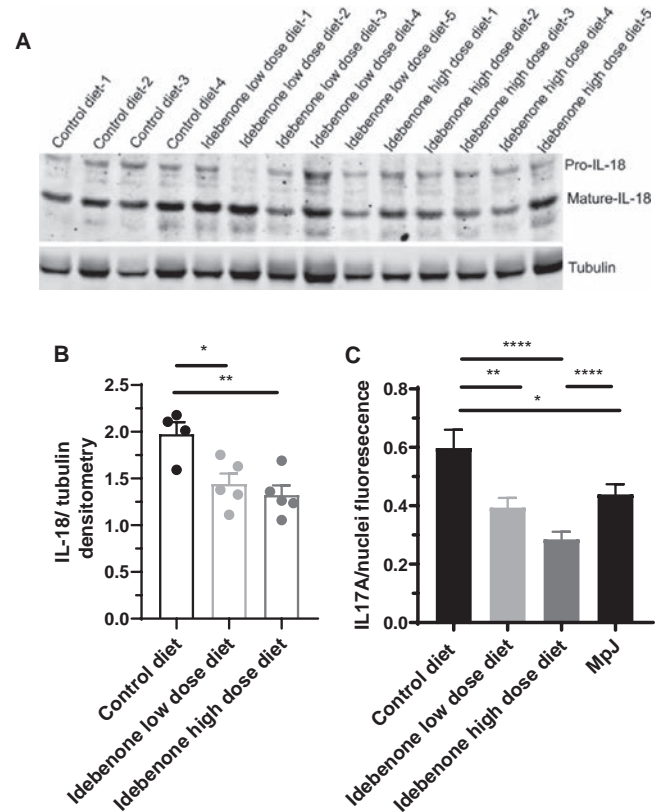


Figure 2. Idebenone modulates inflammasome-associated molecules and interleukin-17 (IL-17) levels in the kidneys of mice with lupus. **A**, Western blot analysis of the expression of pro-IL-18, mature IL-18, and tubulin proteins in the kidneys of MRL/*lpr* mice receiving the control diet or idebenone diets. **B**, Densitometric quantification of mature IL-18 expression in the kidneys of MRL/*lpr* mice receiving the control diet ($n = 4$) or either the low- or high-dose idebenone diet ($n = 5$ mice/group). **C**, Quantification of IL-17A in the glomeruli of MRL/*lpr* or control MpJ mice (4 tissue slides/condition; $n = 10$ MRL/*lpr* mice/group and $n = 3$ MpJ mice). Results are the mean \pm SEM. * = $P < 0.05$; ** = $P < 0.01$; **** = $P < 0.0001$, by Student's unpaired *t*-test.

to mice fed the control diet (Figure 1E). Similarly, renal immune complex deposition was not attenuated by either dose of idebenone compared to animals receiving the control diet. Despite the significant improvement in renal function and reduction in glomerular fibrosis, there was enhanced renal immune complex deposition in both the high-dose and the low-dose idebenone groups compared to the control diet group (Figures 1G–K).

Treatment with either dose of idebenone significantly reduced the renal expression of mature IL-18 compared to that in mice fed the control diet (Figures 2A and B), suggesting that idebenone may modulate inflammasome activation in the murine lupus kidney. In addition, both doses of idebenone significantly reduced IL-17A levels in the kidney (Figure 2C). These results suggest that idebenone can improve kidney function and ameliorate the renal damage characteristic of SLE.

Further support for the beneficial effects of idebenone in lupus renal disease was obtained by administering low-

dose idebenone to NZM2328 mice. Following treatment with low-dose idebenone, NZM2328 mice displayed significant reductions in immune complex deposition and renal inflammation (see Supplementary Figures 3A–E [<http://onlinelibrary.wiley.com/doi/10.1002/art.41128/abstract>]). Overall, these results indicate that idebenone administration modulates lupus glomerulonephritis in murine systems, and that the mechanisms may be complex and appear to differ between mouse strains.

Improvement in endothelium-dependent vasorelaxation and reduction in cardiac lipid peroxidation, but lack of reduction in circulating autoantibodies, with idebenone treatment in murine lupus. Neither the high dose nor the low dose of idebenone modified the serum levels of anti-nRNP, anti-SSA, or anti-dsDNA autoantibodies either in MRL/lpr mice (Figures 3A–C) or in NZM2328 mice (data not shown). In

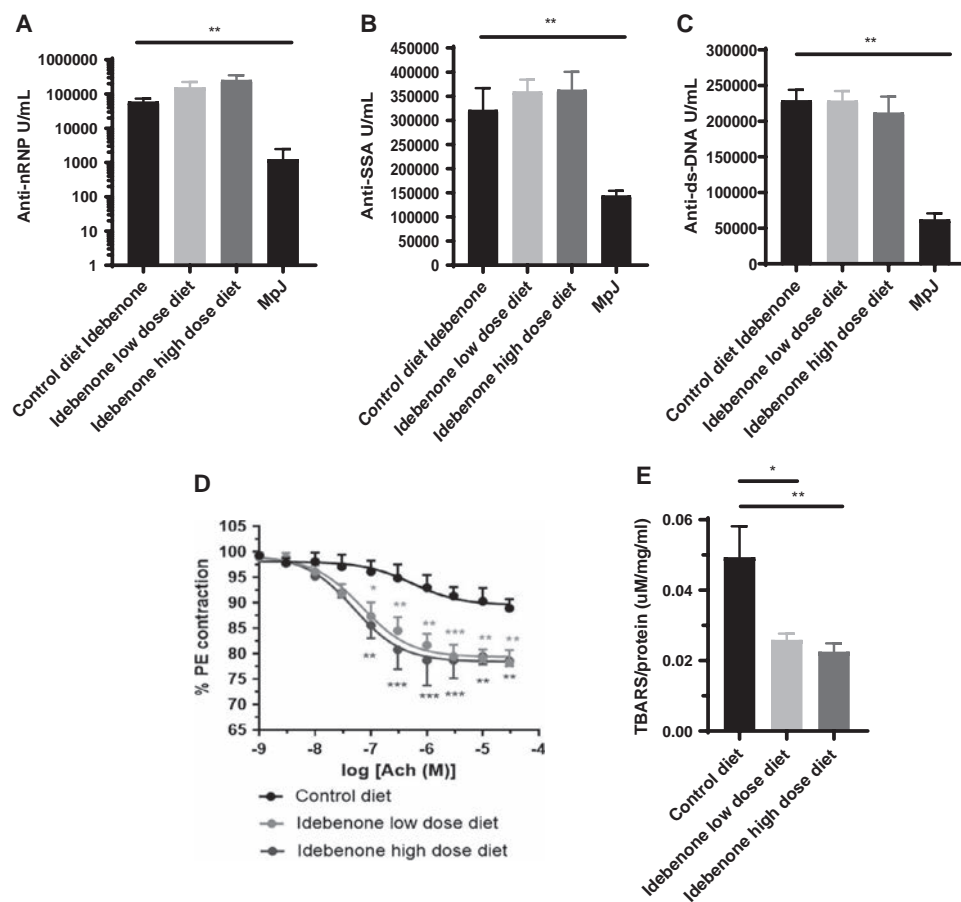


Figure 3. Idebenone has no effect on circulating autoantibodies but modulates endothelium-dependent vasorelaxation and cardiac lipid peroxidation in mice with lupus. **A–C**, Quantification of serum anti-nuclear RNP (anti-nRNP) (**A**), anti-SSA (**B**), and anti-double-stranded DNA (anti-dsDNA) (**C**) antibodies in MRL/lpr mice and control MpJ mice at euthanasia ($n = 10$ mice/group). **D**, Endothelium-dependent vasorelaxation of the aortic rings from MRL/lpr mice ($n = 3$ mice/group), determined according to relaxation of the phenylephrine (PE)-precontracted aortas in response to acetylcholine (ACh) using a myograph. **E**, Quantification of cardiac tissue lipid peroxidation by thiobarbituric acid assay (TBARS) in MRL/lpr mice ($n = 10$ mice/group). Results are the mean \pm SEM. * = $P < 0.05$; ** = $P < 0.01$; *** = $P < 0.001$, by 2-way analysis of variance and Tukey's multiple comparisons test in **D** and by Mann-Whitney U test in **A–C** and **E**.

contrast, both doses of idebenone induced significant improvements in endothelium-dependent vasorelaxation (Figure 3D), suggesting that this compound can beneficially modulate lupus vasculopathy.

In further support of the idea that idebenone can improve cardiovascular physiology, cardiac lipid peroxidation (a phenomenon associated with enhanced oxidative damage and cardiovascular disease) was significantly diminished by both doses of idebenone compared to the control diet group (Figure 3E). These results indicate that idebenone significantly improves parameters of cardiovascular risk in lupus-prone mice.

Attenuation of inflammation pathways and immune dysregulation with idebenone treatment in murine lupus. Spleen size, a parameter of murine lupus disease activity, was reduced following treatment with both doses of idebenone, with the low-dose group showing significant differences com-

pared to the control diet group (Figure 4A). There were no significant differences in total splenic T cell numbers between the idebenone and control diet groups (Figure 4B). Similarly, there were no significant changes in the numbers of double-negative T cells (CD4⁻CD8⁻) (Figure 4C). However, when the maturation and activation status of T cells was assessed, treatment with low-dose idebenone significantly reduced the numbers of effector memory T cells (CD44⁺CD62L⁻) (Figures 4D–E) and effector memory CD4⁺ T helper cells (Figure 4F and Supplementary Figure 4 [http://onlinelibrary.wiley.com/doi/10.1002/art.41128/abstract]). In contrast, high-dose idebenone did not affect the proportions of spleen cells significantly when compared to the control diet. There was no difference in the numbers of other splenic cell subsets, including B cells, plasma cells, naive B cells, marginal zone B cells, plasmablasts, plasmacytoid dendritic cells, monocytes, and neutrophils, between the control diet and either dose of idebenone (see Supplementary

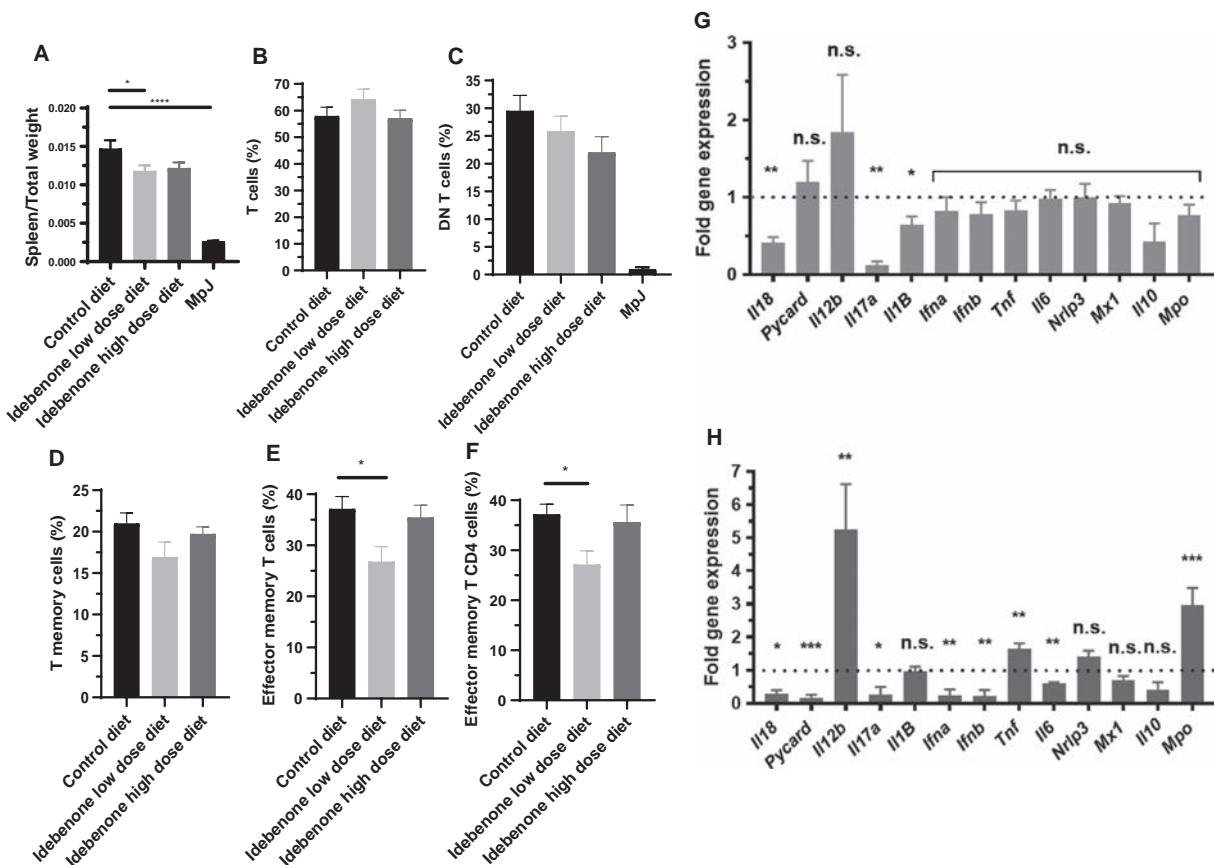


Figure 4. Idebenone decreases spleen size, reduces the number of effector memory T cells, and modulates inflammatory gene expression in mice with lupus. **A**, Size of the spleens relative to total weight in MRL/lpr mice and control MpJ mice. **B–F**, Percentage of splenic T cells (CD45⁺CD3⁺) (**B**), double-negative (DN) T cells (CD45⁺CD3⁺CD4⁻CD8⁻) (**C**), memory T cells (CD45⁺CD3⁺CD4⁺CD8⁻CD44⁺CD62L⁻) (**D**), effector memory T cells (CD45⁺CD3⁺CD44⁺CD62L⁻) (**E**), and effector memory CD4⁺ T helper cells (CD45⁺CD3⁺CD4⁺CD8⁻CD44⁺CD62L⁻) (**F**). Results in **A–F** are the mean \pm SEM of 10 mice/group. **G** and **H**, Expression of representative type I interferon-regulated genes, proinflammatory cytokines, and inflammasome-related genes in splenocytes from MRL/lpr mice treated with the low-dose (**G**) or high-dose (**H**) idebenone diet. Gene expression is measured as the fold change in the idebenone groups adjusted for the control diet group (normalized to a value of 1 [broken horizontal line]). Results are the mean \pm SEM of 4 mice per group. * = $P < 0.05$; ** = $P < 0.01$; *** = $P < 0.001$; **** = $P < 0.0001$, by Mann-Whitney U test. NS = not significant.

Figure 5 [http://onlinelibrary.wiley.com/doi/10.1002/art.41128/abstract]). These results suggest that idebenone preferentially reduces the number of effector memory CD4⁺ T cells in mice with lupus, and that the effect differs between doses of the compound.

Gene expression analysis of splenocytes showed that selected type I IFNs and type I IFN-regulated genes and other proinflammatory genes (such as *Tnf* and *Il6*) were not significantly modified by treatment with low-dose idebenone, whereas splenocyte expression of *Il18*, *Il17a*, and *Il1B* was significantly decreased (Figure 4G) as compared to the control diet. The high-dose idebenone diet significantly inhibited splenocyte expression of *Il18*, *Pycard*, *IL17a*, *Ifna*, *Ifnb*, and *Il6*, whereas it significantly induced splenocyte expression of *Il12b*, *Tnf*, and *Mpo* (Figure 4H), when compared to the control diet.

These findings were supported by the findings in NZM2328 mice, in which treatment with low-dose idebenone also significantly reduced splenomegaly and decreased splenocyte gene expression of *Ifna1*, *Mx1*, *Il6*, *Il1B*, and *Il10* (see Supplementary Figures 3A and F [http://onlinelibrary.wiley.com/doi/10.1002/art.41128/abstract]). These results indicate

that idebenone may modify inflammatory gene expression in lupus-prone mice.

Modulation of mitochondrial metabolism with idebenone treatment in lupus-prone mice.

We quantified the modulation of mitochondrial metabolism by idebenone in mouse splenocytes and BM-derived neutrophils using a Seahorse Analyzer. In both the splenocytes (Figures 5A–C) and neutrophils (Figures 5E–G), low-dose idebenone significantly enhanced mitochondrial basal respiration (Figures 5A and E), maximal respiration (Figures 5B and F), and ATP production (Figures 5C and G) as compared to the control diet. Trends were similar in the high-dose idebenone group, but differences compared to the control diet did not reach statistical significance (Figures 5A–C and E–G).

Low-dose idebenone increased the ratio of mitochondrial gene:nuclear gene (*16S:B2m*) transcription compared to the control diet, whereas conversely, this ratio was decreased with high-dose idebenone (Figure 5D). Overall, these results suggest that mitochondrial immunometabolism is improved by idebenone treatment in lupus-prone mice.

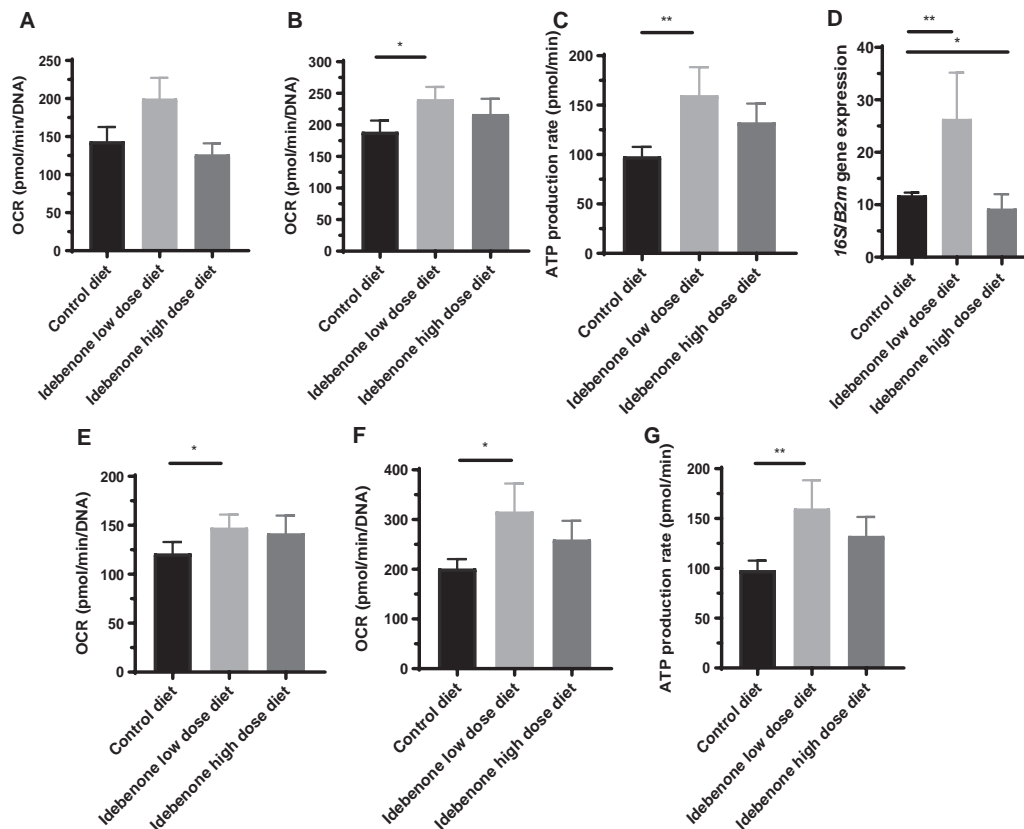


Figure 5. Mitochondrial immunometabolism is modulated by idebenone. **A–C** and **E–G**, Mitochondrial metabolism was analyzed in splenocytes (**A–C**) and bone marrow–derived neutrophils (**E–G**) from MRL/*lpr* mice receiving the control or idebenone diets. Mice were analyzed for basal respiration (**A** and **E**), maximal respiration (**B** and **F**), and ATP production (**C** and **G**) ($n = 10$ mice/group). **D**, The ratio of transcription of the mitochondrial gene *16S* to that of the nuclear gene *B2m* was analyzed by quantitative reverse transcription–polymerase chain reaction in splenocytes from MRL/*lpr* mice ($n = 10$ mice/group). Results are the mean \pm SEM. * = $P < 0.05$; ** = $P < 0.01$, by Mann-Whitney U test. OCR = oxygen consumption rate.

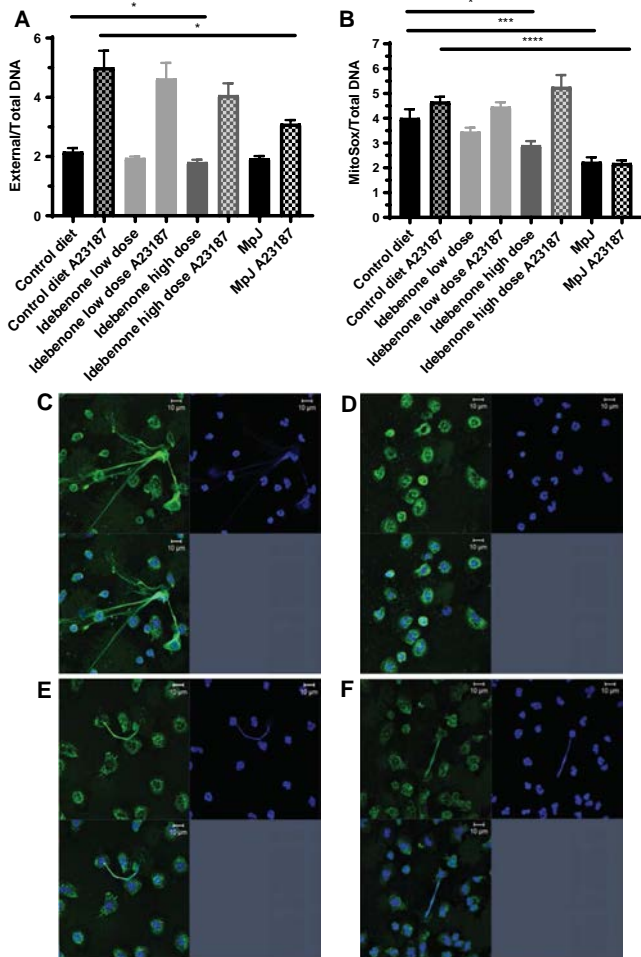


Figure 6. Idebenone modulates spontaneous murine and human neutrophil extracellular trap (NET) formation and murine mitochondrial reactive oxygen species (ROS) synthesis. **A**, Ex vivo spontaneous and ionophore (A23187)-induced NET formation in neutrophils, quantified by Sytox plate assay at 2 hours poststimulation, from the bone marrow (BM) of MRL/*lpr* mice receiving the control or idebenone diets and control MpJ mice. **B**, Mitochondrial ROS synthesis, determined as the ratio of MitoSox to Picogreen fluorescence, in BM-derived neutrophils from each group of mice. Results in **A** and **B** are the mean \pm SEM of 10 mice per group. * = $P < 0.05$; *** = $P < 0.001$; **** = $P < 0.0001$, by Mann-Whitney U test. **C–F**, Assessment of NET formation in human lupus low-density granulocytes (LDGs) (**C** and **D**) compared to normal-density granulocytes (NDGs) (**E** and **F**) in the presence of idebenone treatment (10 μ M) (**D** and **F**) or absence of idebenone treatment (**C** and **E**), as quantified by immunofluorescence after 2 hours of incubation. Images are representative of 3 different patients analyzed. Green fluorescence indicates neutrophil elastase, and blue fluorescence indicates DNA. The upper panels in **C–F** are single fluorochromes, and the bottom left panel shows the merged fluorescence. Original magnification $\times 40$.

To further characterize the pathways modulated by idebenone in murine lupus, we measured the specific activity of mitochondrial complex II in splenic extracts. We found mitochondrial complex II activity to be enhanced in splenocytes from MRL/*lpr* exposed

to low-dose idebenone compared to the control diet. This effect in the low-dose idebenone group was inhibited by both of the mitochondrial complex II-specific inhibitors tested, malonate and TTFA (see Supplementary Figure 6 [http://onlinelibrary.wiley.com/doi/10.1002/art.41128/abstract]).

Modulation of NET formation with idebenone treatment in lupus-prone mice and human patients with SLE.

The capacity of idebenone to modulate antioxidants and immunometabolism could potentially modify the amount of mROS that is synthesized by myeloid cells. Since mROS are implicated in pathogenic NET formation (2), we quantified this process ex vivo in BM-derived neutrophils from idebenone-treated mice after euthanasia (Figure 6A). Spontaneous NET formation by neutrophils from MRL/*lpr* mice was significantly decreased in the high-dose idebenone-treated mice but not in the low-dose idebenone-treated mice, as compared to the control diet group (Figure 6A), while no differences in ionophore-induced NET formation were observed.

Similarly, synthesis of mROS in MRL/*lpr* mouse neutrophils was significantly decreased in the high-dose idebenone group but not in the low-dose idebenone group (Figure 6B) compared to the control diet. These results suggest that mROS production is enhanced in murine lupus neutrophils, and that idebenone can modulate NET formation by, at least in part, reducing mROS generation.

The in vitro effect of idebenone on NET formation was also analyzed in neutrophils from human patients with SLE. We have previously described a pathogenic neutrophil subset in patients with SLE, referred to as lupus LDGs, which are primed to form NETs in an mROS-dependent manner, whereas NET formation in normal-density granulocytes (NDGs), which are less prone to NETs, occurs independent of mROS (2). Treatment with idebenone significantly inhibited spontaneous NET formation by lupus LDGs, whereas it did not affect this process in NDGs (Figures 6C–F). These observations suggest that the beneficial effects of idebenone are operational when dysfunctional/inflamed cells are exposed to it, and that human lupus neutrophils could be modulated by this drug.

DISCUSSION

A key role of mitochondrial dysfunction in the pathogenesis of lupus and other autoimmune diseases has been suggested (2,21–24). The results of the present study further support the notion that the use of compounds that modulate mitochondrial function and also act as antioxidants may attenuate lupus-associated organ damage and immune dysregulation associated with this disease. Importantly, idebenone was well-tolerated and modified the rate of survival in these murine lupus models. Some aspects of lupus immune dysregulation, organ damage, and immunometabolism were similarly modified by both doses of idebenone, while other aspects were differentially modulated

by only 1 of the 2 doses tested or showed opposite effects. This suggests that the putative pleiotropic roles of idebenone in immune function, inflammation, tissue repair/fibrosis, and oxidative damage may be, in several instances, dose-dependent, and this should be taken into consideration for potential future studies, both preclinical and clinical.

With regard to regulation of immune responses, idebenone treatment led to a decrease in the number of effector memory CD4+ T cells in MRL/lpr mice. The mechanisms by which idebenone specifically modifies the number of these T cells is unclear and could be either direct (through effects on cell metabolism that impact the phenotype/differentiation of these cells) or indirect (through reduction of cytokines that impact their development) (25–27). Despite the reduction in activated T cells as a result of idebenone treatment, autoantibody levels were not affected by this compound. The reason for these differential effects on specific cell subsets remains unclear, and could potentially be related to the timing of administration, to distinct effects on subsets of T cells involved in direct stimulation of B cell function, or to lack of a direct impact on autoreactive B cells and/or long-lived plasma cells.

Of note, endothelium-dependent vasorelaxation significantly improved with idebenone administration. Since endothelial dysfunction, vasculopathy, and premature atherosclerosis occur at an increased frequency in human patients with SLE, these findings suggest that idebenone could have potential beneficial effects in vascular health in this disease (28–30). This is also emphasized by the observation of decreased cardiac lipid peroxidation by idebenone, a phenomenon that may also promote enhanced vascular health (31).

Recent findings have implicated inflammasome activation in the pathogenesis of murine and human SLE and in vasculopathy (32). Idebenone down-regulated mRNAs of components of the inflammasome pathway and reduced the expression of mature IL-18 in the mouse kidney tissue. As one of the putative mechanisms of action of idebenone is through its ability to bypass the dysfunctional mitochondrial complex I, it may dampen enhanced mROS synthesis and subsequent inflammasome activation (33). Indeed, both splenocytes and neutrophils showed improved mitochondrial function in animals treated with low-dose idebenone. Importantly, idebenone had an inhibitory effect on NET formation in proinflammatory neutrophil subsets from lupus patients, but not in other neutrophil subsets not considered to play a major role in SLE pathogenesis. This could be reassuring when considering testing this or similar compounds in SLE patients in the future, since the drug may preferentially target aberrant immune cell subsets. Idebenone has been reported to be safe in the treatment of human patients with a variety of conditions associated with mitochondrial dysfunction, at doses that are 6–225 times higher than the doses used in this study. This provides a good therapeutic rationale to potentially test this drug in SLE patients in the future (34).

Another potentially immunomodulatory effect of idebenone in SLE could be secondary to the reduction of IL-17 expression

in the spleen and kidneys. Blockade of the IL-17 pathway has been reported to reduce renal disease and immune dysregulation in murine and human SLE (35–38). The observation that idebenone modulated renal involvement in 2 mouse models of SLE imply that targeting mitochondrial dysfunction can have pleiotropic effects on organ damage or would have high relevance to this disease. Again, the effects on histopathologic features in the kidney varied between the 2 doses of idebenone and the mouse model studied, indicating that future studies should focus on further characterizing the effects of this compound on tissue repair and fibrosis/evolution to end-stage renal disease. Low-dose idebenone significantly reduced the expression of *Il10* in NZM2328 mice; this finding may be relevant in the context of the putative role of IL-10 in the pathogenesis of SLE (39).

In summary, the results of this study indicate that idebenone improves immune dysregulation, organ damage, vasculopathy, and mitochondrial function in murine SLE through pleiotropic effects on the immune compartment, immunometabolism, and tissue damage. Our study suggests that targeting mitochondrial dysfunction should be further explored as a putative strategy in lupus and potentially other autoimmune conditions.

ACKNOWLEDGMENT

We thank the NIAMS/NIH Office of Science and Technology, Intramural Research Program for technical support.

AUTHOR CONTRIBUTIONS

All authors were involved in drafting the article or revising it critically for important intellectual content, and all authors approved the final version to be published. Dr. Kaplan had full access to all of the data in the study and takes responsibility for the integrity of the data and the accuracy of the data analysis.

Study conception and design. Blanco, Kaplan.

Acquisition of data. Blanco, Pedersen, Wang, Lightfoot, Seto, Carmona-Rivera, Yu, Hoffmann, Yuen.



Analysis and interpretation of data. Blanco.

REFERENCES

1. Yang SK, Zhang HR, Shi SP, Zhu YQ, Song N, Dai Q, et al. The role of mitochondria in systemic lupus erythematosus: a glimpse of various pathogenetic mechanisms. *Curr Med Chem* 2019;26:1–15.
2. Lood C, Blanco LP, Purmalek MM, Carmona-Rivera C, De Ravin SS, Smith CK, et al. Neutrophil extracellular traps enriched in oxidized mitochondrial DNA are interferogenic and contribute to lupus-like disease. *Nat Med* 2016;22:146–53.
3. Oaks Z, Winans T, Caza T, Fernandez D, Liu Y, Landas SK, et al. Mitochondrial dysfunction in the liver and antiphospholipid antibody production precede disease onset and respond to rapamycin in lupus-prone mice. *Arthritis Rheumatol* 2016;68:2728–39.
4. Cheng SW, Ko CH, Yau SK, Mak C, Yuen YF, Lee CY. Novel use of idebenone in Leber's hereditary optic neuropathy in Hong Kong. *Hong Kong Med J* 2014;20:451–4.
5. Lyseng-Williamson KA. Idebenone: a review in Leber's hereditary optic neuropathy. *Drugs* 2016;76:805–13.

6. McDonald CM, Meier T, Voit T, Schara U, Straathof CS, D'Angelo MG, et al. Idebenone reduces respiratory complications in patients with Duchenne muscular dystrophy. *Neuromuscul Disord* 2016;26:473–80.
7. Zs.-Nagy I. Chemistry, toxicology, pharmacology and pharmacokinetics of idebenone: a review. *Arch Gerontol Geriatr* 1990;11:177–86.
8. Holzerova E, Danhauser K, Haack TB, Kremer LS, Melcher M, Ingold I, et al. Human thioredoxin 2 deficiency impairs mitochondrial redox homeostasis and causes early-onset neurodegeneration. *Brain* 2016;139:346–54.
9. Arend N, Wertheimer C, Laubichler P, Wolf A, Kampik A, Kernt M. Idebenone prevents oxidative stress, cell death and senescence of retinal pigment epithelium cells by stabilizing BAX/Bcl-2 ratio. *Ophthalmologica* 2015;234:73–82.
10. Jaber S, Polster BM. Idebenone and neuroprotection: antioxidant, pro-oxidant, or electron carrier? *J Bioenerg Biomembr* 2015;47:111–8.
11. Gerhardt E, Gräber S, Szegő ÉM, Moiso N, Martins LM, Outeiro TF, et al. Idebenone and resveratrol extend lifespan and improve motor function of HtrA2 knockout mice. *PLoS One* 2011;6:e28855.
12. Heitz FD, Erb M, Anklin C, Robay D, Pernet V, Gueven N. Idebenone protects against retinal damage and loss of vision in a mouse model of Leber's hereditary optic neuropathy. *PLoS One* 2012;7:e45182.
13. Seznec H, Simon D, Monassier L, Criqui-Filipe P, Gansmuller A, Rustin P, et al. Idebenone delays the onset of cardiac functional alteration without correction of Fe-S enzymes deficit in a mouse model for Friedreich ataxia. *Hum Mol Genet* 2004;13:1017–24.
14. National Research Council. Nutrient requirements of laboratory animals. 4th ed. Washington (DC): National Academies Press; 1995.
15. Furumoto Y, Smith CK, Blanco L, Zhao W, Brooks SR, Thacker SG, et al. Tofacitinib ameliorates murine lupus and its associated vascular dysfunction. *Arthritis Rheumatol* 2017;69:148–60.
16. Yuen PST, Dunn SR, Miyaji T, Yasuda H, Sharma K, Star RA. A simplified method for HPLC determination of creatinine in mouse serum. *Am J Physiol-Renal Physiol* 2004;286:F1116–9.
17. Hochberg MC, for the Diagnostic and Therapeutic Criteria Committee of the American College of Rheumatology. Updating the American College of Rheumatology revised criteria for the classification of systemic lupus erythematosus [letter]. *Arthritis Rheum* 1997;40:1725.
18. Denny MF, Yalavarthi S, Zhao W, Thacker SG, Anderson M, Sandy AR, et al. A distinct subset of proinflammatory neutrophils isolated from patients with systemic lupus erythematosus induces vascular damage and synthesizes type I IFNs. *J Immunol* 2010;184:3284–97.
19. Higa R, Roberti SL, Capobianco E, Fornes D, White V, Jawerbaum A. Pro-oxidant/pro-inflammatory alterations in the offspring's heart of mild diabetic rats are regulated by maternal treatments with a mitochondrial antioxidant. *Reprod Toxicol* 2017;73:269–79.
20. Carmona-Rivera C, Simeonov DR, Cardillo ND, Gahl WA, Cadilla CL. A divalent interaction between HPS1 and HPS4 is required for the formation of the biogenesis of lysosome-related organelle complex-3 (BLOC-3). *Biochim Biophys Acta* 2013;1833:468–78.
21. López-López L, Nieves-Plaza M, del R Castro M, Font YM, Torres-Ramos CA, Vilá LM, et al. Mitochondrial DNA damage is associated with damage accrual and disease duration in patients with systemic lupus erythematosus. *Lupus* 2014;23:1133–41.
22. Buskiewicz IA, Montgomery T, Yasewicz EC, Huber SA, Murphy MP, Hartley RC, et al. Reactive oxygen species induce virus-independent MAVS oligomerization in systemic lupus erythematosus. *Sci Signal* 2016;9:ra115.
23. Caza TN, Fernandez DR, Talaber G, Oaks Z, Haas M, Madaio MP, et al. HRES-1/Rab4-mediated depletion of Drp1 impairs mitochondrial homeostasis and represents a target for treatment in SLE. *Ann Rheum Dis* 2014;73:1888–97.
24. Lee HT, Wu TH, Lin CS, Lee CS, Wei YH, Tsai CY, et al. The pathogenesis of systemic lupus erythematosus—from the viewpoint of oxidative stress and mitochondrial dysfunction [review]. *Mitochondrion* 2016;30:1–7.
25. Balomenos D, Rumold R, Theofilopoulos AN. The proliferative in vivo activities of Ipr double-negative T cells and the primary role of p59fyn in their activation and expansion. *J Immunol* 1997;159:2265–73.
26. Balomenos D, Rumold R, Theofilopoulos AN. Interferon- γ is required for lupus-like disease and lymphoaccumulation in MRL-Ipr mice. *J Clin Invest* 1998;101:364–71.
27. Murakami T, Chen X, Hase K, Sakamoto A, Nishigaki C, Ohno H. Splenic CD19⁺CD35⁺B220⁺ cells function as an inducer of follicular dendritic cell network formation. *Blood* 2007;110:1215–24.
28. Rajagopalan S, Somers EC, Brook RD, Kehrer C, Pfenninger D, Lewis E, et al. Endothelial cell apoptosis in systemic lupus erythematosus: a common pathway for abnormal vascular function and thrombosis propensity. *Blood* 2004;103:3677–83.
29. Manzi S, Meilahn EN, Rairie JE, Conte CG, Medsger TA Jr, Jansen-McWilliams L, et al. Age-specific incidence rates of myocardial infarction and angina in women with systemic lupus erythematosus: comparison with the Framingham Study. *Am J Epidemiol* 1997;145:408–15.
30. Esdaile JM, Abrahamowicz M, Grodzicky T, Li Y, Panaritis C, du Berger R, et al. Traditional Framingham risk factors fail to fully account for accelerated atherosclerosis in systemic lupus erythematosus. *Arthritis Rheum* 2001;44:2331–7.
31. Bianchi P, Kunduzova O, Masini E, Cambon C, Bani D, Raimondi L, et al. Oxidative stress by monoamine oxidase mediates receptor-independent cardiomyocyte apoptosis by serotonin and postischemic myocardial injury. *Circulation* 2005;112:3297–305.
32. Kahlenberg JM, Yalavarthi S, Zhao W, Hodgins JB, Reed TJ, Tsuji NM, et al. An essential role of caspase 1 in the induction of murine lupus and its associated vascular damage. *Arthritis Rheumatol* 2014;66:152–62.
33. Groß CJ, Mishra R, Schneider KS, Médard G, Wettmarshausen J, Dittlein DC, et al. K⁺ efflux-independent NLRP3 inflammasome activation by small molecules targeting mitochondria. *Immunity* 2016;45:761–73.
34. Becker C, Bray-French K, Drewe J. Pharmacokinetic evaluation of idebenone. *Expert Opin Drug Metab Toxicol* 2010;6:1437–44.
35. Amarilyo G, Lourenço EV, Shi FD, La Cava A. IL-17 promotes murine lupus. *J Immunol* 2014;193:540–3.
36. Crispín JC, Oukka M, Bayliss G, Cohen RA, Van Beek CA, Stillman IE, et al. Expanded double negative T cells in patients with systemic lupus erythematosus produce IL-17 and infiltrate the kidneys. *J Immunol* 2008;181:8761–6.
37. Lee SY, Lee SH, Seo HB, Ryu JG, Jung K, Choi JW, et al. Inhibition of IL-17 ameliorates systemic lupus erythematosus in Roquin^{san/san} mice through regulating the balance of TFH cells, GC B cells, Treg and Breg. *Sci Rep* 2019;9:5227.
38. Saber NZ, Maroof SH, Soliman DA, Fathi MS. Expression of T helper 17 cells and interleukin 17 in lupus nephritis patients. *Egypt Rheumatol* 2017;39:151–7.
39. Teichmann LL, Kashgarian M, Weaver CT, Roers A, Müller W, Shlomchik MJ. B cell-derived IL-10 does not regulate spontaneous systemic autoimmunity in MRL.Fas(Ipr) mice. *J Immunol* 2012;188:678–85.

Using Autoantibodies and Cutaneous Subset to Develop Outcome-Based Disease Classification in Systemic Sclerosis

Svetlana I. Nihtyanova,¹  Alper Sari,² Jennifer C. Harvey,¹ Anna Leslie,¹ Emma C. Derrett-Smith,¹ Carmen Fonseca,¹ Voon H. Ong,¹ and Christopher P. Denton¹ 

Objective. To describe the associations between autoantibodies, clinical presentation, and outcomes among patients with systemic sclerosis (SSc) in order to develop a novel SSc classification scheme that would incorporate both antibodies and the cutaneous disease subset as criteria.

Methods. Demographic and clinical characteristics, including cutaneous subset, time of disease and organ complication onset, and autoantibody specificities, were determined in a cohort of SSc subjects. Survival analysis was used to assess the effect of the autoantibodies on organ disease and death.

Results. The study included 1,325 subjects. Among the antibody/skin disease subsets, anticentromere antibody-positive patients with limited cutaneous SSc (lcSSc) ($n = 374$) had the highest 20-year survival (65.3%), lowest incidence of clinically significant pulmonary fibrosis (PF) (8.5%) and scleroderma renal crisis (SRC) (0.3%), and lowest incidence of cardiac SSc (4.9%), whereas the frequency of pulmonary hypertension (PH) was similar to the mean value in the SSc cohort overall. The anti-Scl-70+ groups of patients with lcSSc ($n = 138$) and patients with diffuse cutaneous SSc (dcSSc) ($n = 149$) had the highest incidence of clinically significant PF (86.1% and 84%, respectively, at 15 years). Anti-Scl-70+ patients with dcSSc had the lowest survival (32.4%) and the second highest incidence of cardiac SSc (12.9%) at 20 years. In contrast, in anti-Scl-70+ patients with lcSSc, other complications were rare, and these patients demonstrated the lowest incidence of PH (6.9%) and second highest survival (61.8%) at 20 years. Anti-RNA polymerase antibody-positive SSc patients ($n = 147$) had the highest incidence of SRC (28.1%) at 20 years. The anti-U3 RNP+ SSc group ($n = 56$) had the highest incidence of PH (33.8%) and cardiac SSc (13.2%) at 20 years. Among lcSSc patients with other autoantibodies ($n = 295$), the risk of SRC and cardiac SSc was low at 20 years (2.7% and 2.4%, respectively), while the frequencies of other outcomes were similar to the mean values in the full SSc cohort. Patients with dcSSc who were positive for other autoantibodies ($n = 166$) had a poor prognosis, demonstrating the second lowest survival (33.6%) and frequent organ complications.

Conclusion. These findings highlight the importance of autoantibodies, cutaneous subset, and disease duration when assessing morbidity and mortality in patients with SSc. Our novel classification scheme may improve disease monitoring and benefit future clinical trial designs in SSc.

INTRODUCTION

Autoantibody testing has become an essential part of the assessment of patients with systemic sclerosis (SSc). The most commonly observed and strongly scleroderma-specific antibodies are the anticentromere antibodies (ACAs), anti-topoisomerase I (anti-topo I; anti-Scl-70) antibodies, and anti-RNA polymerase (anti-RNAP) antibodies, which, together, are found in 50–80% of SSc patients (1,2).

Whereas positivity for anti-topo I is predictive of the development of pulmonary fibrosis (PF) and positivity for anti-RNAP is predictive of severe skin disease and scleroderma renal crisis (SRC), the risk of lung- and kidney-based organ disease is reduced in the presence of ACAs (3). Much rarer, but still very disease specific, are the antifibrillar antibodies (anti-U3 RNP), anti-Th/To antibodies, and anti-U11/U12 RNP antibodies, while anti-PM/Scl and anti-Ku antibodies are associated with scleroderma overlap syndromes (4–10).

Supported in part by Scleroderma & Raynaud's UK (SRUK grant reference RF33) and the Royal Free Charity (fund 97).

¹Svetlana I. Nihtyanova, MSc, MD, Jennifer C. Harvey, MSc, Anna Leslie, MBBS, Emma C. Derrett-Smith, PhD, MRCP, Carmen Fonseca, MD, PhD, Voon H. Ong, PhD, FRCP, Christopher P. Denton, PhD, FRCP: UCL Division of Medicine, Royal Free Hospital, London, UK; ²Alper Sari, MD: UCL Division of Medicine, Royal Free Hospital, London, UK, and Hacettepe Üniversitesi, Ankara, Turkey.

No potential conflicts of interest relevant to this article were reported.

Address correspondence to Christopher P. Denton, PhD, FRCP, Royal Free Campus, UCL Centre for Rheumatology and Connective Tissue Diseases, UCL Medical School Building 2nd Floor, Rowland Hill Street, London NW3 2PF, UK. E-mail: c.denton@ucl.ac.uk.

Submitted for publication February 20, 2019; accepted in revised form October 29, 2019.

The majority of studies that have demonstrated associations between autoantibodies and organ disease have been cross-sectional and have provided sparse information on the timing of the development of organ complications (11). In a previous study, we demonstrated time-dependent effects of anti-topo I antibodies on the hazard of clinically significant PF (12). Some studies have suggested that anti-RNAP+ SSc patients tend to develop PF later in the disease course, in contrast to SSc patients with anti-topo I antibodies, in whom PF is an early complication (13,14). A major caveat for these types of analyses would be that the disease duration differs between subjects at study entry, which could significantly bias the estimation of time to event (15).

Similarly, skin thickness and change in the modified Rodnan skin thickness score (MRSS) over the disease course vary substantially among SSc patients (16,17). While several reports have described change in the MRSS over time and its role in SSc risk stratification, those studies tended to use a small number of skin assessments, often at fixed time points (17–19). Even when multiple MRSS assessments are analyzed, the mathematical modeling approaches generally assume constant change in skin thickness, i.e., linear association between time and MRSS (20,21). Since it is widely accepted that the MRSS trajectory is nonlinear, the timing of assessment is very likely to be an important predictor of both the absolute MRSS and the subsequent change in MRSS (22). Autoantibodies are associated strongly with MRSS changes, and frequencies of the hallmark SSc antibodies are very different in patients with the diffuse cutaneous (dcSSc) subtype, whose MRSS scores are initially high compared to those with milder skin disease (16,23).

SSc is a rare disorder with substantial clinical and serologic heterogeneity. Several authors have proposed classification schemes for the disease based on the varying extent of skin involvement (24,25), although patients are still most commonly classified into either the dcSSc or limited cutaneous SSc (lcSSc) subset, as proposed by LeRoy and colleagues in 1988 (26). Subdividing SSc cases into more than 2 cutaneous subsets does not improve risk stratification (27). Conversely, autoantibodies are a very strong predictor of organ involvement; therefore, a combination of autoantibodies and the skin subset of SSc could substantially refine risk stratification (17,28,29).

Thus, in the present study, we used a large, well-characterized cohort of patients with SSc to describe the associations between autoantibodies and changes in skin thickness over time, the frequency and timing of organ complications, and survival among SSc patients. Based on our observations, we propose a simple classification scheme for SSc that incorporates both antibodies and the cutaneous disease subset into the classification criteria.

PATIENTS AND METHODS

Cohort selection. All patients fulfilled the American College of Rheumatology/European League Against Rheumatism 2013 classification criteria for SSc (30). We included patients

with disease onset between January 1, 1995 and December 31, 2007 for all analyses of time to organ complications and death. As the definition of clinically significant PF included pulmonary function test (PFT) results, we aimed to avoid bias in the estimation of timing of this complication by including only subjects who had undergone at least 1 PFT within the first 3 years after disease onset. For the analysis of the changes in skin thickness score over time, we focused on patients with dcSSc and at least 1 MRSS assessment. In order to increase the number of subjects, we did not set any restrictions on the time of disease onset for this group.

This project was conducted in compliance with the Declaration of Helsinki. Data used were obtained through 2 studies, involving collection of routine data and samples from patients seen in our center. The 2 studies have been approved by the London-Hampstead and London-Fulham Research Ethics Committees.

Disease characteristics and outcome definitions.

Disease onset was defined as the time of first occurrence of a non-Raynaud's symptom of SSc, as recalled by the patient or as observed by a physician. Skin thickness was assessed using the MRSS (score range 0–51). Cutaneous subset was defined as limited (lcSSc) when skin thickening did not extend proximally to the elbows and knees; otherwise, the subset was defined as diffuse (dcSSc) (26). Patients were recorded as having PF if this diagnosis was confirmed on high-resolution computed tomography (HRCT). PF was considered clinically significant if 1 of the following criteria were fulfilled: 1) forced vital capacity (FVC) <70% predicted; 2) FVC \leq 80% and a documented absolute decline in the FVC of \geq 15%; 3) diffusing capacity for carbon monoxide (DLco) <70%, with no history of pulmonary hypertension (PH) or development of PH in the 3 years after DLco dropped below 70%; or 4) DLco \leq 80% and a documented decline in DLco of \geq 15%, with no history of PH or development of PH in the 3 years after DLco dropped below 70%.

PH was defined as a mean pulmonary artery pressure of \geq 25 mm Hg at rest, with pulmonary artery wedge pressure of \leq 15 mm Hg on right-sided heart catheterization. This included patients in group 1 (those with connective tissue disease-associated pulmonary arterial hypertension) and group 3 (those with interstitial lung disease-associated PH). Cardiac scleroderma was defined as hemodynamically significant arrhythmias, pericardial effusion, or congestive heart failure (left ventricular ejection fraction below 50%) requiring specific treatment, in the absence of other known cardiac causes. Scleroderma renal crisis (SRC) was defined as new-onset systemic hypertension of >150/85 mm Hg and a documented decrease in the estimated glomerular filtration rate of >30% or confirmed features of SRC on renal biopsy. Details on the distribution and assessment of autoantibodies are available in the Supplementary Patients and Methods (Autoantibodies section) and Supplementary Tables 1 and 2 (available on the *Arthritis & Rheumatology*

web site at <http://onlinelibrary.wiley.com/doi/10.1002/art.41153/abstract>).

Autoantibody associations. For the analysis of associations between antibodies and morbidity/mortality, we focused on SSc-specific antibodies (ACAs, anti-topo I, anti-RNAP, anti-U3 RNP, anti-PM/Scl). Patients who were positive for >1 antibody were included in the antibody group that was specific to SSc. Patients positive for antinuclear antibodies (ANA+) and negative for anti-extractable nuclear antigen (ENA-) formed a separate group. Patients who carried any other defined antibodies (U1 RNP, Th/To, SL, Ku, Jo-1, Ro, La, XR, PL-7, heterogeneous nuclear RNP, and Sm antibodies) as well as ANA- patients were included in the group classified as "other."

Classification development. For the development of this novel SSc classification, subjects were divided into 14 initial subgroups by antibody specificity (ACAs, anti-topo I, anti-RNAP, anti-U3 RNP, anti-PM/Scl, ANA+ENA-, or other autoantibodies) and skin subset (diffuse or limited). The end points of interest were survival and cumulative incidence of organ complications at 5, 10, 15, and 20 years from disease onset; these were calculated for each subgroup. Within each end point, subgroups were ranked in

terms of survival/cumulative incidence of organ disease estimates, and the subgroups that showed similar ranking in multiple end points were then merged.

Statistical analysis. Survival was analyzed using Kaplan-Meier (KM) survival estimates, while the incidence of organ complications was calculated using both the 1 - KM estimate and the cumulative incidence function (CIF) estimate, accounting for competing risks. The KM method works under the assumption of noninformative censoring, which does not hold in those cases where death occurs before an organ complication has developed, and may therefore result in overestimation (31). For that reason, the 1 - KM estimate and the CIF estimate accounting for death as a competing risk were compared. Discreet-time hazard rates were calculated within intervals of 12 months over the follow-up, in order to assess the timing of highest rates of death and organ complication development. The effect of antibody specificities on the hazards was assessed using Cox proportional hazards regression analysis. Proportionality of hazards assumption was tested using log-log plots, plots of Scaled Schoenfeld residuals, comparison between observed KM and Cox model-predicted survival, and through the incorporation of time-varying effects in the models. Linear mixed-effects models were used to assess

Table 1. Characteristics of the cohort overall and by organ complications and cutaneous disease subset*

	Overall cohort (n = 1,325)	Clinically significant pulmonary fibrosis cohort (n = 654)	dcSSc skin cohort (n = 581)
Follow-up, mean ± SD years	12.3 ± 5.6	11.2 ± 5.8	12.2 ± 7.9
Age at onset, mean ± SD years	46.8 ± 13.6	47.8 ± 13.1	44.0 ± 13.8
Male, no. (%)	222 (16.8)	112 (17.1)	131 (22.6)
dcSSc subset, no. (%)	476 (35.9)	329 (50.3)	581 (100)
Overlap syndromes, no. (%)	262 (19.8)	114 (17.4)	102 (17.6)
Autoantibody subset, no. (%)			
Anticentromere	391 (29.5)	139 (21.3)	17 (2.9)
Anti-topoisomerase I	287 (21.7)	157 (24.0)	178 (30.6)
Anti-RNA polymerase	149 (11.3)	113 (17.3)	161 (27.7)
Anti-U3 RNP	56 (4.2)	34 (5.2)	39 (6.7)
Anti-PM/Scl	56 (4.2)	27 (4.1)	27 (4.7)
Other†	214 (16.2)	95 (14.5)	79 (13.6)
ANA+ENA-	196 (14.8)	103 (15.8)	95 (16.4)
ANA-	58 (4.4)	28 (4.3)	24 (4.1)
Organ complications, no. (%)			
Pulmonary fibrosis, any	575 (43.4)‡	326 (49.9)	316 (54.4)§
Clinically significant pulmonary fibrosis	520 (39.3)‡	308 (47.1)	-
Pulmonary hypertension (groups 1 and 3)¶	172 (13.0)	84 (12.8)	54 (9.3)
Pulmonary arterial hypertension	134 (10.1)	64 (9.8)	34 (5.9)
Cardiac scleroderma	63 (4.8)	41 (6.3)	43 (7.4)
Scleroderma renal crisis	94 (7.1)	63 (9.6)	84 (14.5)
Death, no. (%)	441 (33.3)	257 (39.3)	189 (32.5)

* dcSSc = diffuse cutaneous systemic sclerosis; ENA- = anti-extractable nuclear antigen negative.

† Includes anti-U1 RNP, anti-Th/To, anti-SL, anti-Ku, anti-Jo-1, anti-Ro, anti-La, anti-XR, anti-PL-7, anti-heterogeneous nuclear RNP, and anti-Sm, as well as patients who were antinuclear antibody negative (ANA-).

‡ Missing pulmonary fibrosis data for 10 (0.8%) of the patients.

§ Missing pulmonary fibrosis data for 11 (1.9%) of the patients.

¶ Group 1 comprised patients with connective tissue disease-associated pulmonary arterial hypertension, and group 3 comprised those with interstitial lung disease-associated pulmonary hypertension.

associations between autoantibody specificities and changes in the MRSS over time.

RESULTS

Cohort description. Of the 1,354 SSc patients who met the inclusion criteria, 29 did not have information on antibody specificity and were therefore excluded from the analysis. The demographic and clinical characteristics of the remaining 1,325 subjects are summarized in Table 1. For 10 patients (0.8%), information on the presence of PF was missing. In 115 patients (8.7%), we found multiple autoantibody specificities. Nine patients had dual SSc hallmark antibodies. Three patients were ACA+ and anti-topo I+, 2 were ACA+ and anti-U3 RNP+, and 1 was ACA+ and anti-PM/Scl+; all of these patients were classified into their respective non-ACA antibody group, since,

in all cases, ACAs were not detected on the first serology testing. In 2 patients, the antibody specificity had switched from anti-topo I to anti-RNAP at a later stage of their disease; these patients were classified as anti-topo I+. One patient was anti-RNAP+ and anti-PM/Scl+, but the anti-PM/Scl positivity was very weak, and therefore the patient was classified as anti-RNAP+.

Autoantibodies and survival. Survival of patients in the full SSc cohort at 5, 10, 15, and 20 years from disease onset was 91.8%, 82.2%, 67.5%, and 53.8%, respectively. Survival at these time points was much lower among patients with dcSSc (84.4%, 72%, 53.9%, and 39.7%, respectively) compared to patients with lcSSc (95.8%, 87.7%, 74.6%, and 61%, respectively; $P < 0.001$). The patients who carried ACAs had the highest survival, while the group of patients who were ANA+ENA- had the lowest survival (Table 2

Table 2. Survival estimates and estimates of cumulative incidence of organ complications within each antibody subgroup of patients with systemic sclerosis at different time points after disease onset*

Subgroup, time point	Clinically significant pulmonary fibrosis		Pulmonary hypertension		Cardiac scleroderma		Scleroderma renal crisis		Survival, KM
	1 – KM	CIF	1 – KM	CIF	1 – KM	CIF	1 – KM	CIF	
Anticentromere									
5 years	7.5	7.5	5.0	5.0	1.3	1.3	0.8	0.8	96.1
10 years	8.4	8.3	10.2	10.0	1.6	1.6	0.8	0.8	89.3
15 years	8.4	8.3	14.6	14.0	2.4	2.3	0.8	0.8	78.3
20 years	8.4	8.3	22.4	20.9	5.3	4.8	0.8	0.8	64.7
Anti-topoisomerase I									
5 years	80.3	79.3	1.1	1.1	3.6	3.6	4.7	4.6	91.0
10 years	85.0	83.2	6.1	5.5	6.2	6.0	5.6	5.5	80.3
15 years	87.0	84.7	11.4	9.8	10.1	9.0	6.4	6.1	60.1
20 years	87.0	84.7	13.3	11.1	11.5	10.0	6.4	6.1	46.5
Anti-RNA polymerase									
5 years	34.1	33.4	4.6	4.4	1.4	1.4	23.3	23.3	88.0
10 years	44.0	42.1	10.0	9.4	2.3	2.2	25.1	24.9	74.6
15 years	46.9	44.5	16.0	14.6	2.3	2.2	29.0	28.1	62.6
20 years	46.9	44.5	26.8	23.3	2.3	2.2	29.0	28.1	47.1
Anti-U3 RNP									
5 years	19.2	17.9	6.0	5.7	9.2	9.1	11.3	11.0	85.4
10 years	19.2	17.9	19.9	17.7	13.8	13.2	11.3	11.0	76.0
15 years	24.3	21.5	38.6	33.8	13.8	13.2	11.3	11.0	66.0
20 years	24.3	21.5	38.6	33.8	13.8	13.2	11.3	11.0	60.5
Anti-PM/Scl									
5 years	40.7	40.7	2.0	2.0	1.9	1.9	3.8	3.8	98.2
10 years	40.7	40.7	4.1	4.0	1.9	1.9	5.8	5.8	96.1
15 years	50.6	49.8	11.1	10.1	1.9	1.9	5.8	5.8	68.5
20 years	50.6	49.8	11.1	10.1	1.9	1.9	5.8	5.8	58.8
ANA+ENA-									
5 years	56.8	53.4	4.7	4.3	3.9	3.7	10.6	10.4	82.8
10 years	56.8	53.4	7.6	6.8	4.7	4.3	10.6	10.4	69.7
15 years	56.8	53.4	20.3	16.3	6.0	5.2	10.6	10.4	53.2
20 years	56.8	53.4	27.0	20.8	6.0	5.2	10.6	10.4	39.0
Other antibodies†									
5 years	51.5	51.5	4.7	4.6	3.7	3.6	3.5	3.5	95.9
10 years	55.8	55.6	10.7	10.2	4.3	4.2	4.1	4.1	86.0
15 years	57.8	57.4	18.8	17.5	5.1	4.9	4.1	4.1	73.7
20 years	57.8	57.4	27.6	24.7	5.1	4.9	4.1	4.1	56.0

* Values are the percentage of patients. KM = Kaplan-Meier; CIF = cumulative incidence function; ENA- = anti-extractable nuclear antigen negative.

† Includes anti-U1 RNP, anti-Th/To, anti-SL, anti-Ku, anti-Jo-1, anti-Ro, anti-La, anti-XR, anti-PL-7, anti-heterogeneous nuclear RNP, and anti-Sm, as well as patients who were antinuclear antibody negative (ANA-).

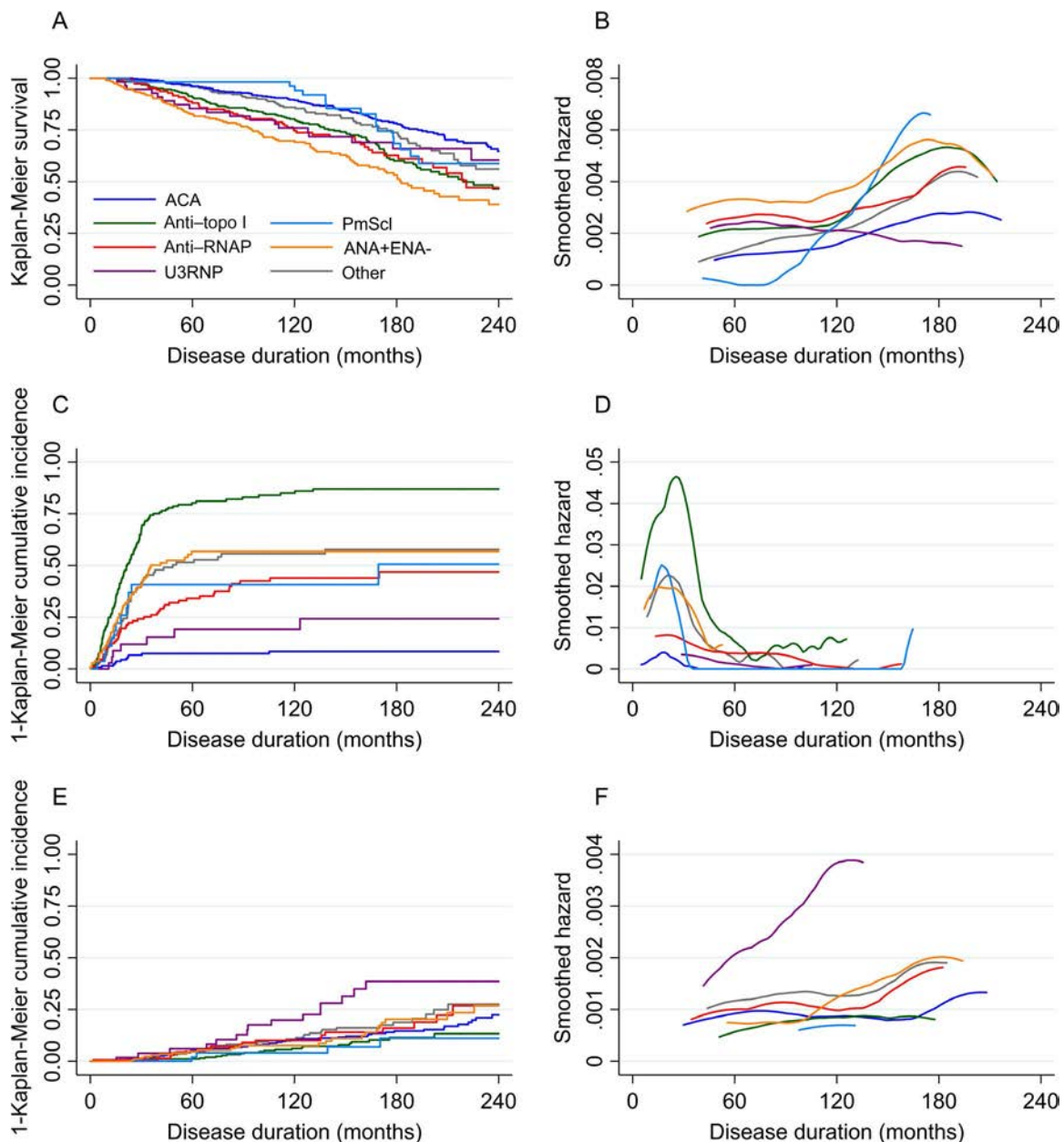


Figure 1. Associations of autoantibodies with survival estimates and incidence of organ complications over time in patients with systemic sclerosis. **A** and **B**, Kaplan-Meier (KM) survival estimates (**A**) and smoothed hazards of death over time (**B**) in subgroups by antibody specificity. **C** and **E**, 1 – KM estimates of cumulative incidence of clinically significant pulmonary fibrosis (**C**) and pulmonary hypertension (**E**) in subgroups by antibody specificity. **D** and **F**, Smoothed hazards of clinically significant pulmonary fibrosis (**D**) and pulmonary hypertension (**F**) over time in subgroups by antibody specificity. ACA = anticentromere antibodies; anti-topo I = anti-topoisomerase I antibodies; anti-RNAP = anti-RNA polymerase antibodies; ANA+ = antinuclear antibody positive; ENA– = anti-extractable nuclear antigen negative. Information on the numbers at risk at the different time points is available in Supplementary Figures 4–6 (see the *Arthritis & Rheumatology* web site at <http://onlinelibrary.wiley.com/doi/10.1002/art.41153/abstract>).

and Figure 1A). The hazard of death appeared to gradually increase over time for the majority of antibody groups, although among anti-U3 RNP+ patients, this declined over time (Figure 1B).

Thus, we fitted an extended Cox proportional hazards model to allow for time-varying effects of the antibodies (Table 3). The data in this model showed that even though anti-U3 RNP+ patients had a higher hazard of death compared to the other

antibody groups in the earlier years of disease, long-term survival was better and the hazard of death was lower in the later years of disease. Conversely, anti-PM/Scl+ subjects appeared to be at a very low risk of death in the first 10 years of disease, whereas the risk of death increased significantly and became higher than in the other antibody groups in the second decade of the disease.

Table 3. Cox proportional hazards models for associations of outcomes with each autoantibody subgroup*

Outcome, autoantibody subgroup	HR	95% CI	P
Clinically significant pulmonary fibrosis			
Anti-topo I	Referent		
ACA	0.048	(0.026–0.089)	<0.001
Anti-RNA polymerase	0.303	(0.216–0.425)	<0.001
Anti-U3 RNP	0.141	(0.066–0.301)	<0.001
Anti-PM/Scl	0.350	(0.193–0.633)	0.001
ANA+ENA–	0.487	(0.354–0.669)	<0.001
Other	0.458	(0.328–0.639)	<0.001
Pulmonary hypertension			
Anti-U3 RNP	Referent		
ACA	0.420	(0.237–0.742)	0.003
Anti-topo I	0.271	(0.141–0.523)	<0.001
Anti-RNA polymerase	0.499	(0.254–0.983)	0.044
Anti-PM/Scl	0.221	(0.073–0.665)	0.007
ANA+ENA–	0.473	(0.247–0.906)	0.024
Other	0.562	(0.305–1.036)	0.065
Cardiac scleroderma			
Anti-U3 RNP	Referent		
ACA	0.171	(0.069–0.426)	<0.001
Anti-topo I	0.535	(0.238–1.202)	0.130
Anti-RNA polymerase	0.149	(0.040–0.562)	0.005
Anti-PM/Scl	0.114	(0.014–0.915)	0.041
ANA+ENA–	0.351	(0.135–0.911)	0.031
Other	0.294	(0.114–0.763)	0.012
Scleroderma renal crisis			
Anti-RNA polymerase	Referent		
ACA	0.025	(0.008–0.080)	<0.001
Anti-topo I	0.187	(0.104–0.335)	<0.001
Anti-U3 RNP	0.367	(0.155–0.869)	0.023
Anti-PM/Scl	0.178	(0.055–0.578)	0.004
ANA+ENA–	0.363	(0.211–0.624)	<0.001
Other	0.132	(0.062–0.283)	<0.001
Death			
Anti-U3 RNP	Referent		
ACA	0.172	(0.065–0.454)	<0.001
Anti-topo I	0.424	(0.166–1.085)	0.074
Anti-RNA polymerase	0.609	(0.223–1.666)	0.334
Anti-PM/Scl	0.078	(0.016–0.382)	0.002
ANA+ENA–	0.909	(0.358–2.306)	0.840
Other	0.206	(0.073–0.580)	0.003
Antibody × time interaction†			
ACA × time	1.013	(1.004–1.022)	0.005
Anti-topo I × time	1.010	(1.001–1.019)	0.023
Anti-RNA polymerase × time	1.007	(0.998–1.017)	0.136
Anti-PM/Scl × time	1.020	(1.008–1.032)	0.001
ANA+ENA– × time	1.007	(0.998–1.015)	0.148
Other antibodies × time	1.014	(1.004–1.023)	0.004

* The group with the highest associated hazard has been used as the referent in the calculation of each hazard ratio (HR). 95% CI = 95% confidence interval; anti-topo I = anti-topoisomerase I; ACA = anticentromere antibody; ANA+ = antinuclear antibody positive; ENA– = anti-extractable nuclear antigen negative.

† Antibody interaction with time since disease onset.

Associations between autoantibodies and cumulative incidence and timing of organ complications. *Clinically significant pulmonary fibrosis.* A subgroup of 654 patients who had PFT results available within the first 3 years after disease onset was included in the analysis of incidence of clinically significant PF (Table 1). Among these patients, 308 (47.1%) developed clinically significant PF, with the majority developing

it within the first 5 years from disease onset (1 – KM estimate 44.8%) and with a much lower incidence rate thereafter (48.3% at year 10 and 50.3% at year 15, and no additional cases after 15 years). Cutaneous subset was strongly associated with the development of clinically significant PF, with 5-year, 10-year, and 15-year cumulative incidence rates of clinically significant PF of 37.4%, 39.3%, and 41.2%, respectively, in patients with lcSSc

compared to 52.5%, 58.0%, and 60.1%, respectively, in patients with dcSSc ($P < 0.001$).

Analysis within the autoantibody subgroups confirmed the very low risk of clinically significant PF among ACA+ subjects, and the remarkably high risk among anti-topo I+ patients, the majority of whom ultimately developed this organ complication over time (Table 2). Rates of clinically significant PF among anti-RNAP+ patients were higher than those in ACA+ patients, but still much lower than those seen in anti-topo I+ patients. Even after 20 years of follow-up, the cumulative incidence of clinically significant PF among anti-RNAP+ patients was about one-half that seen in anti-topo I+ patients (Table 2 and Figure 1C).

Comparison between the 1 – KM estimate and the CIF estimate accounting for death as a competing risk revealed some small differences. The 1 – KM calculation overestimated the incidence of clinically significant PF in the later stages of the disease by ~2% among anti-topo I+ and anti-RNAP+ patients, and by 3% among anti-U3 RNP+ and ANA+ENA– patients (Table 2).

The hazard of clinically significant PF development in the overall SSc cohort peaked in the second year from disease onset, and this observation was replicated in the antibody subgroup analysis (Figure 1D). Among anti-topo I+ patients, the hazard of clinically significant PF was 30% in year 1 and 45.7% in year 2, peaked at 57.4% in year 3, and went down sharply thereafter. Although it was much lower among ACA+ patients, the hazard of clinically significant PF in this antibody subgroup was highest in the second year from disease onset (1.5%, 5.5%, and 0.8% in years 1, 2, and 3, respectively). In anti-RNAP+ patients, the hazard of clinically significant PF also peaked in year 2 (12.3%, 13.1%, and 5% at years 1, 2, and 3, respectively) and declined thereafter. For the remaining antibody subgroups, the hazard of developing clinically significant PF at 1, 2, and 3 years from the time of SSc onset was 3%, 10%, and 3.9%, respectively, in anti-U3 RNP+ patients, 11.8%, 34.2%, and 6.3%, respectively, in anti-PM/Scl+ patients, 17.1%, 26%, and 25.9%, respectively, in ANA+ENA– patients, and 15%, 27.7%, and 17.8%, respectively, in the combined group of patients with other antibodies. Cox regression analyses confirmed that, compared to anti-topo I antibodies, the presence of other antibodies lowered the hazard of clinically significant PF, and the presence of ACAs was associated with the greatest reduction in the hazard of clinically significant PF (Table 3).

Pulmonary hypertension. Cumulative incidence of PH in the full SSc cohort at 5, 10, 15, and 20 years from disease onset was 4%, 9.2%, 16.2%, and 22.6%, respectively. Incidence of PH at 5, 10, 15, and 20 years was nearly identical between the 2 cutaneous subsets (4.1%, 9.5%, 16.5%, and 22.7%, respectively, in patients with lcSSc versus 3.7%, 8.5%, 15.6%, and 22.3%, respectively, in patients with dcSSc; $P = 0.981$).

Autoantibody specificity was strongly associated with the risk of PH, and the highest incidence was observed among anti-U3 RNP+ patients, while there was very little difference among

patients with other antibodies (Table 2 and Figure 1E). Death as a competing risk had an effect on the estimates of PH incidence in most antibody subgroups, with the greatest overestimation seen among anti-U3 RNP+ and ANA+ENA– subjects, in whom the incidence of PH at 15 and 20 years from disease onset was overestimated by ~5% with the 1 – KM estimate compared to the CIF estimate. The hazard of PH was very low in the first years from disease onset, and for most patients, it varied between 1% and 2% per year from year 3 onward, with some gradual increase during the later stages of disease, generally after 10 years (Figure 1F). Anti-topo I+ and anti-PM/Scl+ patients had the lowest hazard of PH development, while the hazard of PH among ACA+ patients was similar to the mean value in the cohort overall (Table 3). Equivalent results were obtained when the data were reanalyzed with only pulmonary arterial hypertension (group 1 PH) included as an end point (see Supplementary Patients and Methods [Organ Complication Associations section], Supplementary Figure 1, and Supplementary Tables 3 and 4 available on the *Arthritis & Rheumatology* web site at <http://onlinelibrary.wiley.com/doi/10.1002/art.41153/abstract>).

Cardiac scleroderma. Cardiac involvement was a rare complication, affecting fewer than 5% of the cohort, with 1 – KM estimates of cumulative incidence of cardiac SSc at 5, 10, 15, and 20 years of 2.9%, 4.1%, 5.4%, and 6.8%, respectively. Patients with dcSSc had a significantly higher incidence of cardiac SSc at 5, 10, 15, and 20 years compared to patients with lcSSc (1 – KM estimate 6.2%, 8.6%, 10%, and 10%, respectively, among patients with dcSSc versus 1.2%, 1.8%, 3.1%, and 4.9%, respectively, among patients with lcSSc; $P < 0.001$). Autoantibodies were significantly associated with cardiac SSc development, and the 2 with the strongest positive association were anti-U3 RNP and anti-topo I (Table 2 and Supplementary Figure 2, available on the *Arthritis & Rheumatology* web site at <http://onlinelibrary.wiley.com/doi/10.1002/art.41153/abstract>). Comparison between the 1 – KM and CIF estimates of cardiac SSc development did not reveal any substantial differences (Table 2). Except for anti-topo I antibodies, all other antibodies were associated with a significantly reduced hazard of cardiac SSc development as compared to anti-U3 RNP+ patients (Table 3). There was no clear association between disease duration and cardiac SSc development, and hazards fluctuated over time, with cardiac complications developing both in early disease and in late disease.

Scleroderma renal crisis. More than 90% of the patients with SRC developed this complication within 5 years from SSc onset (1 – KM estimate at 5, 10, and 15 years 6.5%, 7.1%, and 7.6%, respectively, with no cases after 14 years), and 9 of 94 patients had SRC at presentation. SRC was much more common among patients with dcSSc (1 – KM estimate at 5, 10, and 15 years 14.1%, 15.5%, and 17.4%, respectively) than among patients with lcSSc (1 – KM estimate 2.4% at 5 years and 2.5% at 10 years, with no SRC cases after year 7; $P < 0.001$).

Autoantibodies demonstrated significant associations with SRC development, with the highest hazard seen in anti-RNAP+ subjects and the lowest in ACA+ subjects (Table 3 and Supplementary Figure 3, available on the *Arthritis & Rheumatology* web site at <http://onlinelibrary.wiley.com/doi/10.1002/art.41153/>

abstract). As this was a very early complication, the estimation of cumulative incidence of SRC was not affected by death as a competing risk (Table 2). For all antibody groups, the hazards of SRC were highest in the first year of disease, except in the anti-PM/Scl+ group, the majority of whom developed SRC in years 5 and 6.

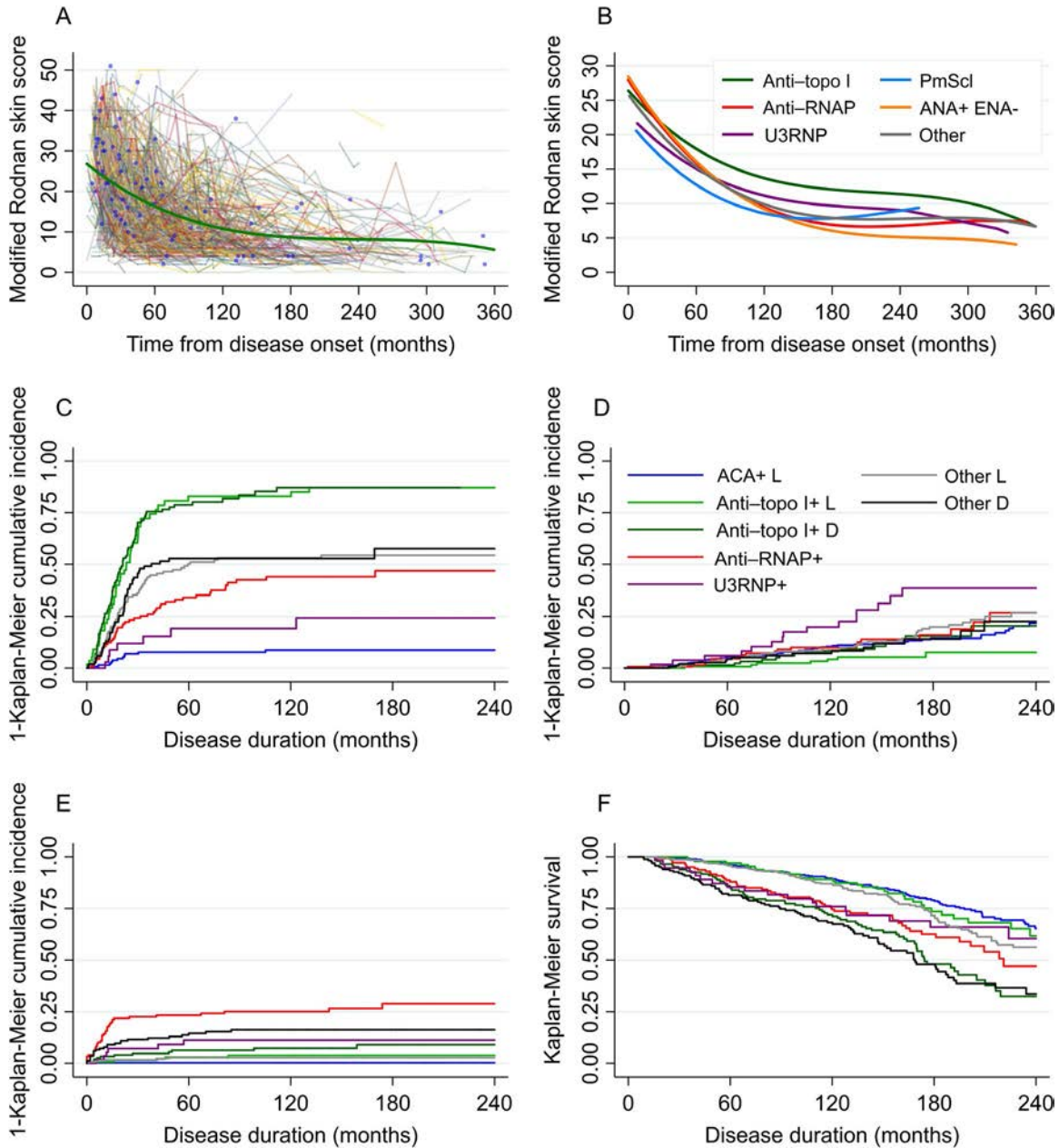


Figure 2. A and B, Modified Rodnan skin thickness score changes over time in the entire cohort of patients with systemic sclerosis (SSc) (A) and in subgroups by autoantibody specificity (B). In A, the thick line represents the model-predicted average skin score; the thin lines and dots represent individual patient skin scores from patients with multiple and single skin score assessments, respectively. C–F, Kaplan-Meier (KM) survival estimates (F) and 1 – KM estimates of cumulative incidence of pulmonary fibrosis (C), pulmonary hypertension (D), and scleroderma renal crisis (E) in the 7 new classification groups. The groups are defined in the key in D. The group of “Other” antibodies includes anti-U1 RNP, anti-Th/To, anti-SL, anti-Ku, anti-Jo-1, anti-Ro, anti-La, anti-XR, anti-PL-7, anti-heterogeneous nuclear RNP, and anti-Sm, as well as patients who were antinuclear antibody negative (ANA–). Anti-topo I = anti-topoisomerase I antibodies; anti-RNAP = anti-RNA polymerase antibodies; ENA– = anti-extractable nuclear antigen negative; ACA+ = anticentromere antibody positive; L = limited cutaneous SSc; D = diffuse cutaneous SSc. Information on the numbers at risk at the different time points is available in Supplementary Figures 7–10 (see the *Arthritis & Rheumatology* web site at <http://onlinelibrary.wiley.com/doi/10.1002/art.41153/abstract>).

Autoantibodies and skin changes over time. The cohort included in the analysis of skin score changes over time consisted of 581 patients with dcSSc (Table 1). At least 3 MRSS assessments were available from 413 subjects (71.1%), 2 were available from 88 subjects (15.2%), and 1 was available from 80 subjects (13.8%). The first MRSS assessment was performed within 3 years from disease onset for 383 subjects (65.9%).

The mean ± SD MRSS at 12 months from disease onset was 24.2 ± 9.2 (95% confidence interval 23.3–25.2), and this gradually declined, with the scores following a nonlinear trajectory (MRSS = 24.2 – 2.5 × years + 0.13 × years² – 0.002 × years³; *P* < 0.001 for all parameters). Thus, improvement in skin thickness scores was greater in earlier disease, with a mean drop in the MRSS of 2.3 between years 1 and 2, 2.1 between years 2 and 3, 1.9 between years 3 and 4, 1.6 between years 4 and 5, and 0.8 between years 9 and 10 (Figure 2A and Supplementary Table 6, available on the *Arthritis & Rheumatology* web site at <http://onlinelibrary.wiley.com/doi/10.1002/art.41153/abstract>). There was a moderately strong, negative association between the MRSS at 1 year and drop in MRSS

over time (correlation coefficient –0.6), suggesting that higher initial skin thickness scores are associated with greater subsequent improvement.

Autoantibodies showed a significant association both with the baseline MRSS and with the change in MRSS over time. At 1 year from disease onset, the highest mean MRSS was observed in ANA+ENA– patients (mean MRSS 25.5) and anti-RNAP+ patients (mean MRSS 25). Compared to ANA+ENA– patients, the mean MRSS was 24.3 in anti-topo I+ patients (*P* = 0.421), 21 in anti-U3 RNP+ patients (*P* = 0.041), 19.6 in anti-PM/Scl+ patients (*P* = 0.022), and 23.3 in patients with other antibodies (*P* = 0.216). Over subsequent years, the greatest improvement was observed in ANA+ENA– and anti-RNAP+ patients, in whom the mean drop in the MRSS between year 1 and year 5 was 9.4 units and 9.1 units, respectively. The mean drop in the MRSS was 6.4 in anti-topo I+ patients (*P* = 0.004 for anti-topo I+ × time interaction versus ANA+ENA– × time interaction), compared to a mean drop in MRSS of 6 in anti-U3 RNP+ patients (*P* = 0.029), 6.9 in anti-PM/Scl+ patients (*P* = 0.206), and 7.9 in patients with other antibodies (*P* = 0.265). This followed a nonlinear trajectory, with a greater reduction in the MRSS in earlier years (Figure 2B and Supplementary Table 8,

Table 4. Cumulative incidence function estimates of organ complications and Kaplan-Meier estimates of all-cause mortality in the final 7 classification groups of patients with SSc*

Outcome, time point	Classification group						
	ACA+ lcSSc	Anti-topo I+ lcSSc	Anti-topo I+ dcSSc	Anti-RNAP+	Anti-U3 RNP+	Other antibodies lcSSc	Other antibodies dcSSc
Clinically significant PF							
5 years	7.7	82.2	77.7	33.4	17.9	49.9	50.2
10 years	8.5	82.2	84.0	42.1	17.9	52.8	50.2
15 years	8.5	86.1	84.0	44.5	21.5	53.9	53.8
20 years	8.5	86.1	–	44.5	21.5	53.9	53.8
Pulmonary hypertension							
5 years	5.1	0.8	1.4	4.4	5.7	4.2	3.9
10 years	10.3	4.1	7.0	9.4	17.7	8.6	6.1
15 years	13.9	6.9	12.5	14.6	33.8	18.5	11.1
20 years	20.4	6.9	15.3	23.3	33.8	24.3	16.4
Cardiac scleroderma							
5 years	1.4	0.0	7.0	1.4	9.1	1.0	7.6
10 years	1.7	1.6	10.1	2.2	13.2	1.4	8.4
15 years	2.4	5.0	12.9	2.2	13.2	2.4	8.4
20 years	4.9	7.0	12.9	2.2	13.2	2.4	8.4
Scleroderma renal crisis							
5 years	0.3	3.0	6.2	23.3	11.0	2.7	14.1
10 years	0.3	3.8	7.0	24.9	11.0	2.7	15.6
15 years	0.3	3.8	8.3	28.1	11.0	2.7	15.6
20 years	0.3	3.8	8.3	28.1	11.0	2.7	15.6
Mortality							
5 years	4.1	3.0	14.6	12.0	14.6	4.2	18.5
10 years	10.7	10.9	28.0	25.4	24.0	12.9	31.7
15 years	20.9	26.4	51.9	37.4	34.0	28.4	52.1
20 years	34.7	38.2	67.6	52.9	39.5	43.8	66.4

* Cumulative incidence function estimates were calculated for each outcome accounting for death as a competing risk. Values are the percentage of patients. SSc = systemic sclerosis; ACA+ = anticentromere antibody positive; lcSSc = limited cutaneous SSc; anti-topo I+ = anti-topoisomerase I positive; dcSSc = diffuse cutaneous SSc; anti-RNAP+ = anti-RNA polymerase positive; PF = pulmonary fibrosis.

available on the *Arthritis & Rheumatology* web site at <http://online.library.wiley.com/doi/10.1002/art.41153/abstract>).

Proposed classification of SSc using autoantibodies and skin subset as criteria. We calculated KM estimates of all-cause mortality and 1 – KM estimates for the incidence of organ complications in the original 14 groups of patients classified by autoantibody specificity and cutaneous disease subset (see Supplementary Table 10, available on the *Arthritis & Rheumatology* web site at <http://onlinelibrary.wiley.com/doi/10.1002/art.41153/abstract>). Merging all subgroups that had similar rankings within different end points resulted in 7 final classification groups. Five of those groups included patients with SSc-specific antibodies, while the last 2 groups had all remaining patients with other antibodies, including ANA+ENA– and ANA–subjects (Table 4 and Figures 2C–F).

ACA+ lcSSc group. The group of ACA+ patients with lcSSc was the largest ($n = 374$, 28.2% of the cohort). These patients had the highest survival, lowest incidence of clinically significant PF and SRC, very low incidence of cardiac SSc, and an incidence of PH similar to the mean value in the total cohort.

Anti-topo I+ lcSSc group. The group of anti-topo I+ patients with lcSSc consisted of 138 subjects (10.4% of the cohort). Although the incidence of clinically significant PF among these patients was extremely high, other complications were rare, and they had the lowest incidence of PH and second highest survival of all 7 groups.

Anti-topo I+ dcSSc group. The subjects in the anti-topo I+ dcSSc group ($n = 149$, 11.3% of the cohort) had the worst prognosis, since they had the lowest survival and the second highest incidence of cardiac SSc of all groups. The incidence of clinically significant PF was almost identical to that among anti-topo I+ lcSSc patients.

Anti-RNAP+ group. As expected, anti-RNAP+ SSc patients ($n = 147$, 11.1% of the cohort) had the highest incidence of SRC. However, they had the lowest incidence of cardiac scleroderma, while the incidence of other organ complications and survival were similar to the mean values in the total cohort.

Anti-U3 RNP+ group. Only 4.2% of the cohort ($n = 56$) was included in the group of anti-U3 RNP+ SSc patients. Although long-term survival among these subjects was higher than the mean value in the total cohort, they had the highest incidence of PH and cardiac SSc.

Other antibodies lcSSc group. The group of lcSSc patients with other antibodies ($n = 295$, 22.3% of the cohort) had a low overall risk of SRC and cardiac SSc, while the frequencies of other outcomes were similar to the mean values in the total cohort.

Other antibodies dcSSc group. Conversely, the group of dcSSc patients with other antibodies ($n = 166$, 12.5% of the cohort) had a poor prognosis, with the second lowest survival and above average rates of clinically significant PF, cardiac scleroderma, and SRC.

DISCUSSION

Herein we have described a large, single-center cohort of patients with SSc, focusing on the effect of autoantibodies on the timing of organ complication development and disease prognosis. Our observations confirm that double SSc-specific autoantibody positivity is extremely rare (<1% of the cohort). These findings highlight the importance of careful and accurate antibody analysis to inform patient monitoring and prognosis.

Although it is often suggested that ACA positivity is strongly predictive of the development of PH, there is in fact very little evidence in the literature to support this, and studies either have been based on enriched cohorts or have not used robust definitions for PH (6,32–34). We found no evidence to indicate an association between ACAs and PH. The incidence of PH in the ACA+ group was similar to the mean value in the SSc cohort overall. We confirmed the strong association between ACAs and low incidence rates of other major organ-based complications and mortality, suggesting that ACA positivity in SSc patients is a good prognostic sign.

Similarly, good outcomes were observed in anti-PM/Scl+ subjects, who overall demonstrated a low incidence of PH, SRC, and cardiac SSc, although approximately one-half of these patients did develop clinically significant PF within the first 15 years of disease (35). Mortality rates, although low in the first 10 years of disease, appeared to increase faster than among the other antibody groups in the second decade of disease, possibly being related to the progression of clinically significant PF or to the development of malignancies (36).

As expected, anti-topo I antibody positivity was associated with a substantial risk of clinically significant PF, with no difference in incidence between the cutaneous subsets. Despite this finding, the long-term prognosis was strikingly different between lcSSc and dcSSc patients with this antibody, with much better survival and low risk of other organ complications among lcSSc patients (29).

Anti-U3 RNP+ patients had the highest incidence of both PH and cardiac scleroderma, which is consistent with the findings in previously published studies (4,5). This antibody group also had very high mortality rates in the early stages of the disease, although long-term survival was among the highest, suggesting that patients with this antibody are at much higher risk in the first 10 years of disease.

Our analysis clearly demonstrated that there is no difference in the timing of clinically significant PF development between patients with different antibodies. In all groups, the hazards peaked within the first 3 years and rapidly declined thereafter. Hazards for SRC peaked even earlier, within the first year of disease. Conversely, the hazard of PH was very low early on and gradually increased, especially in the second decade. For all antibody subgroups, except anti-U3 RNP, the hazard of death was low initially and gradually increased over time. In anti-U3 RNP+ patients, the

hazard of death showed an early peak, suggesting that patients with this antibody would require more active management early in the disease course.

Skin involvement is an important aspect of SSc morbidity, and a large proportion of clinical trials have utilized the MRSS as a primary end point. Spontaneous improvement in the MRSS occurs in the majority of dcSSc patients, and we demonstrated that, at a group level, the MRSS declines over time. The greatest improvement is early in the disease, while during later stages, there is little change. Similar to previous studies, we found a negative association between the change in MRSS and both baseline MRSS and disease duration (21). We also confirmed that skin change was significantly associated with autoantibodies, with higher skin scores in early disease observed in anti-RNAP+ and ANA+ENA- patients, while at the same time, those groups experienced greater improvement and had lower mean MRSS scores compared to patients with the other antibodies in the later stages of disease. Antibody specificities only partly explained the changes in MRSS, with considerable residual variance even after accounting for antibodies and their interaction with time (see Supplementary Tables 6 and 8 [<http://onlinelibrary.wiley.com/doi/10.1002/art.41153/abstract>]).

Our study had several important limitations. There was a relatively small number of patients who had at least 1 MRSS assessment within the first 12 months of disease, which could explain why an initial increase in the MRSS was not observed in the overall cohort and, indeed, only a very small number of patients had deterioration in the MRSS. Nevertheless, a sensitivity analysis demonstrated that the results remained similar when only subjects with the first MRSS <3 years after disease onset were analyzed (see Supplementary Tables 7 and 9 and Supplementary Figures 11 and 12 [<http://onlinelibrary.wiley.com/doi/10.1002/art.41153/abstract>]).

We could not use HRCT scans to assess the severity of PF as the imaging for a number of patients was performed prior to the introduction of electronic imaging storage or was done in another hospital. However, since the severity of PF was determined on the basis of PFTs, even when HRCT had not been done, the absence of clinically significant PF could be reasonably assumed, based on preserved and stable lung function. When HRCT information was not available to confirm the presence of PF, and the PFT results showed abnormalities, we considered this to be missing data. As a result, it is likely that we underestimated the overall presence of PF (any degree) among the study subjects, but the estimate of clinically significant PF incidence should be comparatively accurate.

To avoid immortal time bias, we included an incident cohort with disease onset during a fixed time window. In addition, the tendency for severe cases to be referred early means that it is unlikely that our cohort was biased toward patients with milder disease, who would survive long enough to be seen in a specialist center.

Some of the autoantibodies (anti-U3 RNP, anti-Th/To) were defined on the basis of indirect immunofluorescence (IIF) analysis with no confirmatory test, and SSc-specific antibody testing may not be available in some hospitals, where physicians may only receive a result reporting a nucleolar pattern on IIF. For that reason we repeated the analysis of associations between autoantibodies and end points according to the subclassifications ACA+, anti-topo I+, anti-RNAP+, ANA+ with nucleolar pattern, and other (see Supplementary Table 5 [<http://onlinelibrary.wiley.com/doi/10.1002/art.41153/abstract>]).

By combining autoantibody specificity and extent of skin involvement, we propose a simple classification for SSc in which patients are classified into 1 of 7 groups. This enables more precise risk stratification of patients, compared to the simple division into dcSSc and lcSSc, and reflects widespread opinion that the current subset classification fails to take account of the variability of organ-based complications (37). Techniques to test for the more common and SSc-specific antibodies are available to most rheumatologists, and cutaneous subset is easy to determine, which makes this classification easy to apply in everyday clinical practice. Patients could be classified at their initial visit and would remain in the same group, even if other characteristics of the disease subsequently change. Once validated in other cohorts, this classification could be used to inform prognosis and disease monitoring in routine practice and for cohort enrichment in event-driven clinical trials.

AUTHOR CONTRIBUTIONS

All authors were involved in drafting the article or revising it critically for important intellectual content, and all authors approved the final version to be published. Dr. Denton had full access to all of the data in the study and takes responsibility for the integrity of the data and the accuracy of the data analysis.

Study conception and design. Nihtyanova, Sari, Denton.

Acquisition of data. Nihtyanova, Sari, Harvey, Leslie, Derrett-Smith, Fonseca, Ong, Denton.


Analysis and interpretation of data. Nihtyanova, Denton.

REFERENCES

1. Kuwana M. Circulating anti-nuclear antibodies in systemic sclerosis: utility in diagnosis and disease subsetting. *J Nippon Med Sch* 2017;84:56–63.
2. Mecoli CA, Casciola-Rosen L. An update on autoantibodies in scleroderma. *Curr Opin Rheumatol* 2018;30:548–53.
3. Nihtyanova SI, Denton CP. Autoantibodies as predictive tools in systemic sclerosis. *Nat Rev Rheumatol* 2010;6:112–6.
4. Tormey VJ, Bunn CC, Denton CP, Black CM. Anti-fibrillarin antibodies in systemic sclerosis. *Rheumatology (Oxford)* 2001;40:1157–62.
5. Aggarwal R, Lucas M, Fertig N, Oddis CV, Medsger TA Jr. Anti-U3 RNP autoantibodies in systemic sclerosis. *Arthritis Rheum* 2009;60:1112–8.
6. Mitri GM, Lucas M, Fertig N, Steen VD, Medsger TA Jr. A comparison between anti-Th/To- and anticentromere antibody-positive systemic sclerosis patients with limited cutaneous involvement. *Arthritis Rheum* 2003;48:203–9.

7. Fertig N, Domsic RT, Rodriguez-Reyna T, Kuwana M, Lucas M, Medsger TA Jr, et al. Anti-U11/U12 RNP antibodies in systemic sclerosis: a new serologic marker associated with pulmonary fibrosis. *Arthritis Rheum* 2009;61:958–65.
8. McMahan ZH, Domsic RT, Zhu L, Medsger TA, Casciola-Rosen L, Shah AA. Anti-RNPC (U11/U12) antibodies in systemic sclerosis are associated with moderate-to-severe gastrointestinal dysmotility. *Arthritis Care Res (Hoboken)* 2019;71:1164–70.
9. D'Acoust J, Hudson M, Tatibouet S, Wick J, the Canadian Scleroderma Research Group, Mahler M, et al. Clinical and serologic correlates of anti-PM/Scl antibodies in systemic sclerosis: a multicenter study of 763 patients. *Arthritis Rheumatol* 2014;66:1608–15.
10. Hoa S, Hudson M, Troyanov Y, Proudman S, Walker J, Stevens W, et al. Single-specificity anti-Ku antibodies in an international cohort of 2140 systemic sclerosis subjects: clinical associations. *Medicine (Baltimore)* 2016;95:e4713.
11. Steen VD. Autoantibodies in systemic sclerosis. *Semin Arthritis Rheum* 2005;35:35–42.
12. Nihtyanova SI, Schreiber BE, Ong VH, Rosenberg D, Moynadeh P, Coghlan JG, et al. Prediction of pulmonary complications and long-term survival in systemic sclerosis. *Arthritis Rheumatol* 2014;66:1625–35.
13. Foocharoen C, Suwannachat P, Netwijitpan S, Mahakkanukrauh A, Suwannaroj S, Nanagara R. Clinical differences between Thai systemic sclerosis patients with positive versus negative anti-topoisomerase I. *Int J Rheum Dis* 2016;19:312–20.
14. Hoffmann-Vold AM, Midtvedt Ø, Tennøe AH, Garen T, Lund MB, Aaløkken TM, et al. Cardiopulmonary disease development in anti-RNA polymerase III-positive systemic sclerosis: comparative analyses from an unselected, prospective patient cohort. *J Rheumatol* 2017;44:459–65.
15. Nihtyanova SI, Denton CP. Scleroderma lung involvement, autoantibodies, and outcome prediction: the confounding effect of time [editorial]. *J Rheumatol* 2017;44:404–6.
16. Shand L, Lunt M, Nihtyanova S, Hoseini M, Silman A, Black CM, et al. Relationship between change in skin score and disease outcome in diffuse cutaneous systemic sclerosis: application of a latent linear trajectory model. *Arthritis Rheum* 2007;56:2422–31.
17. Perera A, Fertig N, Lucas M, Rodriguez-Reyna TS, Hu P, Steen VD, et al. Clinical subsets, skin thickness progression rate, and serum antibody levels in systemic sclerosis patients with anti-topoisomerase I antibody. *Arthritis Rheum* 2007;56:2740–6.
18. Maurer B, Graf N, Michel BA, Müller-Ladner U, Czirják L, Denton CP, et al. Prediction of worsening of skin fibrosis in patients with diffuse cutaneous systemic sclerosis using the EUSTAR database. *Ann Rheum Dis* 2015;74:1124–31.
19. Dobrota R, Maurer B, Graf N, Jordan S, Mihai C, Kowal-Bielecka O, et al. Prediction of improvement in skin fibrosis in diffuse cutaneous systemic sclerosis: a EUSTAR analysis. *Ann Rheum Dis* 2016;75:1743–8.
20. Amjadi S, Maranian P, Furst DE, Clements PJ, Wong WK, Postlethwaite AE, et al, for the Investigators of the D-Penicillamine, Human Recombinant Relaxin, and Oral Bovine Type I Collagen Clinical Trials. Course of the modified Rodnan skin thickness score in systemic sclerosis clinical trials: analysis of three large multicenter, double-blind, randomized controlled trials. *Arthritis Rheum* 2009;60:2490–8.
21. Merkel PA, Silliman NP, Clements PJ, Denton CP, Furst DE, Mayes MD, et al, for the Scleroderma Clinical Trials Consortium. Patterns and predictors of change in outcome measures in clinical trials in scleroderma: an individual patient meta-analysis of 629 subjects with diffuse cutaneous systemic sclerosis. *Arthritis Rheum* 2012;64:3420–9.
22. Medsger TA Jr. Natural history of systemic sclerosis and the assessment of disease activity, severity, functional status, and psychologic well-being. *Rheum Dis Clin North Am* 2003;29:255–73.
23. Herrick AL, Pan X, Peytrignet S, Lunt M, Hesselstrand R, Mouthon L, et al. Treatment outcome in early diffuse cutaneous systemic sclerosis: the European Scleroderma Observational Study (ESOS). *Ann Rheum Dis* 2017;76:1207–18.
24. Maricq HR, Valter I. A working classification of scleroderma spectrum disorders: a proposal and the results of testing on a sample of patients. *Clin Exp Rheumatol* 2004;22 Suppl 33:S5–13.
25. Giordano M, Valentini G, Migliaresi S, Picillo U, Vatti M. Different antibody patterns and different prognoses in patients with scleroderma with various extent of skin sclerosis. *J Rheumatol* 1986;13:911–6.
26. LeRoy EC, Black C, Fleischmajer R, Jablonska S, Krieg T, Medsger TA Jr, et al. Scleroderma (systemic sclerosis): classification, subsets and pathogenesis. *J Rheumatol* 1988;15:202–5.
27. Cottrell TR, Wise RA, Wigley FM, Boin F. The degree of skin involvement identifies distinct lung disease outcomes and survival in systemic sclerosis. *Ann Rheum Dis* 2014;73:1060–6.
28. Srivastava N, Hudson M, Tatibouet S, Wang M, Baron M, Fritzler MJ. Thinking outside the box—the associations with cutaneous involvement and autoantibody status in systemic sclerosis are not always what we expect. *Semin Arthritis Rheum* 2015;45:184–9.
29. Boonstra M, Mertens BJ, Bakker JA, Ninaber MK, Ajmone Marsan N, van der Helm-van Mil AH, et al. To what extent do autoantibodies help to identify high-risk patients in systemic sclerosis? *Clin Exp Rheumatol* 2018;36 Suppl 113:109–17.
30. Van den Hoogen F, Khanna D, Fransen J, Johnson SR, Baron M, Tyndall A, et al. 2013 classification criteria for systemic sclerosis: an American College of Rheumatology/European League Against Rheumatism collaborative initiative. *Arthritis Rheum* 2013;65:2737–47.
31. Putter H, Fiocco M, Geskus RB. Tutorial in biostatistics: competing risks and multi-state models. *Stat Med* 2007;26:2389–430.
32. Coghlan JG, Denton CP, Grünig E, Bonderman D, Distler O, Khanna D, et al. Evidence-based detection of pulmonary arterial hypertension in systemic sclerosis: the DETECT study. *Ann Rheum Dis* 2014;73:1340–9.
33. Walker UA, Tyndall A, Czirják L, Denton C, Farge-Bancel D, Kowal-Bielecka O, et al. Clinical risk assessment of organ manifestations in systemic sclerosis: a report from the EULAR Scleroderma Trials And Research group database. *Ann Rheum Dis* 2007;66:754–63.
34. Hudson M, Mahler M, Pope J, You D, Tatibouet S, Steele R, et al. Clinical correlates of CENP-A and CENP-B antibodies in a large cohort of patients with systemic sclerosis. *J Rheumatol* 2012;39:787–94.
35. Hanke K, Brückner CS, Dähnrich C, Huscher D, Komorowski L, Meyer W, et al. Antibodies against PM/Scl-75 and PM/Scl-100 are independent markers for different subsets of systemic sclerosis patients. *Arthritis Res Ther* 2009;11:R22.
36. Bruni C, Lages A, Patel H, Harvey J, Nihtyanova SI, Green B, et al. Resolution of paraneoplastic PM/Scl-positive systemic sclerosis after curative resection of a pancreatic tumour [letter]. *Rheumatology (Oxford)* 2017;56:317–8.
37. Johnson SR, Soowamber ML, Fransen J, Khanna D, Van Den Hoogen F, Baron M, et al. There is a need for new systemic sclerosis subset criteria: a content analytic approach. *Scand J Rheumatol* 2018; 47:62–70.

Spontaneous Pulmonary Hypertension Associated With Systemic Sclerosis in P-Selectin Glycoprotein Ligand 1–Deficient Mice

Rafael González-Tajuelo,¹ María de la Fuente-Fernández,¹ Daniel Morales-Cano,² Antonio Muñoz-Callejas,¹ Elena González-Sánchez,¹ Javier Silván,¹ Juan Manuel Serrador,³ Susana Cadenas,⁴ Bianca Barreira,² Marina Espartero-Santos,¹ Carlos Gamallo,¹ Esther F. Vicente-Rabaneda,¹ Santos Castañeda,⁵ Francisco Pérez-Vizcaíno,² Ángel Cogolludo,² Luis Jesús Jiménez-Borreguero,⁶ and Ana Urzainqui¹ 

Objective. Pulmonary arterial hypertension (PAH), one of the major complications of systemic sclerosis (SSc), is a rare disease with unknown etiopathogenesis and noncurative treatments. As mice deficient in P-selectin glycoprotein ligand 1 (PSGL-1) develop a spontaneous SSc-like syndrome, we undertook this study to analyze whether they develop PAH and to examine the molecular mechanisms involved.

Methods. Doppler echocardiography was used to estimate pulmonary pressure, immunohistochemistry was used to assess vascular remodeling, and myography of dissected pulmonary artery rings was used to analyze vascular reactivity. Angiotensin II (Ang II) levels were quantified by enzyme-linked immunosorbent assay, and Western blotting was used to measure Ang II type 1 receptor (AT₁R), AT₂R, endothelial cell nitric oxide synthase (eNOS), and phosphorylated eNOS expression in lung lysates. Flow cytometry allowed us to determine cytokine production by immune cells and NO production by endothelial cells. In all cases, there were 4–8 mice per experimental group.

Results. PSGL-1^{-/-} mice showed lung vessel wall remodeling and a reduced mean ± SD expression of pulmonary AT₂R (expression ratio [relative to β-actin] in female mice age >18 months: wild-type mice 0.799 ± 0.508 versus knockout mice 0.346 ± 0.229). With aging, female PSGL-1^{-/-} mice had impaired up-regulation of estrogen receptor α (ERα) and developed lung vascular endothelial dysfunction coinciding with an increase in mean ± SEM pulmonary Ang II levels (wild-type 48.70 ± 5.13 pg/gm lung tissue versus knockout 78.02 ± 28.09 pg/gm lung tissue) and a decrease in eNOS phosphorylation, leading to reduced endothelial NO production. These events led to a reduction in the pulmonary artery acceleration time:ejection time ratio in 33% of aged female PSGL-1^{-/-} mice, indicating pulmonary hypertension. Importantly, we found expanded populations of interferon-γ-producing PSGL-1^{-/-} T cells and B cells and a reduced presence of regulatory T cells.

Conclusion. The absence of PSGL-1 induces a reduction in Treg cells, NO production, and ERα expression and causes an increase in Ang II in the lungs of female mice, favoring the development of PAH.

Supported by the Spanish Ministry of Economy and Competitiveness (grants SAF2015-69396-R, SAF2011-28150, and SAF2014-55399) and the Spanish Ministry of Health and Instituto de Salud Carlos III (cofinanced by Fondos FEDER; grants AC17-00027, FIS-PI14-01698, FIS-PI17-01819, and FIS-PI12-01578, Red de Investigación de Enfermedades Reumáticas [RIER] RD12/0009/0017). The Centro Nacional de Investigaciones Cardiovasculares (CNIC) is supported by the Ministerio de Economía, Industria y Competitividad, and the Pro CNIC Foundation and is a Severo Ochoa Center of Excellence (SEV-2015-0505).

¹Rafael González-Tajuelo, PhD, María de la Fuente-Fernández, MS, Antonio Muñoz-Callejas, MS, Elena González-Sánchez, PhD, Javier Silván, MS, Marina Espartero-Santos, BS, Carlos Gamallo, PhD, MD, Esther F. Vicente-Rabaneda, PhD, MD, Ana Urzainqui, PhD: Fundación de Investigación Biomédica-Hospital de la Princesa, IIS-Princesa, Servicio de Inmunología, Madrid, Spain; ²Daniel Morales-Cano, PhD, Bianca Barreira, BS, Francisco Pérez-Vizcaíno, PhD, Ángel Cogolludo, PhD: University Complutense of Madrid School of Medicine and Ciber Enfermedades Respiratorias, Madrid,

Spain; ³Juan Manuel Serrador, PhD: Centro de Biología Molecular Severo Ochoa (CBMSO) and Instituto de Física Teórica CSIC/Universidad Autónoma de Madrid (UAM), Madrid, Spain; ⁴Susana Cadenas, PhD: Fundación de Investigación Biomédica-Hospital de la Princesa, IIS-Princesa, and CBMSO, CSIC-UAM, Madrid Spain; ⁵Santos Castañeda, PhD, MD: Fundación de Investigación Biomédica-Hospital de la Princesa, IIS-Princesa, and Catedra UAM-ROCHE, Madrid, Spain; ⁶Luis Jesús Jiménez-Borreguero, MD: Hospital de la Princesa and Centro Nacional de Investigaciones Cardiovasculares (CNIC), Madrid, Spain.

Ms de la Fuente-Fernández and Dr. Morales-Cano contributed equally to this work.

No potential conflicts of interest relevant to this article were reported.

Address correspondence to Ana Urzainqui, PhD, Hospital de la Princesa, Calle de Diego de León 62, 28006 Madrid, Spain. E-mail: ana.urzainqui@salud.madrid.org.

Submitted for publication February 22, 2019; accepted in revised form September 3, 2019.

INTRODUCTION

Pulmonary arterial hypertension (PAH) is a rare and progressive disease that mainly affects women. PAH is characterized by hypertrophic distal pulmonary vascular remodeling resulting from endothelial dysfunction, dysregulated vascular smooth muscle cell proliferation, and inflammation, which together promote medial thickening of pulmonary arteries and luminal obliteration (1). These pathologic events increase pulmonary vascular resistance and pulmonary artery pressure (PAP), leading to an increased hemodynamic load on the right ventricle (RV). The RV adapts with a compensatory increase in wall thickness and contractility (2,3). PAH develops in 7–12% of patients with systemic sclerosis (SSc), constituting a leading cause of death (4–6). Indeed, SSc is a major cause of connective tissue disease (CTD)-associated PAH (4).

Several molecular mechanisms have been implicated in the control of pulmonary pressure and are dysregulated in PAH. Pulmonary artery endothelial cells (ECs) from patients with idiopathic PAH produce reduced amounts of nitric oxide (NO) (4). Angiotensin II (Ang II) plays a major role in the control of blood pressure and vascular tone in peripheral blood vessels (7–9). In this context, the binding of Ang II to Ang II receptor 1 (AT₁R) induces vasoconstriction, while binding to AT₂R triggers vasodilation (7). Thus, elevated levels of renin, angiotensin-converting enzyme (ACE), Ang II, and AT₁R have been observed in experimental models as well as in patients with pulmonary hypertension (PH) (10–12).

P-selectin glycoprotein ligand 1 is a leukocyte receptor responsible for the initial contacts between white blood cells and endothelium. PSGL-1 interacts with P-, E-, and L-selectin, allowing leukocyte tethering and rolling before extravasation to the inflammatory foci (13). The PSGL-1–P-selectin interaction triggers a tolerogenic program in human monocyte-derived dendritic cells, which drive Treg cell generation (14). Accordingly, disease exacerbation has been described in PSGL-1-deficient (PSGL-1^{-/-}) mice in different experimental inflammatory models (15–19). More importantly, PSGL-1^{-/-} mice progressively develop an autoimmune syndrome which shares multiple features with human SSc, such as autoantibody production, dermal fibrosis, and vascular damage (15).

Given that PSGL-1^{-/-} mice develop an autoimmune syndrome similar to SSc, and that there are not good mouse models for SSc associated with PAH (SSc-PAH), we questioned whether, as a part of the scleroderma-like syndrome, these mice develop PH. Interestingly, Doppler echocardiography is now considered a validated noninvasive method to assess the systolic pressure in the pulmonary artery and right ventricle (20,21). The reduction in the ratio of pulmonary artery acceleration time (PAAT) to ejection time (ET) is associated with high PAP in humans and in mice (20–23). In the present study, we analyzed the lungs and heart of PSGL-1^{-/-} mice, finding pulmonary small vessel remodeling and increased PAP in female mice, and we examined the possible molecular events implicated in this phenotype.

MATERIALS AND METHODS

Animals. C57BL/6 PSGL-1^{-/-} mice were kindly provided by Dr. M. K. Wild and Dr. D. Vestweber (Max Planck Institute for Molecular Biomedicine, Münster, Germany). Wild-type (WT) C57BL/6 mice were obtained from The Jackson Laboratory and were backcrossed with PSGL-1^{-/-} mice. Mice were kept in pathogen-free conditions at the Animal Facility of the School of Medicine, Universidad Autónoma de Madrid and the Animal Facility of the Centro Nacional de Investigaciones Cardiovasculares. Mice were killed by cervical dislocation, and internal organs were extracted for analysis. All experiments and breeding were performed in accordance with national and institutional guidelines for animal care (EU Directive 2010/63/EU for animal experiments). The experimental procedures were approved by the Director General de Medio Ambiente of Madrid (ref. PROEX 69/14 and PROEX 162/15).

Immunohistochemistry and vessel wall thickness calculation. Immunohistochemistry analysis using antibody against murine α -smooth muscle actin (α -SMA) was performed in paraffin-embedded lung sections. Small blood vessel (diameter <50 μ m) wall thickness was calculated by measuring the internal and total vessel diameter of anti- α -SMA-stained lungs and calculating the vessel wall area occupied by the vessel wall using ImageJ (National Institutes of Health). Vessels were clustered according to their diameter, and the mean wall thickness area was calculated.

Transthoracic Doppler echocardiography and Fulton index calculation. All transthoracic echocardiography measurements were obtained with an echocardiography system (VEVO 2100; Visualsonics) and an 18–38 -Hz ultrasound probe. Chest hair was removed with hypoallergenic depilatory cream, and animals were anesthetized with a continuous influx of 2% isoflurane with an oxygen flow rate of 1.5 liter/minute. Pulsed wave Doppler mode was used to measure the PAAT and ET of blood flow in the pulmonary artery at the level of the pulmonary valve. The PAAT:ET ratio was then calculated and used as an indirect measure of systolic pulmonary artery blood pressure. M-mode in transversal and longitudinal axis was used to measure the systolic and diastolic left ventricular internal diameters (LVIDs) and the longitudinal length of the LV. LV end systolic volume (LVESV) and LV end diastolic volume (LVEDV) were estimated as follows: LVESV = (7/[2.4 + systolic LVID]) \times systolic LVID³; LVEDV = (7/[2.4 + diastolic LVID]) \times diastolic LVID³. The ejection fraction was then calculated as the ratio (LVEDV – LVESV):LVEDV. Diastolic function was assessed using analyses of transmitral blood flow by pulsed wave Doppler. E wave (early ventricular filling) and A wave (late ventricular filling caused by atrial contraction) velocity were measured, and the E/A ratio was calculated.

Systemic pressure measurements. Systemic arterial pressure was measured using a BP-2000 system (Visitech Systems), and data were analyzed with BP-2000 Analysis Software.

Eighteen-month-old female WT and PSGL-1^{-/-} mice were subjected to pressure measurement for a week for protocol habituation. Next, consecutive measurements were obtained over 5 days, and the mean systolic pressure value was calculated.

Vascular reactivity. Murine pulmonary arteries were carefully dissected free of surrounding tissue and cut into rings (1.8–2 mm in length). Vessel segments were mounted on a wire myograph in Krebs physiologic solution. Buffer solutions were continuously bubbled with 21% O₂, 5% CO₂, and 74% N₂ (PO₂/4 17–19 kPa) (24), and stretched to a transmural pressure equivalent to 30 mm Hg. Contractility was recorded with an isometric force transducer and a displacement device coupled with a digitalization and data acquisition system (PowerLab). To confirm smooth muscle viability, arteries were first stimulated by raising the K⁺ concentration of the buffer to 80 mmoles/liter. Thereafter, concentration-response curves to acetylcholine (10⁻⁹–10⁻⁵ moles/liter) and sodium nitroprusside (10⁻¹¹–10⁻⁵ moles/liter) were performed using cumulative addition to analyze the endothelium-dependent and endothelium-independent vasodilatation, respectively. For the reactive oxygen species (ROS) scavenging experiments, the concentration of superoxide dismutase (SOD)–polyethylene glycol (Sigma) used was 50 units/ml.

Enzyme-linked immunosorbent assay (ELISA). The left lung was mechanically disrupted in 1× phosphate buffered saline (PBS). After 4 freeze/thaw cycles to break cell membranes, samples were centrifuged at 5,000g for 5 minutes at 4°C, and supernatants were recovered. Ang II concentrations were measured using an Ang II ELISA kit (CSB-E04495 ml; Cusabio).

Western blotting. The right lung was frozen, pulverized, and diluted in radioimmunoprecipitation assay buffer (1% Triton X-100, 0.24M sodium deoxycholate, 0.35M sodium dodecyl sulfate in 1× Tris buffered saline) with protease and phosphatase inhibitors. Lung lysates were used for Western blot assays. The following primary antibodies were used: rabbit anti-AT₁R and anti-AT₂R (1:1,000; Novus Biologicals), rabbit anti-β-actin (1:5,000; Sigma), rabbit antivinculin (1:2,000; Sigma), mouse anti-eNOS (1:1,000; BD Pharmingen), mouse anti-phosphorylated eNOS Ser¹¹⁷⁶ (1:1,000; BD Pharmingen), mouse anti-estrogen receptor α (ERα) (1:1,000; R&D), rabbit anti-ERβ (1:1,000; ThermoFisher Scientific), and mouse anti-GAPDH (1:1,000; Biologend).

Bound antibodies were visualized by chemiluminescence with a Luminata Forte Western HRP Substrate (Merck KGaA) using either a horseradish peroxidase-conjugated goat anti-rabbit or goat anti-mouse IgG secondary antibody. Band intensity was analyzed using ImageJ, and results were normalized to the expression of β-actin, GAPDH, or vinculin, as loading controls.

Flow cytometry. Lungs were weighed, minced into ~1-mm² pieces, and digested for 1 hour with 1 mg/ml collagenase A (Sigma), 2.5 mg/ml Dispase II (Roche), and 40 μg/ml DNase (Sigma) in

RPMI 1640 medium. Cell aggregates and undigested pieces of tissue were eliminated using a 70-μm cell strainer (BD Falcon). Cells were then washed with 25 ml of PBS, 0.5% bovine serum albumin, 5 mM EDTA, concentrated in 700 μl, and filtered through a 30-μm cell strainer (BD Pharmingen). After incubation with 1:200 Fc Block (BD Pharmingen), cells were stained with the cocktail of surface antibodies for 15 minutes at 4°C. Subsequently, cells were permeabilized with 2 ml of fluorescence-activated cell sorting (FACS) Lysing Solution (BD Pharmingen) for 15 minutes, washed, and stained for 30 minutes at 4°C with a cocktail of antibodies directed against intracellular cytokines. For intranuclear FoxP3 staining, a fluorescein isothiocyanate (FITC)-conjugated anti-mouse/rat FoxP3 staining set was used according to the instructions of the manufacturer (eBioscience). Flow cytometry was performed using a FACSCanto II and FACS Diva Software (BD Pharmingen).

Cell gating strategy and flow cytometry reagents. T cells and B cells were gated as CD45.2+CD3+CD19-/B220- and CD45.2+CD19+CD3- or CD45.2+B220+CD3-, respectively. Neutrophils were gated as CD45+Ly-6G+ and Ly-6C+ (see Supplementary Figure 1, on the *Arthritis & Rheumatology* web site at <http://onlinelibrary.wiley.com/doi/10.1002/art.41100/abstract>). Alveolar macrophages were gated as CD45.2+CD11c+Siglec F+, interstitial macrophages were gated as CD45.2+MHC-II+Siglec F-CD11c-CD11b+, and dendritic cells were gated as CD45.2+Siglec F-MHC-II+CD11c+ (Supplementary Figure 1). The expression of interleukin-10 (IL-10), IL-17, and interferon-γ (IFNγ) was analyzed in these subsets. Lung ECs were identified as CD45.2-CD31+. Antibodies used for the identification of the aforementioned cell populations were as follows: phycoerythrin (PE)-Cy7-conjugated CD11c (1:50; eBioscience), PE-Cy7-conjugated CD3ε (1:200; eBioscience), allophycocyanin (APC)-conjugated CD31 (1:200; BD Pharmingen), FITC- and BV421-conjugated CD45.2 (1:200; BD Pharmingen), APC-Cy7-conjugated IL-17A (1:200; BD Pharmingen), APC-conjugated IFNγ (1:50; Miltenyi Biotec), VioBlue-conjugated CD19 (1:50; Miltenyi Biotec), APC-Vio770-conjugated B220 (1:50; Miltenyi Biotec), PerCP-Cy5.5-conjugated IL-10 (1:100; BioLegend), Gr-1- and APC-conjugated Ly-6G/Ly-6C (1:100; BD Pharmingen), APC-conjugated CD11b (1:50; Miltenyi Biotec), PerCP-Vio 700-conjugated major histocompatibility complex class II (MHC-II) (1:100; Miltenyi Biotec), and PE-conjugated Siglec F (1:100; BD Pharmingen). CountBright absolute counting beads (Invitrogen) were used for the quantification of absolute cell numbers.

Intracellular NO evaluation. After blocking and surface molecule staining (CD45 and CD31), cells were washed and incubated with the NO-sensing fluorescent probe diaminorhodamine-4M acetoxymethyl ester (DAR-4M AM) (5 μm; Sigma) in PBS for 30 minutes at 37°C. Finally, cells were fixed and analyzed with a FACSCanto II cytometer. Cells that were not incubated with the probe were used as negative controls for fluorescence. Two groups of cells could be distinguished according to the

fluorescence levels at Em 580 nm. The fold change in the DAR-4M AM mean fluorescence intensity (MFI) for ECs from WT mice and PSGL-1^{-/-} mice was calculated as the ratio of the MFI obtained in each mouse in relation to the average MFI for all WT mice analyzed.

Statistical analysis. Statistical significance between 2 groups was calculated using Student's 2-tailed *t*-test for parametric variables and the Mann-Whitney U test for nonparametric variables. Statistical significance between 3 groups was calculated using one-way analysis of variance (ANOVA) with the Bonferroni post hoc test. For dose-dependent relaxation studies, statistical significance was calculated using two-way ANOVA. *P* values less than 0.05 were considered significant. All statistical analyses were performed using SPSS, version 15.0 (IBM).

RESULTS

Altered echocardiographic parameters consistent with PH in PSGL-1^{-/-} mice. Given the elevated rate of death in PSGL-1^{-/-} mice after reaching 1 year of age (15), echocardiography was used to measure the PAAT:ET ratio (Figure 1A), an indirect evaluation of pulmonary pressure. Since preliminary data suggested differences in the PAAT:ET ratio between WT and PSGL-1^{-/-} mice, follow-up transthoracic Doppler echocardiography was performed on WT

and PSGL-1^{-/-} littermates between 1.5 and 18 months of age. A recurrent tendency toward a reduced PAAT:ET ratio was observed in female PSGL-1^{-/-} mice from 3 months of age (Figure 1B). Considering that a group of 3 female PSGL-1^{-/-} mice (33% of all female PSGL-1^{-/-} mice) died between 15 and 18 months of age, we differentiated between the dead and survivor groups. The group of PSGL-1^{-/-} mice that died prematurely showed increased PAP, detected by a reduced PAAT:ET ratio, compared to WT mice and to the surviving group of PSGL-1^{-/-} mice (Figure 1B). PSGL-1^{-/-} mice that survived maintained a PAAT:ET ratio below that observed in WT mice. In contrast, both male WT and male PSGL-1^{-/-} mice exhibited similar PAAT:ET ratios throughout the experiment (Figure 1C).

No differences in the ejection fraction and the E/A ratio were found between the 3 groups (Supplementary Figures 2A and B, <http://onlinelibrary.wiley.com/doi/10.1002/art.41100/abstract>). In addition, systolic arterial pressure and the PAAT:ET ratio were measured in another cohort of aged female WT and PSGL-1^{-/-} mice, and WT and KO mice showed similar systolic arterial pressure (Supplementary Figure 2C).

Remodeling of pulmonary small vessels in PSGL-1^{-/-} mice. The presence of pulmonary vascular remodeling that could explain the increase in pulmonary pressure was analyzed. Immunohistochemical staining, using an antibody against α -SMA, of lung

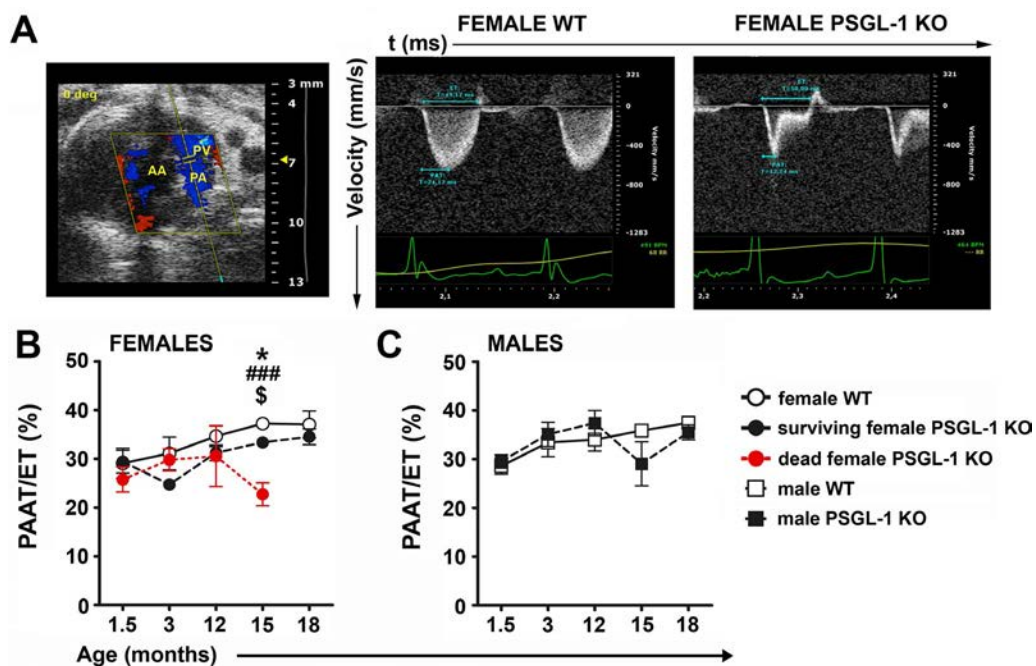


Figure 1. Development of pulmonary hypertension with aging in female PSGL-1^{-/-} mice. **A**, B-mode showing the echocardiographic plane used for Doppler pulmonary flow acquisition (left), and representative Doppler pulmonary artery flow of female wild-type (WT) mice (middle) and PSGL-1-knockout (KO) mice (right). **B**, Longitudinal study of the pulmonary artery acceleration time:ejection time (PAAT:ET) ratio between 1.5 and 18 months of age in female WT mice (*n* = 4), surviving female PSGL-1^{-/-} mice (*n* = 6), and female PSGL-1^{-/-} mice that died prematurely (*n* = 3). **C**, Longitudinal study of the PAAT:ET ratio between 1.5 and 18 months of age in male WT mice (*n* = 6) and male PSGL-1^{-/-} mice (*n* = 6). Results are representative of 3 replicate experiments. Values are the mean \pm SD. * = *P* < 0.05, WT versus surviving PSGL-1^{-/-} mice; ### = *P* < 0.005, WT versus dead PSGL-1^{-/-} mice; \$ = *P* < 0.05, surviving PSGL-1^{-/-} versus dead PSGL-1^{-/-} mice, all by one-way analysis of variance with Bonferroni post hoc test. AA = ascending aorta; PV = pulmonary valve; PA = pulmonary artery.

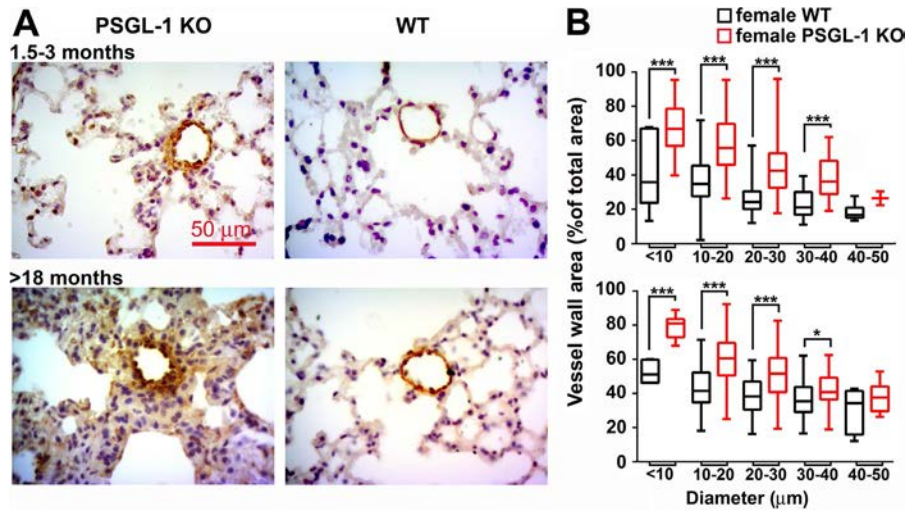


Figure 2. Vascular remodeling in pulmonary small vessels from female PSGL-1^{-/-} mice. **A**, Representative photomicrographs of anti- α -smooth muscle actin-immunostained lung sections from mice ages 1.5–3 months and >18 months. **B**, Percentage of vessel wall area in <50- μ m-diameter pulmonary blood vessels in mice ages 1.5–3 months (top) and >18 months (bottom). Fewer than 150 vessels were analyzed for each age group ($n = 5$ –7 per group). Data are presented as box plots, where the boxes represent the 25th to 75th percentiles, the lines within the boxes represent the median, and the lines outside the boxes represent the 10th and 90th percentiles. * = $P < 0.05$; *** = $P < 0.005$, by Student's 2-tailed t -test. See Figure 1 for definitions. Color figure can be viewed in the online issue, which is available at <http://onlinelibrary.wiley.com/doi/10.1002/art.41100/abstract>.

sections from female WT and PSGL-1^{-/-} mice revealed a thicker medial wall of small vessels in PSGL-1^{-/-} mouse lungs (Figure 2A). Quantification demonstrated a significant increase of the relative wall area in almost all groups of PSGL-1^{-/-} mouse vessels, independent of age (Figure 2B).

Decreased endothelial NO-dependent relaxing response in pulmonary arteries of aged female PSGL-1^{-/-} mice.

Vascular reactivity in pulmonary and mesenteric arterial rings was assessed using wire myography. When compared to female WT littermates, pulmonary arteries isolated from female PSGL-1^{-/-} mice showed increased vasoconstriction in response to 80 mM KCl (Figure 3A). The vasodilating response to acetylcholine was impaired in PSGL-1^{-/-} mouse arterial rings (Figure 3B); however, the addition of an external NO donor (sodium nitroprusside) was sufficient to

fully relax both WT and PSGL-1^{-/-} mouse arterial rings (Figure 3C). Conversely, vascular reactivity did not differ between mesenteric arterial rings of PSGL-1^{-/-} and WT littermates (Supplementary Figures 3A and B, <http://onlinelibrary.wiley.com/doi/10.1002/art.41100/abstract>), which suggests that the endothelial dysfunction is restricted to the pulmonary circulation. The inhibition of ROS production by addition of SOD did not restore the relaxation capability of PSGL-1^{-/-} mouse lung arteries, thus ruling out the notion of NO scavenging by ROS (Supplementary Figure 3C).

Reduced pulmonary endothelial NO production and eNOS phosphorylation in aged female PSGL-1^{-/-} mice.

To understand the molecular mechanisms responsible for the impaired EC-dependent relaxation of pulmonary arteries, NO production by ECs was assessed. The percentage of NO-producing lung ECs

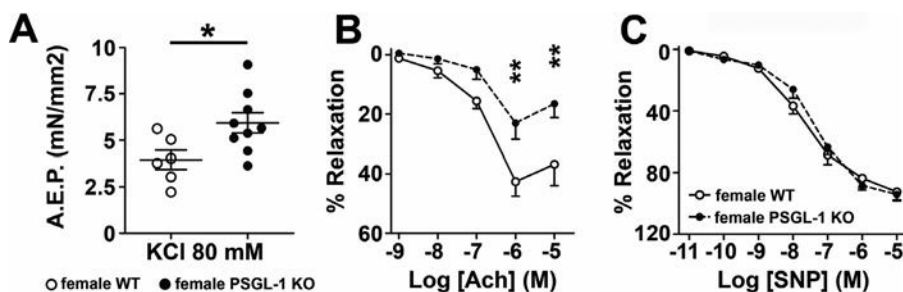


Figure 3. Vascular response to vasoconstrictor and vasodilator agents. **A**, Contractile response to KCl in pulmonary arterial rings obtained from female mice >18 months of age. Symbols represent individual mice; bars show the mean \pm SEM. **B** and **C**, Vasodilating response to acetylcholine (ACh) (**B**) and sodium nitroprusside (SNP) (**C**) in pulmonary arterial rings obtained from female mice >18 months of age. Values are the mean \pm SEM. * = $P < 0.05$; ** = $P < 0.01$, by Student's 2-tailed t -test (**A**) and by two-way analysis of variance (**B**). AEP = active effective pressure (see Figure 1 for other definitions).

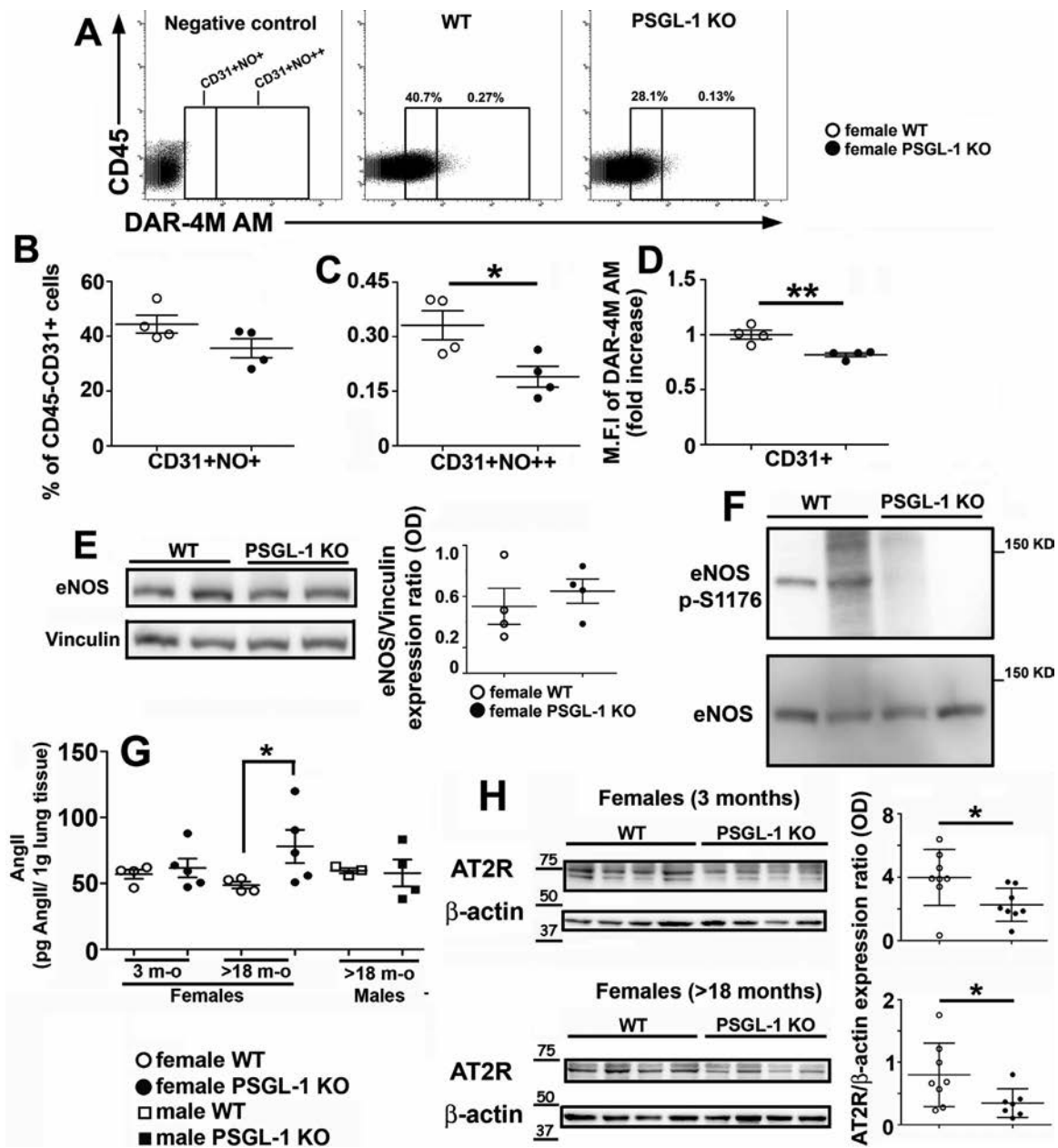


Figure 4. Quantification of nitric oxide (NO) production and assessment of endothelial cell nitric oxide synthase (eNOS) phosphorylation. **A**, Dot plots of diaminorhodamine-4M acetoxymethyl ester (DAR-4M AM) signal in female mice >18 months of age. Highly positive population is shown to the right of the internal vertical line. **B** and **C**, Percentage of lung endothelial cells producing moderate (**B**) or high (**C**) amounts of NO measured in WT and PSGL-1^{-/-} female mice >18 months of age. **D**, Fold change of mean fluorescence intensity (MFI) for the NO-sensing probe DAR-4M AM measured in lung endothelial cells of female WT and PSGL-1^{-/-} mice >18 months of age (n = 4–6 per group). **E**, Western blot showing eNOS expression in the lungs of female mice >18 months of age (left) and densitometric quantification (right). Vinculin was used as a loading control. **F**, Western blot showing phosphorylated eNOS expression in the lungs of female mice >18 months of age. **G**, Angiotensin II (Ang II) concentration in lung lysates from mice (n = 5 per group). **H**, Immunoblots showing Ang II type 2 receptor (AT₂R) expression in the lungs of mice (n = 7–8 per group) and densitometric quantification. β -actin was used as a loading control. In **B–E**, **G**, and **H**, symbols represent individual mice; bars show the mean \pm SEM (**B–E** and **G**) or the mean \pm SD (**H**). * = $P < 0.05$; ** = $P < 0.01$, by Mann-Whitney U test. See Figure 1 for other definitions.

was reduced in aged female PSGL-1^{-/-} mice (Figures 4A–C), although this was significant only within the highest NO-producing EC subset (Figure 4C). Additionally, the MFI for the NO-sensing probe DAR-4M AM was lower in lung ECs from aged PSGL-1^{-/-} mice than in those from aged WT mice (Figure 4D). These changes

were not observed in 3-month-old female mice (Supplementary Figures 4A–C, <http://onlinelibrary.wiley.com/doi/10.1002/art.41100/abstract>). Remarkably, although eNOS protein expression was measured in lung lysates and no differences were found between female WT and PSGL-1^{-/-} mice (Figure 4E), reduced lev-

els of eNOS phosphorylation at the Ser¹¹⁷⁶ activator site were found in the lung lysates of aged female PSGL-1^{-/-} mice (Figure 4F).

Increased pulmonary levels of Ang II and reduced expression of AT₂R in aged female PSGL-1^{-/-} mice. No differences were found in the pulmonary concentration of Ang II between young female WT and PSGL-1^{-/-} mice; however, the mean ± SEM Ang II concentration was significantly higher in

aged female PSGL-1^{-/-} mice (78.02 ± 28.09 pg/gm lung tissue) than in aged female WT mice (48.70 ± 5.13 pg/gm lung tissue) (Figure 4G). In contrast, Ang II levels in aged males were similar between the 2 genotypes (Figure 4G).

Regarding Ang II receptors, the mean ± SD expression of AT₂R was lower in both young and aged female PSGL-1^{-/-} mice than in WT mice (expression ratio [relative to β-actin] in young WT 3.983 ± 1.765 versus young KO 2.266 ± 1.045; in aged WT

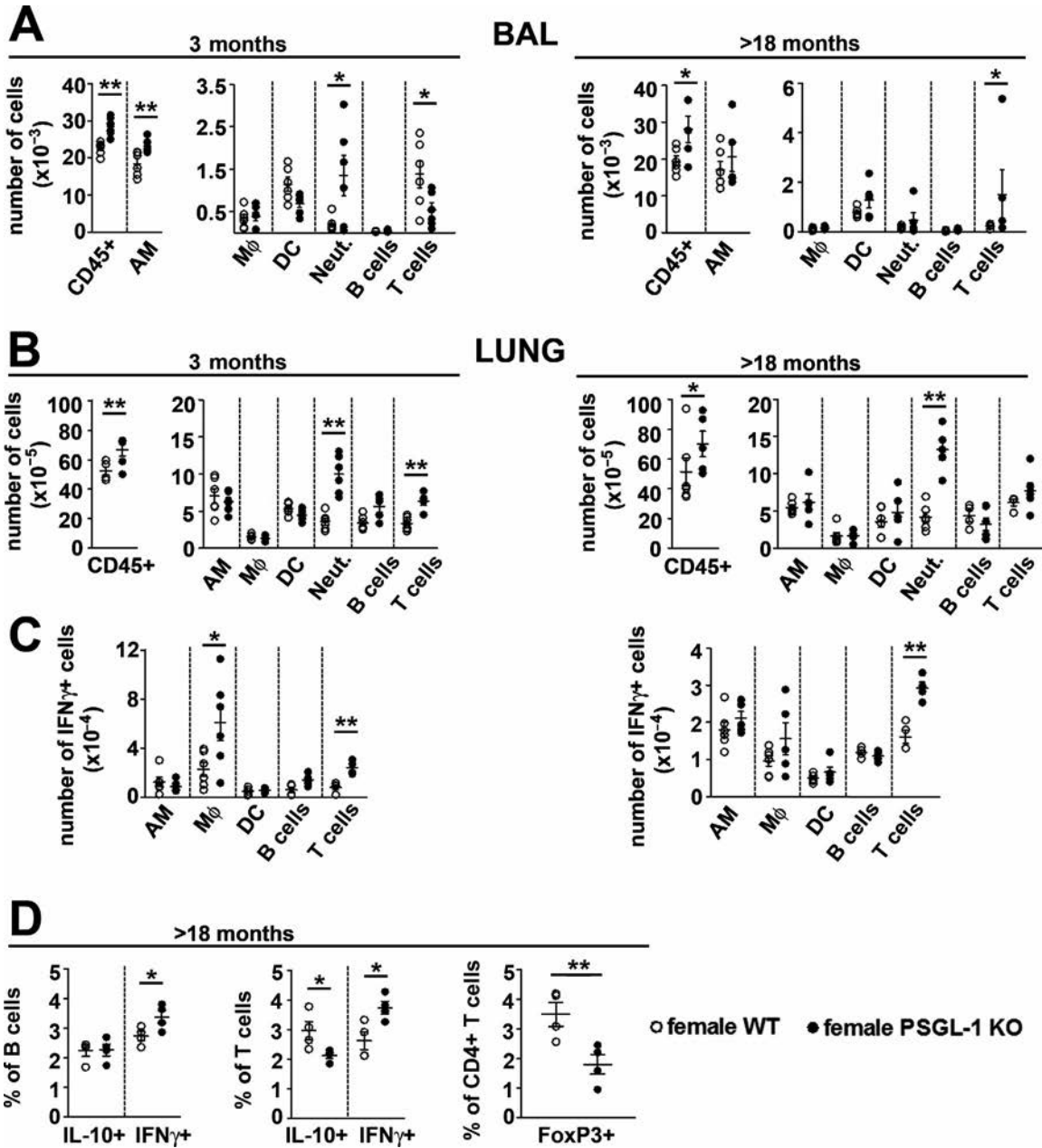


Figure 5. Immune system analysis of the lungs of female wild-type (WT) and PSGL-1^{-/-} mice. **A**, Absolute numbers of immune cell populations isolated from the bronchoalveolar lavage (BAL) fluid of female WT and PSGL-1^{-/-} mice. **B**, Absolute numbers of immune cell populations found in the whole lungs of female WT and PSGL-1^{-/-} mice. **C**, Absolute numbers of interferon- γ (IFN γ)-positive cells obtained from the whole lungs of female WT and PSGL-1^{-/-} mice. **D**, Percentage of interleukin-10 (IL-10)- and IFN γ -producing cells in the B cell and T cell populations and the frequency of Treg cells (FoxP3+) in the CD4+ T cell subset in lungs isolated from mice (n = 4–6 per group). Symbols represent individual mice; bars show the mean ± SEM. * = P < 0.05; ** = P < 0.01, by Student's 2-tailed t-test with Bonferroni post hoc test. AM = alveolar macrophages; MΦ = interstitial macrophages; DC = dendritic cells; Neut. = neutrophils.

0.799 ± 0.508 versus aged KO 0.346 ± 0.229) (Figure 4H), whereas no differences in expression were found for AT_1R in any case (Supplementary Figure 4D, <http://onlinelibrary.wiley.com/doi/10.1002/art.41100/abstract>).

Increased IFN γ -producing T cells, B cells, and macrophages and reduced Treg cells in the lungs of aged female PSGL-1 $^{-/-}$ mice. Because PSGL-1 is a leukocyte receptor, the pulmonary immune system was analyzed in female WT and PSGL-1 $^{-/-}$ mice. The total number of CD45+ cells was increased in the bronchoalveolar lavage (BAL) fluid and lung tissue of young and aged female PSGL-1 $^{-/-}$ mice (Figures 5A and B). Deeper analysis showed that the BAL fluid in young female mice had higher numbers of alveolar macrophages and neutrophils, and aged female mice had an increased number of neutrophils (Figure 5A). In the lung tissue, female PSGL-1 $^{-/-}$ mice showed increased numbers of neutrophils and T cells at a young age and an increased number of neutrophils when elderly (Figure 5B).

Because IFN γ has been associated with vascular dysfunction (25,26), the presence of IFN γ -producing cells was analyzed in the lung tissue. Interestingly, IFN γ -producing interstitial macrophages and T cell populations were increased in the lung tissue of young female PSGL-1 $^{-/-}$ mice, and the IFN γ -producing T cell subset was increased in aged female PSGL-1 $^{-/-}$ mice (Figure 5C and Supplementary Figure 5, <http://onlinelibrary.wiley.com/doi/10.1002/art.41100/abstract>). Notably, the analysis of B cell and T cell populations in the lung tissue showed that aged female PSGL-1 $^{-/-}$ mice had reduced percentages of IL-10-producing T cells and increased IFN γ -producing T cells and B cells (Figure 5D and Supplementary Figure 5), while the percentage of IL-17-producing populations was similar in WT and KO mice (Supplementary Figures 5A and B). Importantly, the percentage of Treg cells was

highly reduced in the T cell population, which increased the Th1/Treg cell balance in the lung tissue of aged female PSGL-1 $^{-/-}$ mice (Figure 5D and Supplementary Figure 5A).

Reduced ER α expression in aged female PSGL-1 $^{-/-}$ mice. To elucidate the molecular mechanisms responsible for the sex bias implicated in the development of pulmonary hypertension in female PSGL-1 $^{-/-}$ mice, the expression of estrogen receptors was quantified in lung lysates. Aging induced a reduction in the expression of ER β in a genotype- and sex-independent manner, with no differences between WT and KO mice (Figures 6A–C). In contrast, ER α expression increased with aging in female WT mice but not in female PSGL-1 $^{-/-}$ mice, while aging did not affect the expression of ER α in males, and no differences between male WT and PSGL-1 $^{-/-}$ mice were found (Figures 6D–F).

DISCUSSION

PAH is a particularly severe life-threatening complication of some CTDs that leads to RV remodeling, right heart failure, and premature death (27). Although many efforts have been made in searching for an efficient treatment for PAH, no curative therapy is available. Our work shows that female mice deficient in PSGL-1 exhibit reduced expression of pulmonary AT_2R and thickened small vessel walls. With aging, female PSGL-1 $^{-/-}$ mice show increased pulmonary levels of Ang II, which coincides with decreased eNOS phosphorylation and reduced NO production by lung ECs and leads to RV dysfunction and death. Interestingly, aged female PSGL-1 $^{-/-}$ mice have impaired ER α up-regulation.

The increase in relative wall vessel area in lung vasculature has been described as a histologic marker of PAH in both animal models and patients (1,4,27) and is thought to be one of the

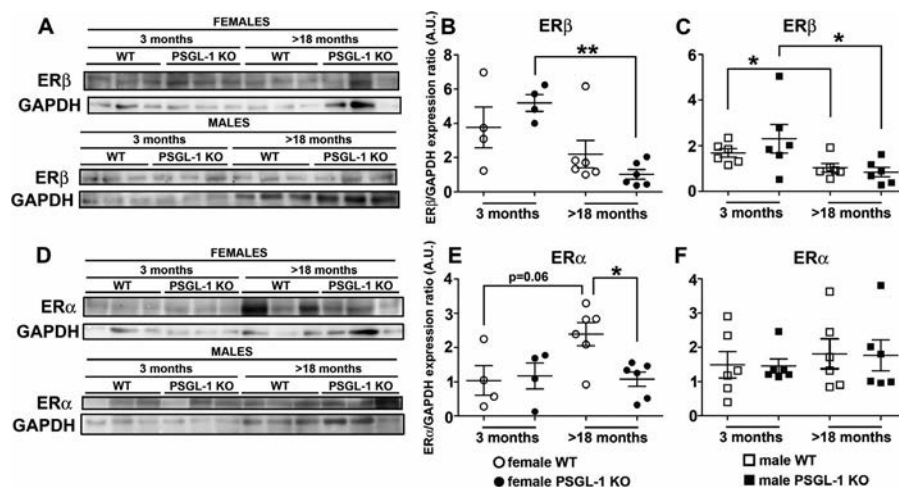


Figure 6. Analysis of estrogen receptor β (ER β) and ER α expression in the lungs of mice. **A–C,** Western blot (**A**) and quantification of the expression of ER β in the lungs of female (**B**) and male (**C**) wild-type (WT) and PSGL-1 $^{-/-}$ mice. **D–F,** Representative Western blot (**D**) and quantification of the expression of ER α in the lungs of female (**E**) and male (**F**) WT and PSGL-1 $^{-/-}$ mice. Symbols represent individual mice; bars show the mean \pm SEM. * = $P < 0.05$; ** = $P < 0.01$, by Mann-Whitney U-test.

first events that occurs in the development of PAH (2,12). The vascular remodeling observed in PSGL-1^{-/-} mice might cause an increase in the lung vascular resistance to blood flow, the main consequence of which would be the elevation of pressure in the pulmonary artery.

Transthoracic Doppler echocardiography is a noninvasive diagnostic tool for patients with suspected PAH, providing information not only about diagnosis but also about the causes or consequences of PAH (27,28). This method has been validated for estimating PAP in PAH patients and in rat and mouse models (20–23,29) and is becoming increasingly more relevant in murine models of heart diseases (30). Using this echocardiography modality, and in accordance with the pulmonary vessel remodeling, we found a reduced PAAT:ET ratio in the pulmonary arteries of 3-month-old female PSGL-1^{-/-} mice, suggesting that PSGL-1^{-/-} mice are susceptible to PH at young age. Importantly, female PSGL-1^{-/-} mice had preserved ejection fraction and E/A ratio, indicating that the incremental increase in PAP was not a consequence of an alteration in LV systolic/diastolic function or an elevated systemic arterial pressure, which suggests primary PAH.

Reduced expression of AT₂R, together with increased Ang II concentration, reduced eNOS phosphorylation at Ser¹¹⁷⁶, and NO production by ECs, was found in the lungs of aged female PSGL-1^{-/-} mice. This might explain the higher contractility and reduced relaxation capability of lung arteries at this age, which ultimately leads to an elevated flow resistance and then to increased pulmonary pressure and a reduced PAAT:ET ratio. In this context, pentraxin 3, a soluble ligand of P-selectin that interferes with the PSGL-1–P-selectin interaction (31,32), induced endothelial dysfunction and increased blood pressure (32), suggesting that PSGL-1 binding to P-selectin may be involved in the maintenance of correct endothelial function and integrity.

Molecular systems involved in the control of vascular tone, such as endothelin 1, Ang II, and NO, have been described as being altered in several animal models and in patients with PAH (4,7,27). In our model, we found elevated lung concentrations of Ang II in aged female PSGL-1^{-/-} mice. Thus, hypoxic and monocrotaline-treated rats showed increased Ang II and AT₁R levels (11,33,34), and patients with PAH showed higher levels of pulmonary Ang II due to increased activity of ACE, as well as increased expression and signaling of AT₁R, resulting in augmented vascular smooth muscle cell (VSMC) proliferation (35). Inhibitors of the renin–angiotensin–aldosterone system (RAAS) have been shown to have an effect in reducing PAP and other PAH signs in some animal models and in pilot studies with small patient cohorts, highlighting the role of RAAS in the pathology of PAH. For example, treatment with losartan (AT₁R antagonist) or captopril (ACE inhibitor) was able to reduce mean PAP, RV hypertrophy, and lung VR in rats exposed to hypobaric hypoxia for 14 days (35,36). Although no differences in ACE expression were found in the lungs of female WT and PSGL-1^{-/-} mice, the increased levels of pulmonary Ang II found in aged female PSGL-1^{-/-} mice might

be explained by enhanced ACE activity, which has previously been reported in patients with PAH and in animal models (35,37).

NO is a critical regulator of vascular homeostasis, not only by modulating vascular tone but also by controlling VSMC proliferation and migration and leukocyte adhesion to endothelium (27,38). Accordingly, reduced NO production by PSGL-1^{-/-} mouse lung ECs, together with a reduction of eNOS phosphorylated on Ser¹¹⁷⁶ in lung lysates, suggests an impairment of eNOS activation (39). Interestingly, the reduction of NO is not due to NO sequestering by ROS. It has been reported that an increase in Ang II could lead to eNOS uncoupling, which results in reduced NO production (25).

Several studies have highlighted the relevant role of inflammation and the immune system in endothelial dysfunction (25,26,40). Importantly, the Treg cell population is reduced and the balance between effector cells in each leukocyte subset is altered in aged PSGL-1^{-/-} mice, as previously described in the colon and skin of these mice (15,16). In this context, it was observed that vascular dysfunction in aortic ECs can be mediated by inflammatory monocytes and natural killer cells producing IFN γ and IL-12 in an Ang II–dependent manner (25,26). A similar mechanism could be operating in the pulmonary vasculature of female PSGL-1^{-/-} mice, in which aging increases IFN γ production in B cells and T cells as well as pulmonary Ang II levels that can account for the endothelial dysfunction with the ensuing reduction in the endothelial NO. Moreover, we found a reduction in the lung Treg cell population. In this regard, hypoxic mice treated with Treg cells showed reduced RV systolic pressure and Fulton index scores, accompanied by a reduction of the expression of proinflammatory cytokines (41). Furthermore, patients with CTD-associated PAH showed reduced numbers of circulating Treg cells, illustrating the importance of this T cell subset in the pathogenesis of PAH (42).

The mechanisms that mediate sex bias in pulmonary hypertension have not yet been described. It has been suggested that 17 β estradiol exerts vasoprotective actions through both ER α and ER β (43). In ECs, ER α promotes eNOS phosphorylation in a phosphatidylinositol 3-kinase– and Akt-dependent manner (44–48). In addition, treatment with Ang II promotes vascular adhesion and migration of leukocytes, which can be abolished through treatment with 17 β estradiol (49,50) and exacerbated by incubation with L-N^G-nitroarginine methyl ester (51). Moreover, coculture with Treg cells induces the up-regulation of ER α and ER β in human cardiac microvascular ECs and increases culture supernatant concentrations of plasma prostacyclin and IL-10 (52). In female PSGL-1^{-/-} mice, the reduction in the percentage of Treg cells could explain why the pulmonary levels of ER α were not increased with aging, declining at the same time as the phosphorylation of eNOS and NO production. Our data also indicate that the increase in ER α expression along with aging may prevent the increase of Ang II in female WT mice, which has recently been described in the context of hepatic ischemia-reperfusion injury (53). Notably, ER α expression in males is not regulated by aging, suggesting that it is not as crucial in males as in females to control

Ang II elevation and to increase NO production. These observations may explain why female PSGL-1^{-/-} mice develop PAH. Since PSGL-1 might participate in the control of ER α expression with aging, it would be of great interest to understand the molecular mechanisms implicated.

Our findings demonstrate that, with aging, female PSGL-1^{-/-} mice develop PH as part of an SSc-like autoimmune syndrome. Our study highlights the importance of leukocyte–endothelium interactions for the maintenance of vascular homeostasis in lungs and protection against PAH. Leukocytic deficiency of PSGL-1, which interacts with P-selectin and E-selectin on the surface of activated endothelium, reduces the presence of Treg cells in the lungs and the expression of ER α in females and also promotes endothelial dysfunction characterized by reduced vasodilation response due to impaired NO production. This impairment in endothelial function leads to vascular remodeling, PH, and, ultimately, premature death in mice.

ACKNOWLEDGMENTS

We thank the UAM and CNIC animal facilities for animal breeding and care. We are indebted to Ana Vanesa Alonso and Lorena Flores (Vascular Imaging Unit at CNIC) for performing echocardiography examinations. We also thank the Cytometry Unit and Statistical and Methodological Support Unit of the Hospital de la Princesa for technical support. We thank Dr. Kenneth McCreath for manuscript editing.

AUTHOR CONTRIBUTIONS

All authors were involved in drafting the article or revising it critically for important intellectual content, and all authors approved the final version to be published. Dr. Urzainqui had full access to all of the data in the study and takes responsibility for the integrity of the data and the accuracy of the data analysis.

Study conception and design. González-Tajuelo, Urzainqui.

Acquisition of data. González-Tajuelo, de la Fuente-Fernández, Morales-Cano, Muñoz-Callejas, González-Sánchez, Silván, Serrador, Cadenas, Barreira, Espartero-Santos, Jiménez-Borreguero, Urzainqui.





Analysis and interpretation of data. González-Tajuelo, Serrador, Gamallo, Vicente-Rabaneda, Castañeda, Pérez-Vizcaino, Cogolludo, Jiménez-Borreguero, Urzainqui.

REFERENCES

- Farber H, Loscalzo J. Pulmonary arterial hypertension. *N Engl J Med* 2004;351:1655–65.
- Leopold JA, Maron BA. Molecular mechanisms of pulmonary vascular remodeling in pulmonary arterial hypertension. *Int J Mol Sci* 2016;17:E761.
- Vonk Noordegraaf A, Westerhof B, Westerhof N. The relationship between the right ventricle and its load in pulmonary hypertension. *J Am Coll Cardiol* 2017;69:236–43.
- Montani D, Günther S, Dorfmueller P, Perros F, Girerd B, Garcia G, et al. Pulmonary arterial hypertension [review]. *Orphanet J Rare Dis* 2013;8:97.
- Derrett-Smith EC, Dooley A, Gilbane AJ, Trinder SL, Khan K, Baliga R, et al. Endothelial injury in a transforming growth factor β -dependent mouse model of scleroderma induces pulmonary arterial hypertension. *Arthritis Rheum* 2013;65:2928–39.
- Rhee RL, Gabler NB, Praestgaard A, Merkel PA, Kawut SM. Adverse events in connective tissue disease-associated pulmonary arterial hypertension. *Arthritis Rheumatol* 2015;67:2457–65.
- Maron BA, Leopold JA. The role of the renin-angiotensin-aldosterone system in the pathobiology of pulmonary arterial hypertension (2013 Grover Conference Series) [review]. *Pulm Circ* 2014;4:200–10.
- Gaddam RR, Chambers S, Bhatia M. ACE and ACE2 in inflammation: a tale of two enzymes. *Inflamm Allergy Drug Targets* 2014;13:224–34.
- Liu SS, Wang HY, Tang JM, Zhou XM. Hypoxia-induced collagen synthesis of human lung fibroblasts by activating the angiotensin system. *Int J Mol Sci* 2013;14:24029–45.
- Bruce E, Shenoy V, Rathinasabapathy A, Espejo A, Horowitz A, Oswald A, et al. Selective activation of angiotensin AT2 receptors attenuates progression of pulmonary hypertension and inhibits cardiopulmonary fibrosis. *Br J Pharmacol* 2015;172:2219–31.
- Yuan YM, Luo L, Guo Z, Yang M, Ye RS, Luo C. Activation of renin-angiotensin-aldosterone system (RAAS) in the lung of smoking-induced pulmonary arterial hypertension (PAH) rats. *J Renin Angiotensin Aldosterone Syst* 2015;16:249–53.
- Maron BA, Loscalzo J. Pulmonary hypertension: pathophysiology and signaling pathways. In: Humbert M, Evgenov OV, Stasch JP editors. *Pharmacotherapy of pulmonary hypertension*. Heidelberg: Springer, 2013. p. 31–58.
- Zarbock A, Ley K, McEver RP, Hidalgo A. Leukocyte ligands for endothelial selectins: specialized glycoconjugates that mediate rolling and signaling under flow. *Blood* 2011;118:6743–51.
- Urzainqui A, Martínez del Hoyo G, Lamana A, de la Fuente H, Barreiro O, Olazabal IM, et al. Functional role of P-selectin glycoprotein ligand 1/P-selectin interaction in the generation of tolerogenic dendritic cells. *J Immunol* 2007;179:7457–65.
- Pérez-Frías A, González-Tajuelo R, Núñez-Andrade N, Tejedor R, García-Blanco MJ, Vicente-Rabaneda E, et al. Development of an autoimmune syndrome affecting the skin and internal organs in P-selectin glycoprotein ligand 1 leukocyte receptor-deficient mice. *Arthritis Rheumatol* 2014;66:3178–89.
- Núñez-Andrade N, Lamana A, Sancho D, Gisbert JP, Gonzalez-Amaro R, Sanchez-Madrid F, et al. P-selectin glycoprotein ligand-1 modulates immune inflammatory responses in the enteric lamina propria. *J Pathol* 2011;224:212–21.
- He X, Schoeb TR, Panoskaltis-Mortari A, Zinn KR, Kesterson RA, Zhang J, et al. Deficiency of P-selectin or P-selectin glycoprotein ligand-1 leads to accelerated development of glomerulonephritis and increased expression of CC chemokine ligand 2 in lupus-prone mice. *J Immunol* 2006;177:8748–56.
- Rivera-Nieves J, Burcin T, Olson T, Morris MA, McDuffie M, Cominelli F, et al. Critical role of endothelial P-selectin glycoprotein ligand 1 in chronic murine ileitis. *J Exp Med* 2006;203:907–17.
- Angiari S, Rossi B, Piccio L, Zinselmeyer BH, Budui S, Zenaro E, et al. Regulatory T cells suppress the late phase of the immune response in lymph nodes through P-selectin glycoprotein ligand-1. *J Immunol* 2013;191:5489–500.
- Thibault H, Kurtz B, Raheer M, Shaik RS, Waxman A, Derumeaux G, et al. Noninvasive assessment of murine pulmonary arterial pressure: validation and application to models of pulmonary hypertension. *Circ Cardiovasc Imaging* 2010;3:157–63.
- Yared K, Noseworthy P, Weyman A, McCabe E, Picard MH, Baggish AL. Pulmonary artery acceleration time provides an accurate estimate of systolic pulmonary arterial pressure during transthoracic echocardiography. *J Am Soc Echocardiogr* 2011;24:687–92.
- Urboniene D, Haber I, Fang YH, Thenappan T, Archer SL. Validation of high-resolution echocardiography and magnetic resonance imaging vs. high-fidelity catheterization in experimental pulmonary hypertension. *Am J Physiol Lung Cell Mol Physiol* 2010;299:401–12.

23. Tania NP, Maarsingh H, Bos ST, Mattiotti A, Prakash S, Timens W, et al. Endothelial follistatin-like-1 regulates the postnatal development of the pulmonary vasculature by modulating BMP/Smad signaling. *Pulm Circ* 2017;7:219–31.
24. Cogolludo A, Frazziano G, Briones A, Cobeño L, Moreno L, Lodi F, et al. The dietary flavonoid quercetin activates BKCa currents in coronary arteries via production of H₂O₂. Role in vasodilatation. *Cardiovasc Res* 2007;73:424–31.
25. Kossmann S, Hu H, Steven S, Schönfelder T, Fraccarollo D, Mikhed Y, et al. Inflammatory monocytes determine endothelial nitric-oxide synthase uncoupling and nitro-oxidative stress induced by angiotensin II. *J Biol Chem* 2014;289:27540–50.
26. Kossmann S, Schwenk M, Hausding M, Karbach SH, Schmidgen MI, Brandt M, et al. Angiotensin II-induced vascular dysfunction depends on interferon- γ -driven immune cell recruitment and mutual activation of monocytes and NK-cells. *Arterioscler Thromb Vasc Biol* 2013;33:1313–9.
27. Rabinovitch M. Molecular pathogenesis of pulmonary arterial hypertension. *J Clin Invest* 2012;122:4306–13.
28. Bleeker GB, Steendijk P, Holman ER, Yu CM, Breithardt OA, Kaandorp TA, et al. Assessing right ventricular function: the role of echocardiography and complementary technologies. *Heart* 2006;92:i19–26.
29. Brittain E, Penner NL, West J, Hemnes A. Echocardiographic assessment of the right heart in mice. *J Vis Exp* 2013;81:50912.
30. Chen G, Li Y, Tian J, Zhang L, Jean-Charles P, Gobara N, et al. Application of echocardiography on transgenic mice with cardiomyopathies. *Biochem Res Int* 2012;2012:7151972.
31. Deban L, Russo RC, Sironi M, Moalli F, Scanziani M, Zambelli V, et al. Regulation of leukocyte recruitment by the long pentraxin PTX3. *Nat Immunol* 2010;11:328–34.
32. Carrizzo A, Lenzi P, Procaccini C, Damato A, Biagioni F, Ambrosio M, et al. Pentraxin 3 induces vascular endothelial dysfunction through a P-selectin/matrix metalloproteinase-1 pathway. *Circulation* 2015;131:1495–505.
33. Becker MO, Kill A, Kutsche M, Guenther J, Rose A, Tabeling C, et al. Vascular receptor autoantibodies in pulmonary arterial hypertension associated with systemic sclerosis. *Am J Respir Crit Care Med* 2014;190:808–17.
34. Li G, Liu Y, Zhu Y, Liu A, Xu Y, Li X, et al. ACE2 activation confers endothelial protection and attenuates neointimal lesions in prevention of severe pulmonary arterial hypertension in rats. *Lung* 2013;191:327–36.
35. De Man FS, Tu L, Handoko ML, Rain S, Ruitter G, François C, et al. Dysregulated renin–angiotensin–aldosterone system contributes to pulmonary arterial hypertension. *Am J Respir Crit Care Med* 2012;186:780–9.
36. Morrell N, Morris K, Stenmark KR. Role of angiotensin-converting enzyme and angiotensin II in development of hypoxic pulmonary hypertension. *Am J Physiol* 1995;269:1186–94.
37. Shenoy V, Qi Y, Katovich MJ, Raizada MK. ACE2, a promising therapeutic target for pulmonary hypertension. *Curr Opin Pharmacol* 2011;11:150–5.
38. Martinelli R, Gegg M, Longbottom R, Adamson P, Turowski P, Greenwood J. ICAM-1-mediated endothelial nitric oxide synthase activation via calcium and AMP-activated protein kinase is required for transendothelial lymphocyte migration. *Mol Biol Cell* 2009;20:995–1005.
39. Zhao Y, Vanhoutte PM, Leung SW. Vascular nitric oxide: beyond eNOS. *J Pharmacol Sci* 2015;129:83–94.
40. Stenmark K, Meyrick B, Galie N, Mooi WJ, McMurtry IF. Animal models of pulmonary arterial hypertension: the hope for etiological discovery and pharmacological cure. *Am J Physiol Lung Cell Mol Physiol* 2009;297:L1013–32.
41. Chu Y, Xiangli X, Xiao W. Regulatory T cells protect against hypoxia-induced pulmonary arterial hypertension in mice. *Mol Med Rep* 2015;11:3181–7.
42. Gaowa S, Zhou W, Yu L, Zhou X, Liao K, Yang K, et al. Effect of Th17 and Treg axis disorder on outcomes of pulmonary arterial hypertension in connective tissue diseases. *Mediators Inflamm* 2014;2014:247372.
43. Austin ED, Lahm T, West J, Tofovic SP, Johansen AK, MacLean MR, et al. Gender, sex hormones and pulmonary hypertension. *Pulm Circ* 2013;3:294–314.
44. Lantin-Hermoso RL, Rosenfeld CR, Yuhanna IS, German Z, Chen Z, Shaul PW. Estrogen acutely stimulates nitric oxide synthase activity in fetal pulmonary artery endothelium. *Am J Physiol* 1997;273:L119–26.
45. Chambliss K, Shaul PW. Estrogen modulation of endothelial nitric oxide synthase. *Endocr Rev* 2002;23:665–86.
46. Simoncini T, Hafezi-Moghadam A, Brazil DP, Ley K, Chin WW, Liao JK. Interaction of oestrogen receptor with the regulatory subunit of phosphatidylinositol-3-OH kinase [letter]. *Nature* 2000;407:538–41.
47. Hisamoto K, Ohmichi M, Kurachi H, Hayakawa J, Kanda Y, Nishio Y, et al. Estrogen induces the Akt-dependent activation of endothelial nitric-oxide synthase in vascular endothelial cells. *J Biol Chem* 2001;276:3459–67.
48. Stirone C, Boroujerdi A, Duckles SP, Krause DN. Estrogen receptor activation of phosphoinositide-3 kinase, akt, and nitric oxide signaling in cerebral blood vessels: rapid and long-term effects. *Mol Pharmacol* 2005;67:105–13.
49. Álvarez Á, Cerdá-Nicolás M, Nabah YN, Mata M, Issekutz AC, Panés J, et al. Direct evidence of leukocyte adhesion in arterioles by angiotensin II. *Blood* 2004;104:402–8.
50. Alvarez A, Hermenegildo C, Issekutz A, Esplugues J, Sanz MJ. Estrogens inhibit angiotensin II-induced leukocyte-endothelial cell interactions in vivo via rapid endothelial nitric oxide synthase and cyclooxygenase activation. *Circ Res* 2002;91:1142–50.
51. Nabah YN, Mateo T, Cerdá-Nicolás M, Alvarez A, Martinez M, Issekutz AC, et al. L-NAME induces direct arteriolar leukocyte adhesion, which is mainly mediated by angiotensin-II. *Microcirculation* 2005;12:443–53.
52. Tamosiuniene R, Manouvakhova O, Mesange P, Saito T, Qian J, Sanyal M, et al. Dominant role for regulatory T cells in protecting females against pulmonary hypertension. *Circ Res* 2018;122:1689–702.
53. Li W, Li D, Sun L, Li Z, Yu L, Wu S. The protective effects of estrogen on hepatic ischemia-reperfusion injury in rats by downregulating the Ang II/AT1R pathway. *Biochem Biophys Res Commun* 2018;503:2543–8.

Multicenter Prospective Study of the Efficacy and Safety of Combined Immunosuppressive Therapy With High-Dose Glucocorticoid, Tacrolimus, and Cyclophosphamide in Interstitial Lung Diseases Accompanied by Anti-Melanoma Differentiation-Associated Gene 5-Positive Dermatomyositis

Hideaki Tsuji,¹ Ran Nakashima,¹  Yuji Hosono,² Yoshitaka Imura,³ Masato Yagita,³ Hajime Yoshifuji,¹ Shintaro Hirata,⁴  Takaki Nojima,⁴ Eiji Sugiyama,⁴ Kazuhiro Hatta,⁵ Yoshio Taguchi,⁵ Masaki Katayama,⁶  Kiminobu Tanizawa,¹ Tomohiro Handa,¹ Ryuji Uozumi,¹  Shuji Akizuki,¹ Kosaku Murakami,¹ Motomu Hashimoto,¹ Masao Tanaka,¹ Koichiro Ohmura,¹ and Tsuneyo Mimori¹

Objective. Interstitial lung disease (ILD) accompanied by anti-melanoma differentiation-associated gene 5 (anti-MDA-5)-positive dermatomyositis (DM) is often rapidly progressive and associated with poor prognosis. Because there is no established treatment, we undertook this study to prospectively evaluate the efficacy and safety of a combined immunosuppressive regimen for anti-MDA-5-positive DM patients with ILD.

Methods. Adult Japanese patients with new-onset anti-MDA-5-positive DM with ILD ($n = 29$) were enrolled at multiple study centers from 2014 to 2017. They were treated with a regimen of high-dose glucocorticoids (GCs), tacrolimus, and intravenous cyclophosphamide (IV CYC). Plasmapheresis was used if a patient's condition worsened after the regimen started. The primary end point was 6-month survival, which was compared between this group of patients and a historical control group ($n = 15$) consisting of anti-MDA-5-positive DM patients with ILD who received step-up treatment (high-dose GC and stepwise addition of immunosuppressant). Secondary end points were 12-month survival rate, adverse events, and changes in laboratory data.

Results. The combined immunosuppressive regimen group showed significantly higher 6-month survival rates than the step-up treatment group (89% versus 33%; $P < 0.0001$). Over a period of 52 weeks, improvements in anti-MDA-5 titers, serum ferritin levels, vital capacity, and chest high-resolution computed tomography scores were observed. The combined immunosuppressive regimen group received IV CYC nearly 20 days earlier with shorter intervals and tended to receive plasmapheresis more often than patients undergoing step-up treatment. Cytomegalovirus reactivation was frequently observed over 52 weeks.

Conclusion. A combined immunosuppressive regimen is effective for anti-MDA-5-positive DM patients with ILD. Plasmapheresis can be used for additional effect in intractable disease. Patients should be carefully monitored for opportunistic infections during treatment.

INTRODUCTION

Idiopathic inflammatory myopathies (IIMs) are heterogeneous autoimmune diseases that affect skeletal muscle and various

organs, including the skin, lungs, heart, and joints. IIMs have been categorized on the basis of clinical phenotype or histopathologic characteristics; however, recent studies have focused on the utility of myositis-specific autoantibodies (MSAs) for

Supported in part by the Japan Society for the Promotion of Science (grants JP25293222 and 16H05341 to Dr. Mimori).

¹Hideaki Tsuji, MD, Ran Nakashima, MD, PhD, Hajime Yoshifuji, MD, PhD, Kiminobu Tanizawa, MD, PhD, Tomohiro Handa, MD, PhD, Ryuji Uozumi, PhD, Shuji Akizuki, MD, Kosaku Murakami, MD, PhD, Motomu Hashimoto, MD, PhD, Masao Tanaka, MD, PhD, Koichiro Ohmura, MD, PhD, Tsuneyo Mimori, MD, PhD: Kyoto University Graduate School of Medicine, Kyoto, Japan; ²Yuji

Hosono, MD, PhD: National Institute of Arthritis and Musculoskeletal and Skin Diseases, NIH, Bethesda, Maryland; ³Yoshitaka Imura, MD, PhD, Masato Yagita, MD, PhD: Kitano Hospital, Osaka, Japan; ⁴Shintaro Hirata, MD, PhD, Takaki Nojima, MD, PhD, Eiji Sugiyama, MD, PhD: Hiroshima University Hospital, Hiroshima, Japan; ⁵Kazuhiro Hatta, MD, Yoshio Taguchi, MD: Tenri Hospital, Tenri, Japan; ⁶Masaki Katayama, MD, PhD: Osaka Red Cross Hospital, Osaka, Japan.

subcategorization of IIMs and corresponding clinical management (1). Clinically amyopathic dermatomyositis (CADM) is defined as a manifestation of typical skin lesions of dermatomyositis (DM) with few or no features of myopathy. Anti-melanoma differentiation-associated gene 5 (anti-MDA-5) antibody, an MSA, is reportedly strongly associated with CADM (2). Anti-MDA-5-positive DM/CADM patients often exhibit rapidly progressive interstitial lung disease (ILD), which results in substantial mortality due to respiratory failure (3,4). Rapidly progressive ILD in patients with anti-MDA-5-positive DM/CADM is more frequent in Asian populations than in European or American populations (39–71% versus 22–57%) (3–10); furthermore, anti-MDA-5 is one of the most important prognostic factors in DM/CADM patients with ILD in Asia. The source of rapidly progressive ILD has not been fully clarified, but is thought to be affected by genetic susceptibility and environmental factors (11–14).

A standard treatment for rapidly progressive ILD in patients with anti-MDA-5-positive DM/CADM has not yet been established. The 6-month survival rate of patients undergoing conventional treatment with glucocorticoids (GCs) alone or a combination of GCs and additional immunosuppressants (step-up therapy) is 28–66% in Asian patients (1,3,7). Failure of these treatments seems to be partly related to rapid progression of alveolar damage before achieving sufficient immunosuppression. Recently, some case reports have suggested that a combined immunosuppressive therapy might be efficacious; this type of therapy includes high-dose GCs, calcineurin inhibitors (CNIs), and intravenous cyclophosphamide (IV CYC), which are administered beginning in the early phase of rapidly progressive ILD with DM/CADM (15–18). In addition, we have observed the effectiveness of such combination therapy in the early stage of rapidly progressive ILD in Japanese patients with anti-MDA-5-positive DM/CADM, compared to those receiving step-up therapy (75% versus 29%) at our hospital

(1). However, there has not been a prospective trial examining the efficacy and safety of this combination therapy. Therefore, we conducted a single-arm clinical trial to assess the efficacy and safety of a combined immunosuppressive regimen comprising high-dose GCs, tacrolimus, and IV CYC for anti-MDA-5-positive DM/CADM with ILD. To the best of our knowledge, this is the first prospective trial involving DM/CADM patients with ILD and a particular MSA, anti-MDA-5, who show relatively uniform clinical characteristics and pathophysiology.

PATIENTS AND METHODS

Design overview. This study was conducted at 5 hospitals between July 1, 2014 and August 31, 2017. Figure 1 outlines the study design. In this clinical study, anti-MDA-5-positive DM/CADM patients with ILD who were treated with a combined immunosuppressive regimen (high-dose GCs, tacrolimus, and IV CYC) were compared to an existing historical control group, which comprised patients who were treated with step-up treatment (control group A: high-dose GCs were initially used and immunosuppressants were added stepwise based on deterioration of the patients' clinical conditions). An additional historical control group of patients who were treated with a combined immunosuppressive regimen without plasmapheresis prior to this study (control group B) was compared to the group of patients who participated in this prospective study.

DM was diagnosed in accordance with the criteria developed by Bohan and Peter (19); CADM was diagnosed when patients had typical cutaneous lesions of DM without clinical evidence of myositis and with minimal or no increase in serum creatine kinase (CK) levels, as described previously (20,21). The diagnosis of ILD was based on respiratory symptoms, physical examinations, chest high-resolution computed tomography (HRCT) findings, and pulmonary function tests. Patients were eligible to be enrolled

Dr. Nakashima has received speaking fees from Bristol-Myers Squibb and Astellas Pharma (less than \$10,000 each) and research support from Medical & Biological Laboratories Co. Dr. Yagita owns the licensing rights for a patent owned by Onkimmune for a cell line. Dr. Yoshifuji has received speaking fees and/or honoraria from Nippon Shinyaku Co., Actelion, Mochida Pharmaceutical, Bayer, and Eisai (less than \$10,000 each) and from Chugai Pharma (more than \$10,000) and research support from Astellas Pharma. Dr. Hirata has received consulting fees, speaking fees, and/or honoraria from AbbVie, Asahi Kasei Pharma, Asahi Kasei Medical, Astellas Pharma, AYUMI, Bristol-Myers Squibb, Celgene, Chugai Pharmaceutical, Eisai, Eli Lilly, Janssen, Kissei, Novartis, Pfizer, Sanofi, Takeda Chemical Industries, Mitsubishi Tanabe Pharma, and UCB (less than \$10,000 each) and research support from those companies. Dr. Nojima has received consulting fees, speaking fees, and/or honoraria from Asahi Kasei Pharma, Astellas Pharma, AYUMI, Bristol-Myers Squibb, Chugai Pharmaceutical, Eisai, Eli Lilly, Janssen, Pfizer, Sanofi, Takeda Chemical Industries, Mitsubishi Tanabe Pharma, and UCB (less than \$10,000 each) and research support from those companies. Dr. Taguchi has received speaking fees from Boehringer Ingelheim (more than \$10,000 each). Dr. Tanizawa has received research support from Eisai and Mitsubishi Tanabe Pharma. Dr. Handa owns stock or stock options in Teijin and has received research support from Teijin. Dr. Uozumi has received consulting fees from Eisai (less than

\$10,000) and from CAC Croit (more than \$10,000). Dr. Murakami has received research support from Eisai and Mitsubishi Tanabe Pharma. Dr. Hashimoto has received speaking fees from Astellas Pharma and Eisai (less than \$10,000 each) and from Bristol-Myers Squibb and Mitsubishi Tanabe Pharma (more than \$10,000 each) and research support from Bristol-Myers Squibb, Astellas Pharma, Mitsubishi Tanabe Pharma, Eisai Chugai Pharmaceutical, AYUMI, and UCB. Dr. Tanaka has received speaking fees from Pfizer, Asahi Kasei Pharma, Taisho Pharmaceutical, Eisai, Takeda Chemical Industries, Bristol-Myers Squibb, Chugai Pharmaceutical, Eli Lilly, UCB, Janssen, Mitsubishi Tanabe Pharma, and Novartis (less than \$10,000 each) and from AbbVie GK and Astellas Pharma (more than \$10,000 each) and research support from Pfizer, Astellas Pharma, AbbVie GK, Taisho Toyama Pharmaceutical Co., Takeda Chemical Industries, Mitsubishi Tanabe Pharma, Chugai Pharmaceutical, AYUMI, UCB, and Eisai. Dr. Mimori has received speaking fees from Bristol-Myers Squibb, Chugai Pharmaceutical, Pfizer, and Mitsubishi Tanabe Pharma (less than \$10,000 each) and research support from Actelion, Astellas Pharma, Asahi Kasei Pharma, AYUMI, Chugai Pharmaceutical, Daiichi Sankyo, Eisai, JB Chemicals and Pharmaceuticals, Mitsubishi Tanabe Pharma, MSD, Nippon Shinyaku, Pfizer, Sanofi, and Takeda Chemical Industries. No other disclosures relevant to this article were reported.

Address correspondence to Ran Nakashima, MD, PhD, Kyoto University Graduate School of Medicine, Department of Rheumatology and Clinical Immunology, Kyoto 606-8507, Japan. E-mail: ranran@kuhp.kyoto-u.ac.jp.

Submitted for publication April 19, 2019; accepted in revised form September 10, 2019.

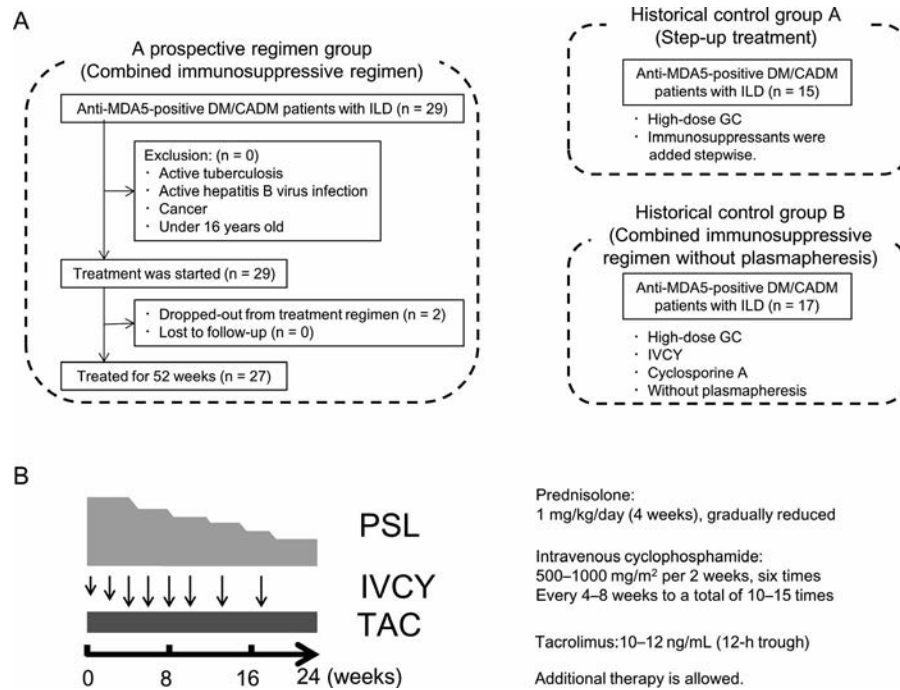


Figure 1. Study participants and combined immunosuppressive regimen. **A**, Flow diagram of the study participants. **B**, Combined immunosuppressive therapy regimen for anti-melanoma differentiation-associated gene 5 (anti-MDA-5)-positive dermatomyositis (DM)/clinically amyopathic dermatomyositis (CADM) patients with rapidly progressive interstitial lung disease (ILD). High-dose prednisolone (PSL), oral tacrolimus (TAC), and intravenous cyclophosphamide (IVCY) were used in combination. GC = glucocorticoid.

in the study if they were diagnosed as having definite, probable, or possible DM or CADM with ILD—without immunosuppressive treatment—before admission to one of the registered hospitals. Serum anti-MDA-5 was detected by immunoprecipitation (IP) assay using ³⁵S-labeled HeLa cells and confirmed by anti-MDA-5 enzyme-linked immunosorbent assay (ELISA; Mesacup). Patients with the following conditions were excluded: active tuberculosis, active hepatitis B virus infection, cancer, and patients <16 years of age. The follow-up period was 52 weeks. This study was conducted in accordance with the Declaration of Helsinki and its amendments, and it was approved by the ethics committee at each institution and registered in the University Hospital Medical Information Network (UMIN00014344). Written informed consent was obtained from all patients prior to enrollment.

Combined immunosuppressive regimen. The combined immunosuppressive regimen consisted of prednisolone, tacrolimus, and IV CYC. The treatment was initiated soon after a patient received a diagnosis of DM or CADM with ILD (Figure 1). Prednisolone was initially administered at 1 mg/kg/day for 4 weeks; thereafter, the existing dose was reduced by 10% every 2 weeks when the dose was >30 mg daily and every 2–4 weeks when it was <30 mg daily. Tacrolimus was adjusted to retain 12-hour blood trough levels within the range of 10–12 ng/mL. IV CYC was initiated at 500 mg/m² of body surface area biweekly, then gradually increased to a maximum of 1,000 mg/m² of body surface area; this was implemented

with the goal of a nadir leukocyte count of 2,000–3,000/μl or a 50% reduction from baseline. After the sixth administration of IV CYC, the interval was extended to 4–8 weeks. The intended number of IV CYC administrations was 10–15.

Additional therapy was permitted when a patient's condition worsened to the point of requiring oxygen administration during treatment; such therapy included plasmapheresis. Plasmapheresis was performed 1–3 times per week for 3–13 consecutive weeks. During plasmapheresis, 1–1.3 volumes of plasma per session were removed, then replaced with an equivalent amount of fresh frozen plasma (FFP-LR480; Nisseki) or 5% albumin (Albuminar-5; CSL Behring KK). On the day of IV CYC treatment, extracellular fluid (Uromitexan) and mesna (Shionogi & Co.) were injected into the patients to prevent hemorrhagic cystitis (22). During treatment, the patients underwent regular monitoring of serum cytomegalovirus (CMV) antigenemia and β-D-glucan. Trimethoprim/sulfamethoxazole (TMP/SMX) was used for prophylaxis for *Pneumocystis jiroveci* pneumonia (PCP) (23). Patients were treated with antiviral drugs at an early stage if they were positive for CMV antigenemia or showed symptoms due to reactivation of CMV. Patients were treated in the outpatient department after their disease was in remission and their prednisolone dosage was <0.5 mg/kg/day.

Step-up treatment group as a historical control group. We included a historical control group consisting of anti-MDA-5-positive DM/CADM patients with ILD who were treated with a step-up protocol between August 1, 2001 and December

31, 2008 at Kyoto University Hospital (control group A). Anti-MDA-5 antibody levels were retrospectively measured using preserved patient sera.

Combined immunosuppressive regimen group without plasmapheresis as a historical control group. We included an additional historical control group consisting of anti-MDA-5-positive DM/CADM patients with ILD who received a combined immunosuppressive regimen of high-dose GCs, cyclosporin A, and IV CYC, without plasmapheresis, between September 1, 2008 and February 28, 2013 at Kyoto University Hospital (control group B).

Outcome measures: primary and secondary end points. The primary end point was 6-month survival rate, which was compared between the combined immunosuppressive regimen group and the historical control groups. Secondary end points included the following: 12-month survival rate, adverse events, changes in respiratory function, and changes in HRCT scores and laboratory data (i.e., serum ferritin level and anti-MDA-5 titer) during treatment courses.

Clinical and standard laboratory data. Baseline clinical characteristics, including laboratory data, were recorded at the time of admission. After admission to a hospital, electromyography, as well as muscle and skin biopsies, were performed as soon as possible. Chest HRCT and laboratory tests, including blood analysis and urinalysis, were performed at baseline and at 4, 8, 12, 16, 24, and 52 weeks after the initiation of treatment; blood gas tests were performed at baseline and at 12, 24, and 52 weeks, and respiratory function was tested at baseline and at 12 and 24 weeks. Blood tacrolimus trough levels were measured after 12 hours by chemiluminescent enzyme immunoassay (ARCHITECTMi1000; Abbott).

Adverse events. Adverse events associated with the study medication were recorded during the observation periods. Renal disorder during the treatment course was defined as an increase in the level of serum creatinine to >1.5-fold greater than the baseline level (24).

Detection of anti-MDA-5 antibody in IP assay. MSAs in sera were determined by IP assay, as previously described (3). Briefly, 10 μ l of patient sera was mixed with 2 mg of protein A-Sepharose CL-4B (GE Healthcare) in 500 ml of IP buffer (10 mM Tris HCl [pH 8.0], 500 mM NaCl, 0.1% Nonidet P40) and incubated on a rotator device for 2 hours at 4°C. Subsequently, the IgG-coated Sepharose was washed, then suspended in 400 ml of IP buffer for polypeptide studies. HeLa cells (2×10^7) in 100 ml of methionine-free medium were labeled with 18.5 MBq of 35 S-methionine (Perkin Elmer) overnight at 37°C; they were then sonicated in 2 ml of IP buffer, and the supernatant was recovered

by centrifugation. Antibody-coated Sepharose beads were mixed with 100 ml of 35 S-methionine-labeled HeLa cell extracts, then rotated at 4°C for 2 hours. Subsequently, Sepharose beads were washed 5 times, then suspended in sodium dodecyl sulfate sample buffer; polypeptides were then fractionated by 6.5% sodium dodecyl sulfate-polyacrylamide gel electrophoresis and detected by autoradiography.

Anti-MDA-5 antibody ELISA. Anti-MDA-5 titers were measured by ELISA according to the instructions of the manufacturer; these measurements were performed at baseline and at 4, 8, 12, 16, 24, and 52 weeks after the initiation of treatment (2). The cutoff value was 32 units/ml as determined by receiver operating characteristic analysis (25).

Interpretation of chest HRCT images and scores. Chest HRCT scans of the patients were evaluated by trained pulmonologists (KT and TH) in a blinded and independent manner, in accordance with a previously reported classification (26–28). First, the pulmonologists classified chest HRCT results into the following patterns: usual interstitial pneumonia (UIP), probable UIP, nonspecific interstitial pneumonia (NSIP), organizing pneumonia (OP), NSIP with OP, or unclassifiable by chest HRCT. Second, the pulmonologists scored chest HRCT findings including airspace consolidation, ground-glass attenuation, and interlobular septal thickening and/or reticular opacity in each of 6 zones (upper, middle, and lower on both sides) during the treatment courses. Interobserver disagreement was resolved by consensus. Interobserver correlations between the 2 pulmonologists, determined using Spearman's rank correlation coefficient, were 0.79 ($P < 0.0001$) for airspace consolidation, 0.36 ($P = 0.002$) for ground-glass attenuation, and 0.73 ($P < 0.0001$) for interlobular septal thickening and/or reticular opacity.

Statistical analysis. The Mann-Whitney U test, Student's *t*-test, and Fisher's exact test were performed in order to assess associations of clinical features between groups. Survival was calculated from the date of the initial diagnosis to the date of death by any cause. Cumulative survival rates were estimated by Kaplan-Meier analysis; the log rank test was also used to compare survival rates. Pearson's correlation coefficient was used to examine the correlation between blood tacrolimus concentration and renal function. *P* values less than 0.05 were considered significant. *P* values for multiple comparisons were adjusted using the Bonferroni method. Statistical analyses were performed using JMP Pro 12 software (SAS Institute).

RESULTS

Clinical features of anti-MDA-5-positive DM/CADM patients with ILD. We enrolled anti-MDA-5-positive DM/CADM patients with ILD who visited any of the 5 registered hospitals ($n = 29$) (Figure 1). Two patients were withdrawn from the

treatment regimen because their treatment differed from that of the prescribed regimen during the observation period: administration of IV CYC was considerably delayed for 1 patient, and IV CYC was changed to infliximab for the other patient. We established a historical control group in which patients (n = 15) received step-up treatment of immunosuppressants (control group A). When these 2 groups were compared, there were no significant differences in age, sex, serum CK levels, cutaneous symptoms, or muscle symptoms (Table 1). The diffusing capacity for carbon monoxide percent predicted was higher in the combined immunosuppressive regimen group. The vital capacity percent predicted and the forced expiratory volume in 1 second/forced vital capacity did not differ between the 2 groups. In HRCT assessments, OP or unclassifiable patterns were mainly observed in both groups. The HRCT scores did not differ between the 2 groups. The levels of serum ferritin, lactate dehydrogenase (LDH), and anti-MDA-5 were elevated in both groups, relative to standard values.

Next, treatment was compared between the 2 groups. GCs were used for all patients in both groups. However, GC doses were slightly lower in the step-up treatment group. CNI, IV CYC, and combinations of these were used less frequently in the step-up treatment group (see Supplementary Table 1, on the *Arthritis & Rheumatology* web site at <http://onlinelibrary.wiley.com/doi/10.1002/art.41105/abstract>). Patients in the combined regimen group received a mean \pm SD of 9.37 ± 1.57 IV CYC treatments. In IV CYC-treated patients, the dose of cyclophosphamide was similar between the 2 groups (Supplementary Figure 1, <http://onlinelibrary.wiley.com/doi/10.1002/art.41105/abstract>); however, the intervals between IV CYC treatments tended to be longer in the step-up group than in the combined regimen group. Furthermore, we compared the timing of treatment initiation between the 2 groups: the duration from hospitalization to the beginning of IV CYC and CNI was nearly 20 days longer in the step-up treatment group, compared to that in the combined immunosuppressive regimen group (Supplementary Table 2, Supplementary Figure 1, <http://onlinelibrary.wiley.com/doi/10.1002/art.41105/abstract>). The periods from disease onset to the administration of GC, IV CYC, and CNI tended to be longer in the step-up treatment group than in the combined immunosuppressive regimen group, but this difference was not statistically significant. When a patient's condition worsened, additional treatment was applied.

Plasmapheresis tended to be used in more patients in the combined immunosuppressive regimen group than in the step-up treatment group (31% versus 7%), although this difference was not statistically significant (Supplementary Table 1, <http://onlinelibrary.wiley.com/doi/10.1002/art.41105/abstract>). During the combined immunosuppressive treatment, 11 patients exhibited worsened hypoxemia and required oxygen; of these, 9 patients received plasmapheresis (Supplementary Table 1). These patients received a mean \pm SD of 11.6 ± 3.95 plasmapheresis treatments, over a mean \pm SD of 45.6 ± 21.0 days. Among the 11 patients, 6

Table 1. Clinical features of the patients at the time of enrollment*

	Combined immunosuppressive regimen group (n = 29)	Step-up treatment control group (n = 15)
Diagnosis, no. (%)		
DM	14 (48)	9 (60)
CADM	15 (52)	6 (40)
Onset type, no. (%)†		
Acute	8 (30)	3 (20)
Subacute	15 (56)	7 (47)
Chronic	4 (15)	5 (33)
Female sex, no (%)	19 (66)	12 (80)
Age, years	53.4 \pm 13.5	57.6 \pm 9.08
BMI, kg/m ²	21.1 \pm 3.06	21.3 \pm 3.18
Heliotrope rash, no. (%)	13 (46)	7 (54)
Gotttron's sign, no. (%)	28 (97)	13 (87)
Skin ulcer, no. (%)	7 (24)	4 (57)
Proximal muscle weakness, no. (%)	13 (46)	8 (53)
CK, units/liter	284.7 \pm 324.6	357.3 \pm 484.3
Ferritin, ng/ml	689.7 \pm 973.9	1428.4 \pm 1895.7
LDH, units/liter	390.6 \pm 138.9	410 \pm 145.2
Creatinine, mg/dl	0.58 \pm 0.11	0.6 \pm 0.2
CRP, mg/dl	1.47 \pm 2.04	1.5 \pm 1.6
ESR, mm/hour	44.8 \pm 22.9	51.9 \pm 27.8
KL-6, units/ml	689.7 \pm 973.9	951.7 \pm 818.5
SP-D, ng/ml	64.6 \pm 57.2	54.8 \pm 40.5
Pao ₂ , mm Hg	80.3 \pm 13.9	76.0 \pm 7.9
Anti-MDA-5, units/ml	205.0 \pm 46.3‡	171.9 \pm 31.3
VC, % predicted	78.8 \pm 16.1	84.2 \pm 10.8
FEV ₁ /FVC	82.6 \pm 8.40	89.6 \pm 14.7
DLco, ml/minute/mm Hg	16.0 \pm 10.4	11.1 \pm 2.9
DLco, % predicted	62.0 \pm 14.9§	44.6 \pm 13.7
HRCT patterns, no. (%)¶		
NSIP and OP	3 (11)	1 (11)
OP	11 (39)	5 (56)
Unclassifiable	14 (50)	3 (33)
Total HRCT score	10.8 \pm 6.64	12.4 \pm 9.69
Airspace consolidation	3.87 \pm 3.63	3.24 \pm 2.49
Ground-glass attenuation	4.67 \pm 2.97	6.99 \pm 6.59
Interlobular septal thickening and/or reticular opacity	2.25 \pm 3.08	2.18 \pm 3.18

* Except where indicated otherwise, values are the mean \pm SD. DM = dermatomyositis; CADM = clinically amyopathic dermatomyositis; BMI = body mass index; CK = creatine kinase; LDH = lactate dehydrogenase; CRP = C-reactive protein; ESR = erythrocyte sedimentation rate; KL-6 = Krebs von den Lungen 6; SP-D = surfactant protein D; anti-MDA-5 = anti-melanoma differentiation-associated gene 5; VC = vital capacity; FEV₁/FVC = forced expiratory volume in 1 second/forced vital capacity; DLco = diffusing capacity for carbon monoxide; NSIP = nonspecific interstitial pneumonia; OP = organizing pneumonia.

† Acute = within 1 month; subacute = 1–3 months; chronic = >3 months.

‡ P = 0.03 versus step-up treatment control group, by Mann-Whitney U test.

§ P = 0.045 versus step-up treatment control group, by Mann-Whitney U test.

¶ High-resolution computed tomography (HRCT) findings were obtained using data on 28 patients in the combined immunosuppressive regimen group and 9 patients in the step-up treatment control group.

patients treated with plasmapheresis and 2 patients treated without plasmapheresis survived for >6 months.

Primary and secondary outcome measures. Significant improvements in 6-month and 12-month survival rates were observed in the combined immunosuppressive regimen group compared to the step-up treatment group (89% versus 33% and 85% versus 33%, respectively; both $P < 0.0001$) (Figure 2A). All survivors recovered to a state in which oxygenation was not required. Serum levels of C-reactive protein (CRP), LDH, Krebs von den Lungen 6 (KL-6), and ferritin, as well as anti-MDA-5 titers, vital capacity percent predicted, and chest HRCT scores gradually improved in the combined immunosuppressive regimen group (Figure 3). All deaths were due to exacerbation of ILD; however, infections such as CMV reactivation ($n = 3$), PCP ($n = 2$), and sepsis ($n = 2$) seemed to trigger the ILD exacerbation (Supplementary Table 3, [http://](http://onlinelibrary.wiley.com/doi/10.1002/art.41105/abstract)

onlinelibrary.wiley.com/doi/10.1002/art.41105/abstract). PCP occurred in patients who had stopped prophylactic TMP/SMX due to its adverse effects. In the exacerbated state of ILD just before death, 3 patients (75%) showed very high levels of ferritin. In the step-up treatment group, 10 of the 15 patients died. Exacerbation of ILD was the cause of death in all patients. Several infections were observed during the course of treatment in both surviving and deceased patients, but there were no significant differences between groups with respect to the rates of infections (Supplementary Table 4, <http://onlinelibrary.wiley.com/doi/10.1002/art.41105/abstract>).

The step-up treatment group (control group A) was subdivided into 3 groups based on the number of drugs administered within 7 days (0, 1, or 2 of the following: GC, CNI, and IV CYC) or 52 weeks (1, 2, or 3 of the following: GC, CNI, and IV CYC) after admission to hospitals (Figures 2B and C). A higher number of drugs started within 7 days was associated with increased

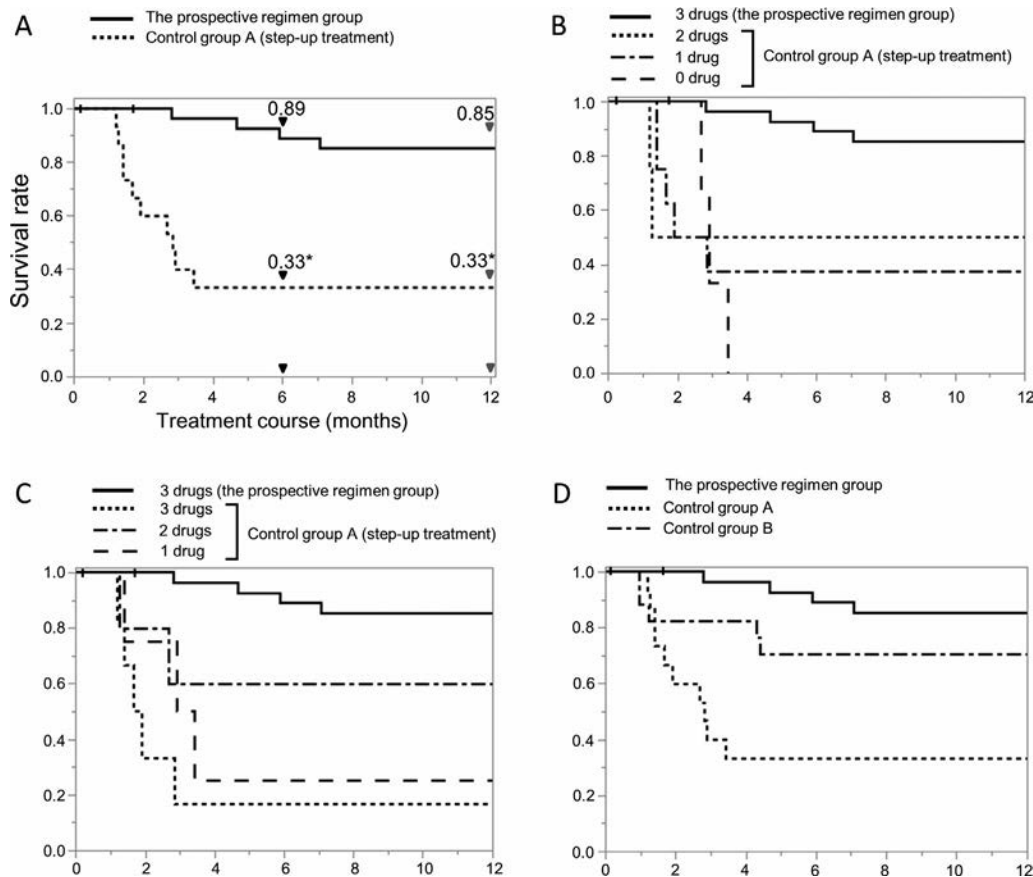


Figure 2. Overall survival in anti-MDA-5-positive DM/CADM patients ($n = 29$ in the prospective regimen group; $n = 15$ in control group A [no drug $n = 3$, 1 drug $n = 8$, 2 drugs $n = 4$ at 7 days; 1 drug $n = 4$, 2 drugs $n = 5$, 3 drugs $n = 6$ within 52 weeks]). **A**, Survival rates in the prospective regimen group (combined immunosuppressive regimen group) and control group A (step-up treatment group). * = $P < 0.0001$ versus the prospective regimen group. **B**, Survival rates stratified according to the number of drugs administered within 7 days after hospital admission. **C**, Survival rates stratified according to the number of drugs administered within 52 weeks after hospital admission. **D**, Effect of additional treatment with plasmapheresis on survival rates. In the prospective regimen group, patients received the combined immunosuppressive regimen with or without plasmapheresis. In control group A ($n = 15$), patients received step-up treatment without plasmapheresis. In control group B ($n = 17$), patients received the combined immunosuppressive regimen without plasmapheresis. Cumulative survival rates were analyzed by Kaplan-Meier test. Plus signs represent censored patients in the prospective regimen group. See Figure 1 for definitions.

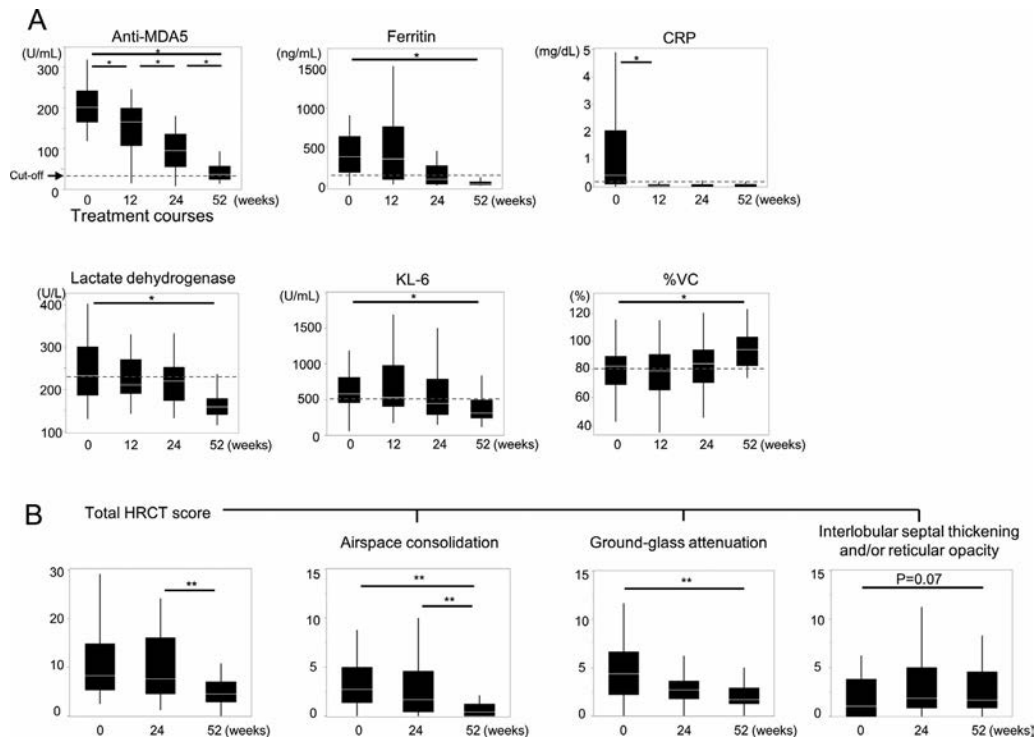


Figure 3. Laboratory data and respiratory function (A) and chest high-resolution computed tomography (HRCT) scores (B) in the combined immunosuppressive regimen group during the treatment course. Data are presented as box plots, where the boxes represent the 25th to 75th percentiles, the lines within the boxes represent the median, and the lines outside the boxes represent the minimum and maximum. * = $P < 0.0125$; ** = $P < 0.0167$, by Student's paired t -test with Bonferroni adjustment. Dotted lines show cutoff values. Anti-MDA-5 = anti-melanoma differentiation-associated gene 5; CRP = C-reactive protein; KL-6 = Krebs von den Lungen 6; VC = vital capacity.

survival. Analysis of the subgroups that were classified based on the number of drugs administered during the 52-week follow-up period showed that survival rates in control group A increased in the following order (from lowest to highest): triple therapy (GC, CNI, and IV CYC), monotherapy (GC), and dual therapy (GC and CNI/IV CYC); survival in the prospective regimen group was highest compared to any subgroup of control group A.

Effectiveness of plasmapheresis. To analyze the effectiveness of plasmapheresis, we compared the prospective regimen group (GC, tacrolimus, and IV CYC) in which plasmapheresis was allowed as an additional treatment to historical control group B that was treated with the regimen (GC, cyclosporin A, and IV CYC) and without plasmapheresis. There were no differences in baseline clinical features of patients or drug usage between the 2 groups (Supplementary Tables 5 and 6, <http://onlinelibrary.wiley.com/doi/10.1002/art.41105/abstract>). The length of the period from hospital admission to the initiation of GC, CNI, and IV CYC did not differ between these 2 groups. However, the length of the period from disease onset to the initiation of these treatments was longer in the prospective regimen group than in historical control group B (Supplementary Table 7, <http://onlinelibrary.wiley.com/doi/10.1002/art.41105/abstract>). Six-month and 12-month survival rates tended to be higher in

the prospective regimen group than in historical control group B (89% versus 71% [$P < 0.09$] and 85% versus 71% [$P < 0.17$], respectively) (Figure 2D).

Comparison between surviving and deceased patients in the combined immunosuppressive regimen group.

When the deceased patients ($n = 4$) and the surviving patients ($n = 23$) in the combined immunosuppressive regimen group were retrospectively compared, cutaneous ulcer was more frequently observed in the deceased patients (75% versus 13%; $P = 0.02$) (Supplementary Table 8, <http://onlinelibrary.wiley.com/doi/10.1002/art.41105/abstract>). Respiratory function and the period from disease onset to the initiation of treatment did not differ between the 2 groups. Laboratory values were compared between surviving patients and patients who died, and levels of ferritin (mean \pm SD 459.9 ± 516.3 ng/ml versus $2,050.3 \pm 1,772.7$ ng/ml; $P = 0.16$), CRP (0.77 ± 1.2 mg/dl versus 2.7 ± 1.1 mg/dl; $P = 0.01$), CK, and LDH before treatment tended to be higher in the deceased patients. During the treatment course, levels of ferritin and CRP were persistently higher in the deceased patients (Supplementary Figure 2, <http://onlinelibrary.wiley.com/doi/10.1002/art.41105/abstract>). Total or airspace consolidation chest HRCT scores showed improvement in surviving patients.

Adverse events during treatment. No severe adverse events directly caused death among the patients in this study. However, some opportunistic infections, insomnia, renal dysfunction, and electrolyte abnormalities were observed (Tables 2 and 3). While antibiotics were more frequently used in the step-up treatment group, there were no differences with respect to bacterial infection between the combined immunosuppressive regimen group and the step-up treatment group. CMV reactivation was more frequently observed in the combined immunosuppressive regimen group; soon after CMV reactivation was determined, patients were treated with antiviral drugs until serum CMV antigenemia was ameliorated. There was no difference in the frequency of PCP, even in patients who stopped using TMP/SMX for prophylaxis.

In both groups, abnormalities in electrolytes were observed. In particular, hyponatremia after IV CYC treatment was often observed; some patients experienced muscle pain (data not shown). To prevent reduction of bone density due to long-term administration of GCs, activated vitamin D and/or bisphosphonates were typically used. Jaw osteomyelitis or jaw bone necrosis was observed in 2 patients in the combined immunosuppressive regimen group; both stopped bisphosphonate use. In addition,

Table 2. Adverse events during immunosuppressive treatment*

	Combined immunosuppressive regimen group (n = 27)	Step-up treatment control group (n = 15)
Infection (total)	23 (85)	12 (80)
Bacterial infection	10 (37)	5 (33)
CMV	23 (85)†	5 (33)
HSV/VZV	2 (7)	2 (13)
Candidiasis	15 (56)	5 (33)
Aspergillus	2 (7)	0 (0)
PCP	3 (11)	2 (13)
Other fungal infections	1 (4)	2 (13)
Use of antibiotics	13 (48)	12 (80)
Prophylaxis of PCP with TMP/SMX	24 (89)	12 (80)
Diabetes mellitus	19 (70)	8 (53)
Hyperglycemia	20 (74)	14 (93)
Hyperlipidemia	24 (89)	13 (87)
Insomnia	22 (81)	10 (67)
Compression fracture	1 (4)	0 (0)
Femoral head necrosis	1 (4)	0 (0)
Hypertension	9 (33)	5 (33)
TMA	2 (7)	0 (0)
Hemorrhagic cystitis	4 (15)	0 (0)
Electrolyte abnormality	24 (89)	13 (87)
Hyponatremia	22 (81)	12 (80)
Hypokalemia	14 (52)	4 (27)
Hyperkalemia	12 (44)	9 (60)
Jaw osteomyelitis/jaw bone necrosis	2 (8)	0 (0)

* Values are the number (%). CMV = cytomegalovirus; HSV/VZV = herpes simplex virus/varicella-zoster virus; PCP = pneumocystis pneumonia; TMP/SMX = trimethoprim/sulfamethoxazole; TMA = thrombotic microangiopathy.

† $P = 0.0015$ versus step-up treatment control group, by Fisher's exact test.

Table 3. Alteration of estimated glomerular filtration rate (eGFR; ml/minute/1.73 m²) during treatment course

	eGFR, mean ± SD	
	Combined immunosuppressive regimen group (n = 29)	Step-up treatment control group (n = 15)
Baseline	98.1 ± 23.9	97.4 ± 26.5
52 weeks	75.3 ± 15.7	67.7 ± 20.2
P^*	5.7×10^{-6}	0.025

* By Student's paired *t*-test.

femoral head necrosis occurred in 1 patient, which was manifested as reduction of body weight. Hemorrhagic cystitis occurred in 4 patients in the combined immunosuppressive regimen group. In 1 patient, several viruses were examined, and adenovirus was detected as the cause of cystitis. IV CYC treatment was discontinued in all 4 patients in whom hemorrhagic cystitis occurred; these patients received IV CYC 5, 7, 9, and 10 times, respectively. Over 52 weeks of treatment, renal function was slightly worsened in both groups (Table 3 and Supplementary Figure 3, <http://onlinelibrary.wiley.com/doi/10.1002/art.41105/abstract>), but there was no significant difference between the 2 groups. Thrombotic microangiopathy (TMA) occurred in 2 patients; 1 of these patients experienced end-stage renal failure and began hemodialysis.

We analyzed the influence of the blood tacrolimus concentration on adverse events such as infection and renal dysfunction in the combined immunosuppressive regimen group. The mean ± SD 12-hour trough level of tacrolimus during the 52-week follow-up period was 7.64 ± 3.45 ng/ml. Mean 12-hour trough levels tended to be correlated with the rate at which creatinine increased (Pearson's correlation coefficient [r] = 0.49, $P = 0.02$) (Supplementary Figure 4, <http://onlinelibrary.wiley.com/doi/10.1002/art.41105/abstract>). Therefore, a high blood concentration of tacrolimus might exhibit some influence on renal function. When we analyzed the influence of tacrolimus concentration on adverse effects, classifying the prospective regimen group according to the occurrence of adverse events (Supplementary Table 9, <http://onlinelibrary.wiley.com/doi/10.1002/art.41105/abstract>), there was no significant difference in 12-hour trough levels of tacrolimus between the 2 groups, except in patients who showed hyperkalemia.

DISCUSSION

The combined immunosuppressive regimen with high-dose GCs, tacrolimus, and IV CYC improved survival of anti-MDA-5-positive DM/CADM patients with ILD, and was well tolerated in this trial. The regimen in this study involved introducing intensive immunosuppressive treatment in the early phase of anti-MDA-5-positive DM/CADM; an additional supportive therapy, plasmapheresis, was used when respiratory function deteriorated faster than disease control could be achieved. No severe adverse events caused death. However, opportunistic infections, such as CMV

reactivation, were frequently observed in patients receiving the combined immunosuppressive regimen, and such events often triggered the exacerbation of ILD activity. Indeed, all deceased patients in this study had experienced opportunistic infections and subsequent exacerbation of ILD, which led to sustained severe respiratory distress, despite appropriate treatment of infection and evidence that microorganisms had disappeared. Thus, prophylaxis for PCP, careful monitoring of other infections (e.g., by checking levels of CRP, CMV antigenemia, and β -D-glucan), and decisions regarding empirical therapeutic intervention are critical when applying this regimen.

The early use of immunosuppressants, such as cyclosporin A, in combination with GCs has been reported to improve survival rates in DM patients with ILD (29). In addition, combination therapy with IV CYC, cyclosporin A, and GCs was shown to be superior to the combination of cyclosporin A and GCs (30). In the present study, when tacrolimus (in place of cyclosporin A) was included as a CNI in the combined immunosuppressive regimen, a satisfactory effect in anti-MDA-5-positive DM/CADM patients with ILD was obtained. In this trial, the administration of immunosuppressants other than GCs after hospitalization occurred nearly 20 days earlier in the combined immunosuppressive regimen group compared to the step-up treatment group. Therefore, treatment delay, even of a few weeks, can greatly affect the outcome in anti-MDA-5-positive DM/CADM patients with rapidly progressive ILD, suggesting the importance of initiating combination therapy with multiple immunosuppressants as soon as possible in these patients.

Plasmapheresis can be an effective additional treatment in patients with ILD (31). Recent studies have shown that many types of inflammatory cytokines and chemokines, such as type I interferon (32), interleukin-6 (IL-6) (33), IL-8, IL-10, IL-15, and IL-18 (32–35), are elevated in the sera of DM/CADM patients with ILD or anti-MDA-5-positive DM patients with ILD (35). In addition, anti-MDA-5 titer has been associated with disease activity (15). In this context, we chose plasmapheresis as an additional supportive therapy with the aim of removing the elevated cytokines/chemokines, as well as anti-MDA-5 antibody, the latter of which might also contribute to the onset or exacerbation of disease. Previously, a randomized controlled trial showed no effect of plasmapheresis on polymyositis or DM, but the enrolled patients were heterogeneous and the trial end points were measurements of muscle disease activity (36). Notably, recent case reports have indicated the efficacy of plasmapheresis in patients with anti-MDA-5-positive rapidly progressive ILD (37–39). Polymyxin B-immobilized fiber column direct hemoperfusion has also been suggested as potentially effective for ILD in CADM or anti-MDA-5-positive rapidly progressive ILD (40,41), although the effect was controversial (42,43). In the future, prospective studies comparing patients who undergo plasmapheresis and those who do not are necessary.

The adverse effect of renal dysfunction showed gradual and irreversible onset (Table 3 and Supplementary Figure 3, <http://online.library.wiley.com/doi/10.1002/art.41105/abstract>). It may have been a result of drug treatment, especially with CNI, which is known to cause renal dysfunction, or of intensive administration of cyclophosphamide. TMA occurred in 2 patients, 1 of whom showed progression of renal dysfunction despite discontinuation of tacrolimus; in that patient, TMA resulted in end-stage renal failure. TMA can be caused both by tacrolimus and by severe DM disease activity. When renal function seems to deteriorate seriously, it may be necessary to reduce or withdraw the potentially contributing medication. In the future, a more detailed investigation of this regimen is needed to avoid overtreatment in patients whose disease activity can be well controlled without such intensive immunosuppression.

There were several limitations to our study. First, this was a historical controlled study, because the enrollment of concurrent controls was not possible due to ethical concerns. Second, plasmapheresis was selected at the attending physician's discretion, so there may have been considerable variation in its application. Third, there was a small number of patients enrolled in this trial, and all were of Japanese ethnicity. Because genetic and environmental backgrounds may contribute to the frequency and severity of ILD in anti-MDA-5-positive patients (11–14), it is necessary to investigate therapeutic adaptations and potential effects in larger populations with different ethnicities. Moreover, further prospective studies are needed, with the combination of immunosuppressants arranged in accordance with the classification of patients' prognostic factors, because the triple regimen will be overtreatment for a portion of the anti-MDA-5-positive patients.

In summary, we showed the efficacy and safety of a combined immunosuppressive regimen that included high-dose GCs, tacrolimus, and IV CYC treatment in Japanese anti-MDA-5-positive DM/CADM patients with rapidly progressive ILD. Early detection of anti-MDA-5, administration of concomitant immunosuppressants, and monitoring of infection are important. Further investigations are needed to aid in the detailed adaptation of the regimen, as well as to determine the efficacy of plasmapheresis as an additional therapy.

ACKNOWLEDGMENTS

We thank Ms Sachi Ibuki for her technical support in the detection of anti-MDA-5 antibody. We thank Ryan Chastain-Gross, PhD (Edanz Group) for editing a draft of the manuscript.

AUTHOR CONTRIBUTIONS

All authors were involved in drafting the article or revising it critically for important intellectual content, and all authors approved the final version to be published. Dr. Nakashima had full access to all of the data in the study and takes responsibility for the integrity of the data and the accuracy of the data analysis.

Study conception and design. Nakashima, Mimori.

Acquisition of data. Tsuji, Nakashima, Hosono, Imura, Yagita, Yoshifuji, Hirata, Nojima, Sugiyama, Hatta, Taguchi, Katayama, Akizuki, Murakami, Hashimoto, Tanaka, Ohmura, Mimori.

Analysis and interpretation of data. Tsuji, Nakashima, Tanizawa, Handa, Uozumi.

REFERENCES

- Nakashima R, Hosono Y, Mimori T. Clinical significance and new detection system of autoantibodies in myositis with interstitial lung disease. *Lupus* 2016;25:925–33.
- Sato S, Hoshino K, Satoh T, Fujita T, Kawakami Y, Fujita T, et al. RNA helicase encoded by melanoma differentiation-associated gene 5 is a major autoantigen in patients with clinically amyopathic dermatomyositis: association with rapidly progressive interstitial lung disease. *Arthritis Rheum* 2009;60:2193–200.
- Nakashima R, Imura Y, Kobayashi S, Yukawa N, Yoshifuji H, Nojima T, et al. The RIG-I-like receptor IFIH1/MDA5 is a dermatomyositis-specific autoantigen identified by the anti-CADM-140 antibody. *Rheumatology (Oxford)* 2010;49:433–40.
- Moghadam-Kia S, Oddis CV, Sato S, Kuwana M, Aggarwal R. Anti-melanoma differentiation-associated gene 5 is associated with rapidly progressive lung disease and poor survival in US patients with amyopathic and myopathic dermatomyositis. *Arthritis Care Res (Hoboken)* 2016;68:689–94.
- Fiorentino D, Chung L, Zwerner J, Rosen A, Casciola-Rosen L. The mucocutaneous and systemic phenotype of dermatomyositis patients with antibodies to MDA5 (CADM-140): a retrospective study. *J Am Acad Dermatol* 2011;65:25–34.
- Chen F, Wang D, Shu X, Nakashima R, Wang G. Anti-MDA5 antibody is associated with A/SIP and decreased T cells in peripheral blood and predicts poor prognosis of ILD in Chinese patients with dermatomyositis. *Rheumatol Int* 2012;32:3909–15.
- Koga T, Fujikawa K, Horai Y, Okada A, Kawashiri SY, Iwamoto N, et al. The diagnostic utility of anti-melanoma differentiation-associated gene 5 antibody testing for predicting the prognosis of Japanese patients with DM. *Rheumatology (Oxford)* 2012;51:1278–84.
- Sato S, Kuwana M, Fujita T, Suzuki Y. Anti-CADM-140/MDA5 autoantibody titer correlates with disease activity and predicts disease outcome in patients with dermatomyositis and rapidly progressive interstitial lung disease. *Mod Rheumatol* 2013;23:496–502.
- Chen Z, Cao M, Plana MN, Liang J, Cai H, Kuwana M, et al. Utility of anti-melanoma differentiation-associated gene 5 antibody measurement in identifying patients with dermatomyositis and a high risk for developing rapidly progressive interstitial lung disease: a review of the literature and a meta-analysis. *Arthritis Care Res (Hoboken)* 2013;65:1316–24.
- Labrador-Horrillo M, Martinez MA, Selva-O'Callaghan A, Trallero-Araguas E, Balada E, Vilardell-Tarres M, et al. Anti-MDA5 antibodies in a large Mediterranean population of adults with dermatomyositis. *J Immunol Res* 2014;2014:290797.
- Muro Y, Sugiura K, Hoshino K, Akiyama M, Tamakoshi K. Epidemiologic study of clinically amyopathic dermatomyositis and anti-melanoma differentiation-associated gene 5 antibodies in central Japan. *Arthritis Res Ther* 2011;13:R214.
- Christensen ML, Pachman LM, Schneiderman R, Patel DC, Friedman JM. Prevalence of coxsackie B virus antibodies in patients with juvenile dermatomyositis. *Arthritis Rheum* 1986;29:1365–70.
- Gono T, Kawaguchi Y, Kuwana M, Sugiura T, Furuya T, Takagi K, et al. Association of HLA-DRB1*0101/*0405 with susceptibility to anti-melanoma differentiation-associated gene 5 antibody-positive dermatomyositis in the Japanese population. *Arthritis Rheum* 2012;64:3736–40.
- Chen Z, Wang Y, Kuwana M, Xu X, Hu W, Feng X, et al. HLA-DRB1 alleles as genetic risk factors for the development of anti-MDA5 antibodies in patients with dermatomyositis. *J Rheumatol* 2017;44:1389–93.
- Matsushita T, Mizumaki K, Kano M, Yagi N, Tennichi M, Takeuchi A, et al. Antimelanoma differentiation-associated protein 5 antibody level is a novel tool for monitoring disease activity in rapidly progressive interstitial lung disease with dermatomyositis. *Br J Dermatol* 2017;176:395–402.
- Hamaguchi Y, Kuwana M, Hoshino K, Hasegawa M, Kaji K, Matsushita T, et al. Clinical correlations with dermatomyositis-specific autoantibodies in adult Japanese patients with dermatomyositis: a multicenter cross-sectional study. *Arch Dermatol* 2011;147:391–8.
- Mukae H, Ishimoto H, Sakamoto N, Hara S, Kakugawa T, Nakayama S, et al. Clinical differences between interstitial lung disease associated with clinically amyopathic dermatomyositis and classic dermatomyositis. *Chest* 2009;136:1341–7.
- Gono T, Sato S, Kawaguchi Y, Kuwana M, Hanaoka M, Katsumata Y, et al. Anti-MDA5 antibody, ferritin and IL-18 are useful for the evaluation of response to treatment in interstitial lung disease with anti-MDA5 antibody-positive dermatomyositis. *Rheumatology (Oxford)* 2012;51:1563–70.
- Bohan A, Peter JB. Polymyositis and dermatomyositis. *N Engl J Med* 1975;292:344–7.
- Gerami P, Schope JM, McDonald L, Walling HW, Sontheimer RD. A systematic review of adult-onset clinically amyopathic dermatomyositis (dermatomyositis sine myositis): a missing link within the spectrum of the idiopathic inflammatory myopathies. *J Am Acad Dermatol* 2006;54:597–613.
- Euwer RL, Sontheimer RD. Amyopathic dermatomyositis: a review. *J Invest Dermatol* 1993;100:124–7.
- Matz EL, Hsieh MH. Review of advances in uroprotective agents for cyclophosphamide- and ifosfamide-induced hemorrhagic cystitis. *Urology* 2017;100:16–9.
- Stern A, Green H, Paul M, Vidal L, Leibovici L. Prophylaxis for *Pneumocystis pneumonia* (PCP) in non-HIV immunocompromised patient [review]. *Cochrane Database Syst Rev* 2014;CD005590.
- Bellomo R, Ronco C, Kellum JA, Mehta RL, Palevsky P. Acute renal failure—definition, outcome measures, animal models, fluid therapy and information technology needs: the Second International Consensus Conference of the Acute Dialysis Quality Initiative (ADQI) Group. *Crit Care* 2004;8:R204–12.
- Sato S, Murakami A, Kuwajima A, Takehara K, Mimori T, Kawakami A, et al. Clinical utility of an enzyme-linked immunosorbent assay for detecting anti-melanoma differentiation-associated gene 5 autoantibodies. *PLoS One* 2016;11:e0154285.
- Sumikawa H, Johkoh T, Colby TV, Ichikado K, Suga M, Taniguchi H, et al. Computed tomography findings in pathological usual interstitial pneumonia: relationship to survival. *Am J Respir Crit Care Med* 2008;177:433–9.
- Sakamoto S, Okamoto M, Kaieda S, Fujimoto K, Nagata S, Tominaga M, et al. Low positive titer of anti-melanoma differentiation-associated gene 5 antibody is not associated with a poor long-term outcome of interstitial lung disease in patients with dermatomyositis. *Respir Investig* 2018;56:464–72.
- Raghu G, Remy-Jardin M, Myers JL, Richeldi L, Ryerson CJ, Lederer DJ, et al. Diagnosis of idiopathic pulmonary fibrosis: an official ATS/ERS/JRS/ALAT clinical practice guideline. *Am J Respir Crit Care Med* 2018;198:e44–68.
- Go DJ, Park JK, Kang EH, Kwon HM, Lee YJ, Song YW, et al. Survival benefit associated with early cyclosporine treatment for dermatomyositis-associated interstitial lung disease. *Rheumatol Int* 2016;36:125–31.
- Kameda H, Nagasawa H, Ogawa H, Sekiguchi N, Takei H, Tokuhira M, et al. Combination therapy with corticosteroids, cyclosporin A, and intravenous pulse cyclophosphamide for acute/subacute interstitial pneumonia in patients with dermatomyositis. *J Rheumatol* 2005;32:1719–26.

31. Kaieda S, Yoshida N, Yamashita F, Okamoto M, Ida H, Hoshino T, et al. Successful treatment of macrophage activation syndrome in a patient with dermatomyositis by combination with immunosuppressive therapy and plasmapheresis. *Mod Rheumatol* 2015;25:962–6.
32. Horai Y, Koga T, Fujikawa K, Takatani A, Nishino A, Nakashima Y, et al. Serum interferon- α is a useful biomarker in patients with anti-melanoma differentiation-associated gene 5 (MDA5) antibody-positive dermatomyositis. *Mod Rheumatol* 2015;25:85–9.
33. Nara M, Komatsuda A, Omokawa A, Togashi M, Okuyama S, Sawada K, et al. Serum interleukin 6 levels as a useful prognostic predictor of clinically amyopathic dermatomyositis with rapidly progressive interstitial lung disease. *Mod Rheumatol* 2014;24:633–6.
34. Gono T, Kawaguchi Y, Sugiura T, Ichida H, Takagi K, Katsumata Y, et al. Interleukin-18 is a key mediator in dermatomyositis: potential contribution to development of interstitial lung disease. *Rheumatology (Oxford)* 2010;49:1878–81.
35. Takada T, Aoki A, Asakawa K, Sakagami T, Moriyama H, Narita I, et al. Serum cytokine profiles of patients with interstitial lung disease associated with anti-CADM-140/MDA5 antibody positive amyopathic dermatomyositis. *Respir Med* 2015;109:1174–80.
36. Miller FW, Leitman SF, Cronin ME, Hicks JE, Leff RL, Wesley R, et al. Controlled trial of plasma exchange and leukapheresis in polymyositis and dermatomyositis. *N Engl J Med* 1992;326:1380–4.
37. Silveira MG, Selva-O'Callaghan A, Ramos-Terrades N, Arredondo-Agudelo KV, Labrador-Horrillo M, Bravo-Masgoret C. Anti-MDA5 dermatomyositis and progressive interstitial pneumonia. *QJM* 2016;109:49–50.
38. Fujita Y, Fukui S, Suzuki T, Ishida M, Endo Y, Tsuji S, et al. Anti-MDA5 antibody-positive dermatomyositis complicated by autoimmune-associated hemophagocytic syndrome that was successfully treated with immunosuppressive therapy and plasmapheresis. *Intern Med* 2018;57:3473–8.
39. Endo Y, Koga T, Suzuki T, Hara K, Ishida M, Fujita Y, et al. Successful treatment of plasma exchange for rapidly progressive interstitial lung disease with anti-MDA5 antibody-positive dermatomyositis: a case report. *Medicine (Baltimore)* 2018;97:e0436.
40. Teruya A, Kawamura K, Ichikado K, Sato S, Yasuda Y, Yoshioka M. Successful polymyxin B hemoperfusion treatment associated with serial reduction of serum anti-CADM-140/MDA5 antibody levels in rapidly progressive interstitial lung disease with amyopathic dermatomyositis. *Chest* 2013;144:1934–6.
41. Sasaki O, Dohi M, Harada H, Imamura M, Tsuchida Y, Yamaguchi K, et al. A case of polymyxin B-immobilized fiber column treatment for rapidly progressive interstitial pneumonia associated with clinically amyopathic dermatomyositis. *Case Rep Med* 2013;2013:750275.
42. Okabayashi H, Ichiyasu H, Hirooka S, Akaike K, Kojima K, Jodai T, et al. Clinical effects of direct hemoperfusion using a polymyxin B-immobilized fiber column in clinically amyopathic dermatomyositis-associated rapidly progressive interstitial pneumonias. *BMC Pulm Med* 2017;17:134.
43. Yasuda H, Ikeda T, Hamaguchi Y, Furukawa F. Clinically amyopathic dermatomyositis with rapidly progressive interstitial pneumonia: the relation between the disease activity and the serum interleukin-6 level. *J Dermatol* 2017;44:1164–7.





DOI: 10.1002/art.41221

Applications Invited for *Arthritis Care & Research* Editor-in-Chief (2021–2026 Term)

The American College of Rheumatology Committee on Journal Publications announces the search for the position of Editor, *Arthritis Care & Research*. The official term of the next *Arthritis Care & Research* editorship is July 1, 2021–June 30, 2026; however, some of the duties of the new Editor will begin during a transition period starting April 1, 2021. ACR/ARP members who are considering applying for this prestigious and rewarding position should submit a nonbinding letter of intent by May 4, 2020 to the Managing Editor, Maggie Parry, at mparry@rheumatology.org, and are also encouraged to contact the current Editor-in-Chief, Dr. Marian Hannan, to discuss details. Initial contact should be made via e-mail to Hannan@hsl.harvard.edu. Applications will be due by June 15, 2020 and will be reviewed during the summer of 2020. Application materials are available on the ACR web site at <https://www.rheumatology.org/Portals/0/Files/ACandR-Editor-Application-Instructions.pdf>.

BRIEF REPORT

Impact of *IL1RN* Variants on Response to Interleukin-1 Blocking Therapy in Systemic Juvenile Idiopathic Arthritis

Claas Hinze,¹  Sabrina Fuehner,¹ Christoph Kessel,¹  Helmut Wittkowski,¹ Elke Lainka,² Melanie Baehr,² Boris Hügle,³  Johannes-Peter Haas,³ Gerd Ganser,⁴ Elisabeth Weißbarth-Riedel,⁵ Annette Jansson,⁶ and Dirk Foell¹ 

Objective. To analyze the reported association of *IL1RN* polymorphisms with response to interleukin-1 (IL-1) blockade in a German cohort of patients with systemic juvenile idiopathic arthritis (JIA), and to assess the impact of other factors on treatment response.

Methods. Sixty-one patients with systemic JIA who had received IL-1 blockade were identified within the German Autoinflammatory Disease registry DNA biobank. Response to IL-1 blockade was assessed according to 1) the clinical response (initially at least a transient response or good response compared to a poor response), 2) switch (or no switch) to anti-IL-6 receptor therapy following IL-1 blockade, 3) achievement of clinically inactive disease within 6 months of IL-1 blockade, 4) improvement in disease activity measured using the modified Juvenile Arthritis Disease Activity Score, and 5) achievement of a glucocorticoid-free state. In addition, basic demographic data, key features of the disease course, laboratory data, and *IL1RN* single-nucleotide polymorphisms (SNPs) were assessed.

Results. Six of 7 *IL1RN* SNPs reported to be associated with response to anakinra therapy were analyzed. These 6 *IL1RN* SNPs were inherited as haplotypes. An association of *IL1RN* haplotypes and SNPs with response to IL-1 blockade could not be confirmed in this cohort of patients with systemic JIA. Patients who received tocilizumab following IL-1 blockade had a longer duration from disease onset to diagnosis than those who did not receive tocilizumab (median 0.27 years versus 0.08 years).

Conclusion. The results of this study could not confirm an impact of *IL1RN* SNPs on response to IL-1 blockade therapy with either anakinra or canakinumab in a cohort of patients with systemic JIA. However, a longer time frame from disease onset to diagnosis was associated with poorer long-term treatment response, thereby supporting the “window of opportunity” hypothesis that suggests improved long-term treatment response with shorter time from disease onset to diagnosis (and treatment).

INTRODUCTION

Systemic juvenile idiopathic arthritis (JIA) is characterized by systemic inflammation and arthritis (1). While, traditionally, glucocorticoids have been an important treatment option for systemic JIA, more recently, cytokine-directed therapies targeting interleukin-1 (IL-1) and IL-6 have also been employed (2). Currently, 3

biologic agents are approved for the treatment of systemic JIA in the European Union: anakinra, a recombinant IL-1 receptor antagonist (IL-1Ra), canakinumab, a human monoclonal IL-1 β antibody, and tocilizumab, a humanized monoclonal IL-6 receptor antibody (in the US, only canakinumab and tocilizumab are approved).

The treatment response to IL-1 blockade is heterogeneous. For example, in a randomized, controlled clinical trial of anakinra

The Autoinflammatory Disease (AID) registry is supported by the BMBF (grant 01 GM 1512D).

¹Claas Hinze, MD, Sabrina Fuehner, Christoph Kessel, PhD, Helmut Wittkowski, MD, Dirk Foell, MD: University Hospital Munster, Munster, Germany; ²Elke Lainka, MD, Melanie Baehr, MD: University Hospital Essen, Essen, Germany; ³Boris Hügle, MD, Johannes-Peter Haas, MD: German Center for Pediatric and Adolescent Rheumatology, Garmisch-Partenkirchen, Germany; ⁴Gerd Ganser, MD: St. Josef-Stift Sendenhorst, Sendenhorst, Germany; ⁵Elisabeth Weißbarth-Riedel, MD: University Hospital Hamburg-Eppendorf, Hamburg, Germany; ⁶Annette Jansson, MD: Dr. von Hauner Children's Hospital, Munich, Germany.

Dr. Hinze has received honoraria from Novartis (less than \$10,000). Dr. Foell has received consulting fees, speaking fees, and/or honoraria from Chugai-Roche, Novartis, and Sobi (less than \$10,000 each). No other disclosures relevant to this article were reported.

Address correspondence to Claas Hinze, MD, Universitätsklinikum Münster, Klinik für Pädiatrische Rheumatologie und Immunologie, Albert-Schweitzer-Campus 1, Gebäude W30, 48149 Münster, Germany. E-mail: claus.hinze@ukmuenster.de.

Submitted for publication March 13, 2019; accepted in revised form October 3, 2019.

in patients with active systemic JIA, ~71% of patients were considered to be responders, according to achievement of the American College of Rheumatology (ACR) Pediatric 30 (Pedi 30) response (3), resolution of fever, and improvement by 50% in the levels of inflammation markers (4). In a randomized, controlled trial of canakinumab, 84% of patients reached a modified ACR Pedi 30 response within 2 weeks of therapy (5). The response rates reported from open-label cohort studies are variable, but are generally in the range of 75–85% (6,7). The reason for the heterogeneity of response to IL-1 blockade is unclear. One hypothesis is that a “window of opportunity” exists, meaning that there is a time frame early in the disease course during which effective therapy may fundamentally improve the long-term outcome and disease course, essentially suggesting that earlier therapy may be associated with an improved treatment response (8). More recently, it was suggested that high-expressing *IL1RN* alleles are associated with a higher risk of nonresponse to anakinra therapy in a cohort of North American patients with systemic JIA (9). The *IL1RN* gene encodes the endogenous IL-1Ra, of which anakinra is a modified version (N2-L-methionyl-26-177-IL-1Ra).

In this study, we analyzed the relationship between treatment response to IL-1 blockade and *IL1RN* variants in a cohort of patients with systemic JIA identified from the DNA biobank of the German Autoinflammatory Disease (AID) registry.

PATIENTS AND METHODS

Patients. The German AID registry and biobank, comprising data from a total of 42 participating centers, enrolled patients with various autoinflammatory diseases, including systemic JIA. Enrollment into the AID registry was based on clinicians' diagnoses and could take place at any time during the disease course. For this study, the biobank was screened for patients who were diagnosed as having systemic JIA ($n = 177$ in total); among these patients, we identified those who had received anakinra and/or canakinumab during the course of their disease ($n = 92$ remaining), and then identified those who had a DNA sample available ($n = 61$ remaining).

Assessment of treatment response. The German AID registry includes detailed longitudinal records of individual patients concerning disease activity and laboratory findings. The main outcome of the study was the treatment response, which was assessed according to 2 different parameters: 1) formal assessment of the clinical response, and 2) patterns of treatment with biologic agents.

The clinical response in patients with systemic JIA was formally assessed according to the following response categories: 1) a good response, if the signs and symptoms of active disease (fever, rash, adenopathy, hepatosplenomegaly, serositis, and arthritis) had resolved and if the levels of inflammation markers

(C-reactive protein [CRP] and erythrocyte sedimentation rate [ESR]) had improved by at least 50% following treatment with anakinra and/or canakinumab, and if this response was maintained for at least 6 months; 2) a transient response, if there was an initial response characterized according to the parameters of a good response for at least 2 months but with later recurrence of disease; or 3) a poor response, if the parameters for improvement were not met. These treatment response criteria had been previously established for the purpose of a separate analysis of the AID registry cohort (10).

Treatment response based on treatment patterns was judged as follows. Patients who initiated treatment with tocilizumab following either anakinra and/or canakinumab therapy were classified into 1 treatment pattern group, and patients who did not receive tocilizumab following anakinra and/or canakinumab therapy were classified into the other treatment pattern group. This approach estimates the drug survival that was supposed to reflect the long-term efficacy of treatment with anakinra and/or canakinumab, essentially a measure of patients “voting with their feet.”

For secondary analyses, we used the following additional improvement criteria: 1) any response, i.e., improvement of fever (if present) and/or arthritis (if present), defined according to the criteria used by Arthur et al (9), 2) improvement in the physician global assessment of disease activity score by at least 30%, 50%, 70%, or 90%, 3) improvement in the modified Juvenile Arthritis Disease Activity Score in 10 joints (JADAS-10), consisting of the sum of the physician global assessment of disease activity score (scale 0–10), the count of joints with active arthritis (scale 0–10), and normalized CRP level (scale 0–10; calculated as $[\text{CRP (in mg/liter)} - 10]/10$, with a CRP level of <10 mg/liter representing a score of 0), 4) development of clinically inactive disease (CID) within 6 months of initiation of IL-1 blockade, defined according to the CID criteria of a physician global assessment of disease activity score of 0 (scale of 0–10), a CRP level or ESR within the normal range, and no documentation of active arthritis, fever, rash, adenopathy, hepatosplenomegaly due to systemic JIA, uveitis, or morning stiffness, and 5) attainment of a glucocorticoid-free state within 6 months of initiation of IL-1 blockade (11,12).

Genotyping. SNP genotyping was performed in the Core Facility Genomics of the University of Munster, assessing the following SNPs in the *IL1RN* gene (with indication of the high-expressing allele in parentheses): rs55663133 (–), rs62158854 (T), rs62158853 (C), rs55709272 (T), rs7580634 (G), rs4251961 (T), and rs55942804/rs555447483 (–). However, the SNP rs55942804/rs555447483, which was also reported by Arthur et al (9), could not be genotyped due to technical issues.

Biomarker analysis. Within the biobank of the AID registry, the serum biomarkers S100A8/A9 and S100A12 were routinely assessed. In addition, the biobank was queried, and

Table 1. Characteristics of the 61 patients with systemic juvenile idiopathic arthritis treated with anakinra and/or canakinumab*

Characteristic	Clinical response pattern		Response based on treatment pattern		P	
	All patients (n = 61)	At least transient response (n = 41)	Poor response (n = 16)	No subsequent switch to TCZ (n = 41)		Subsequent switch to TCZ (n = 20)
Female/male, no. (%)	25 (41)/36 (59)	18 (44)/23 (56)	6 (38)/10 (62)	17 (41)/24 (59)	8 (40)/12 (60)	0.91
Age at disease onset, years	5.2 (0.5–17.3)	5.6 (0.5–17.3)	5.1 (0.6–12.9)	5.6 (0.6–17.3)	4.9 (0.5–12.9)	0.11
Age at diagnosis, years	5.3 (0.5–17.4)	7.0 (0.5–17.4)	5.3 (0.0–16.6)	7.0 (0.7–17.4)	4.9 (0.5–16.6)	0.22
Onset to diagnosis, years	0.09 (0.0–10.6)	0.09 (0.0–3.2)	0.12 (0.0–10.6)	0.08 (0.0–3.2)	0.27 (0.0–10.6)	0.02
Onset to final follow-up, years	5.7 (0.7–27.4)	4.3 (0.7–17.7)	8.6 (0.9–24.0)	3.5 (0.7–27.4)	7.5 (0.9–24.0)	<0.01
Pattern of joint involvement, no. (%)						0.08†
None	6 (9.8)	6 (14.6)	0 (0.0)	4 (9.8)	2 (10.0)	0.76†
Arthralgia	12 (19.7)	10 (24.4)	1 (6.3)	9 (22.0)	3 (15.0)	
Oligoarthritis	7 (11.5)	5 (12.2)	2 (12.5)	5 (12.2)	2 (10.0)	
Polyarthritis	34 (55.7)	19 (46.3)	13 (81.3)	22 (53.7)	12 (60.0)	
Maximum recorded WBC count, × 10 ⁹ /liter	17.3 (5.1–53.5)	25.9 (9.8–48.8)	23.4 (10.1–53.5)	25.6 (9.8–48.8)	26.3 (10.1–53.5)	0.16
Minimum recorded Hgb level, gm/dl	11.9 (5–14.6)	11.9 (9.2–14.9)	12.0 (9.9–15.3)	11.9 (8.2–14.9)	12.0 (9.6–15.3)	0.85
Maximum recorded CRP level, mg/liter	138.5 (1.0–930.0)	150.7 (9.4–930.0)	163.7 (130.9–302.8)	74.0 (1.0–930.0)	143.2 (15.0–302.8)	0.03
Maximum recorded ESR, mm/hour	80 (4–143)	77 (6–143)	117 (4–135)	77 (5–125)	99 (4–143)	0.05
Maximum recorded S100A8/A9 level, ng/ml	2,565 (200–45,390)	2,940 (200–45,390)	1,520 (490–12,050)	2,580 (200–29,230)	2,940 (490–45,390)	0.84
Maximum recorded S100A12 level, ng/ml	450 (14–22,730)	2,160 (47–22,730)	340 (76–1,470)	2,160 (47–22,730)	450 (76–17,850)	0.66
Modified JADAS-10 score at initiation of IL-1 blockade‡	17.0 (5.0–30.0)	15.5 (10.0–28.0)	20.1 (13.0–30.0)	14.8 (5–29)	20.1 (13–30)	0.06
On glucocorticoid therapy at initiation of IL-1 blockade, no. (%)	49 (80.3)	34 (82.9)	13 (81.3)	32 (78.0)	17 (85.0)	0.52
Prednisone-equivalent dose at time of initiation of IL-1 blockade, mg/kg	0.17 (0–15)	0.20 (0–15)	0.18 (0–10)	0.15 (0–15)	0.22 (0–2)	0.43
Off glucocorticoid therapy within 6 months of IL-1 blockade, no./total (%)	25/49 (51.0)	19/34 (55.9)	5/13 (38.4)	20/33 (60.6)	5/16 (31.3)	0.05
Prednisone-equivalent dose at time of discontinuation of glucocorticoid, mg/kg	0.00 (0.00–0.77)	0.00 (0.00–0.40)	0.13 (0.00–0.77)	0.00 (0.00–0.20)	0.15 (0.00–0.77)	<0.01
Biologic treatment, no. (%)						ND
Anakinra	57 (93.4)	39 (95.1)	16 (100.0)	37 (90.2)	20 (100.0)	ND
Canakinumab	15 (24.6)	9 (22.0)	4 (25.0)	9 (22.2)	6 (30.0)	
Anakinra and canakinumab	11 (18.0)	7 (17.1)	4 (25.0)	5 (12.2)	6 (30.0)	
Any TCZ	23 (37.7)	10 (24.4)	13 (81.3)	3 (7.3)	20 (100.0)	
TCZ after IL-1 blockade	20 (32.8)	7 (17.1)	13 (81.3)	0 (0.0)	20 (100.0)	

* Except where indicated otherwise, values are the median (range). P values were determined by Mann-Whitney U test for continuous variables and by chi-square test for categorical variables. TCZ = tocilizumab; WBC = white blood cell; Hgb = hemoglobin; ESR = erythrocyte sedimentation rate; IL-1 = interleukin-1; ND = not determined.

† P for trend.

‡ The Juvenile Arthritis Disease Activity Score in 10 joints (JADAS-10) is the sum of the physician global assessment of disease activity score (scale 0–10), count of joints with active arthritis (scale 0–10), and normalized C-reactive protein (CRP) level (scale 0–10; calculated as [CRP (in mg/liter) – 10]/10, with a CRP level <10 mg/liter representing a score of 0).

for each of the patients in this cohort, at least 2 additional serum samples were examined. Many of the patients had a large number of serum samples stored within the AID registry biobank (up to 60 serum samples). For all of the available serum samples, the levels of S100A12, a calgranulin that shows a strong correlation with disease activity in systemic JIA (13,14), had already been recorded. In order to achieve some degree of standardization for each patient, the serum sample with the highest S100A12 level and the serum sample with lowest S100A12 level, supposedly reflecting the highest and lowest overall inflammatory activity, respectively, for that individual patient were examined. Luminex multiplex analysis of the following cytokines was performed: CXCL9, IL-1 β , IL-1Ra, IL-6, IL-17A, IL-18, and S100A12.

Statistical analysis. Descriptive statistics concerning the relationship between the various clinical parameters and treatment response were calculated. The relationship between the different *IL1RN* homozygous polymorphisms and treatment response was assessed using the chi-square test. Receiver operating characteristic (ROC) curve analysis was performed to assess the accuracy of the continuous variables regarding outcomes. A plot of linkage disequilibrium was prepared using the Haploview software package (Broad Institute of MIT and Harvard).

RESULTS

Patient characteristics and treatment responses.

The patient cohort consisted of 61 patients who were treated with anakinra and/or canakinumab during the course of their disease; 57 (93.4%) of 61 patients had received anakinra, 15 (24.6%) had received canakinumab, and 11 (18.0%) had received both. Of the 61 patients, 41 (67%) showed at least a transient clinical response and 16 (26%) had a poor clinical response, while for 4 patients (7%), an assessment of the clinical response was not available. Twenty-three patients had received/switched to tocilizumab, including 20 (33%) who switched following prior therapy with anakinra and/or canakinumab, and 3 who switched prior to receiving anakinra and/or canakinumab, meaning that 41 patients (67%) had not switched to tocilizumab following the initiation of IL-1 blockade (Table 1). The treatment responses in these 2 groups overlapped to some degree, as indicated by the distribution of treatment responses in Table 2.

Analysis of the basic characteristics indicated that patients who did not experience a switch to tocilizumab had a lower duration from disease onset to diagnosis than those who had to later switch to tocilizumab (median 0.08 years compared to 0.27 years; $P = 0.02$). ROC curve analysis of the duration from disease onset to diagnosis and future switch to tocilizumab showed an area under the ROC curve of 0.69 (95% confidence interval 0.54–0.83). Furthermore, there were differences concerning the total duration of follow-up between these 2 response groups (median follow-up

Table 2. Distribution of response to treatment with interleukin-1 blocking agents*

Treatment response	No. of responders based on lack of subsequent tocilizumab therapy	No. of nonresponders based on subsequent tocilizumab therapy	Total no.
Clinical response†			
Good	33	4	37
Transient	1	3	4
Poor/absent	3	13	16
Not classifiable	4	0	4
Any response‡			
Yes	39	11	50
No	1	9	10
Not classifiable	1	0	1
PGA30 within 6 months			
Yes	27	12	39
No	4	7	11
Not classifiable	10	1	11
PGA50 within 6 months			
Yes	27	8	35
No	4	11	15
Not classifiable	10	1	11
PGA70 within 6 months			
Yes	21	6	27
No	10	13	23
Not classifiable	10	1	11
PGA90 within 6 months			
Yes	14	3	17
No	17	16	33
Not classifiable	10	1	11
Modified JADAS-10 score ≤ 5 within 6 months			
Yes	14	1	15
No	6	15	21
Not classifiable	21	4	25
CID within 6 months			
Yes	17	2	19
No	22	17	39
Not classifiable	2	1	3
Off glucocorticoid therapy within 6 months			
Yes	20	5	25
No	13	11	24
Not classifiable	8	4	12

* PGA30 = 30% improvement in the physician global assessment of disease activity score; JADAS-10 = Juvenile Arthritis Disease Activity Score in 10 joints; CID = clinically inactive disease.

† A good response was defined as the resolution of signs and symptoms of active disease (fever, rash, adenopathy, hepatosplenomegaly, serositis, and arthritis) and improvement by at least 50% in the levels of inflammation markers (C-reactive protein and erythrocyte sedimentation rate).

‡ Defined as improvement in fever (if present) and/or arthritis (if present).

3.5 years in those who did not switch to tocilizumab compared to 7.5 years in those who did switch; $P < 0.01$).

In addition, the maximum recorded CRP and ESR values were higher in patients who later switched to tocilizumab than in those who did not switch (median CRP 143 mg/liter versus 74 mg/liter; median ESR 99 mm/hour versus 77 mm/hour). Other parameters, including sex, age at onset, age at diagnosis, proportion of patients treated with glucocorticoids, and the median dose of glucocorticoids at initiation of IL-1 blockade, maximum recorded white blood cell count, minimum recorded hemoglobin level, and maximum recorded S100A8/A9 and S100A12 protein levels were not different between the response groups.

IL1RN haplotypes and treatment responses. Six previously reported SNPs in the *IL1RN* gene were genotyped. Genotyping of the rs55663133, rs62158853, rs62158854, rs55709272, rs7580634, and rs4251961 SNPs was successful in 55 patients (90.1%), 54 patients (88.5%), 57 patients (93.4%), 60 patients (98.3%), 58 patients (95.0%), and 61 patients (100%), respectively. We observed that there was strong linkage disequilibrium (see Supplementary Figure 1, available on the *Arthritis & Rheumatology* web site at <http://onlinelibrary.wiley.com/doi/10.1002/art.41130/abstract>), suggesting that the SNPs were present as haplotypes, i.e., either homozygous ($n = 22$ [36.1%]), heterozygous ($n = 32$ [52.5%]), or null ($n = 7$ [11.5%]) for the target genotypes.

We pursued analyses comparing the frequencies of the different genotypes across different outcomes, including 1) clinical response, 2) subsequent switch (or no switch) to tocilizumab, 3) improvement in the physician global assessment of disease activ-

ity score by at least 30%, 50%, 70%, and 90%, 4) achievement of a modified JADAS-10 score of 5 or better within 6 months of IL-1 blockade, 5) achievement of CID within 6 months of IL-1 blockade, and 6) attainment of a glucocorticoid-free state (Table 3 and Supplementary Table 1, available on the *Arthritis & Rheumatology* web site at <http://onlinelibrary.wiley.com/doi/10.1002/art.41130/abstract>). None of these outcomes was associated with the *IL1RN* haplotype.

IL1RN alleles and treatment responses. When the proportions of the individual effect alleles between the key outcomes were analyzed, similar to that in the analysis by Arthur et al, (9), the frequencies were not different between patients with systemic JIA who demonstrated at least a transient response to IL-1 blockade and those who experienced either a poor or absent response (see Supplementary Table 2 at <http://onlinelibrary.wiley.com/doi/10.1002/art.41130/abstract>). A different grouping, i.e., comparing patients with a good clinical response to those with only a transient or poor response, did not yield significant differences in individual effect allele frequencies (see Supplementary Table 3 at <http://onlinelibrary.wiley.com/doi/10.1002/art.41130/abstract>). There were also no significant differences in individual effect allele frequencies when response was evaluated according to the second outcome measure, i.e., patients who received tocilizumab following anakinra and/or canakinumab therapy versus those who did not. Furthermore, the findings did not differ when assessed according to those patients who had received IL-1 blockade with anakinra only (and not with canakinumab) (see Supplementary Table 4 at <http://onlinelibrary.wiley.com/doi/10.1002/art.41130/abstract>).

Table 3. *IL1RN* haplotypes in patients with systemic juvenile idiopathic arthritis and relationship to clinical treatment responses*

	Patients with available data, no.	Haplotype, no./total (%)		
		Homozygous	Heterozygous	Null
Clinical response				
At least transient	57	15/21 (71.4)	22/31 (71.0)	4/5 (80.0)
Good	57	13/21 (61.9)	20/31 (64.5)	4/5 (80.0)
No switch to tocilizumab	61	13/22 (59.1)	22/32 (68.8)	6/7 (85.7)
Any response†	60	18/22 (81.8)	27/32 (84.4)	5/6 (83.3)
Physician global assessment score within 6 months of IL-1 blockade				
Improved at least 30%	50	11/16 (68.8)	26/30 (86.7)	2/4 (50)
Improved at least 50%	50	9/16 (56.3)	24/30 (80.0)	2/4 (50)
Improved at least 70%	50	8/16 (50)	17/30 (56.7)	2/4 (50)
Improved at least 90%	50	6/16 (38)	11/30 (36.7)	0/4 (0)
Best modified JADAS-10 score ≤ 5 within 6 months of IL-1 blockade‡	36	5/12 (42)	7/20 (35)	3/4 (75)
CID within 6 months of IL-1 blockade	58	9/21 (42.9)	9/31 (29.0)	1/6 (16.7)
Off glucocorticoid therapy within 6 months of IL-1 blockade	49	11/18 (61.1)	11/27 (40.7)	3/4 (75.0)

* Differences between the haplotypes (P values by chi-square test) were not significant for any response group. IL-1 = interleukin-1; CID = clinically inactive disease.

† Defined as improvement in fever (if present) and/or arthritis (if present).

‡ The Juvenile Arthritis Disease Activity Score in 10 joints (JADAS-10) is the sum of physician global assessment of disease activity score (scale 0–10), count of joints with active arthritis (scale 0–10), and normalized C-reactive protein level (scale 0–10; calculated as [CRP (in mg/liter) – 10]/10, with a CRP level <10 mg/liter representing a score of 0).

Serum biomarkers and treatment responses. The comparison of several serum biomarkers obtained from the bio-bank sample with the highest serum S100A12 level for each individual patient demonstrated that only the IL-1Ra level was different between the different response groups. In analyses with treatment response defined as at least a transient clinical response or according to a treatment pattern of not switching to tocilizumab, those who were designated as responders had higher serum IL-1Ra levels (see Supplementary Table 5 at <http://onlinelibrary.wiley.com/doi/10.1002/art.41130/abstract>). The other biomarkers measured did not differ between the response groups.

Further analysis of nonparametric correlations between the different biomarkers across all samples tested indicated a substantial degree of correlation between the levels of most of the biomarkers, but not for IL-1Ra (see Supplementary Figure 2 at <http://onlinelibrary.wiley.com/doi/10.1002/art.41130/abstract>). Subsequently, the database was further queried in order to determine whether patients were receiving anakinra therapy at the time of serum sampling. Indeed, many of the patients were receiving anakinra at the time of sampling. Measured IL-1Ra serum levels were, on average, approximately an order of magnitude higher in patients receiving anakinra therapy (see Supplementary Figure 3 at <http://onlinelibrary.wiley.com/doi/10.1002/art.41130/abstract>), indicating that the measured IL-1Ra levels likely represent the presence of anakinra, i.e., recombinant IL-1Ra. Assessment of IL-1Ra serum levels measured both in the individual samples with the highest S100A12 serum levels and in those with the lowest S100A12 serum levels did not demonstrate any correlation with the different *IL1RN* haplotypes (data not shown).

DISCUSSION

In this real-world cohort of well-characterized German patients with systemic JIA who had received IL-1 blockade with anakinra and/or canakinumab, we cannot confirm an association of 6 *IL1RN* gene polymorphisms or the *IL1RN* haplotype with various definitions of an adequate treatment response. Such an association was previously reported by Arthur et al for 7 *IL1RN* gene polymorphisms in a small cohort of US patients with systemic JIA who had received anakinra therapy (9). Although we were unable to genotype 1 of the reported 7 SNPs (rs55942804/rs555447483) due to technical issues, we do not believe that this had an impact on our conclusions, the reason being that this SNP generally is part of the same strongly conserved haplotype as the other 6 SNPs. The data previously presented by Arthur et al (9) support a compelling hypothesis. On the one hand, higher-expressing *IL1RN* alleles, i.e., higher endogenous IL-1Ra production, may be associated with a lower risk of developing systemic JIA. On the other hand, once systemic JIA is present, it carries a higher risk of nonresponse to treatment with anakinra (recombinant IL-1Ra).

It is unclear as to why such an association was not seen in this German cohort. Interestingly, whereas an association of the differ-

ent *IL1RN* SNPs with risk of systemic JIA was seen in several of the systemic JIA cohorts (from the US, UK, Turkey, Italy, Brazil, Argentina, Canada, and Spain) reported by Arthur et al (9), most prominently, for rs55663133, we did not observe any association in the German cohort. Therefore, it is possible that genetic risk factors for systemic JIA and for treatment nonresponse vary in different populations. Clearly, systemic JIA is very heterogeneous, both phenotypically—for example, ranging from a rather benign condition with a monophasic disease course to a serious condition with chronic destructive arthritis or complicated by life-threatening macrophage activation syndrome—and genetically, as outlined by Arthur et al (9). In the cohort described in the study by Arthur et al, the patients were not characterized in more detail, so that further comparisons with our cohort are not feasible. Furthermore, whereas 38 patients were evaluated in the study by Arthur et al (9), the cohort was somewhat larger, comprising 61 patients, in the present study.

Considering other potential predictors of nonresponse to therapy with IL-1 blockade, there is some indication that patients with a long-term nonresponse, based on a subsequent switch to IL-6 blockade with tocilizumab, have a longer duration from onset of symptoms to diagnosis when compared to those with a persistent response (median 0.27 years compared to 0.08 years). This observation supports the “window of opportunity” hypothesis, i.e., early diagnosis (and treatment) may positively influence the long-term outcome of the disease (8). However, we did not observe a significant association of duration from onset to diagnosis and a different measure of treatment response (clinical response).

While we attempted to correlate serum IL-1Ra levels with 1) the different *IL1RN* SNPs, and 2) treatment response, this was fraught with difficulty. First, an association of the different SNPs with serum IL-1Ra levels was not observed. Second, while higher IL-1Ra serum levels were detected, this was most likely attributable to the ongoing treatment with anakinra in these patients, since the assay used does not distinguish between the endogenous IL-1Ra and anakinra (N2-L-methionyl-26-177-IL-1Ra), i.e., the analyte of interest represents the active treatment that was given to many of the patients.

Our study has several limitations. Some of the patients had a disease onset after the age of 16 years, and therefore they did not fulfill the International League of Associations for Rheumatology criteria for systemic JIA (15). However, these criteria are a subject of controversy, and potentially more appropriate criteria have been suggested (16,17). The present study focuses on a cohort of patients with variable duration of follow-up, which may have an impact on the treatment outcomes; for example, a patient with a much longer disease course may have a higher chance to receive tocilizumab following IL-1 blockade. We were unable to extract more formal response criteria from the registry, such as the modified ACR Pedi 30 response criteria or the complete JADAS criteria, each of which have been used in controlled clinical trials. This was because some of the criteria, such as patient global assessment of disease activity (5), were not recorded.

Nevertheless, from a clinical standpoint, we believe that our assessment of treatment response, i.e., clinical response concerning systemic inflammation and drug survival, was valid. Because patients were often not enrolled in the registry early during the disease, the laboratory data recorded in the registry almost certainly do not represent the most prominent changes, since such data are often present at the onset of disease; therefore, conclusions on the impact of certain laboratory abnormalities on treatment outcomes are very limited. Furthermore, assessment of serum cytokine levels, including IL-1Ra, is presumably strongly influenced by multiple factors, such as degree of systemic inflammation and current medications (18), for which we did not control; therefore, based on our current data, it would not be possible to draw conclusions on the effect of *IL1RN* SNPs on IL-1Ra expression. It would be desirable to extend genetic studies to cohorts that could be better characterized and prospectively followed up.

In summary, despite the limitations mentioned, in this German cohort of patients with systemic JIA treated with IL-1 blockade, we could not find any evidence of an impact of *IL1RN* SNPs on treatment response to IL-1 blockade. In contrast, this study provides evidence of a “window of opportunity” in this cohort, i.e., improved long-term treatment response with shorter time from disease onset to diagnosis (and treatment, presumably).

AUTHOR CONTRIBUTIONS

All authors were involved in drafting the article or revising it critically for important intellectual content, and all authors approved the final version to be published. Dr. Hinze had full access to all of the data in the study and takes responsibility for the integrity of the data and the accuracy of the data analysis.

Study conception and design. Hinze, Foell.

Acquisition of data. Hinze, Fuehner, Kessel, Wittkowski, Lainka, Baehr, Hügler, Haas, Ganser, Weißbarth-Riedel, Jansson, Foell.

Analysis and interpretation of data. Hinze, Kessel, Wittkowski, Lainka, Foell.

REFERENCES

- Mellins ED, Macaubas C, Grom AA. Pathogenesis of systemic juvenile idiopathic arthritis: some answers, more questions [review]. *Nat Rev Rheumatol* 2011;7:416–26.
- Hinze CH, Holzinger D, Lainka E, Haas JP, Speth F, Kallinich T, et al, and PRO-KIND SJA project collaborators. Practice and consensus-based strategies in diagnosing and managing systemic juvenile idiopathic arthritis in Germany. *Pediatr Rheumatol Online J* 2018;16:7.
- Giannini EH, Ruperto N, Ravelli A, Lovell DJ, Felson DT, Martini A. Preliminary definition of improvement in juvenile arthritis. *Arthritis Rheum* 1997;40:1202–9.
- Quartier P, Allantaz F, Cimaz R, Pillet P, Messiaen C, Bardin C, et al. A multicentre, randomised, double-blind, placebo-controlled trial with the interleukin-1 receptor antagonist anakinra in patients with systemic-onset juvenile idiopathic arthritis (ANAJIS trial). *Ann Rheum Dis* 2011;70:747–54.
- Ruperto N, Brunner HI, Quartier P, Constantin T, Wulffraat N, Horneff G, et al, for the PRINTO and PRCSSG. Two randomized trials of canakinumab in systemic juvenile idiopathic arthritis. *N Engl J Med* 2012;367:2396–406.
- Gattorno M, Piccini A, Lasigliè D, Tassi S, Brisca G, Carta S, et al. The pattern of response to anti-interleukin-1 treatment distinguishes two subsets of patients with systemic-onset juvenile idiopathic arthritis. *Arthritis Rheum* 2008;58:1505–15.
- Pascual V, Allantaz F, Arce E, Punaro M, Banchereau J. Role of interleukin-1 (IL-1) in the pathogenesis of systemic onset juvenile idiopathic arthritis and clinical response to IL-1 blockade. *J Exp Med* 2005;201:1479–86.
- Nigrovic PA. Is there a window of opportunity for treatment of systemic juvenile idiopathic arthritis? [review]. *Arthritis Rheumatol* 2014;66:1405–13.
- Arthur VL, Shuldiner E, Remmers EF, Hinks A, Grom AA, Foell D, et al. *IL1RN* variation influences both disease susceptibility and response to recombinant human interleukin-1 receptor antagonist therapy in systemic juvenile idiopathic arthritis. *Arthritis Rheumatol* 2018;70:1319–30.
- Bielak M, Husmann E, Weyandt N, Haas JP, Hügler B, Horneff G, et al. IL-6 blockade in systemic juvenile idiopathic arthritis—achievement of inactive disease and remission (data from the German AID-registry). *Pediatr Rheumatol Online J* 2018;16:22.
- Wallace CA, Giannini EH, Huang B, Irtter L, Ruperto N, for the Childhood Arthritis and Rheumatology Research Alliance (CARRA), Pediatric Rheumatology Collaborative Study Group (PRCSG), Paediatric Rheumatology International Trials Organisation (PRINTO). American College of Rheumatology provisional criteria for defining clinical inactive disease in select categories of juvenile idiopathic arthritis. *Arthritis Care Res (Hoboken)* 2011;63:929–36.
- Consolaro A, Ruperto N, Bazso A, Pistorio A, Magni-Manzoni S, Filocamo G, et al, for the Paediatric Rheumatology International Trials Organisation. Development and validation of a composite disease activity score for juvenile idiopathic arthritis. *Arthritis Rheum* 2009;61:658–66.
- Foell D, Wittkowski H, Hammerschmidt I, Wulffraat N, Schmeling H, Frosch M, et al. Monitoring neutrophil activation in juvenile rheumatoid arthritis by S100A12 serum concentrations. *Arthritis Rheum* 2004;50:1286–95.
- Wittkowski H, Frosch M, Wulffraat N, Goldbach-Mansky R, Kallinich T, Kueemmerle-Deschner J, et al. S100A12 is a novel molecular marker differentiating systemic-onset juvenile idiopathic arthritis from other causes of fever of unknown origin. *Arthritis Rheum* 2008;58:3924–31.
- Petty RE, Southwood TR, Manners P, Baum J, Glass DN, Goldenberg J, et al, and the International League of Associations for Rheumatology. International League of Associations for Rheumatology classification of juvenile idiopathic arthritis: second revision, Edmonton, 2001 [abstract]. *J Rheumatol* 2004;31:390–2.
- Martini A, Ravelli A, Avcin T, Beresford MW, Burgos-Vargas R, Cuttica R, et al, for the Pediatric Rheumatology International Trials Organization (PRINTO). Toward new classification criteria for juvenile idiopathic arthritis: first steps, Pediatric Rheumatology International Trials Organization International Consensus. *J Rheumatol* 2019;46:190–7.
- Beukelman T, Nigrovic PA. Juvenile idiopathic arthritis: an idea whose time has gone? [editorial]. *J Rheumatol* 2019;46:124–6.
- Gårdlund B, Sjölin J, Nilsson A, Roll M, Wickerts CJ, Wretling B. Plasma levels of cytokines in primary septic shock in humans: correlation with disease severity. *J Infect Dis* 1995;172:296–301.

LETTERS

DOI 10.1002/art.41137

Immune checkpoint inhibitors in preexisting autoimmune disease: comment on the article by Tison et al

To the Editor:

We read with great interest the article by Tison et al, profiling the safety and efficacy of immune checkpoint inhibitor (ICI) treatment in individuals with cancer and preexisting autoimmune disease (1). In this nationwide, multicenter cohort study, with the largest study population other than the one reported by Kehl et al (2), the occurrence of flare of preexisting autoimmune disease and/or other immune-related adverse effects (IRAEs) was frequent but mostly manageable without the need to discontinue use of ICIs. However, some issues should be addressed.

First, a previous study based on a relatively small sample size indicated differences in flare rates among patients with preexisting autoimmune diseases of different systems (i.e., rheumatologic, dermatologic, endocrine, neurologic), and the occurrence of flare was more likely in patients with rheumatologic disorders (14 of 27 [52%]) (3). Therefore, we propose that the authors should additionally classify preexisting autoimmune disease according to system and subsequently assess differences in the rate of flare among systems. The results could be interesting and may be of clinical value.

Second, some important missing messages should be presented. During the median follow-up of 8 months, a flare of the preexisting autoimmune disease was reported in 53 patients, and 42% of patients experienced IRAEs not related to their preexisting autoimmune disease. We suggest the median time to flare (with range or interquartile range) and the rate of IRAEs in the overall cohort, including patients without preexisting autoimmune disease, should be reported to provide more clinically relevant data.

Third, there seem to be 2 mistakes in the Results section, under the “Flare of preexisting autoimmune disease” heading. Tison et al stated “A flare of the preexisting autoimmune disease was reported in 53 patients (47%), and 84% of the flares were similar to previous flares. Of the 50 patients for whom Common Terminology Criteria for Adverse Events grades were available, the flare was mild for 35 patients (70%) but severe in 15 (30%).” We believe that 84% is incorrect and it should be 83% (if there were 44 patients) or 85% (if there were 45 patients). The total number of patients experiencing mild and severe flare is 50 (100%), but Tison and colleagues reported there were 53 patients who experienced flare.

Wen-hui Xie, PhD 
Zhuo-li Zhang, MD, PhD
Peking University First Hospital
Beijing, China

1. Tison A, Quéré G, Misery L, Funck-Brentano E, Danlos FX, Routier E, et al. Safety and efficacy of immune checkpoint inhibitors in patients with cancer and preexisting autoimmune disease: a nationwide multicenter cohort study. *Arthritis Rheumatol* 2019;71:2100–11.
2. Kehl KL, Yang S, Awad MM, Palmer N, Kohane IS, Schrag D. Preexisting autoimmune disease and the risk of immune-related adverse events among patients receiving checkpoint inhibitors for cancer. *Cancer Immunol Immunother* 2019;68:917–26.
3. Menzies AM, Johnson DB, Ramanujam S, Atkinson VG, Wong ANM, Park JJ, et al. Anti-PD-1 therapy in patients with advanced melanoma and preexisting autoimmune disorders or major toxicity with ipilimumab. *Ann Oncol* 2017;28:368–76.

DOI 10.1002/art.41139

Reply

To the Editor:

We thank Drs. Xie and Zhang for their interest in our study on the safety and efficacy of ICIs in patients with cancer and preexisting autoimmune disease.

First, the authors suggested classifying preexisting autoimmune diseases according to systems in order to assess if rheumatic disorders were more likely to flare with ICIs. Such trends have been reported in other studies (1,2), with the limitation that the highest percentage of preexisting autoimmune diseases in the cohorts studied were rheumatic disorders ($n = 27$ [52%] in ref. 1 and $n = 25$ [45%] in ref. 2). This trend was also reported in other series (3,4). In Table 3 of our article, we presented the percentage of flares according to the 5 main preexisting autoimmune diseases in our cohort (84 of 112 patients [75%]), dominated by rheumatic disorders (rheumatoid arthritis, polymyalgia rheumatica/giant cell arteritis, spondyloarthritis). Other preexisting autoimmune diseases were heterogeneous and with a small sample size for each system, which does not allow firm conclusions. For example, both the respiratory system and the neurologic system were represented by 3 patients (pulmonary sarcoidosis and 1 myasthenia gravis, 1 multiple sclerosis, and 1 autoimmune hypophysitis), and the hematologic system was represented by only 2 patients. Furthermore, several preexisting autoimmune diseases had systemic features (4 patients with systemic

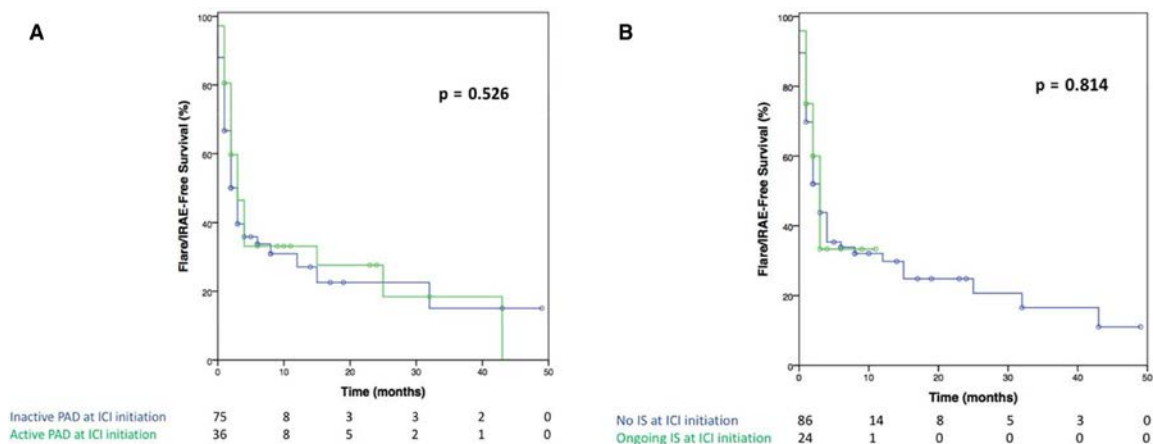


Figure 1. Flare/immune-related adverse effect (IRAE)-free survival at immune checkpoint inhibitor (ICI) initiation in patients with active or inactive preexisting autoimmune disease (PAD) (A) and in patients receiving ongoing or no immunosuppressive (IS) treatment (B).

lupus erythematosus, 3 with systemic sclerosis, 2 with antineutrophil cytoplasmic antibody-associated vasculitis, 1 with antiphospholipid syndrome, and 1 with dermatomyositis), precluding their classification in a single organ system. For these reasons, we consider it more meaningful to classify the diseases according to the diagnosis, with a larger sample size, even if a classification by system might add clinical value. Interestingly, more flares were reported in the psoriasis group in our cohort, and 50% of patients with inflammatory bowel disease (IBD) experienced a flare, compared to lower flare frequencies reported in other retrospective cohorts (1–4). IBD represented a larger sample size in our cohort.

Second, the authors inquired about the median time before a flare/IRAE occurrence. Considering only the first course of ICI treatment, the median time before the worst flare was 6.6 weeks (range 0–183), and the median time before the worst grade IRAE was 9.6 weeks (range 0.6–137), which was consistent with safety data on ICI in the general population (5,6). Weber et al reported a median time to treatment-related select AEs ranging from 5.0 weeks for skin AEs to 15.1 weeks for renal AEs (6). Notably there were no differences in our cohort in worst flare/IRAE-free survival in patients with active versus inactive preexisting autoimmune diseases at baseline, or in ongoing versus no immunosuppressive therapy at baseline ($P = 0.526$ and $P = 0.814$; Figures 1A and B).

Third, Xie and Zhang asked about the median time before IRAE in patients without preexisting autoimmune disease. Since our cohort included only patients with a preexisting autoimmune disease at ICI initiation, we can only respond based on current available literature. In a prospective study, Danlos et al reported a higher frequency of IRAE grade ≥ 2 in the preexisting autoimmune disease group versus the group of patients without preexisting autoimmune disease (44% versus 29%), and IRAE-free survival was significantly shorter in patients with preexisting autoimmune diseases (median 5.4 months versus 13 months, $P = 2.1 \times 10^{-4}$) (7). In a recent systematic literature review performed to inform ongoing European League Against Rheumatism recommendations, the median time of exposure to ICI


was 120 days for patients without preexisting autoimmune diseases experiencing de novo arthritis, 60 days for patients with polymyalgia rheumatica-like syndrome, and 25 days for patients with myositis (Kostine M, et al: unpublished observations).

Last, Xie and Zhang were concerned about the numbers reported in the section entitled “Flare of preexisting autoimmune disease.” We reported a flare of preexisting autoimmune disease in 53 patients (47%), in which 43 of 51 (84%) were similar to previous flares. There were indeed missing data on this for 2 patients. With regard to patients experiencing mild and severe flares a similar explanation applies, with data missing for 3 of 53 patients.


Alice Tison, MD

CHRU Brest

Brest, France

Marie Kostine, MD, PhD 

Centre Hospitalier Universitaire de Bordeaux
Bordeaux, France

Divi Cornec, MD, PhD 

CHRU Brest

Brest, France

1. Menzies AM, Johnson DB, Ramanujam S, Atkinson VG, Wong ANM, Park JJ, et al. Anti-PD-1 therapy in patients with advanced melanoma and preexisting autoimmune disorders or major toxicity with ipilimumab. *Ann Oncol* 2017;28:368–76.
2. Leonardi GC, Gainor JF, Altan M, Kravets S, Dahlberg SE, Gedmintas L, et al. Safety of programmed death-1 pathway inhibitors among patients with non-small-cell lung cancer and preexisting autoimmune disorders. *J Clin Oncol* 2018;36:1905–12.
3. Johnson DB, Sullivan RJ, Ott PA, Carlino MS, Khushalani NI, Ye F, et al. Ipilimumab therapy in patients with advanced melanoma and preexisting autoimmune disorders. *JAMA Oncol* 2016;2:234–40.
4. Kähler KC, Eigentler TK, Gesierich A, Heinzerling L, Loquai C, Meier F, et al. Ipilimumab in metastatic melanoma patients with pre-existing autoimmune disorders. *Cancer Immunol Immunother* 2018;67:825–34.
5. Friedman CF, Proverbs-Singh TA, Postow MA. Treatment of the immune-related adverse effects of immune checkpoint inhibitors: a review. *JAMA Oncol* 2016;2:1346–53.
6. Weber JS, Hodi FS, Wolchok JD, Topalian SL, Schadendorf D, Larkin J, et al. Safety profile of nivolumab monotherapy: a pooled

analysis of patients with advanced melanoma. *J Clin Oncol* 2017; 35:785–92.

7. Danlos FX, Voisin AL, Dyevre V, Michot JM, Routier E, Taillade L, et al. Safety and efficacy of anti-programmed death 1 antibodies in patients with cancer and pre-existing autoimmune or inflammatory disease. *Eur J Cancer* 2018;91:21–9.

DOI 10.1002/art.41155

The first epidemiologic perspective on takotsubo syndrome in patients with Takayasu arteritis and its impact on inpatient outcomes: comment on the report by Lim et al

To the Editor:

Takayasu arteritis (TAK) is a chronic inflammatory condition of large blood vessels primarily affecting the aorta and its

main branches (1). Although more prevalent in Asians, it has a worldwide distribution. Increased oxidative stress perpetuating the inflammatory response and activity of matrix metalloproteinases are commonly proposed mechanisms for the occurrence of TAK (2). The persistent inflammatory response in TAK can lead to involvement of the pulmonary/coronary artery or myocardium (3). Takotsubo (stress) cardiomyopathy (TC) has been recently reported to result in poor outcomes, comparable to those associated with acute coronary syndrome (4). A variety of risk factors make certain individuals more susceptible to TC and adversely influence outcome (5). Recently, Lim et al presented the first report describing TC in a patient with TAK (6). The epidemiology of TC in patients with TAK and outcomes in patients with coexistent TC and TAK have not been reported.

Table 1. Hospital admissions with, and outcomes of takotsubo cardiomyopathy in, patients with versus those without coexistent Takayasu arteritis*

	All takotsubo cardiomyopathy (n = 156,506)	Takotsubo cardiomyopathy without Takayasu arteritis (n = 156,428)	Takotsubo cardiomyopathy with Takayasu arteritis (n = 78)	P
Age at hospitalization, median (IQR) years	68 (58–77)	68 (58–77)	66 (52–73)	0.004
Female	87.0	87.0	93.6	0.082
Race				0.030
White	82.5	82.5	92.5	
Nonwhite	17.5	17.5	–†	
Nonelective admission	90.9	90.9	100.0	0.005
Location/teaching status of hospital				0.001
Rural	7.2	7.2	–†	
Urban non-teaching	32.9	32.9	50.2	
Urban teaching	60.0	60.0	38.0	
Region of hospital				0.001
Northeast	19.5	19.5	–†	
Midwest	26.3	26.3	38.5	
South	33.3	33.3	24.6	
West	20.9	20.9	30.5	
Comorbidities				
Hypertension	63.0	63.0	56.5	0.230
Diabetes, uncomplicated	18.6	18.6	–†	0.191
Diabetes, chronic complications	3.1	3.1	–†	0.085
Dyslipidemia	43.3	43.3	38.0	0.385
Prior MI/PCI/CABG	13.8	13.8	19.2	0.166
Smoking	31.5	31.5	43.3	0.022
Peripheral vascular disease	8.0	8.0	19.7	<0.001
Congestive heart failure	18.2	18.2	19.7	0.817
Chronic obstructive pulmonary disease	27.9	27.9	44.4	0.001
Any psychiatric disorder	51.0	51.0	75.2	<0.001
In-hospital outcomes				
All-cause in-hospital mortality	4.7	4.7	–†	0.474
Cardiogenic shock	5.3	5.3	–†	0.672
Arrhythmia	29.0	29.0	18.8	0.058
Venous thromboembolism	3.5	3.5	–†	0.090
Stroke	2.2	2.2	–†	0.01
Respiratory failure	17.4	17.4	30.6	0.002
Intubation/mechanical ventilation	18.8	18.8	30.6	0.007
Routine discharge	58.6	58.6	42.3	<0.001
Transfer to other facility (SNF, ICF, etc.)	19.4	19.4	19.7	<0.001
Home health care	14.2	14.1	32.0	<0.001
Length of stay, median (IQR) days	4 (2–8)	4 (2–8)	4 (2–7)	0.209
Total hospital charges, median (IQR) dollars	38,413 (22,411–72,885)	38,396 (22,411–72,866)	49,730 (37,331–79,789)	0.048

* Except where indicated otherwise, values are the percent. IQR = interquartile range; MI = myocardial infarction; PCI = percutaneous coronary intervention; CABG = coronary artery bypass grafting; SNF = skilled nursing facility; ICF = intermediate care facility.

† Data not reported per privacy guidelines (<https://www.hcup.us.ahrq.gov/db/publishing.jsp>), because total number of hospitalizations was <11.

Using the National Inpatient Sample (2007–2014) and International Classification of Diseases, Ninth Revision, Clinical Modification codes, we identified TC (code 429.83)– and TAK (code 446.7)–related hospitalizations among adults and the frequency of TAK among patients with TC. Baseline characteristics and outcomes of TC-related hospitalizations with TAK versus other triggers were analyzed. This is the first study to explore the epidemiology of TC in patients with TAK and outcomes in hospitalized patients.



The prevalence of TAK among all TC-related hospitalizations was 0.05% (78 of 156,506) (Table 1). The proportion of women in the TC-TAK cohort was higher than that in the non-TAK TC cohort (93.6% versus 87.0%), although the difference did not reach statistical significance. A female predilection in both conditions could be the reason for this observation (5). The TC-TAK cohort was younger (median age 66 years [interquartile range 52–73] versus 68 years [interquartile range 58–77]; $P = 0.004$) and had a higher proportion of patients who were white (92.5% versus 82.5%; $P = 0.03$) and whose admission was not elective (100% versus 90.9%; $P = 0.005$).

We observed a higher prevalence of peripheral vascular disease (19.7% versus 8.0%; $P < 0.001$) and smoking (43.3% versus 31.5%; $P = 0.02$) in the TC-TAK cohort. Smoking-induced endothelial dysfunction and platelet activation can lead to early atherosclerosis. Endothelial dysfunction is believed to be a key factor in coronary microvascular dysfunction, which also plays a role in the pathogenesis of TC (5). These shared pathologic mechanisms, including atherosclerosis, endothelial dysfunction, and hypercoagulability state, could be the key reasons for the susceptibility to TC among patients with TAK. We also found a higher frequency of psychiatric disorders (75.2% versus 51.0%; $P < 0.001$) in the TC-TAK cohort, as reported earlier in TC patients (5). Patients with mood disorder and anxiety may have intensified sympathetic responses to stressors, making them susceptible to stress-related cardiac dysfunction and poor outcomes (5). The frequency of chronic obstructive pulmonary disease (COPD) was higher in the TC-TAK cohort (44.4% versus 27.9%; $P = 0.001$), possibly due to increased risk of pulmonary artery involvement and chronic/recurrent alveolar hemorrhage in TAK. Respiratory failure and COPD exacerbations are also known triggers of TC (5), which likely explains the observed high burden of respiratory failure (30.6% versus 17.4%; $P = 0.002$) and use of mechanical ventilation (30.6% versus 18.8%; $P = 0.007$).

There was no significant difference in all-cause mortality between the groups ($P = 0.47$); however, the TC-TAK cohort had a higher frequency of stroke ($P = 0.01$). Among TAK patients, a high burden of stroke has been reported earlier (~12%) (1). The atherosclerotic changes and activation of the coagulation cascade causing a thromboembolic state can contribute to stroke events in these patients. TAK patients remain more vulnerable to infections owing to glucocorticoid and immunosuppressive treatment, leading to sepsis, pneumonia, or cellulitis necessitating prolonged hospitalization (1). High complication rates and

greater need for diagnostic/therapeutic modalities in the TC-TAK cohort could have amplified health care costs and resource utilization (1).

In conclusion, the frequency of TAK was 0.05% among all TC-related admissions. The TC-TAK cohort showed a higher frequency of stroke, respiratory failure/mechanical ventilation, and health care resource utilization as compared to the non-TAK TC cohort. This study highlights the possible role of TAK and other chronic inflammatory states in the development and worse prognosis of TC.

Rupak Desai, MBBS 
Veterans Affairs Medical Center
Atlanta, GA
 Sandeep Singh, MBBS
Amsterdam University Medical Center
Amsterdam, The Netherlands
 Rajesh Sachdeva, MD 
Veterans Affairs Medical Center
Morehouse School of Medicine
and Emory University School of Medicine
Atlanta, GA
and Medical College of Georgia
Augusta, GA
 Gautam Kumar, MD
Veterans Affairs Medical Center
and Emory University School of Medicine
Atlanta, GA

1. Ungprasert P, Wijarnpreecha K, Cheungpasitporn W, Thongprayoon C, Kroner PT. Inpatient prevalence, burden and comorbidity of Takayasu's arteritis: nationwide inpatient sample 2013-2014. *Semin Arthritis Rheum* 2019;49:136–9.
2. Mahajan N, Dhawan V, Malik S, Jain S. Implication of oxidative stress and its correlation with activity of matrix metalloproteinases in patients with Takayasu's arteritis disease. *Int J Cardiol* 2010;145:286–8.
3. Takeda N, Takahashi T, Seko Y, Maemura K, Nakasone H, Sakamoto K, et al. Takayasu myocarditis mediated by cytotoxic T lymphocytes. *Intern Med* 2005;44:256–60.
4. Templin C, Ghadri JR, Diekmann J, Napp LC, Bataiosu DR, Jaguszewski M, et al. Clinical features and outcomes of takotsubo (stress) cardiomyopathy. *N Engl J Med* 2015;373:929–38.
5. Ghadri JR, Wittstein IS, Prasad A, Sharkey S, Dote K, Akashi YJ, et al. International expert consensus document on takotsubo syndrome (part I): clinical characteristics, diagnostic criteria, and pathophysiology. *Eur Heart J* 2018;39:2032–46.
6. Lim SL, Ong CC, Dissanayake DP, Teo LL, Tay SH. Takotsubo and Takayasu—a reason to rhyme? *Arthritis Rheumatol* 2019;71:1726.

DOI 10.1002/art.41151

Reply

To the Editor:

The comments from Dr. Desai et al regarding the epidemiology and outcomes of TC in patients with TAK, following our recent report of the first-described case of TC with concomitant TAK, are of interest. Cardiac involvement is a major cause of morbidity and

mortality in TAK (1–3). Any structure of the heart can potentially be affected, with predominant involvement of the ascending aorta leading to aortic aneurysm with aortic regurgitation, coronary vasculitis, and myocarditis leading to dilated cardiomyopathy. Nearly half of the patients with TAK have cardiac involvement at some point during the course of their disease (4–6). It has been estimated that up to 60% of TAK patients have angiographic evidence of coronary artery involvement, but with symptoms evident in only 5–20% (1–3). Vascular inflammation is the main mechanism of coronary arteriopathy. In addition, premature atherosclerosis secondary to hypertension and chronic inflammation may play contributory roles (6). Up to 50% of TAK patients are reported to have myocardial involvement, but interestingly, the majority are asymptomatic. Increased expression of perforins and major histocompatibility complex molecules within inflammatory lesions suggests that cell-mediated cytotoxicity may be one of the mechanisms of injury (7). Our patient had moderate aortic regurgitation and arteriographic abnormalities involving the thoracic aorta, right brachiocephalic trunk, left common carotid, left subclavian artery, and main and bilateral pulmonary arteries—only discovered at the time of presentation with asthma.

The pathophysiology of TC is not completely understood. While it was previously thought to be a consequence of direct catecholamine effects on the coronary circulation as well as catecholamine toxicity to the myocardium (8–10), the role of inflammation, and possibly autoimmunity, in TC has been increasingly recognized (11,12). Circulating T cells are generally tolerant to cardiac antigens, such as cardiac myosin and cardiac troponin I, as self-reactive T cells undergo negative selection during the maturation process in the thymus. However, some autoreactive T cells may be incompletely deleted during thymic development and can recognize cardiac self antigens (13,14). In the setting of catecholamine-induced myocardial damage exposing these cardiac antigens, these autoreactive T cells can recognize cardiac self antigens and activate an immunologic response cascade against the cardiomyocytes, resulting in global cardiac dysfunction, contributing to the development of TC.

Given the epidemiologic overlap between TAK and TC as described by Desai et al, the low prevalence of TAK among more than 156,000 TC-related hospitalizations between 2007 and 2014 is surprising. This can potentially be explained by the immunosuppressive treatment used in TAK. Patients receiving immunosuppressive therapy may not mount such an exaggerated inflammatory response to catecholamine-induced myocardial damage, thus protecting against the development of full-blown TC.

The intersection of cardiology and rheumatology is a rich area for basic science and clinical investigation. Exposure to classic presentations of cardiac and rheumatic syndromes, as well as an

understanding of cardioimmunology, are essential for cardiologists and rheumatologists.

Sen Hee Tay, MBBS, MRCP 
 D. P. S. Dissanayake, MBBS, MD, MRCP
 Shir Lynn Lim, MBBS, MRCP
 Weiqin Lin, MBBS, MRCP
*National University Health System
 Singapore, Singapore*

1. Park MC, Lee SW, Park YB, Chung NS, Lee SK. Clinical characteristics and outcomes of Takayasu's arteritis: analysis of 108 patients using standardized criteria for diagnosis, activity assessment, and angiographic classification. *Scand J Rheumatol* 2005;34:284–92.
2. Soto ME, Espinola N, Flores-Suarez LF, Reyes PA. Takayasu arteritis: clinical features in 110 Mexican Mestizo patients and cardiovascular impact on survival and prognosis. *Clin Exp Rheumatol* 2008; 26 Suppl 49:S9–15.
3. Cong XL, Dai SM, Feng X, Wang ZW, Lu QS, Yuan LX, et al. Takayasu's arteritis: clinical features and outcomes of 125 patients in China. *Clin Rheumatol* 2010;29:973–81.
4. Bicakcigil M, Aksu K, Kamali S, Ozbalkan Z, Ates A, Karadag O, et al. Takayasu's arteritis in Turkey: clinical and angiographic features of 248 patients. *Clin Exp Rheumatol* 2009;27 Suppl 52:S59–64.
5. Maksimowicz-McKinnon K, Clark TM, Hoffman GS. Limitations of therapy and a guarded prognosis in an American cohort of Takayasu arteritis patients. *Arthritis Rheum* 2007;56:1000–9.
6. Seyahi E, Ugurlu S, Cumali R, Balci H, Seyahi N, Yurdakul S, et al. Atherosclerosis in Takayasu arteritis. *Ann Rheum Dis* 2006;65:1202–7.
7. Takeda N, Takahashi T, Seko Y, Maemura K, Nakasone H, Sakamoto K, et al. Takayasu myocarditis mediated by cytotoxic T lymphocytes. *Intern Med* 2005;44:256–60.
8. Galiuto L, de Caterina AR, Porfidi A, Paraggio L, Barchetta S, Locorotondo G, et al. Reversible coronary microvascular dysfunction: a common pathogenetic mechanism in apical ballooning or Tako-Tsubo syndrome. *Eur Heart J* 2010;31:1319–27.
9. Abraham J, Mudd JO, Kapur NK, Klein K, Champion HC, Wittstein IS. Stress cardiomyopathy after intravenous administration of catecholamines and β -receptor agonists. *J Am Coll Cardiol* 2009; 53:1320–5.
10. Giavarini A, Chedid A, Bobrie G, Plouin PF, Hagege A, Amar L. Acute catecholamine cardiomyopathy in patients with pheochromocytoma or functional paraganglioma. *Heart* 2013;99:1438–44.
11. Sattler S, Couch LS, Harding SE. Takotsubo syndrome: latest addition to the expanding family of immune-mediated diseases? *JACC Basic Transl Sci* 2018;3:779–81.
12. Scally C, Abbas H, Ahearn T, Srinivasan J, Mezincescu A, Rudd A, et al. Myocardial and systemic inflammation in acute stress-induced (takotsubo) cardiomyopathy. *Circulation* 2019;139:1581–92.
13. Lv H, Havari E, Pinto S, Gottumukkala RV, Cornivelli L, Raddassi K, et al. Impaired thymic tolerance to α -myosin directs autoimmunity to the heart in mice and humans. *J Clin Invest* 2011; 121:1561–73.
14. Göser S, Andrassy M, Buss SJ, Leuschner F, Volz CH, Ottl R, et al. Cardiac troponin I but not cardiac troponin T induces severe autoimmune inflammation in the myocardium. *Circulation* 2006;114: 1693–702.

ACR Announcements

AMERICAN COLLEGE OF RHEUMATOLOGY
2200 Lake Boulevard NE, Atlanta, Georgia 30319-5312
www.rheumatology.org

ACR Meetings

State-of-the-Art Clinical Symposium
March 27–29, 2020, New Orleans

Pediatric Rheumatology Symposium
April 29–May 2, 2020, New Orleans

For additional information, contact the ACR office.

Applications Invited for *Arthritis Care & Research* Editor-in-Chief (2021–2026 Term)

The American College of Rheumatology Committee on Journal Publications announces the search for the position of Editor, *Arthritis Care & Research*. The official term of the next *Arthritis Care & Research* editorship is July 1, 2021–June 30, 2026; however, some of the duties of the new Editor will begin during a transition period starting April 1, 2021. ACR/ARP members who are considering applying for this prestigious and rewarding position should submit a nonbinding letter of intent by May 4, 2020 to the Managing Editor, Maggie Parry, at mparry@rheumatology.org, and are also encouraged to contact the current Editor-in-Chief, Dr. Marian Hannan, to discuss details. Initial contact should be made via e-mail to Hannan@hsl.harvard.edu. Applications will be due by June 15, 2020 and will be reviewed during the summer of 2020. Application materials are available on the ACR web site at <https://www.rheumatology.org/Portals/0/Files/ACandR-Editor-Application-Instructions.pdf>.

ACR 2020 State-of-the-Art Clinical Symposium

Join the ACR in New Orleans for rheumatology's premier weekend symposium, complete with cutting-edge clinical best practices and emerging trends, without taking time from work! What's new in 2020? The first full day of the 2020 meeting kicks off with a wellness yoga session to help you avoid physician burnout and get a healthy jumpstart to the weekend. Cap off the day in New Orleans

style with Cocktails & Cases, an event designed to encourage discussion and networking. You'll also be able to participate in a lively panel discussion after each group session. Experience the exceptional educational programs yourself, March 27–29 in New Orleans, LA. Advance registration ends March 11. After March 11, you may register on-site. To take advantage of special housing rates, reserve your room by March 6. Visit rheumatology.org/Learning-Center/Educational-Activities to learn more and register.

ACR 2020 Pediatric Rheumatology Symposium

Join your pediatric colleagues from across the country at the Pediatric Rheumatology Symposium (PRSYM), a scientific meeting dedicated exclusively to pediatric rheumatology. In 2020, PRSYM is being held in New Orleans for the first time ever! The most cutting-edge pediatric rheumatology research will be on display in the poster hall, where a variety of abstracts will provide enlightening content to bring back to your team. Get an interactive learning experience with panel discussions, as well as several key networking opportunities. Take part in the exciting educational programs, April 29–May 2 in New Orleans. Register by March 4 for early-bird rates or by April 15 for advance registration rates, or register on-site. Reserve your room early to take advantage of special rates (until April 8). Visit rheumatology.org/Learning-Center/Educational-Activities to learn more and register.

Education Programs

Precision Medicine in Autoimmunity. March 11–13, 2020, Denver, CO. Expert speakers will present scientific and clinical advances related to precision medicine in rheumatoid arthritis, juvenile inflammatory arthritis, systemic lupus erythematosus, psoriasis and psoriatic arthritis, ankylosing spondylitis, inflammatory bowel disease, myositis, and scleroderma, and on checkpoint inhibitors and immune-related adverse events, influence of lifestyle factors on autoimmunity, and patient-reported outcomes. Registration fee is \$475. For additional information, visit the web site www.precisionmedicineautoimmunity.org.